

https://dspace.org/

Effect of high-volume fly ash, curing temperature and water to cement ratio on strength development and durability of concrete

Hlabangana, Mthulisi

2020
https://hdl.handle.net/10539/31341

Downloaded from a DSpace repository. https://dspace.org/

UNIVERSITY OF THE WITWATERSRAND, JOHANNESBURG

FACULTY OF ENGINEERING AND THE BUILT ENVIRONMENT

School of Civil and Environmental Engineering

EFFECT OF HIGH-VOLUME FLY ASH, CURING TEMPERATURE AND WATER TO CEMENT RATIO ON STRENGTH DEVELOPMENT AND DURABILITY OF CONCRETE

Prepared By:

Mthulisi Hlabangana
Student Number: 494284

Supervisor:

Prof. Sunday Nwaubani

October 2019

A research report submitted to the Faculty of Engineering and the Built Environment, University of the Witwatersrand, in partial fulfilment of the requirements for the degree of Master of Science in Engineering

Johannesburg 2019

DECLARATION

I **MTHULISI HLABANGANA** declare that this research report is my own unaided work. It is being submitted for the Degree of Master of Science in Engineering to the University of the Witwatersrand, Johannesburg. It has not been submitted before for any degree or examination to any other University.



……

(Signature of Candidate)

16/10/2019

…….. ……

(Date)

ABSTRACT

High volume fly ash concrete presents a sustainable and environmentally friendly alternative to production of construction materials. However, it has not been fully embraced in high strength concrete applications due to the challenge of reduced early age compressive strength. This study investigated the influence of high volume fly ash replacement, curing temperature, water to cement ratio and $Ca(OH)_2$ activation on compressive strength and durability of concrete. High strength concrete incorporating ordinary Portland cement and ultra-fine fly ash contents of 25%, 35% and 50% was used to prepare samples for compressive strength and durability testing. Ultra-fine fly ash was used in order to attain high strength concrete. A total of 16 concrete mixes were prepared. Eight concrete mixes had a w/c ratio of 0.45 and the other eight mixes had a w/c ratio of 0.35. $Ca(OH)_2$ was added to eight concrete mixes in order to activate the fly ash and improve early age compressive strength and durability. Concrete cubes of 100mm dimensions were cast and cured in water at either 23^0C or 40^0C. The concrete properties measured included compressive strength, chloride conductivity, oxygen permeability and water absorption.

Compressive strength tests were done at 1 day, 3 days, 7 days, 28 days, 90 days and 180 days. The results showed that some fly ash concrete mixes yielded higher compressive strength compared to the ordinary portland cement concrete mixes. Adding $Ca(OH)_2$ and curing at 40ºC significantly improved the rate of compressive strength development of fly ash concrete. Durability index tests were conducted at the age of 28 days in accordance with the South African durability index testing methods. Concrete with water to cement ratio of 0.35 yielded higher compressive strength and durability results compared to concrete with water to cement ratio of 0.45. Curing at 40ºC reduced the late age strength of ordinary Portland cement concrete whereas curing at 40ºC and adding $Ca(OH)_2$ improved the strength of fly ash concrete. 50% fly ash concrete was the most responsive to $Ca(OH)_2$ activation and high temperature curing. The chloride conductivity index for ordinary Portland cement concrete was significantly higher than that of fly ash concrete. Fly ash concrete cured at 40^0C was more resistant to chloride penetration compared to fly ash concrete cured at 23^0C. All the durability index test results signified concrete of high quality. An economic analysis for the binder material indicates that high volume fly ash replacement yielded significant economic benefits.

ACKNOWLEDGEMENTS

I wish to express my tender gratitude and appreciation to the following persons for their contribution towards making this research possible:

Professor Sunday Nwaubani, my research supervisor, for his guidance, valuable time and support.

Concrete lab Staff, for availing the lab resources and assistance in concrete mixing and sample preparation.

The concrete materials research group, for the feedback and constructive criticism during departmental seminar presentations.

My family for their patience, encouragement and support throughout the duration of the study

CONTENTS

1. INTRODUCTION 1
   1.1 Background 1
   1.2 Rationale of the Study 3
   1.3 Research Question 3
   1.4 Aim 3
   1.5 Research Objectives 4
   1.6 Scope of the study 4
   1.7 Structure of the research report 5
2. LITERATURE REVIEW 6
   2.1 Introduction 6
   2.2 High Volume Fly Ash (HVFA) Concrete 7
   2.3 Economic Benefits of High-Volume Fly Ash Concrete 8
   2.4 Fly Ash (FA) 9
      2.4.1 Physical Composition of Fly Ash 10
      2.4.2 Chemical Composition of Fly Ash 10
   2.5 Pozzolanic and Hydration Reactions 11
   2.6 Fly Ash Activation 12
   2.7 Effects of HVFA on Concrete Properties 16
      2.7.1 Effects of HVFA on Concrete Setting Time 17
      2.7.2 Effect of HVFA on Workability 18
      2.7.3 Effect of HVFA on heat of hydration 18
      2.7.4 Effect of HVFA on Strength Development 19
      2.7.5 Effect of HVFA on Durability 20
   2.8 Maturity Concept in Concrete 24
   2.9 Curing of Concrete 26
   2.10 South African Durability Index tests 29
      2.10.1 Chloride Conductivity Index (CCI) Test 29
      2.10.2 Oxygen Permeability Index (OPI) Test 30
      2.10.3 Water Sorptivity Index (WSI) Test 31

2.11 Conclusion 32
3. EXPERIMENTAL METHODS AND PROCEDURES 33
3.1 Introduction 33
3.2 Materials and Sources 34
3.3 Material Properties and Tests 34
3.3.1 Cement Properties 34
3.3.2 Cement Tests 34
3.3.3 Fly Ash Properties 36
3.3.4 Fly Ash Tests 37
3.3.5 Aggregate Properties and Tests 38
3.3.6 Absorption Tests for Fine Aggregates 40
3.3.7 Coarse Aggregate Properties and Tests 41
3.3.8 Water Absorption Test for Coarse Aggregates 42
3.3.9 Admixtures 42
3.3.10 Mixing Water 42
3.4 Concrete Mix Design 43
3.5 Concrete Mix Design Trial Tests 45
3.6 Concrete Mixing 45
3.6.1 Mixing of Concrete With w/c Ratio of 0.45 46
3.6.2 Mixing of Concrete With w/c Ratio of 0.35 52
3.7 Superplasticizer Dosage 56
3.8 Curing of Concrete 58
3.9 Hardened Concrete Testing 59
3.9.1 Compressive Strength Test 59
3.9.2 Durability Tests 61
4. RESULTS AND DISCUSIONS 70
4.1 Compressive Strength Test Results 70
4.1.1 Influence of Fly Ash Content on Compressive Strength 70
4.1.2 Influence of Curing Temperature and $Ca(OH)_2$ Activation 92
4.1.3 Influence Of Water To Cement Ratio on Compressive Strength 106
4.1.4 Comparison of compressive strength Results with Published Data 109

4.1.5 Relationship Between Compressive Strength, Age and Fly Ash Content 113
4.2 X-Ray Diffraction Analysis 115
4.3 Durability Index Test Results 122
4.3.1 Chloride Conductivity Index (CCI) Test Results 123
4.3.2 Water Sorptivity Test 133
4.3.3 Oxygen Permeability Index (OPI) Test 141
4.3.4 Summary of durability Index Tests 144
4.3.5 Regression Analysis of Durability and Compressive Strength Results 145
5. Economic Analysis of High Strength High Volume Fly Ash Concrete 149
5.1 Engineering Benefits 149
5.2 Environmental Benefits 149
5.3 Cost Benefits 150
5.4 Conclusion 156
6. CONCLUSIONS 158
7. RECOMMENDATIONS FOR FUTURE RESEARCH 162
8. REFERENCES 163
9. Annexures 172

Table 3-1: Materials and Sources 34
Table 3-2: Properties of Cement (PPC, 2014) 34
Table 3-3: XRF Analysis Data for Cement 34
Table 3-4: Cement and Fly Ash Fineness Parameters 36
Table 3-5: XRF Analysis Data for Fly Ash 37
Table 3-6: Fine Aggregate Properties 38
Table 3-7: Fine Aggregate Particle Size Proportions 39
Table 3-8: Fine Aggregate Water Absorption Test Results 40
Table 3-9: Coarse Aggregates Proportions 41
Table 3-10: Coarse Aggregate Water Absorption Test Results 42
Table 3-11: Superplasticiser Properties (Sika, 2016) 42
Table 3-12: Typical Mix Proportions for high strength HVFA Concrete (Mehta, 2004) 43

Table 3-13: Concrete Mix Proportions Investigated in the Study 44
Table 3-14: Concrete Mixes Investigated in the Study 46
Table 3-15: Quantities for Concrete Mix 3 and 4: w/c ratio = 0.45 46
Table 3-16: Wet Density for Concrete Mix 3 and 4 47
Table 3-17: Quantities for Concrete Mix 7 and 8: w/c ratio = 0.45 48
Table 3-18: Wet Density for Concrete Mix 7 and 8 48
Table 3-19: Quantities for Concrete Mix 11 and 12: w/c ratio = 0.45 49
Table 3-20: Wet Density for Concrete Mix 11 and 12 49
Table 3-21: Quantities for Concrete Mix 15 and 16: w/c ratio = 0.45 50
Table 3-22: Wet Density for Concrete Mix 15 and 16 50
Table 3-23: Concrete Slump Values for Concrete with w/c ratio of 0.45 51
Table 3-24: Quantities for Concrete Mix 1 and 2: w/c ratio = 0.35 52
Table 3-25: Wet Density for Concrete Mix 1 and 2 53
Table 3-26: Quantities for Concrete Mix 5 and 6: w/c ratio = 0.35 53
Table 3-27: Wet Density for Concrete Mix 5 and 6 54
Table 3-28: Quantities for Concrete Mix 9 and 10: w/c ratio = 0.35 54
Table 3-29: Wet Density for Concrete Mix 9 and 10 54
Table 3-30: Quantities for Concrete Mix 13 and 14: w/c ratio = 0.35 55
Table 3-31: Wet Density for Concrete Mix 13 and 14 55
Table 3-32: Concrete Slump Values for Concrete with w/c ratio of 0.35 56
Table 3-33: Superplasticiser Dosage 56
Table 3-34: Hardened Concrete Cubes Tested for Compressive Strength 60
Table 3-35: Concrete Samples Tested for Chloride Conductivity 64
Table 3-36: Concrete Samples for Oxygen Permeability Test 67
Table 3-37: Concrete Samples for Water Sorptivity Test 69
Table 4-1: Compressive Strength for Concrete Cured at 23^{0}C without $Ca(OH)_2$ Activator (w/c = 0.45) 71
Table 4-2: Relative Strength of Concrete as a Percentage of OPC Concrete Strength (23^{0}C : Without $Ca(OH)_2$: w/c = 0.45) 72
Table 4-3: Compressive Strength for Concrete Cured at 23^{0}C with $Ca(OH)_2$ Activator (w/c = 0.45) 73
Table 4-4: Relative Strength of Concrete as a Percentage of OPC Concrete Strength (23^{0}C : $Ca(OH)_2$ Activator : w/c = 0.45) 75

Table 4-5: Compressive Strength for Concrete Cured at 40°C without $Ca(OH)_2$ Activator (w/c = 0.45) 76
Table 4-6: Relative Strength of Concrete as a Percentage of OPC Concrete Strength (40°C : No Activator : w/c = 0.45) 78
Table 4-7: Compressive Strength for Cubes Cured at 40°C with $Ca(OH)_2$ Activator (w/c = 0.45) 79
Table 4-8: Relative Strength of Concrete as a Percentage of OPC Concrete Strength (40°C : $Ca(OH)_2$ Activator : w/c = 0.45) 80
Table 4-9: Compressive Strength for Concrete Cured at 23°C without $Ca(OH)_2$ Activator (w/c = 0.35) 81
Table 4-10: Relative Strength of Concrete as a Percentage of OPC Concrete Strength (23°C : No Activator : w/c = 0.35) 83
Table 4-11: Compressive Strength for Concrete Cured at 23°C with $Ca(OH)_2$ Activation (w/c = 0.35) 84
Table 4-12: Relative Strength of Concrete as a Percentage of OPC Concrete Strength (23°C : $Ca(OH)_2$ Activator : w/c = 0.35) 85
Table 4-13: Compressive Strength for Concrete Cured at 40°C without $Ca(OH)_2$ Activator (w/c = 0.35) 86
Table 4-14: Relative Strength of Concrete as a Percentage of OPC Concrete Strength (40°C : No Activator : w/c = 0.35) 88
Table 4-15: Compressive Strength for Concrete Cured at 40°C with $Ca(OH)_2$ Activator (w/c = 0.35) 89
Table 4-16: Relative Strength of Concrete as a Percentage of OPC Concrete Strength (40°C : $Ca(OH)_2$ Activator : w/c = 0.35) 91
Table 4-17: Compressive Strength of High Volume Fly Ash Concrete Mixes 110
Table 4-18: Compressive Strength Values Suggested by Fly Ash Supplier (Ash Resources) 112
Table 4-19: Chloride Conductivity Index for Samples with w/c = 0.35 123
Table 4-20: Chloride Conductivity Index for Samples with w/c = 0.45 124
Table 4-21: Suggested Ranges for Durability Classification Index Values (Alexander et al., 1999) 128
Table 4-22: Acceptance Limits for Durability Indexes (Alexander et al., 2001) 128
Table 4-23: Comparison of Chloride Conductivity Index Results with values suggested by Alexander et al, 1999 128
Table 4-24: Porosity Results from CCI Tests (w/c = 0.35) 130

Table 4-25: Porosity Results from CCI Tests (w/c = 0.45)..... 130
Table 4-26: Sorptivity Test Results for Specimens with w/c = 0.45 133
Table 4-27: Sorptivity Test Results for Specimens with w/c = 0.35 134
Table 4-28: Comparison of Water Sorptivity Index Results with values suggested by Alexander et al, (1999)..... 135
Table 4-29: Porosity Results from Water Sorptivity Tests (w/c = 0.45)..... 137
Table 4-30: Porosity Results from Water Sorptivity Tests (w/c = 0.35)..... 138
Table 4-31: Oxygen Permeability Index Results for Specimens with w/c ratio of 0.45..... 141
Table 4-32: Oxygen Permeability Index Results for Specimens with w/c ratio of 0.35..... 142
Table 4-33: Comparison of Oxygen Permeability Index results with values suggested by Alexander et al, (1999)..... 143
Table 5-1: Regression Functions for 28 Day Compressive Strength Graphs..... 151
Table 5-2: Eight 60MPa Concrete Mixes Incorporating Fly Ash Contents Derived from Regression Trendlines 152
Table 5-3: Cost Comparison Between OPC and Fly Ash Binder Material..... 153
Table 5-4: Projected Cost of Binder Material Which Yields 28 Day Compressive Strength of 60MPa 153
Table 5-5: Carbon Tax Cost Per Cubic Metre of Concrete with Projected 28 Day Strength of 60MPa 153
Table 5-6: Possible binder material cost savings..... 154
Table 5-7: Possible Carbon Tax Cost Savings 154
Table 5-8: Increase or decrease in 28 Day Compressive Strength Compared to OPC Concrete Strength: w/c=0.45..... 155
Table 5-9: Increase or Decrease in 28 Day Compressive Strength Compared to OPC Concrete Strength: w/c=0.35..... 155
Table 9-1: Compressive Strength Test Results 172
Table 9-2: Chloride Conductivity Index Test Results..... 184
Table 9-3: Porosity Test Results Determined in Terms of CCI Test..... 187
Table 9-4: Water Sorptivity Index Test Results..... 191
Table 9-5: Porosity Test Results Determined In Terms of Water Sorptivity Test 194
Table 9-6: Oxygen Permeability Index Test Results..... 198

Figure 2.1: Conceptual model for geopolymerization (Duxson et al., 2007) 15
Figure 2.2: Proposed reaction sequence of geopolymerization (Provis et al., 2005) 15
Figure 2.3: Effect of moist curing time on strength gain of concrete (Kosmatka and Wilson, 2011) 27
Figure 3.1: Experimental Work Flow Chart..... 33
Figure 3.2: XRD Pattern for OPC Cement..... 35
Figure 3.3: Cement and Fly Ash Particle Size Distribution Graph 36
Figure 3.4: XRD Pattern for Fly Ash 37
Figure 3.5: Cement and Fly Ash SEM Images 38
Figure 3.6: Fine Aggregates Sieving 39
Figure 3.7: Fine Aggregate Particle Size Distribution 39
Figure 3.8: Coarse Aggregate Particle Size Distribution 41
Figure 3.9: Slump for Concrete Mix 3 with Superplasticiser 47
Figure 3.10: Concrete Slump for Mix 7 and 8 With Superplasticiser 48
Figure 3.11: Slump for Concrete Mix 11 and 12 With Superplasticiser 49
Figure 3.12: Slump for Concrete Mix 15 and 16 with Superplasticiser 51
Figure 3.13: Slump for Concrete Mix 1 With Superplasticiser 53
Figure 3.14: Slump for Concrete Mix 13 and 14 With Superplasticiser 55
Figure 3.15: Superplasticiser Dosage 57
Figure 3.16: Comparison of superplasticiser dosages..... 57
Figure 3.17: Plastic Wrapped Concrete Moulds in Curing Bath 58
Figure 3.18: Concrete Cubes in Curing Water Bath 58
Figure 3.19: Amsler Compressive Strength Testing Machine 59
Figure 3.20: Vacuum Saturation Tank Apparatus 62
Figure 3.21: Chloride Conductivity Cell (Durability Index Testing Procedure Manual, 2018) 62
Figure 3.22: Chloride Conductivity Test Circuit Arrangement (SANS 3001-CO3-3:2015) 63
Figure 3.23: Chloride Conductivity Test Apparatus 63
Figure 3.24: Oxygen Permeability Index Test Specimens..... 65
Figure 3.25: Oxygen Permeability Test Setup (Durability Index Testing Procedure Manual, 2018) 66
Figure 3.26: Oxygen Permeability Index Test Apparatus 66

Figure 3.27: Water Sorptivity Test Setup..... 68
Figure 4.1: Compressive Strength for Concrete Cured at 23°C without $Ca(OH)_2$ Activator (w/c = 0.45) 71
Figure 4.2: Reduction or Increase in Strength as a Percentage of OPC Concrete Strength (23°C : No Activator: w/c = 0.45)..... 73
Figure 4.3: Compressive Strength for Cubes Cured at 23°C with $Ca(OH)_2$ Activation (w/c = 0.45) . 74
Figure 4.4: Reduction or Increase in Strength as a Percentage of OPC Concrete Strength (23°C : With $Ca(OH)_2$: w/c = 0.45) 75
Figure 4.5: Compressive Strength for Concrete Cured at 40°C without $Ca(OH)_2$ Activator (w/c = 0.45) 76
Figure 4.6: Reduction or Increase in Strength as a Percentage of OPC Concrete Strength (40°C:Without $Ca(OH)_2$:w/c = 0.45) 78
Figure 4.7: Compressive Strength for Concrete Cured at 40°C with $Ca(OH)_2$ Activator (w/c = 0.45) 79
Figure 4.8: Reduction or Increase in Strength as a Percentage of OPC Concrete Strength (40°C : With $Ca(OH)_2$: w/c = 0.45) 81
Figure 4.9: Compressive Strength for Concrete Cured at 23°C without $Ca(OH)_2$ Activator (w/c = 0.35) 82
Figure 4.10: Reduction or Increase in Strength as a Percentage of OPC Concrete Strength (23°C : No Activator : w/c = 0.35)..... 83
Figure 4.11: Compressive Strength for Concrete Cured at 23°C with $Ca(OH)_2$ Activation (w/c = 0.35) 84
Figure 4.12: Reduction or Increase in Strength as a Percentage of OPC Concrete Strength (23°C : $Ca(OH)_2$: w/c= 0.35) 86
Figure 4.13: Compressive Strength for Concrete Cured at 40°C without Activator (w/c = 0.35) 87
Figure 4.14: Reduction or Increase in Strength as a Percentage of OPC Concrete Strength (40°C : No Activator : w/c = 0.35)..... 88
Figure 4.15: Compressive Strength for Concrete Cured at 40°C with $Ca(OH)_2$ Activator (w/c = 0.35) 90
Figure 4.16: Reduction or Increase in Strength as a Percentage of OPC Concrete Strength (40°C:$Ca(OH)_2$: w/c = 0.35) 91
Figure 4.17: Compressive Strength Results of OPC Concrete with w/c ratio of 0.45 92
Figure 4.18: Compressive Strength Results of OPC Concrete with w/c ratio of 0.45 93
Figure 4.19: Effect of Curing Temperature on Compressive Strength (Zemajtis, 2014)..... 94

Figure 4.20: Compressive Strength Results for OPC Concrete with w/c ratio of 0.35 96
Figure 4.21: Compressive Strength Results for OPC Concrete with w/c of 0.35..... 96
Figure 4.22: Compressive Strength Results for 25%FA Concrete with w/c ratio of 0.45..... 97
Figure 4.23: Compressive Strength Results for 25%FA Concrete with w/c ratio of 0.45..... 98
Figure 4.24: Compressive Strength Results for 25%FA Concrete with w/c ratio of 0.35..... 99
Figure 4.25: Compressive Strength Results for 25%FA Concrete with w/c ratio of 0.35..... 99
Figure 4.26: Compressive Strength Results for 35%FA Concrete with w/c ratio of 0.45..... 100
Figure 4.27: Compressive Strength Results for 35% FA Concrete with w/c ratio of 0.45 101
Figure 4.28: Compressive Strength Results for 35%FA Concrete with w/c ratio of 0.35..... 102
Figure 4.29: Compressive Strength Results for 35%FA Concrete with w/c ratio of 0.35..... 102
Figure 4.30: Compressive Strength Results for 50%FA Concrete with w/c ratio of 0.45..... 103
Figure 4.31: Compressive Strength Results for 50%FA Concrete with w/c ratio of 0.45..... 104
Figure 4.32: Compressive Strength Results for 50%FA Concrete with w/c ratio of 0.35..... 105
Figure 4.33: Compressive Strength Results for 50%FA Concrete with w/c ratio of 0.35 105
Figure 4.34: Comparison of Compressive Strength of Concrete with Different w/c Ratios..... 107
Figure 4.35: Comparison of Compressive Strength of Concrete with Different w/c Ratios..... 108
Figure 4.36: Effect of curing temperature rise on compressive strength development (Berry and Malhotra, 1987)..... 111
Figure 4.37: Typical Regression Lines for The Relationship Between Compressive Strength and Concrete Age 113
Figure 4.38: Typical Regression Lines for Relationship Between Compressive Strength and FA Content..... 114
Figure 4.39: XRD Patterns for OPC and 50%FA Concrete cured at 40^0C with $Ca(OH)_2$ Activator 118
Figure 4.40: XRD Patterns for OPC and 50%FA Concrete cured at 40^0C without Activator..... 119
Figure 4.41: XRD Patterns for OPC and 50%FA Concrete cured at 23^0C with $Ca(OH)_2$ Activator 120
Figure 4.42: XRD Patterns for OPC and 50%FA Concrete cured at 23^0C without Activator..... 121
Figure 4.43: Relationship between FA content and Chloride Conductivity Index for Samples with w/c = 0.35 124
Figure 4.44: Relationship between FA content and Chloride Conductivity Index for Samples with w/c = 0.45 125

Figure 4.45: Chloride Conductivity Index Results for Specimens with w/c of 0.35 and 0.45 129
Figure 4.46: Porosity Results from CCI Tests (w/c = 0.35)..... 130
Figure 4.47: Porosity Results from CCI Tests (w/c = 0.45) 131
Figure 4.48: Porosity Results for Specimens with w/c of 0.35 and 0.45 based on CCI Test. 132
Figure 4.49: Water Sorptivity Index Results for Specimens with w/c of 0.45..... 134
Figure 4.50: Water Sorptivity Index Results for Specimens with w/c of 0.35..... 135
Figure 4.51: Water Sorptivity Index Results for Specimens with w/c of 0.35 and 0.45 136
Figure 4.52: Porosity Results for Specimens with w/c of 0.45..... 137
Figure 4.53: Porosity Results for Specimens with w/c of 0.35..... 138
Figure 4.54: Porosity Results for Specimens with w/c of 0.35 and 0.45 139
Figure 4.55: Oxygen Permeability Index Results for Specimens with w/c ratio of 0.45..... 142
Figure 4.56: Oxygen Permeability Index Results for Specimens with w/c ratio of 0.35..... 142
Figure 4.57: Typical Regression Trendlines for the Relationship between FA content and Chloride Conductivity Index 145
Figure 4.58: Relationship between Chloride Conductivity Index and Porosity Determined Using CCI Test 146
Figure 4.59: Relationship between Compressive Strength and Porosity Determined Using **Chloride Conductivity Index** Test 147
Figure 4.60: Relationship between Compressive Strength and Porosity Determined Using **Water Sorptivity Index** Test..... 147
Figure 4.61: Relationship between Compressive Strength and Water Sorptivity Index 148
Figure 5.1: Relationship between 28 Day Compressive Strength and Fly Ash Content..... 150
Figure 5.2: Trendlines for the Relationship Between 28 Day Compressive Strength and Fly Ash Content based on Regression Functions Presented in Table 5-1..... 151
Figure 5.3: Increase or Decrease in 28 Day Compressive Strength vs Cost Reduction (w/c=0.45) 156
Figure 5.4: Increase or Decrease in 28 Day Compressive Strength vs Cost Reduction (w/c=0.35) 156
Figure 9.1: Compressive Strength for Concrete Cured at 23^{0}C without $Ca(OH)_2$ Activator (w/c = 0.45) 175
Figure 9.2: Compressive Strength for Concrete Cured at 23^{0}C with $Ca(OH)_2$ Activator (w/c = 0.45) 175
Figure 9.3: Compressive Strength for Concrete Cured at 40^{0}C without $Ca(OH)_2$ Activation (w/c = 0.45) 176
Figure 9.4: Compressive Strength for Concrete at 40^{0}C with $Ca(OH)_2$ Activator (w/c = 0.45) 176

Figure 9.5: Compressive Strength for Concrete Cured at 23°C without $Ca(OH)_2$ Activator (w/c = 0.35) 177
Figure 9.6: Compressive Strength for Concrete Cured at 23°C with $Ca(OH)_2$ Activation (w/c = 0.35) 177
Figure 9.7: Compressive Strength for Concrete Cured at 40°C without $Ca(OH)_2$ Activator (w/c = 0.35) 178
Figure 9.8: Compressive Strength for Concrete Cured at 40°C with $Ca(OH)_2$ Activator (w/c = 0.35) 178
Figure 9.9: Relationship Between Compressive strength and FA Content (23°C: w/c 0.45: No Activator)..... 179
Figure 9.10: Relationship between Compressive strength and FA Content (23°C: w/c 0.45: $Ca(OH)_2$ Activator) 179
Figure 9.11: Relationship Between Compressive strength and FA Content (40°C: w/c 0.45: No Activator)..... 180
Figure 9.12: Relationship Between Compressive strength and FA Content (40°C: w/c 0.45: $Ca(OH)_2$ Activator) 180
Figure 9.13: Relationship Between Compressive strength and FA Content (23°C: w/c 0.35: No Activator)..... 181
Figure 9.14: Relationship Between Compressive strength and FA Content (23°C: w/c 0.35: $Ca(OH)_2$ Activator) 181
Figure 9.15: Relationship Between Compressive strength and FA Content (40°C: w/c 0.35: No Activator)..... 182
Figure 9.16: Relationship Between Compressive strength and FA Content (40°C: w/c 0.35: $Ca(OH)_2$ Activator) 182
Figure 9.17: Particle Size Distribution for Ultra Fine Fly Ash, Silica Fume and Standard Fly Ash (Source: Seedat, 2003)..... 203

Acronyms

ACAA : American Coal Ash Association
$Ca(OH)_2$: Calcium Hydroxide
CCI : Chloride Conductivity Index
C&CI : Cement and Concrete Institute
CH : Calcium Hydroxide
CSH : Calcium Silicate Hydrate
CO_2 : Carbon Dioxide
FA : Fly Ash
GGBS : Ground Granulated Blast Furnace Slag
HVFA : High Volume Fly Ash
LOI : Loss on Ignition
OPC : Ordinary Portland Cement
OPI : Oxygen Permeability Index
PCA : Portland Cement Association
PFA : Pulverised Fuel Ash
PSD : Particle Size Distribution
SANS : South Africa National Standards
SEM : Scanning Electron Microscopy
SCM : Supplementary Cementitious Material
UN : United Nations
UNFCCC : United Nations Framework Convention On Climate Change
VAT : Value Added Tax
W/C : Water to Cementitious Material
WSI : Water Sorptivity Index
XRD : X-Ray Diffraction
XRF : X-Ray Fluorescence

Keywords

High volume fly ash (HVFA), high strength concrete, compressive strength, durability, curing temperature, water to cement ratio, Calcium Hydroxide

1. INTRODUCTION

1.1 Background

Huge quantities of industrial by-products are considered waste materials which are disposed into the environment. In some instances, the disposal of industrial waste materials is contributing to environmental pollution. Re-use of such industrial waste as construction material greatly contributes towards sustainable development and environmental conservation. Concrete is used nearly in all small and large-scale infrastructure projects. The cementitious material that is often used in concrete is ordinary Portland cement (OPC) which is primarily made up of cement clinker which is produced by burning raw materials at high temperature. Hasanbeigi, et al., (2012) states that the cement manufacturing process consumes a lot of energy and it is one of the biggest producers of carbon dioxide accounting for approximately five percent of carbon dioxide (CO_2) emissions. They estimate that for each tonne of cement produced there is approximately one tonne of carbon dioxide produced. Having such a high carbon footprint, cement production is not environmentally friendly and cement cannot be classified as a green building material. The carbon dioxide released during cement manufacturing adds on to other greenhouse gas emissions which contribute to climate change. The devastating effects of climate change and high cost of construction materials have made it imperative to explore alternative, sustainable, renewable and environmentally friendly approaches to production of construction materials. One of such alternative approaches is the use of high-volume fly ash (HVFA) as a cementitious material in concrete. The American Coal Ash Association estimates that using fly ash in concrete can eliminate thirteen million tonnes of carbon emissions annually (American Coal Ash Association, 2015). Bold (2013) estimates that for every tonne of fly ash used in concrete there is a reduction of approximately one tonne of CO_2 released during cement manufacturing. Reducing the quantity of OPC used in concrete by using high volume fly ash as a supplementary cementitious material will go a long way in providing sustainable, cost effective and environmentally friendly solutions to infrastructure development. However, it is imperative to fully understand the effects of using high-volume fly ash on the properties of concrete.

High volume fly ash utilisation can help reduce the cost of disposing fly ash in compliance with environmental regulations (Barough et al.). Replacing a substantial part of OPC in concrete with cheap and readily available fly ash presents great economic and engineering benefits. Fly ash is a more abundant resource due to increased reliance on coal as a fuel for power generation. Eskom (2016) estimates that power stations that use coal as a source of fuel can produce up-to seventeen thousand tonnes of ash in a day. The quantity of fly ash produced by Eskom activities in a year is estimated to be approximately twenty-five million tonnes of which nearly 1,2 million tonnes is used by cement manufacturers as a cement extender (Eskom, 2016). The bulk of the ash produced from Eskom power generation activities is considered waste material and it is dumped in ash disposal sites which presents environmental challenges. The Medupi Power Station which is currently under construction is expected to have a capacity of 4800 Megawatts. This implies that when it is fully operational, the volume of fly ash produced by Eskom activities will be significantly increased.

High volume fly ash concrete promotes the effective utilisation and beneficiation of fly ash. Utilisation of significant quantities of fly ash as a construction material will greatly contribute to sustainability and reduce the amount of fly ash that is disposed with consequent environment pollution. This study explored the use of high-volume fly ash as a supplementary cementitious material in concrete and investigated its effects on the performance of concrete. The study assessed the influence of high-volume fly ash on compressive strength development and durability of concrete. It investigated the effects of varying curing temperature and water to cement ratio on the properties of OPC and fly ash concrete. Thomas (2007) states that high volume fly ash presents challenges such as longer setting time and reduced early-age strengths which slow down construction activities. However, he opined that there is a possibility of using high-volume fly ash in a beneficial way without affecting the engineering properties of concrete.

1.2 Rationale of the Study

Fly ash has been widely utilised as a supplementary cementitious material in concrete at levels of up-to 30% by mass of cementitious material. Thomas (2007) highlighted that replacing cement with high volume fly ash results in low early age strength. As such, the use of high-volume fly ash has been limited to mass concrete applications such as dam construction where it is primarily used for its ability to regulate the heat of hydration rather than for its contribution to strength development. The study seeks to encourage the use of higher proportions of fly ash in the production of high strength concrete. The study explored the suitability and performance of high-volume ultra-fine fly ash concrete in high strength concrete applications by investigating compressive strength development patterns and evaluating the durability properties using the South African durability index testing methods. Ultra-fine fly ash was used as a cement replacement material in order to achieve high strength concrete. The study evaluated concrete properties such as compressive strength, oxygen permeability, water sorptivity and chloride conductivity. The study also investigated the influence of w/c ratio, curing temperature and chemical activation on the properties of HVFA concrete. The study will contribute to the current body of knowledge on high strength high volume fly ash concrete.

1.3 Research Question

Does high volume fly ash concrete have sufficient compressive strength and durability properties that make it suitable for use in high strength concrete applications?

1.4 Aim

The study is aimed at determining the influence of high-volume fly ash, curing temperature, water content and chemical activation on compressive strength development and durability of concrete. The study seeks to encourage the use of high-volume fly ash in the production of high strength concrete.

1.5 Research Objectives

The objectives of the research are to;

i. Carryout laboratory investigations to determine the influence of high-volume fly ash replacement on strength development and durability of high strength concrete.
ii. Establish the maximum replacement level to achieve high strength concrete with 28-day compressive strength of 60MPa.
iii. Evaluate the effects of curing temperature and calcium hydroxide activation on compressive strength and durability of HVFA concrete.
iv. Investigate the influence of water to cement ratio on compressive strength and durability of HVFA concrete.
v. Use the South African durability index testing methods to evaluate the durability of HVFA concrete.
vi. Evaluate the economic benefits of using high volume fly ash and encourage higher substitutions of fly ash in the production of high strength concrete.

1.6 Scope of the study

The study investigated the influence of HVFA on strength development and durability of concrete. The study also focused on the influence of w/c ratio, curing temperature and calcium hydroxide activation on strength development and durability of HVFA concrete. Tests on properties of fresh concrete were limited to slump tests. Experimental work on strength development and durability of hardened concrete was limited to compressive strength, water sorptivity, oxygen permeability and chloride conductivity tests. Tests on binder materials were limited to X-Ray diffraction, X-Ray fluorescence, particle size distribution and scanning electron microscopy. An economic analysis was carried out for binder material in order to encourage the use of high strength high volume fly ash concrete. The economic analysis focused on the economic benefits of incorporating high volume fly ash in high strength concrete. Non-standard fly ash classified as ultra-fine fly ash was used in the study in order to attain high strength concrete.

1.7 Structure of the research report

This research report consists of six chapters as follows:

Chapter one gives an introduction of the study. The chapter covers the benefits of using high volume fly ash as a supplimentary cementitiuos material in concrete production and it discusses the study rationale, key research question and aim. The chapter also covers the scope and objectives of the study.

Chapter two gives a comprehensive review of the literature on the effects of high volume fly ash replacement, curing temperature and w/c ratio on properties of concrete. The chapter discusses the environmental and economic benefits of utilising fly ash in concrete. It also gives an overview of fly ash and its composition, activation techniques, as well as the chemistry of pozzolanic and hydration reactions.

Chapter three details the experimental methods and procedures used in the project. It starts by giving an overview of the materials used in the study and goes on to detail the types of materials used, their sources and properties. Tests conducted on the characterisation of materials used and results obtained are all outlined in this chapter. The chapter further gives an outline of the concrete mix design, specimen preparation and the experimental procedures carried out in the study.

Chapter four gives a presentation, discussion and analysis of the results of compressive strength and durability tests. The relationships between compressive strength, FA content, w/c ratio, curing temperature and $Ca(OH)_2$ content are analysed and discussed in detail. The chapter also presents the durability index test results. It outlines the relationship between fly ash content and durability index results. The discussion further relates the results to published research work.

Chapter five presents an economic analysis of high volume fly ash concrete. The chapter discuses the environmental and cost benefits of high volume fly ash utilisation. The chapter gives an analysis on the cost savings resulting from cement replacement with fly ash.

Chapter six presents the conclusions derived from the analysis of test results

Chapter seven gives recommendations for future research on high volume fly ash concrete.

2. LITERATURE REVIEW

2.1 Introduction

Climate change and sustainability have become major discussion topics due to the devastating weather events being felt all over the world. The United Nations warns that emission of greenhouse gases has increased significantly and climate change effects such as global warming and extreme weather are now affecting every part of the world resulting in huge economic losses (United Nations, 2015a). Climate change is directly linked to the emission of greenhouse gases such as carbon dioxide. Initiatives and international policies have been developed to reduce emissions of greenhouse gases. Key among such initiatives was the Kyoto Protocol that set reduction targets of greenhouse gases which include carbon dioxide (UNFCCC, 2008). The current UNFCCC Paris Agreement seeks to mitigate climate change by taking actions that will result in low carbon emissions in the future (United Nations, 2015b). In line with the Paris Agreement, the South African government has introduced the Carbon Tax Bill which will enable South Africa to play its role in enforcing reduction of greenhouse gas emissions (South African Government, 2018). The Carbon Tax Bill promotes emissions reduction through the polluter pays principle and it is likely to impact on the cement manufacturing industry which is one of the major contributors of carbon emissions. It is now imperative for the local cement manufacturing industry to aggressively pursue alternative and sustainable ways of reducing carbon emissions in order to comply with the initiatives aimed at reducing greenhouse gases. This will enable the cement industry to avoid the cost implications arising from carbon tax.

The environmental impact of the cement manufacturing process as a result of high carbon emissions and energy consumption can be alleviated by reducing the demand of Portland cement. This can be achieved through a paradigm shift in the way the concrete industry views large scale incorporation of supplementary cementitious materials in concrete. Portland cement is derived from finite resources whose continuous extraction leads to environmental degradation. This raises the question of sustainability which can be answered through large scale replacement of cement with industrial waste materials such as fly ash. The abundance and cost of fly ash makes it an ideal material for large scale replacement of Portland cement in concrete. The

benefits of utilising fly ash in the production of concrete outweigh the negative effects. Fly ash reduces the water demand for concrete resulting in concrete with improved workability, compressive strength and durability. High volume fly ash is key in resolving the challenge of heat of hydration in mass concrete structures. Incorporating high volume fly ash in concrete results in significant cost reduction of binder material. From an environmental perspective, increasing fly ash utilisation results in reduced carbon emissions and conservation of material resources used in cement production. High volume fly ash is a tailor-made solution to the environmental challenges presented by the cement manufacture process. It also helps alleviate the ecological challenges arising from the disposal of fly ash into the environment.

High strength concrete incorporating high volume fly ash presents an effective approach to efficient fly ash utilisation. Numerous definitions of high strength concrete have been proposed (ACI, 2010; Owens, 2009; Rashid and Mansur, 2009; Kawai, 2002). Kovacevic and Dzidic (2018) state that it is hard to define high strength concrete with a unique number that distinguishes it from conventional concrete. According to Rashid and Mansur (2009) the bottom range of high strength concrete is dependent on various factors such as time, geographical location, raw materials and expertise. The American Concrete Institute (2010) defines high strength concrete as concrete with compressive strength of 55 MPa or higher. Owens (2009) defines high strength concrete as concrete with 28-day compressive strength ranging from 60MPa and above. Kawai (2002) also defines high strength concrete as concrete with compressive strength of 60MPa and above.

2.2 High Volume Fly Ash (HVFA) Concrete

High-volume fly ash concrete is generally defined as concrete with at least 50% of the Portland cement replaced with fly ash (Arezoumandi et al., 2013). The development of HVFA concrete dates back to 1985 when the Canadian Centre for Mineral and Energy Technology (CANMET) initiated investigations into the use of HVFA concrete in structural applications (Malhotra, 2004). Malhotra (2004) argues that high volume fly ash concrete exhibits all the qualities of high-performance concrete such as excellent mechanical and durability properties. Cross, Stephens and Vollmar (2005)

pushed the frontiers of high-volume fly ash concrete through a study on 100% fly ash concrete. They concluded that concrete with strength and workability properties similar to OPC concrete can be produced using 100% fly ash.

Despite the fact that HVFA can produce competent concrete, its use in the construction industry has remained low. Fly ash has been widely used as a cement extender in quantities ranging from 6% to 30% by mass, however higher volumes of fly ash in excess of 35% by mass are mainly used in mass concrete structures to control the heat of hydration (Thomas, 2007; Zulu and Allopi, 2015). The South African national standard SANS 50197-1 (2013) limits fly ash content in blended cement manufacture to 35%. Obla, Lobo and Kim (2012) identified the primary causes preventing increased use of HVFA in concrete as low early age strength and restrictive specifications on the usage of higher volumes of fly ash. A study conducted by Burke (2012) on HVFA concrete with 50% fly ash demonstrated that HVFA concrete can comply with project specifications while providing cost savings. The study disapproved the belief that early strength development cannot be accomplished with 50% FA content. Burke (2012) achieved 28-day compressive strength of 45MPa with 50%FA content. High volume fly ash concrete can go beyond the normal application in mass concrete and be used in high strength concrete applications without compromising strength development and durability properties. The major challenge of low early age compressive strength can be overcome by using a combination of low w/c ratio and fly ash activation techniques (Bao-min and Li-jiu (2004); Duxson et al., 2007).

2.3 Economic Benefits of High-Volume Fly Ash Concrete

The use of high-volume fly ash should be encouraged in the production of high strength concrete in order to reduce the cost of concrete. The major challenge in producing high strength concrete is the high cost of material used and the quantity of OPC used in the production of high strength concrete is usually high resulting in increased binder cost. Silica fume is a costly supplementary cementitious material that is often used in the production of high strength concrete. Fine fly ash is a generally cheaper alternative material which can be used to produce high strength concrete. Some researchers have proven that incorporating higher volume fly ash in concrete does not adversely impact on the long-term compressive strength and durability

properties of concrete (Poon et al, 2000; Elsageer et al., 2009; Solikin et al., 2013). Hasheela and Ekolu (2010) agree that materials like fly ash can lower the cost of concrete, however they are of the view that there isn't much research that has been done to establish the amount of cost-reduction as a result of using materials like fly ash. Hasheela and Ekolu (2010) investigated the effect of fly ash and slag on the cost of concrete and attained binder material cost reduction of up-to 13% in 30%FA concrete. The cost saving they achieved in 50% fly ash concrete was approximately 24%. Bouzoubaa and Fournier (2002) investigated optimization of fly ash content in concrete. Their cost analysis of fly ash concrete yielded a cost saving of approximately 20% in concrete with fine fly ash content of 50%. In concrete with coarse fly ash content of up to 40%, the cost saving was approximately 10%. Camoes et al. (2003) evaluated fly ash binder material cost using the price of equivalent cement content. They established that binder material with 40% fly ash content yielded a cost reduction of 32% whilst binder material with 60% fly ash content yielded a cost reduction of 48%. The economic benefits of high-volume fly ash concrete are not only limited to the cost aspect. Apart from being economic, high volume fly ash concrete has proven to be effective in overcoming durability challenges encountered in Portland cement concrete. Improved durability properties imply reduced rate of concrete deterioration and this translates to reduced cost of concrete repairs and maintenance.

2.4 Fly Ash (FA)

Fly ash is a powder material collected from the exhaust gases produced during burning of coal in electrical power generation plants (Kosmatka and Wilson, 2011; Kruger, 2003). When coal is burnt at high temperature, it produces CO_2 and fly ash which is predominantly composed of silica and alumina (Kosmatka and Wilson, 2011). Millions of tonnes of fly ash are generated annually all over the world (Manz, 1997; Joshi, 2010). Addition of fly ash in concrete has beneficial effects such as reduced heat of hydration, increased resistance to sulphate attack, reduced porosity, and reduced permeability (Thomas, 2007). The physical, mineralogical and chemical properties of fly ash have significant influence on the properties of concrete. Ultra-fine fly ash with high calcium content has high reactivity which can enhance the properties of concrete (Obla et. al., 2003).

2.4.1 Physical Composition of Fly Ash

Fly ash consists of very tiny spherical glass particles which typically range from less than 1 μm to more than 100 μm with average particle size of less than 20 μm (Kosmatka and Wilson, 2011; Abualrous et. al., 2016). The typical specific surface area of fly ash ranges from 300 m^2/kg to 500 m^2/kg and the relative density of fly ash usually ranges between 1.9 and 2.8 (Kosmatka and Wilson, 2011). The South African National Standard (SANS 50450-1, 2011) groups fly ash into categories in terms of fineness as measured by retention on a 45-micron sieve. The standard categorises FA into two categories namely Category N and Category S. Category N is coarser fly ash which allows for a maximum of 40% to be retained on the 45 μm sieve. Category S is finer fly ash which allows for a maximum of 12% to be retained on a 45 μm sieve (SANS 50450-1, 2011).

2.4.2 Chemical Composition of Fly Ash

Fly ash consists of crystalline and amorphous phases. The amorphous phases of fly ash consists of silica, alumina, calcium oxide, iron oxide and magnesia and these contribute to the reactivity potential of fly ash (Kruse et al., (2013). The crystalline phase consists of anhydrite, mullite, quartz, melite, merwinite, periclase, C_3A, magnetite, hematite and CaO (Kruse et al., 2013). The oxide composition of fly ash determines the reactivity potential. Thomas et al. (1999) states that the calcium content in FA indicates the reactivity of FA and how it will influence the properties of concrete. Heyns and Hassan (2014) contend that the calcium oxide/silicon dioxide ratio is a good indicator of the reactivity potential of fly ash. The unburnt carbon in fly ash increases the water requirement and this impacts on the properties of fly ash concrete (Kruse et al., 2013). A high carbon content in FA will significantly increase the water required to achieved desired workability (Skvarla et. al., 2011). Loss on ignition (LOI) is used to determine the content of carbon in fly ash (American Coal Ash Association, 2003). The South African National Standard (SANS 50450-1, 2011) categorises fly ash on the basis of loss on ignition (LOI). According to SANS 50450-1: 2011, category A fly ash has a LOI of less than 5%, Category B fly ash has LOI of between 2% upto 7% and Category C fly ash has LOI of between 4% and 9%.

ASTM C618 (2005) and SANS 50450-1 (2011) also classify fly ash on the basis of chemical composition of the oxides. Both standards use the combined contents of Alumina, Silica and Ferric Oxide to classify the fly ash as either Class C or Class F. If the sum of SiO_2+AlO+FeO is greater than 70%, the fly ash is classified as Class F and if the sum is between 50%-70%, the fly ash is classified as a Class C (ASTM C618: 2005); SANS 50450-1: 2011). The South African fly ash is categorised as Class F owing to its high content of silica and alumina. Kruse et al., (2013) state that the chemical composition of fly ash is dependent on nature of the parent coal burnt. They further state that anthracite coal produces Class F fly ash whereas lignite coal produces class C fly ash.

2.5 Pozzolanic and Hydration Reactions

FA is a pozzolanic material which does not react with water like Portland cement. It reacts with calcium hydroxide in water to form cementing compounds similar to those formed during Portland cement hydration. The Silica and Alumina in fly ash reacts with $Ca(OH)_2$ to form cementitious substances. ASTM defines a pozzolan as a material that has no cementing potential, however it can react with $Ca(OH)_2$ to form cementitious compounds. The cementitious compound produced by the pozzolanic reaction between fly ash and calcium hydroxide is the Calcium Silicate Hydrate often referred to as CSH gel (Owens, 2009). In OPC and fly ash concrete mixes, the OPC cement will act as an activating agent by reacting with water to form hydration products such as $C_3S_2H_3$ and calcium hydroxide. The calcium hydroxide formed by the hydration process reacts with fly ash to form the cementing calcium silicate hydrates gel. The pozzolanic reaction between fly ash and calcium hydroxide is beneficial to the concrete by increasing the amount of calcium silicate hydrate which enhances the long-term strength and durability of concrete (Thomas, 2007).

Cement consists of four main compounds which play a major role in the hydration process. These compounds are tri-calcium silicate (C_3S), di-calcium silicate (C_2S), tri-calcium aluminate (C_3A) and tetra calcium aluminoferrite (C_4AF) (Owens, 2009). Tri-calcium silicate reacts rapidly and contributes to early strength whereas di-calcium silicate reacts slowly and contributes to strength at later ages. The hydration reaction

between these cement compounds and water is an exothermic reaction which produces cementing compounds. The hydration of cement is best described by the reaction equations 2-1 up to equation 2-4 (Owens, 2009).

$$2C_3S + 6H \rightarrow C_3S_2H_3 + 3CH \qquad \text{Equation 2-1}$$

$$2C_2S + 4H \rightarrow C_3S_2H_3 + CH \qquad \text{Equation 2-2}$$

$$C_3A + CH + 12H \rightarrow C_4AH_{13} \qquad \text{Equation 2-3}$$

$$C_4AF + 4CH + 22H \rightarrow C_4AH_{13} + C_4FH_{13} \qquad \text{Equation 2-4}$$

Where:
C is Calcium Oxide (CaO)
S is Silicon Dioxide (SiO_2)
A is Alumina (Al_2O_3)
F is Ferric Oxide (Fe_2O_3)
H is Water (H_2O)
CH is Calcium Hydroxide, $Ca(OH)_2$ (Owens, 2009)

The reaction of C_3S and C_2S with water results in the formation of calcium silicate hydrates (CSH) and $Ca(OH)_2$. The calcium silicate hydrates are the cementing compounds responsible for the strength of concrete. The $Ca(OH)_2$ produced during the hydration process reacts with Silica and Alumina in the pozzolanic reaction producing CSH gel and hydrated calcium. Equation 2-5 illustrates a simplified pozzolanic reaction between SiO_2 and $Ca(OH)_2$ (Owens, 2009).

$$2S + 3CH = C_3S_2H_3 \qquad \text{Equation 2-5}$$

The equation indicates that the pozzolanic activity of fly ash consumes the $Ca(OH)_2$ resulting in the formation of hydrated compounds such as calcium silicate hydrates.

2.6 Fly Ash Activation

Research work on fly ash concrete has proven that fly ash can be activated in order to accelerate its pozzolanic activity (Bentz, 2010). In geopolymer concrete, fly ash has been used as the sole cementitious material producing good strength and durability results. Work carried out by Shekhovtsova (2015) on alkali-activated binders reported that alkali activated fly ash concrete with good properties comparable to normal concrete can be produced by using 100% FA activated using sodium hydroxide. Bentz (2010) conducted a study on quantifying retardation in high-volume fly ash mixtures.

He examined the performance of retardation mitigation strategies using $Ca(OH)_2$, rapid-set cement and other activators. He reported that out of all the activators used, only $Ca(OH)_2$ activation and addition of rapid-set cement yielded notable reduction in retardation of HVFA mixes of up to 5 hours. He concluded that $Ca(OH)_2$ and rapid-set cement provide feasible solutions to mitigating retardation in HVFA concrete. He argues that $Ca(OH)_2$ and rapid set cement can restore the setting times of HVFA concrete to match those of OPC cement.

Fly ash activation can be achieved through numerous techniques such as the use of chemical substances and mechanical methods in accelerating fly ash reactions. The chemical activators that are commonly used are alkali such as sodium hydroxide and calcium hydroxide (Owens et all., 2010). In fly ash pastes, the pozzolanic reactions requires an alkaline environment in order to continue. The cement hydration reaction produces $Ca(OH)_2$ which is consumed by the fly ash pozzolanic reaction. However, in high volume fly ash pastes, the $Ca(OH)_2$ precipitated by the hydration reaction may not be sufficient to react with fly ash. Myadraboina et al. (2016) calculated the lime requirement for high volume fly ash pastes and observed that beyond 50% fly ash content, the lime produced by hydration reaction was not sufficient for the continued pozzolanic reactions. Dunstan (2011) highlights that not all the $Ca(OH)_2$ produced by the hydration reaction is available to react with pozzolanic materials. He estimates that 25% of the hydration reaction products is free lime and part of it will react to form ettringite. The $Ca(OH)_2$ availability is further reduced in high volume fly ash mixtures where significant quantities of cement are replaced with fly ash. Therefore, any addition of alkali such as $Ca(OH)_2$ to a cement-fly ash paste creates an elevated alkaline pH environment which is conducive for the breakdown of fly ash glassy phases. Owens et al. (2010) suggest that fly ash activation entails the breaking down of fly ash glassy phases. Chemical activators such as $Ca(OH)_2$ break down the silica and alumina, thus accelerating the hydrolysis of Si^{4+} and Al^{3+} resulting in the formation of hydrates as depicted by Equation 2-6 and Equation 2-7 (Bao-min and Li-jiu, 2004).

$$3[Ca(OH)_2] + 2[SiO_2] = [3(CaO).2(SiO_2).3(H_2O)] \quad \text{Equation 2-6}$$

$$3[Ca(OH)_2] + Al_2O_3 + 3[H_2O] = 3(CaO).Al_2O_3.6(H_2O) \quad \text{Equation 2-7 } \textit{(Dunstan, 2011)}$$

Fly ash activation using alkali entails the breaking down of fly ash glassy phases such as alumina and silica in an elevated alkaline pH environment. Fraay et. al. (1989) argue that the cementing compounds in pozzolanic reactions are produced when the glass phase in FA is broken down. They investigated the solubility of the fly ash particles and observed that the glass in fly ash was broken down when the alkalinity was at a pH level above 13. Mehta (cited in Arjunan et al, 2001) states that, the hydroxyl ion promotes the breakdown of alumina and silica. This view is shared by, Fernandez-Jimenez and Palomo (2005) who suggest that the high concentration of the hydroxyl ion is responsible of the breakdown of the bonds in fly ash glass phase. They identify the hydroxyl ion as the catalyst during the pozzolanic reaction. Glukhovsky (cited in Palomo and Fernández-Jiménez, 2011) proposed a three-stage model for the alkali activation of materials consisting of silica and alumina. The proposed model consists of mechanisms which entail the breakdown of fly ash particles. The first mechanism entails the destruction of SiO_2 and Al_2O_3 followed by the formation of coagulated structures which transform to condensed structures. Pacheco-Torgal et al., (2007) states that there is an agreement amongst researchers that the fly ash reaction mechanism basically comprises of the breakdown of SiO_2 followed by the stages of transportation and polycondensation. Fernández and Palomo (2005) investigated the composition and microstructure of alkali activated fly ash paste and proposed that fly ash alkali activation results in the breakdown of fly ash. Duxson et al. (2007) presents a simplified model for fly ash geopolymerization shown in Figure 2.1. The model outlines the transformation of a material like FA. Provis et al., (2005) also proposed a reaction sequence of geopolymerization shown in Figure 2.2.

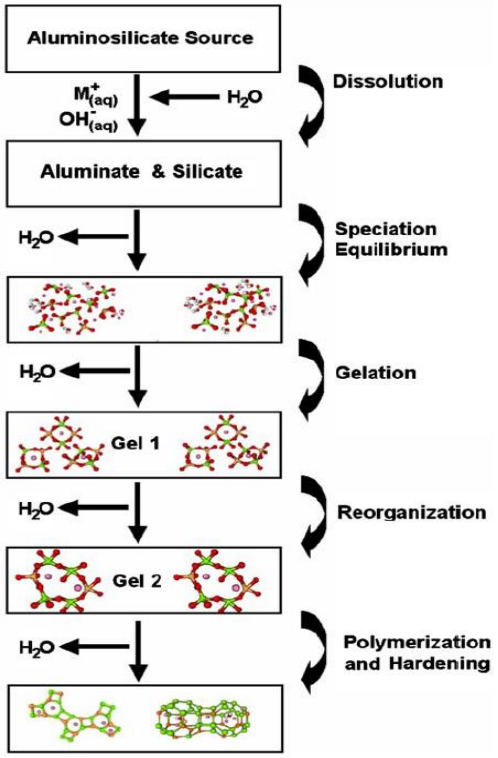

Figure 2.1: Conceptual model for geopolymerization (Duxson et al., 2007)

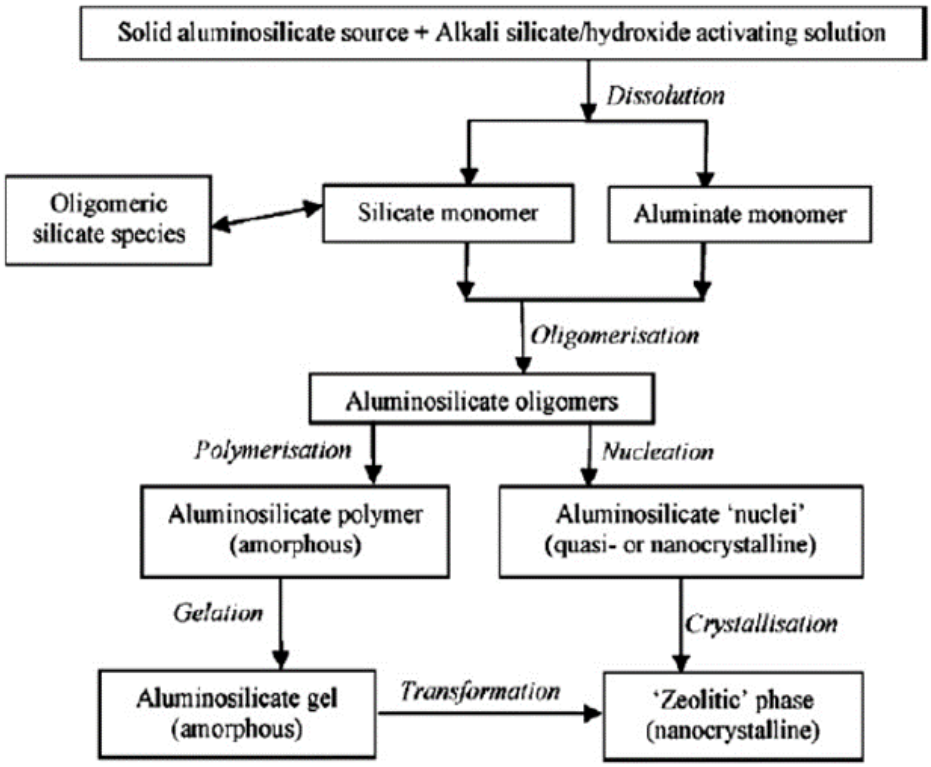

Figure 2.2: Proposed reaction sequence of geopolymerization (Provis et al., 2005)

The threshold values for alkaline activators are dependent on the composition of the binder material (Jiménez et al., 2009). Alonso and Palomo (2001) investigated alkaline activation of calcium hydroxide-metakaolin solid mixtures and established that there is a threshold hydroxyl [OH^-] concentration above which an alkaline polymer was formed and below which calcium silicate hydrate gel was the major reaction product. They concluded that a high hydroxyl concentration impedes calcium hydroxide dissolution. Jiménez et al. (2009) dispel the view that the higher the activator concentration the higher the strength. They argue that there are threshold values above which the strength can decrease and these threshold values are dependent on the composition of binder material. They state that high alkali concentration may result in adverse effects such as increased efflorescence and brittleness. Shi et al. (2006) state that the threshold values for materials rich in SiO_2 and Ca_2O range between 3% and 6 % of the Na_2O by mass with respect to the cementitious material.

The mechanical methods that improve the reactivity potential of fly ash entail the grinding of fly ash in order to improve fineness. Ultra-fine fly ash is more reactive than coarse fly ash owing to its greater surface area. According to Patnaikuni et al (2013), reducing the particle size of fly ash and addition of lime water can assist in developing HVFA concrete mixes which yield compressive strengths similar to OPC concrete.

Bao-min and Li-jiu (2004) allude to physico-chemical techniques that can be used to activate fly ash. These techniques comprise of using heat to activate fly ash reactions. They state that heating can alter the structure of fly ash, however the high heating energy cost hinders the use of this method. Hydrothermal processing introduces ions which activate fly ash glass phases (Bao-min and Li-jiu, 2004). Heat activation creates optimum conditions for fly ash pozzolanic reactions. Fraay et. al. (1989) suggest that the rate of pozzolanic reaction depends on temperature due to the fact that FA solubility and pore water alkalinity are also temperature dependent.

2.7 Effects of HVFA on Concrete Properties

High cement replacement levels may decrease the early age strength of concrete and increase setting time. However, positive results have been reported with use of HVFA as a cementitious material in concrete. Thomas (2007) states that the extent to which

HVFA affects concrete properties does not depend on the fly ash content only. He suggests that parameters such as water content, concrete mix design, curing conditions, admixtures and construction methodologies also affect the performance of HVFA. The water content and curing conditions significantly influence the properties of concrete more than the other parameters.

2.7.1 Effects of HVFA on Concrete Setting Time

The common challenge encountered with HVFA is the increased setting time which leads to construction delays. Bentz (2010) observed excessive retardation of HVFA mixes that he investigated using isothermal calorimetry. The hydration peaks for HVFA mixes increased by eight hours whereas the OPC hydration peaked at 2 hours after mixing. Work carried out by Grieve (1991) on the setting time of FA mixes concluded that replacement of 30% OPC with FA extended the setting times by 2,5 hours. He further established that the setting time of concrete decreases with decreasing w/c ratio. He observed this effect more at low replacement levels of OPC with FA. Grieve and Kruger (1990) investigated the causes of delayed setting time and concluded that boron contributes significantly to retardation in fly ash concrete. A study by Bouzoubaa et al. (2007) established that the setting time duration of HVFA was longer by between 3 and 5 hours compared to the setting time of control OPC concrete.

The challenge of increased setting time can be addressed with the use of accelerators which can reduce the setting time of high-volume fly ash concrete. Sodium hydroxide, $Ca(OH)_2$, high early strength OPC and other activation techniques can be used to restore setting time. Bentz and Ferraris (2010) used rheology and setting time measurements to investigate the setting of high-volume fly ash mixtures. They reported that 5% $Ca(OH)_2$ addition or high early strength OPC significantly reduced the setting time of HVFA mixtures that had retardation. On the contrary, the longer setting times of HVFA concrete can be used as an advantage in ready mix concrete as it allows for longer haulage times and reduced use of retarders.

2.7.2 Effect of HVFA on Workability

High volume fly ash has significant influence on the rheological properties of concrete. It improves workability of concrete and reduces the water requirement. It also promotes cohesion of concrete constituents leading to concrete with less segregation and it helps prevent bleeding in concrete. High volume fly ash content reduces the amount of superplasticiser required to improve workability of a concrete mix. The positive effects can be attributed to the spherical particle shape of fly ash which aids lubrication of concrete mixtures. The effect of reduced water demand cannot be achieved in fly ashes with high LOI due to the fact that carbon has a high-water demand. Grieve (1991) studied the influence of fly ash on workability of concrete and reported that the relationship between increase in FA content and reduction in water demand is linear. On the contrary, Mukheibir (1990) noted that for high strength HVFA, the water demand increased owing to the large quantity of binder material in high strength mixes.

2.7.3 Effect of HVFA on heat of hydration

Replacing cement with high volume fly ash has a significant influence on the hydration reaction. The heat of hydration is significantly reduced in HVFA concrete due to the reduced amount of cement available for the exothermic hydration reaction. The challenges presented by the heat of hydration are often experienced in mass concrete structures where significant temperature rises are encountered owing to the heat liberated by the exothermic hydration reaction between OPC and water. High volume fly ash has been extensively used in mass concrete structures in order to regulate the heat of hydration and also to reduce the effect of thermal stresses generated by the heat of hydration. In high volume fly ash mixes, the heat of cement hydration creates a conducive environment for the acceleration of pozzolanic reactions between fly ash and calcium hydroxide. Balakrishnan et al. (2013) investigated the effect of HVFA concrete in reducing the heat of hydration of concrete and confirmed that using HVFA resulted in a reduction of heat liberated by the hydration process. Their results demonstrated that high volume fly ash has good potential in controlling the heat of hydration of concrete. Ballim and Graham (2009) investigated the heat rate profiles of FA and GGBS and established that the hydration peaks in GGBS or FA pastes

decreased linearly as more GGBS or FA was added. They observed that in HVFA mixes the time required to reach the peak rate increased significantly. Kruger (2003) states that for every ten percent replacement of OPC with fly ash, there is a reduction in the hydration heat of between 5-6%.

2.7.4 Effect of HVFA on Strength Development

Compressive strength is the most important design parameter in the design of concrete structures. It is widely used for prescribing concrete quality and it is the major factor that is used by the construction industry to price concrete and also for acceptance control. For high volume fly ash concrete, strength development is significantly influenced by curing conditions, physical and chemical characteristics of the fly ash. Other factors that affect fly ash concrete strength development are w/c ratio and quantity of binder material in the concrete mix. The most common approach to increasing concrete strength at all ages is to reduce the w/c in concrete. Compressive strength of HVFA concrete is highly influenced by the replacement of cement by high volume fly ash content, resulting in reduced amount of cement available for the hydration reaction which is mainly responsible for early age concrete strength. The pozzolanic reaction between the glass phases of FA and $Ca(OH)_2$ are slow at the early ages and accelerate with time as more $Ca(OH)_2$ is produced by the hydration reaction. Fraay et. al. (1989) allude to an incubation period during which pozzolanic reactions are dormant as a result of low alkalinity of the pore water.

The strength of concrete mainly depends on the w/c ratio and porosity of the concrete. Strength prediction models such as Abrams' model, Powers model, Popovics' model have been developed to correlate strength of concrete with properties of the cement paste (Chidiac et. al., 2013; Popovics, 1998). Abrams' law predicts concrete compressive strength solely on the water-cement ratio and it assumes that concrete is fully compacted with no air voids (Rao and Ramanjaneyulu, 2018). Abrams' law has been criticised by other researchers who have proven that concrete compressive strength does not only depend on the water-cement ratio, but it is also influenced by the composition of the concrete constituents (Özturan et. al., 2008; Moutassem and Chidiac, 2016).

Utilisation of fly ash in concrete has shown that it improves the interfacial transition zones (ITZ) between the cement paste and the aggregate thereby reducing the porosity of concrete (Bhattacharjee). High volume fly ash impacts on early strength gain and significant strength gain is notable at latter ages of concrete due to the continuing pozzolanic reaction that continues to produce more cementing compounds (Thomas, 2007). Fly ash activators can be used in mitigating the delayed setting time and early age strength development. A study by Crouch et al. (2007) established that one day strength of HVFA concrete with 50% FA content exceeded the strength required for removal of formwork. Malhotra (2004) states that high performance HVFA concrete can be produced with cements and fly ashes having different chemical and physical properties. He alludes to HVFA concretes which have attained 28 day compressive strengths of more than 35MPa. A study by Bouzoubaa et al. (2007) on mechanical properties of HVFA concrete established that the 28-day strength of HVFA concrete was similar to that of OPC concrete. Hung (1997) investigated HVFA concrete and established that using FA to simultaneously replace OPC and fine aggregates resulted in increased compressive strength owing to low w/c ratio. He recommended that fly ash should be used to replace both OPC and fine aggregates simultaneously. Nath and Sarker (2011) investigated the effects of FA and concluded that it is possible to make high strength concrete incorporating high volume fly ash content.

2.7.5 Effect of HVFA on Durability

Durability of Concrete

Concrete has proven to be a strong material, however challenges such as corrosion of reinforcement steel, alkali aggregate reactions and abrasion have been encountered during service life of concrete structures. The costs associated with repair and rehabilitation of concrete structures due to concrete deterioration have been on the rise annually and this has led to increased focus on the concept of concrete durability (Gjorv, 2011). Durability refers to the ability of concrete to withstand the design environment without deterioration. Kosmatka and Wilson (2011) defines durability as the ability of concrete to withstand chemical attack, weathering action and

abrasion without deterioration during the service life of a concrete structure. Concrete durability is influenced by the exposure conditions, intrinsic and extrinsic factors of the concrete system (Owens, 2009). The intrinsic factors that influence concrete durability encompass water to cement ratio, aggregates type, penetrability, type of cementitious material and content of cementitious material (Owens, 2009). Exposure conditions that influence concrete durability entail the aggressiveness of the environment such as abrasion, freeze thaw, thermal effects, concentration of external chemical substances, incompatibility of concrete constituents, temperature and relative humidity (Owens, 2009). The extrinsic factors that influence concrete durability entail processes such as concrete mixing, curing and early age temperature history (Ballim, 2015).

Permeability is a major factor that influences concrete durability. Permeability refers to the ease of ingress of fluids through a material. It refers to the capacity of concrete to transfer liquids and gases by permeation (Owens, 2009). Ballim (2015) defines permeability as a measure of the extent of inter-connection of pores in a material. According to Kosmatka and Wilson (2011), concrete permeability refers to the ease of migration of gasses and liquids or diffusion of ions through the concrete pores under a pressure or concentration gradient. Concrete permeability is highly dependent on concrete porosity. A highly porous cement paste matrix exhibits high permeability. Concrete durability failure involves penetration of harmful substances into concrete which subsequently initiate deterioration mechanisms such as ASR, sulphate attack, corrosion, etc (Kosmatka and Wilson, 2011).

Concrete deterioration is governed by transport mechanisms of permeation, diffusion, migration and absorption. Ballim (2015) states that all forms of concrete deterioration involve some form of fluid flow through the concrete pore system. Permeation refers to the movement of fluid through concrete pores under a pressure gradient in saturated concrete (Owens, 2009). Absorption refers to the movement of fluids through unsaturated concrete under the action of capillary forces (Owens, 2010). During absorption, molecules adhere to the pore surfaces by Van Der Waals forces or chemical bonding (Ballim, 2015). Migration refers to the movement of ions in a solution under an electrical field (Owens, 2010). It is the transport mechanism most often used in laboratory accelerated chloride tests such as the Chloride Conductivity Index Test.

Diffusion refers to the movement of fluids and ions through a partially or fully saturated material under a concentration gradient (Owens, 2010). During diffusion, molecules move microscopically under a concentration gradient (Ballim, 2015). Diffusion is the dominant transport mechanism for concrete structures fully submerged in sea water. Diffusion rates are dependent on temperature, moisture content of concrete (Owens, 2010).

Chloride Ion Diffusion

One of the major causes of corrosion in reinforced concrete is the de-passivation of steel due to chloride ion ingress. Chloride ions penetrate concrete through diffusion in saturated concrete and through capillary suction in unsaturated concrete (Owens, 2009). The concrete quality, threshold chloride concentration and exposure conditions are some of the factors that determine how long it will take for the chloride ions to penetrate into concrete and initiate corrosion (Owens, 2009). Replacement of cement with HVFA is effective in reducing the movement of chloride ions in concrete (Thomas 1996). A study conducted by Dhir et al. (1997) concluded that it is not the quality of fly ash that affects chloride ion diffusion. He argues that it is the volume of FA that affects chloride ion diffusion in concrete.

Bouzoubaa et al. (2007) examined HVFA concrete and established that the chloride resistance determined in terms of ASTM C 1202 was significantly higher in FA concrete than in OPC concrete. Nath and Sarker (2011) established that FA concretes with 40% FA yielded better resistance to chloride penetration. Their study proved that it is possible to design high strength concrete with reduced permeability by utilising up to 40% FA. Dhir and Byars (1993) studied chloride diffusion rates and reported that the partial replacement of OPC with FA significantly reduced the coefficient of chloride diffusion of concrete. They observed that the reduction was more as FA content increased. Dhir et al., (1997) investigated chloride binding capacity of FA pastes and concluded that up to a 33% FA level, chloride binding capacity was attributable to the increased concrete resistance to chloride penetration. At FA levels beyond 33% they observed a reduction in chloride binding capacity and also noted an increase in permeability which resulted in increased chloride penetration. Balakrishnan and Awal

(2014) studied the durability properties of concrete containing high volume fly ash and reported that OPC concrete had the highest chloride penetration whereas HVFA concrete had more than 50% lower penetration in 90 days. They attributed the increased resistance of the HVFA concrete to the consumption of $Ca(OH)_2$ which reduced porosity and increased impermeability that hindered the movement of chlorides.

Chloride migration tests measure the electrical current corresponding to movement of chlorides. Filho et al. (2013) argue that the hydroxyl ion is responsible for the intensity of the electrical current in concrete due to its higher ionic conductivity than the chloride ion. They further state that the concrete containing HVFA has low electrical conductivity than concrete OPC concrete due to the pozzolanic activity that consumes the calcium hydroxide in the concrete resulting in a reduction of hydroxyl ions in concrete pore water solution. Thomas (1996) investigated chloride thresholds in marine concrete and reported that 30% FA concrete had lower concentration of hydroxyl ions compared to OPC concrete.

Filho et al. (2013) investigated the chloride diffusion coefficient of HVFA concrete using accelerated tests. They reported that the utilisation of HVFA reduced the charge density passing through the concrete medium and that addition of $Ca(OH)_2$ had no effect on the result. They further stated that colorimetric testing revealed that using FA and $Ca(OH)_2$ lowered the chloride ion diffusion coefficient. They reported an increase in electrical resistivity of FA concrete. The also observed that there was a reduction in the pore sizes of FA which altered the transport properties and reduced the chloride ion diffusion.

Permeability

Permeability of concrete plays a critical role in the durability of concrete. The rate of ingress of deleterious substances depends on the pore structure of the concrete. Fly ash has a filler effect that refines the concrete pore structure which greatly contributes to reduced permeability and improved resistance to penetration of harmful substances. Helmuth (1987) cautions that if concrete is allowed to dry before the OPC and FA have

sufficiently reacted, the FA concrete will be highly permeable compared to OPC concrete. The continued pozzolanic reactions between fly ash and hydration products creates a denser cement paste that is more impermeable. FA produces a denser paste microstructure with improved pore size distribution resulting in reduced permeability. The CSH formed by pozzolanic reaction fills the concrete capillary pores. One of the major durability challenges is the corrosion of steel in concrete as a result of carbonation. When carbon dioxide penetrates the pores of hardened cement paste, it reacts with hydroxides to form carbonates which de-passivate the alkaline layer surrounding reinforcement steel resulting in corrosion of steel (Owens, 2009). HVFA concrete is capable of limiting the rate of carbon dioxide diffusion thereby reducing the rate of movement of the carbonation front (Owens, 2009).

2.8 Maturity Concept in Concrete

The need for construction efficiency and safety has led to the adoption of the maturity concept as a non-destructive, rapid and reliable technique in predicting in-place early age concrete strength (Yikici and Chen, 2015). The concept has been adopted by the construction industry to guide construction activities such as removal of formwork, prestressing time etc (Carino, 1991). Determining concrete strength using the maturity concept is faster than the conventional method which involves casting concrete specimens, curing, testing and transmitting results. The advantage of the maturity concept over the conventional methods is that it uses the actual temperature profile of in-place concrete to predict in-place concrete strength in real-time (NRMCA, 2006). Soutsos et. al., (2018) suggest that failures resulting from premature removal of formwork have led to more interest in real-time compressive strength monitoring through the maturity concept. As such, the maturity concept has been developed and commercialised in the form of maturity meters which make use of maturity functions such as Nurse-Saul, Arrhenius, Rastrup e.t.c (Soutsos et. al., (2018). The maturity method has also been adopted in standards and building codes such as ASTM C1074, ACI 228, (Giatec Scientific, 2019).

The maturity concept was initially proposed in 1950 to account for the collective effects of time and temperature on strength development of steam cured concrete and

subsequently it was implemented in normal curing conditions (Carino, 1991). Since then it has undergone modifications to improve its reliability in accounting for the effects of temperature and time in concrete strength development (Carino, 1991). In 1949 Nurse proved that the effects of temperature and time on strength gain could be expressed as a product of time and temperature (Carino, 1991). This expression was subsequently modified by Saul (1951) to incorporate datum temperature resulting in the development of the Nurse-Saul function. The Nurse-Saul function corelates strength development and temperature using a linear relationship whereas the Arrhenius function assumes an exponential relationship (Carino, 1991).

The maturity method can be used to estimate in-place concrete strength under variable temperature conditions and it accounts for curing temperature effects on strength development of concrete (Brooks et. al., 2007). The maturity concept finds its basis on the temperature dependence of the rate of chemical reactions (Benaicha et. al., (2016). The general principle behind the maturity concept is that concrete strength development is a function of temperature and curing time (Kosmatka and Wilson, 2011). The maturity rule principle states that concrete with similar mix design at the same maturity has the same strength irrespective of temperature and time required to get it to that maturity (Carino, 1991). The maturity index of a specific concrete mix is determined by its temperature-time history and the temperature–time history relates to the hydration process and can be used to predict concrete strength (Yikici and Chen, 2015). The maturity techniques predict concrete strength by monitoring the temperature-time history of concrete and comparing it with laboratory established empirical relationships between temperature–time history and concrete strength of similar concrete (Obla et al., 2012).

Yikici and Chen (2015) investigated the applicability of the maturity concept in the estimation of in-place concrete strength and concluded that the maturity method was accurate in predicting strength of concrete cured at 23 degrees and 40 degrees. They established that concrete cured at 50 degrees had lower strength compared to concrete cured at 23 and 40 degrees. Yang et. al., (2015) evaluated the maturity-strength relationship of high strength concrete and concluded that the maturity concept coupled with the modified equivalent age can be used to evaluate strength

development of high strength concrete. Ballim and Graham (2003) investigated the rate of hydration heat evolution using the maturity concept and concluded that the Arrhenius function is much preferable for normalizing heat rate curves compared to the Nurse-Saul function.

The maturity concept has been found to have some limitations (Rangaraju). Yikici and Chen (2015) highlight concerns pertaining to the short comings of the maturity concept in mass concrete applications where there are variable concrete temperatures. Other limitations to the use of the maturity method include the use of parameters such as datum temperature and activation energy that are not representative of the concrete mix (NRMCA, 2006). Other limitations that have been identified pertain to variations in concrete quality, high early age temperature and poor compaction and curing. Brooks et. al., (2007) states that the composition of binder material has a significant influence on the estimation of concrete strength using the maturity method. Yikici and Chen (2015) highlight that a lot research work has been done on OPC compressive strength prediction using maturity techniques and not much work has been done on concrete with supplementary cementitious materials such as fly ash.

2.9 Curing of Concrete

The key objective of curing is to protect concrete against loss of moisture. Curing maintains adequate moisture and temperature required for hydration. Continued hydration is dependent on availability of moisture and any loss of moisture retards further hydration. The extent to which hydration is completed has a significant influence on the strength and durability properties of concrete (Kosmatka and Wilson, 2011). Loss of moisture from the concrete surface results in plastic shrinkage cracking of concrete surfaces. Curing influences concrete properties such as strength development, durability, volume stability and permeability (Kosmatka and Wilson, 2011).

Concrete curing can be achieved mainly by continuously wetting the concrete surface, preventing moisture loss and applying curing compounds (Concrete NZ, 2017). Concrete surfaces can be kept continuously wet through ponding, sprinkling, using

damp sand or using damp hessian. Moisture loss from concrete surfaces can be achieved by leaving formwork in place or covering concrete with polythene membranes. Applying curing compounds also ensures adequate moisture retention. Ponding is an efficient method of curing horizontal concrete surfaces in small concrete works, however it is not practical for curing large concrete works. Sprinkling can be an efficient curing method when it is done continuously without creating wetting and drying cycles. Spraying water is an efficient way of curing concrete particularly in large concrete structures. Covering concrete with moisture retaining fabrics such as hessian can provide effective curing when the fabrics are kept moist throughout the curing duration. Polythene membranes provide an effective barrier that prevents moisture loss from horizontal and vertical surfaces. Keeping formwork in place also creates a barrier against moisture loss. Membrane forming curing compounds can be applied onto the concrete surfaces by spraying soon after concrete finishing is complete.

Curing duration has influence on concrete strength development. Concrete that is moist cured for a longer period develops strength faster compared to concrete that is cured for a short duration (Zemajtis, 2014). Figure 2.3 indicates that long term moist curing significantly improves the strength of concrete compared to short term curing. The required duration of curing depends mainly on the concrete mix, target strength, ambient temperature, exposure conditions, cementitious material type etc. The curing periods also depend on the type of curing method adopted.

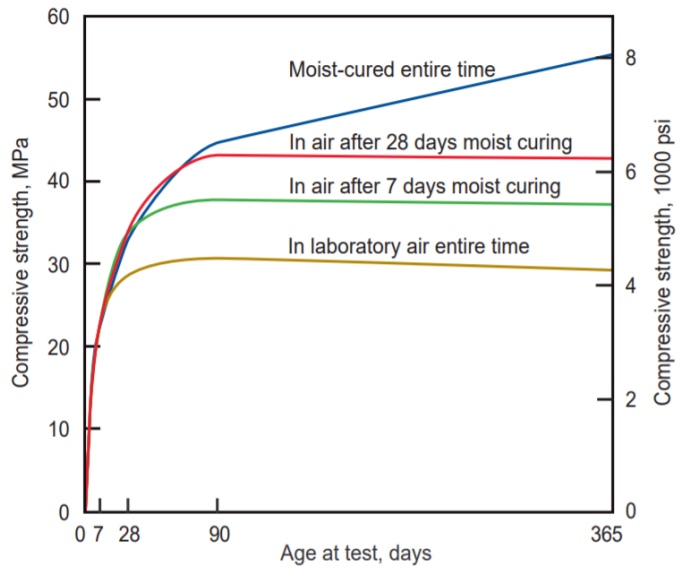

Figure 2.3: Effect of moist curing time on strength gain of concrete (Kosmatka and Wilson, 2011)

Curing concrete at low temperatures has a negative effect on early age strength development. Temperatures below 10°C have a significant impact on the rate of concrete strength development (Kosmatka and Wilson, 2011). The rate of hydration is greatly retarded under freezing temperatures and the hydration process stops at temperatures below −10°C (Nassifa and Petrou, 2013).

High temperature curing accelerates the hydration process and improves the early age strength of concrete, however it has detrimental effects on late age concrete strength (Elkhadiri et. al., 2009). Yikici and Chen (2015) highlight that curing concrete at elevated temperatures accelerates the hydration process resulting in high strength gain at early age. Zemajtis (2014) states that curing at elevated temperature enhances the early age strength of concrete but it reduces concrete strength at 28-days and beyond. Hatzitheodorou et. al., (2017) investigated the effect of curing temperature on the strength development of mortar mixes with GGBS and fly ash and reported that curing at elevated temperatures improves early age strength but it has a negative effect on long term strength development. The reduction in late age strength can be attributed to the rapid formation of hydration products which accumulate around the cement grain surfaces ultimately blocking water penetration towards the partially hydrated cement grain and this results in cement paste with high porosity and non-uniform pore structure (Ekolu, 2006). Carino (1991) highlights that rapid hydration at elevated temperatures produces non-uniformly distributed hydration products with low permeability which form shells around cement grains and impede further hydration of the cement grains resulting in reduced long-term strength. Ekolu (2006) states that the high temperature curing threshold beyond which there are no benefits to engineering properties of concrete ranges between 60°C and 70°C. Ultimate strength reduction and potential for delayed ettringite formation is minimised if curing temperature does not exceed 70°C (Hwang et al, 2012; Kosmatka and Wilson, 2011; Giatec Scientific, 2019).

Pozzolanic reactions are accelerated when concrete is cured at high temperature. Low curing temperatures negatively impacts on strength development and durability of HVFA concrete. Longer curing creates a conducive environment for continued pozzolanic reactions. Obla et al. (2012), investigated HVFA concrete using maturity-

based methods for predicting strength and established that the actual strength of HVFA concrete in a concrete structure is higher than that measured using cylinder tests due to the in-place hydration heat generated by the bigger concrete mass. A study conducted by Ash Resources on the effects of curing temperature on FA concrete concluded that the compressive strength of concrete is affected by curing in cold weather (Kruger, 2003). Grieve (1991) conducted a similar study with FA and concluded that the reduction in strength due to low temperature curing was higher in fly ash concrete compared to OPC concrete.

2.10 South African Durability Index tests

The South African durability index tests have been developed in response to the need for performance-based approach in the design and specification of concrete. The durability index tests are primarily used to evaluate the quality of concrete (Otieno, 2018). The durability indexes measure transport related properties of concrete such as permeation, absorption and diffusion (Owens 2009). The durability index tests consist of the chloride conductivity index (CCI) test, oxygen permeability index (OPI) test and water Sorptivity index (WSI) test (Alexander et al., 1999). Each durability index test is associated with a transport mechanism for the movement of substances through a concrete medium (Owens, 2009). The durability indexes are used in numerous applications such as material characterisation, quality control, performance-based specification and prediction models (Alexander et al., 2010).

2.10.1 Chloride Conductivity Index (CCI) Test

The chloride conductivity index test (CCI) is an accelerated test used to measure the resistance of concrete to chloride ingress by diffusion (Otieno, 2018). The need for accelerated diffusion tests such as the CCI test arose from the fact that chloride ion diffusion in concrete is a slow process which takes months or years to yield significant results (Owens, 2009). The CCI test obtains rapid results by applying voltage across a concrete specimen saturated in a highly concentrated chloride solution (Owens, 2009). The CCI test is sensitive to the type of cementitious material in concrete (Alexander et al., 2008).

The chloride conductivity index is determined by applying a potential difference of approximately 10 V across a saturated concrete specimen and simultaneously reading the electrical current passing through the specimen. The chloride conductivity index is correlated to the applied voltage, electrical current and specimen geometry as shown in Equation 2-8.

$$\sigma = \frac{i.d}{V.A} \qquad \text{Equation 2-8}$$

Where, σ : Chloride conductivity index (mS/cm)
I : Electric current (mA)
d : Specimen thickness (cm)
V : Potential difference (V)
A : Specimen Cross-sectional area (cm2) (Durability Index Testing Manual: 2018)

The chloride conductivity index test has been subjected to numerous evaluations in order to improve its robustness, reproducibility, and repeatability (Otieno and Alexander, 2015). The CCI test has now been incorporated into the South African National Standards as SANS 3001-CO3-3: 2015. Otieno (2018) evaluated the robustness of the CCI test by measuring the effect of concrete quality on its sensitivity to test duration, chloride concentration and variation of potential difference. He concluded that if the correct chloride concentration is used and the correct voltage is applied in the shortest time possible, the CCI test yields valid results that can be relied on.

2.10.2 Oxygen Permeability Index (OPI) Test

The oxygen permeability index (OPI) test evaluates the microstructure and macrostructure of concrete by modelling the movement of the fluids by permeation through a concrete medium (Owens, 2009). The OPI test determines the permeability of concrete by measuring the pressure decay of oxygen passing through a concrete specimen placed in a falling head permeameter (Beushausen and Alexander, 2008). The OPI test is sensitive to the voids and cracks in concrete and it can be used to assess the extent of compaction, bleeding and the degree of continuity of pores (Beushausen and Luco, 2016). The oxygen permeability index values have been used

in service life prediction models such as the carbonation prediction model which predicts the movement of a carbonation front through a concrete medium (Owens, 2009; Mukadam, 2014). Studies carried out on the OPI test have proven that the OPI test correlates well with other oxygen permeability tests such as the Cembureau method and the Torrent Permeability Tester (Owens, 2009). The oxygen permeability index is determined by calculating the D'arcy coefficient (k) of permeability as shown in Equation 2-9. The OPI value is then taken as the negative log of the D'arcy coefficient of permeability (k) i.e. $OPI = -\log_{10}(k)$

$$k = \frac{\omega V g d z}{RAT} \quad ; \qquad z = \frac{\sum\left[\ln\left(\frac{P_0}{P_t}\right)\right]^2}{\sum\left[\ln\left(\frac{P_0}{P_t}\right)t\right]} \qquad \text{Equation 2-9}$$

Where:
- k = Coefficient of permeability (m/s)
- ω = Molecular mass of oxygen (32 g/mol)
- V = Volume of the oxygen permeability cell, (litres)
- g = Gravitational acceleration (9.81 m/s^2)
- d = Specimen thickness (m)
- z = Slope of linear regression line (s^{-1})
- R = Universal gas constant (8.313 Nm/K mol)
- A = Cross-sectional area of the specimen, (m^2)
- T = Absolute temperature (K).
- *t* = Time (seconds)
- P_o = Initial pressure at start of test, t_o (kPa);
- P_t = Pressure reading at time *t,* (kPa). (SANS 3001-CO3-2:2015)

2.10.3 Water Sorptivity Index (WSI) Test

The water Sorptivity index test measures the rate of uni-directional movement of water through a concrete medium under capillary suction (Beushausen and Luco, 2016; Owens, 2009). The water sorptivity index test is sensitive to the type and degree of early age concrete curing and it can be used to investigate the quality of construction (Owens, 2009). The Water Sorptivity Index test is also used to determine concrete porosity. The concrete porosity determined in terms of the Water Sorptivity index test is given by Equation 2-10.

$$n = \frac{Msv - Mso}{Ad\rho_w} \times 100$$ Equation 2-10

Where: M_{sv} = Vacuum saturated mass (grams)
M_{s0} = Mass at start of test) (grams)
A = Specimen cross-sectional area (mm^2)
d = Specimen thickness (mm)
ρ_w = Density of water (g/mm^3) *(Durability Index Testing Manual: 2018)*

2.11 Conclusion

High volume fly ash concrete can contribute towards beneficiation and extensive use of fly ash as a concrete constituent. Utilisation of high-volume fly ash in concrete results in significant improvement of properties of fresh concrete such as reduced heat of hydration, improved workability and reduced bleeding. In hardened concrete, the improvements include increased long-term strength, enhanced resistance to chloride penetration, reduced potential of sulphate attack and alkali-silica reactivity. Despite these beneficial effects, detrimental effects have been reported with regards to delayed setting and early age strength.

The literature review has established that much work has been done on fly ash concrete, however limited work has been done locally on high strength high volume fly ash concrete using South African materials and test methods. There is need for further research on high strength high volume fly ash concrete with respect to improving early age strength development, fly ash activation and durability testing using the South African durability index testing methods. The literature on HVFA concrete has highlighted the challenge of early age strength development. Gaps in current literature have been identified with respect to pushing the content of fly ash beyond the normal replacement levels of up-to 30% in the production of high strength concrete and achieving acceptable early age strengths by using low w/c ratio and fly ash activation techniques such as high temperature curing, calcium hydroxide activation and improved fly ash fineness. Use of ultra-fine fly ash can improve the properties of HVFA concrete. HVFA concrete is highly applicable in marine structures where durability is imperative due to the abundance of deleterious substances such as chlorides and sulphates.

3. EXPERIMENTAL METHODS AND PROCEDURES

3.1 Introduction

This chapter details the experimental methods and procedures followed in this study. It details all the material characterization tests that were done and the results obtained from material tests. The procedures followed in specimen preparation, concrete mix design, compressive strength and durability testing are explained in detail. Figure 3.1 presents an outline of the experimental work flow chart.

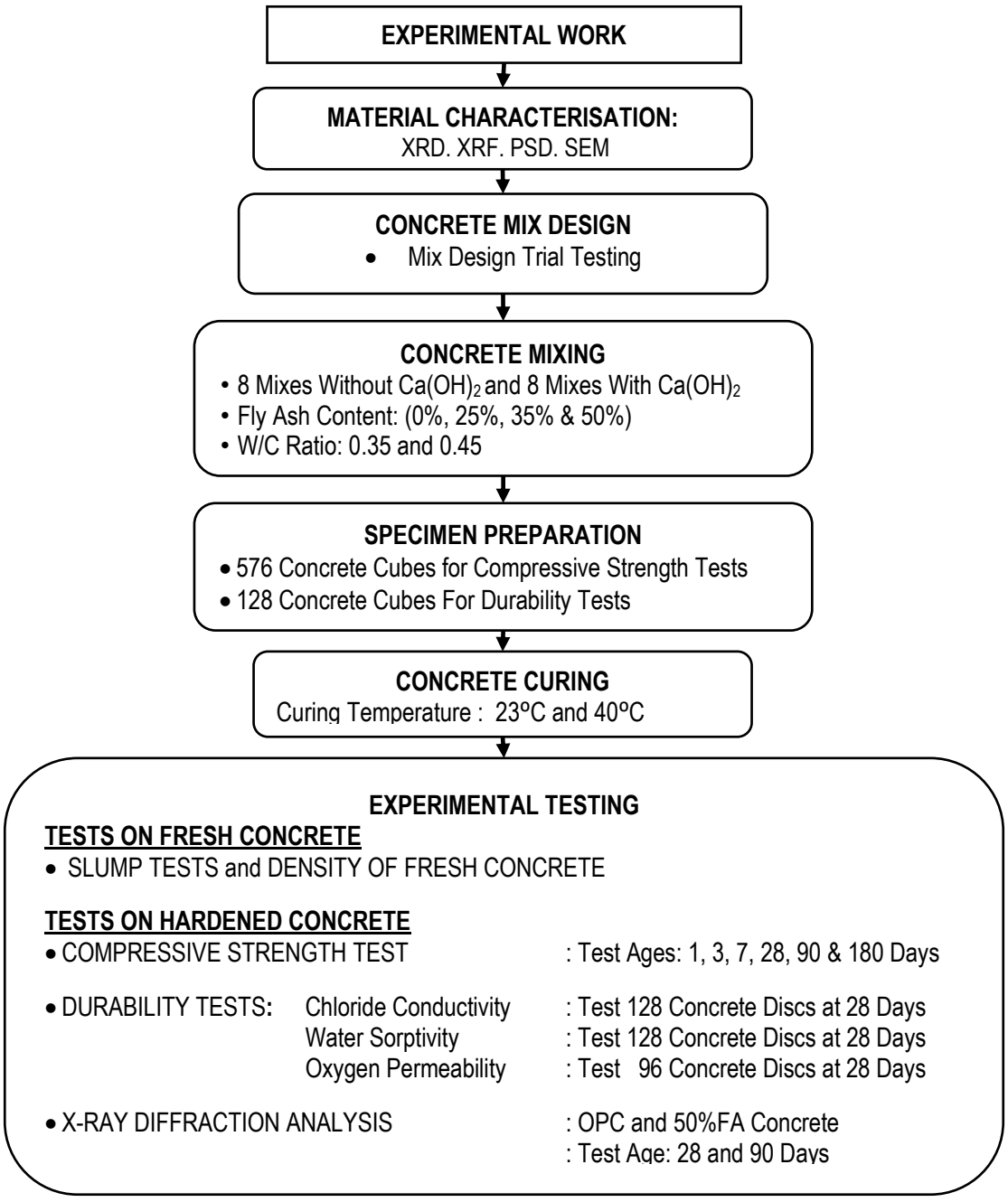

Figure 3.1: Experimental Work Flow Chart

3.2 Materials and Sources

Table 3-1 gives a summary of the materials that were used in the study.

Table 3-1: Materials and Sources

Material	Type	Supplier	Source
Fly Ash	Ultra-Fine Fly Ash (Category S)	Ash Resources	Lethabo Power Station
Cement	CEM1 52.5N	PPC	PPC
Fine Aggregates	Andesite Rock	Afrisam	Eikenhof Quarry
Coarse Aggregates	Andesite Rock	Afrisam	Eikenhof Quarry
Superplasticiser	Chemical Base: Aqueous solution of modified polycarboxylates	Sika	Sika SA

3.3 Material Properties and Tests

3.3.1 Cement Properties

The cement used in the study was OPC CEM 1: 52.5N high early strength cement manufactured by PPC. This type of cement was chosen because it does not contain cement extenders such as fly ash. Table 3-2 shows the cement properties provided by the cement supplier.

Table 3-2: Properties of Cement (PPC, 2014)

Physical Properties	Typical Values
Relative Bulk Density	3.14
Initial Setting time	125 minutes
Final Setting time	2.5 hours
2 Day Compressive Strength (EN196-1 Motor Prism)	28MPa
28 Day Compressive Strength (EN196-1 Motor Prism)	58MPa
Soundness (Le Chatelier Expansion, mm)	1
Insoluble residue	2.0 % by mass

3.3.2 Cement Tests

Cement XRF Analysis

The oxide composition of cement was determined by X-Ray Fluorescence (XRF) analysis which was done at the Wits University Geosciences laboratory. The results of the XRF analysis are detailed in Table 3-3.

Table 3-3: XRF Analysis Data for Cement

Chemical Compound	SiO_2	Al_2O_3	Fe_2O_3	MnO	MgO	CaO	Na_2O	K_2O	TiO_2	P_2O_5	Cr_2O_3	LOI
Content (% by Mass)	21.15	5.37	2.78	0.47	2.5	61.41	0.05	0.25	0.34	0.07	0.06	3.57

Cement XRD Analysis

The crystalline phases of cement were determined by X-Ray Diffraction (XRD) analysis using a Panalytical X'PertPro X-Ray Diffractometer. The XRD pattern for the cement is shown Figure 3.2. The XRD pattern indicates high peaks for the C_3S and C_2S phases that are responsible for strength development. The strong presence of C_3S compounds indicates that the cement has high reactivity and it will develop high early strength upon hydration.

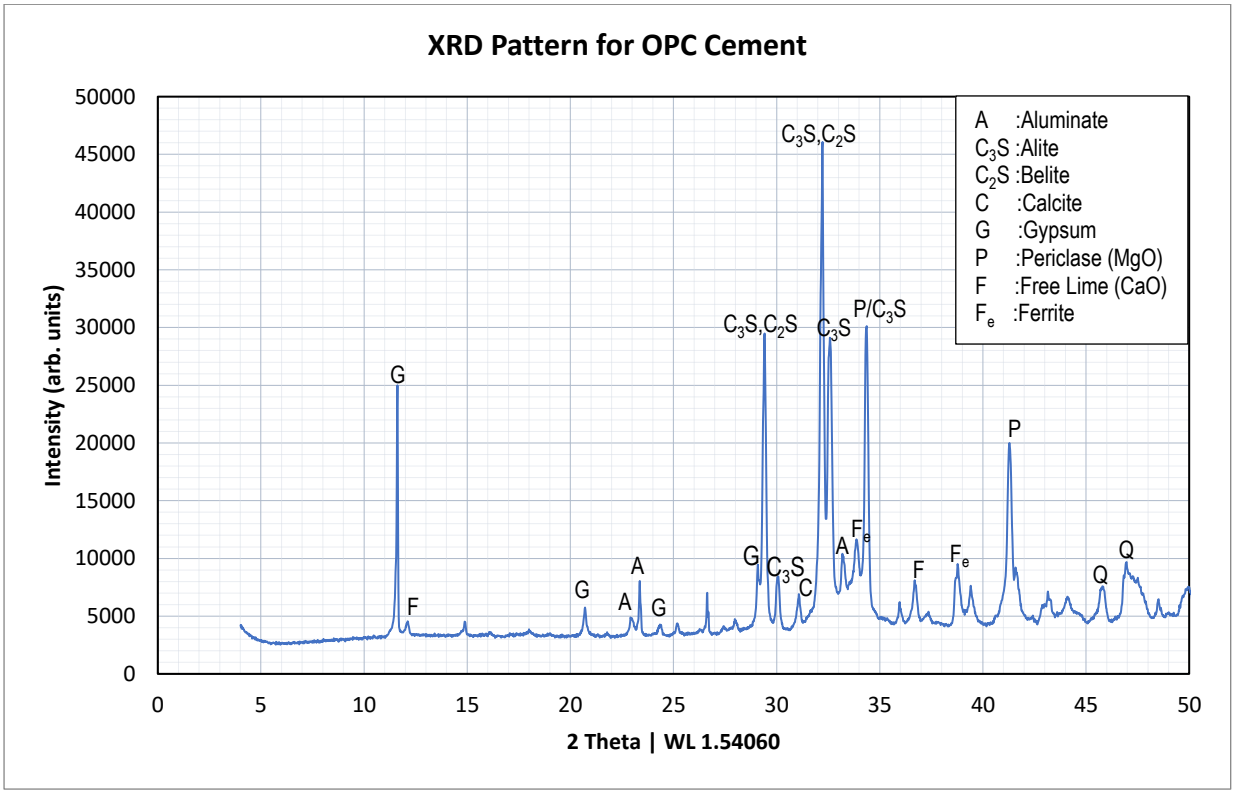

Figure 3.2: XRD Pattern for OPC Cement

Cement Particle Size Distribution

The cement particle size distribution was determined using Malvern Instruments Mastersizer 2000 particle size analyser. The particle size distribution curve for cement is shown in Figure 3.3. The fineness parameters for cement are shown in Table 3-4. The Malvern Instruments Mastersizer 2000 measures particle size distribution using laser diffraction. It produces volume-based particle size distributions of dispersed samples. The cement fineness parameters show that 50% of the sample particles had a size below 12.519µm and 90% of the sample particles had a size below 35.301 µm.

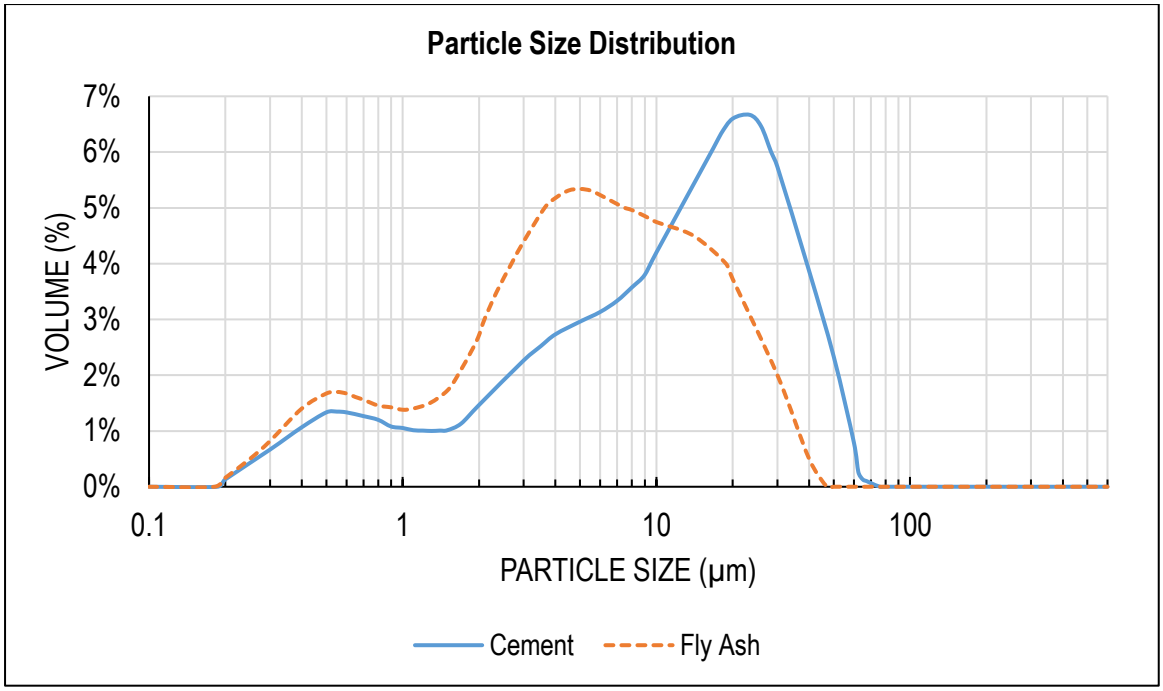

Figure 3.3: Cement and Fly Ash Particle Size Distribution Graph

Table 3-4: Cement and Fly Ash Fineness Parameters

Material	**Specific Surface Area** (m^2/g)	**d(0.1)** (µm)	**d(0.5)** (µm)	**d(0.9)** (µm)
Cement	1.98	1.087	12.519	35.301
Fly Ash	2.78	0.756	5.471	20.476

d(0.1) is particle size below which 10% of the sample lies.
d(0.5) is median of the particle size distribution
d(0.9) is the particle below which 90% of the sample lies. (Malvern Instruments, 2007)

3.3.3 Fly Ash Properties

Fly Ash Particle Size Distribution

Ultra-fine fly ash from Lethabo power station was used in the study. Ultra-fine fly ash was preferred due to its high reactivity potential. The fineness parameters of fly ash are detailed in Table 3-4. The fineness parameters and particle size distribution graph indicate that the fly ash was much finer than cement. The particle size distribution graph comparing fly ash used in this study with silica fume is shown Figure 9.17 in Annexure 8. The ultra-fine fly ash can be used as an extender in high strength concrete instead of silica fume which increases the water demand. The ultrafine fly ash has an added advantage of improving the workability of concrete. The fly ash data sheet provided by the supplier is attached in Annexure 8.

3.3.4 Fly Ash Tests

Fly Ash XRF Analysis

The oxide composition of fly ash was determined by X-Ray Fluorescence (XRF) analysis which was done at the Wits University Geosciences laboratory. The results of the XRF analysis are detailed in Table 3-5. The total sum of Alumina (Al_2O_3), Silica (SiO_2) and Ferric Oxide (Fe_2O_3) is 89.75%. The sum of Al_2O_3 + SiO_2 + Fe_2O_3 is greater than 70%, therefore, in terms of ASTM C618 (2005) and SANS 50450-1 (2011) the fly ash used in this study can be classified as Class F.

Table 3-5: XRF Analysis Data for Fly Ash

Chemical Compound	SiO_2	Al_2O_3	Fe_2O_3	MnO	MgO	CaO	Na_2O	K_2O	TiO_2	P_2O_5	Cr_2O_3	LOI
Content (% by Mass)	53.98	32.55	3.24	0.03	1.25	4.63	0.25	0.87	1.66	0.66	0.05	0.52

Fly Ash XRD Scan

The crystalline phases of fly ash were determined by X-Ray Diffraction (XRD) analysis using Panalytical X'PertPro X-Ray Diffractometer. The XRD pattern for the fly ash is shown in Figure 3.4.

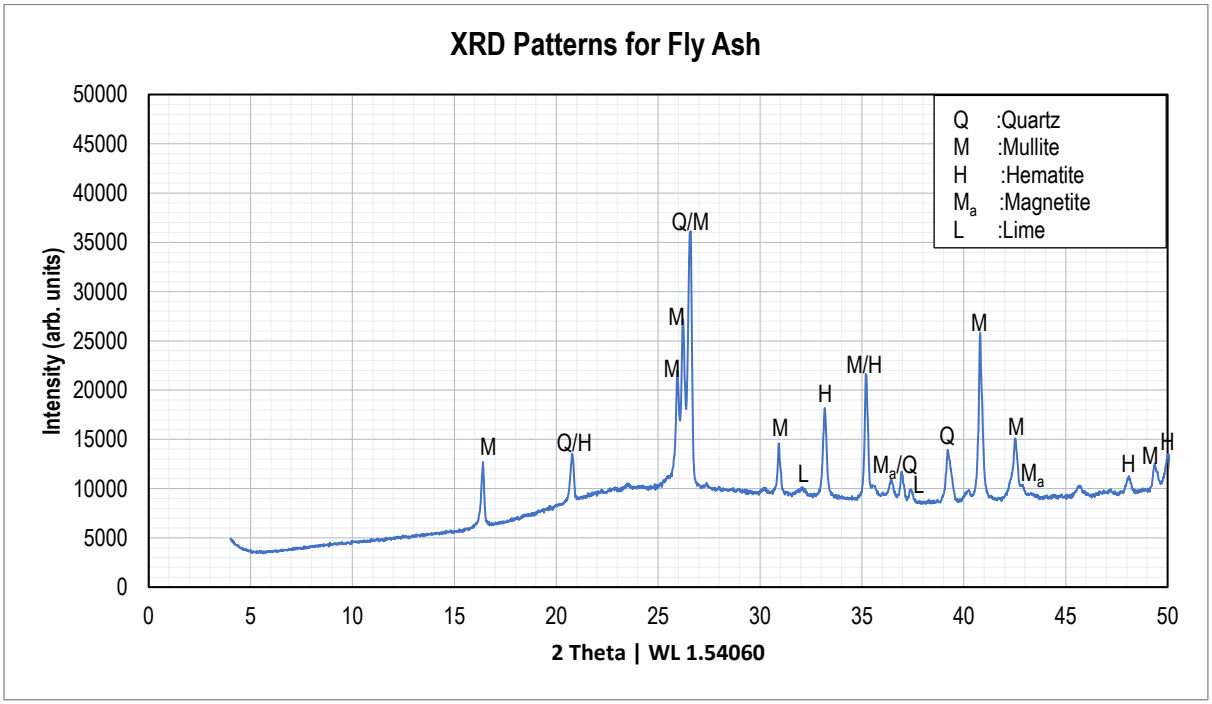

Figure 3.4: XRD Pattern for Fly Ash

Scanning Electron Microscope (SEM)

Figure 3.5 shows the scanning electron microscope images for fly ash and cement. The 100µm line at the bottom of the images can be used to scale the size of the fly ash and cement particles. The SEM images indicate that the fly ash particles are very small compared to the cement particles.

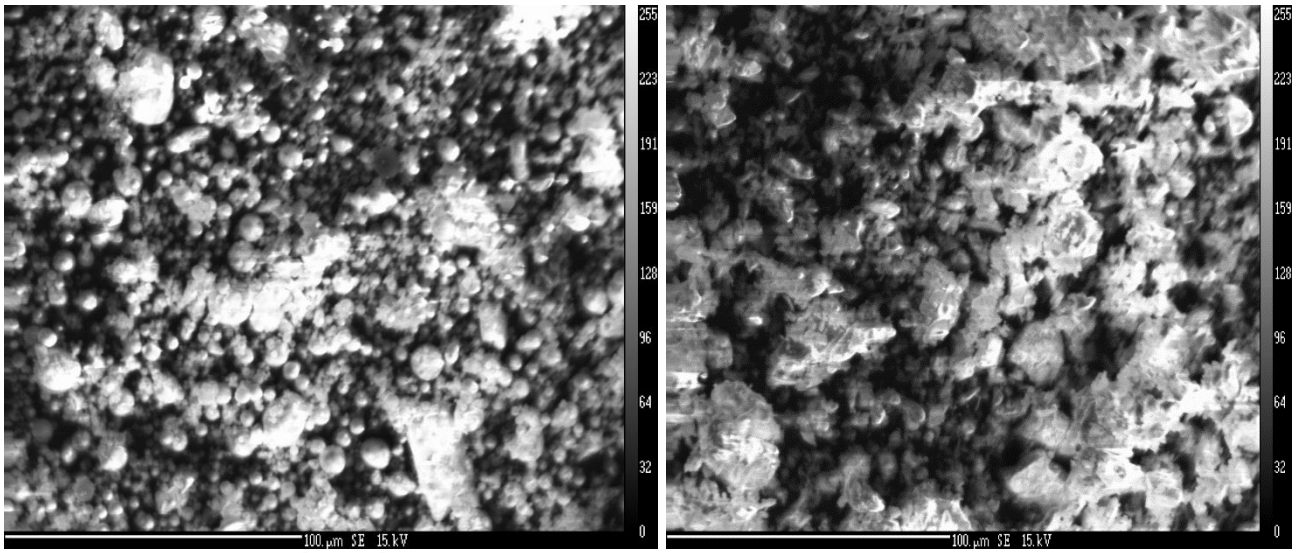

Fly Ash **Cement**

Figure 3.5: Cement and Fly Ash SEM Images

3.3.5 Aggregate Properties and Tests

Fine Aggregates

Crushed andesite rock particles were used as fine aggregates. Table 3-6 gives an outline of the fine aggregate properties. Fine aggregates were sieved and separated according to standard sieve sizes as shown in Figure 3.6 and they were latter on mixed in desired proportions in order to achieve consistency of fine aggregates throughout the study. Table 3-7 shows the fine aggregate particle size proportions that were adopted in this study. Figure 3.7 shows the particle size distribution curve for the fine aggregates in comparison with the suggested fine aggregates limits for Cement and Concrete Institute (Owens, 2009).

Table 3-6: Fine Aggregate Properties

Property	Value
Fineness Modulus	3.55
Relative Density***	2.94

****Source: AfriSam, 2014*

Table 3-7: Fine Aggregate Particle Size Proportions

Sieve Size	4.75mm	2.36mm	1.18mm	600µm	300µm	150µm	75µm	Pan
% Retained	0%	25%	15%	15%	15%	15%	7.50%	7.50%



Figure 3.6: Fine Aggregates Sieving

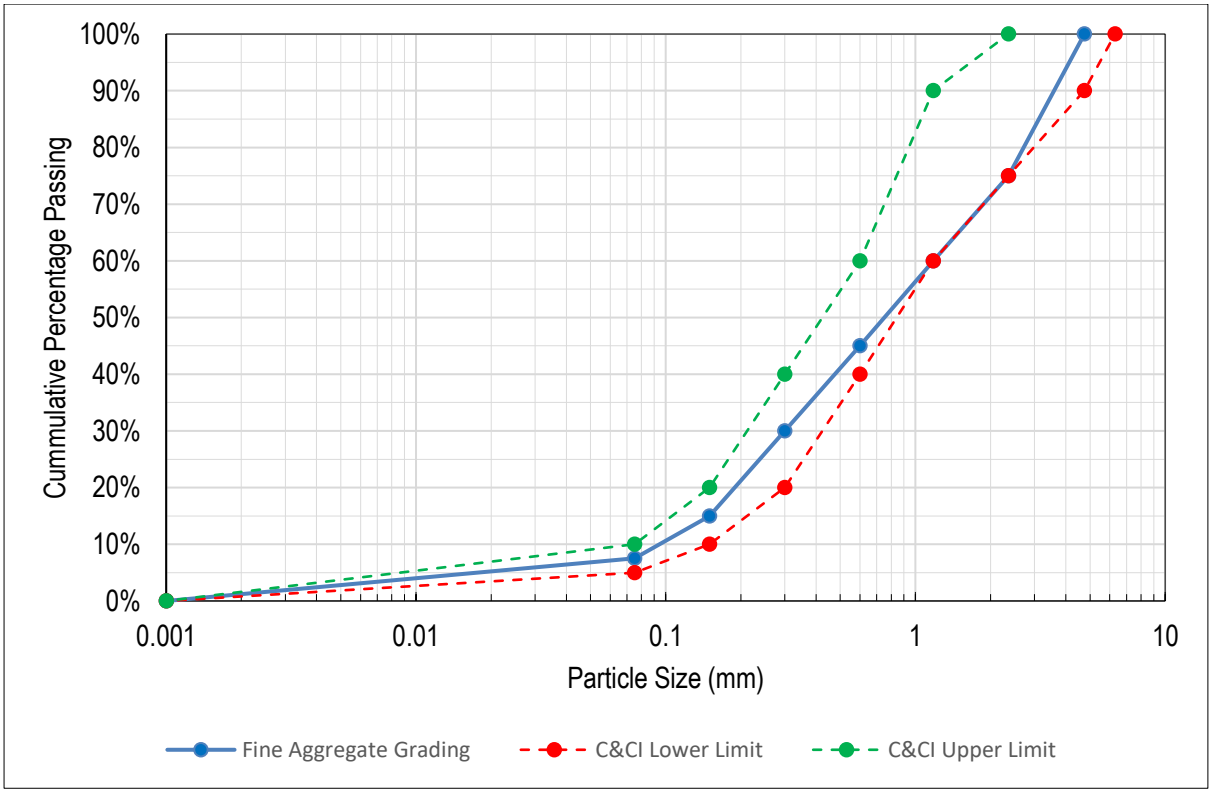

Figure 3.7: Fine Aggregate Particle Size Distribution

3.3.6 Absorption Tests for Fine Aggregates

Water absorption tests were done on the fine aggregates. A sample of the fine aggregates consisting of all the particle size proportions as detailed in Table 3-7 was oven dried to constant weight at a temperature of 110ºC. The sample was air cooled at room temperature before it was saturated in water for a period of 24 hours at room temperature. After 24 hours of saturation, the sample was dried to a Saturated Surface Dry (SSD) condition. The sample was dried with absorbent cloths after which a portion of the sample was then shaped and into a conical form and when it was free flowing that gave the indication that the sample was approximately at Saturated Surface Dry condition. The Saturated Surface Dry sample was weighed and the mass was recorded. The SSD sample was then placed in an oven at a temperature of 110ºC and dried to constant weight. The oven dry mass of the sample was measured and recorded. The results of the water absorption tests are shown in Table 3-8. The constant weight was achieved within a period of 48 hours. All the fine aggregates used in the study were oven dried for forty-eight hours and thereafter kept in an airtight container until concrete mixing. The water absorption was determined using Equation 3-1.

$$A = \left(\frac{M_{SSD} - M_D}{M_D}\right) \times 100\% \quad \text{Equation 3-1}$$

Where: A is Percent Water Absorption
M_{SSD} is Mass of Saturated Surface Dry sample
M_D is Mass of Oven Dry Sample

Table 3-8: Fine Aggregate Water Absorption Test Results

Coarse Aggregate Sizes	Saturated Surface Dry Mass (g)	Oven Dry Mass			Percent Absorption
		Mass One (g)	Mass Two (g)	Mass Three (g)	
2.36mm (25%)	842.30	828.10	827.80	827.30	1.8%
1.18mm (15%)					
600µm (15%)					
300µm (15%)					
150µm (15%)					
75µm (7.5%)					
Pan (7.5%)					

3.3.7 Coarse Aggregate Properties and Tests

Crushed andesite rock particles were used as the coarse aggregates. The coarse aggregate sizes used in the study were 6.7mm, 9.5mm and 13.2mm. The coarse aggregates were combined in desired proportions as shown in Table 3-9 in order to improve particle packing and attain dense, dimensionally stable, strong and durable concrete (Cai, 2017). The relative density of the coarse aggregates is 2.94 (AfriSam 2014). Figure 3.8 illustrates the coarse aggregate particle size distribution after mixing all the stone sizes in desired proportions shown in Table 3-9.

Table 3-9: Coarse Aggregates Proportions

Aggregate Size	**Proportion** *(% by mass)*
13.2mm	50%
9.5mm	30%
6.7mm	20%

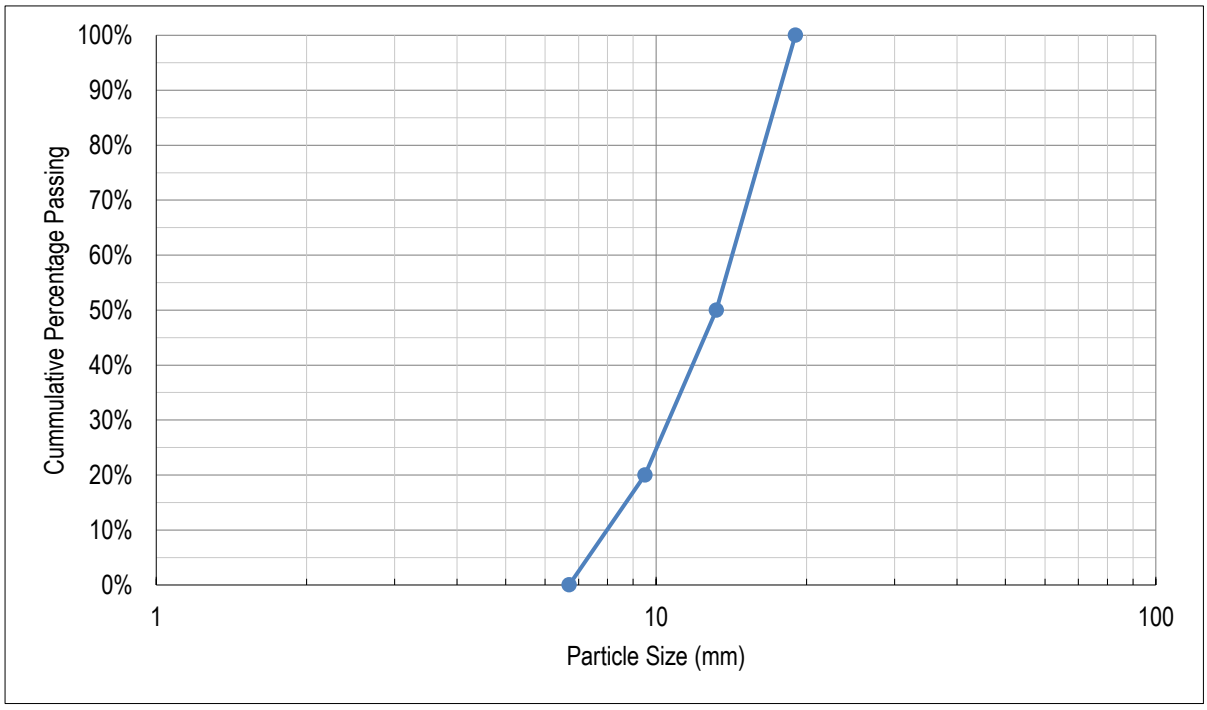

Figure 3.8: Coarse Aggregate Particle Size Distribution

3.3.8 Water Absorption Test for Coarse Aggregates

Water absorption tests were also done for the coarse aggregates. A representative sample of the coarse aggregates with all the stone size proportions as detailed in Table 3-10 was oven dried at a temperature of 110^0C to constant weight and cooled at room temperature. The sample was then saturated in water for a period of 24 hours. After saturation, the sample was dried to a saturated surface dry (SSD) condition. The Saturated Surface Dry (SSD) mass of the sample was determined and recorded. The SSD sample was then placed in an oven at a temperature of 110 ºC and was dried to constant weight. The oven dry mass of the sample was determined and recorded. The results of the water absorption test are shown in Table 3-10. The water absorption was determined using Equation 3-2. All the coarse aggregates used in the study were oven dried for forty-eight hours and kept in an airtight container until concrete mixing.

$$A = \left(\frac{M_{SSD} - M_D}{M_D}\right) \times 100\% \qquad \text{Equation 3-2}$$

Where: A is Percent Water Absorption
M_{SSD} is Mass of Saturated Surface Dry sample
M_D is Mass of Oven Dry Sample

Table 3-10: Coarse Aggregate Water Absorption Test Results

Coarse Aggregate Sizes	Saturated Surface Dry Mass (g)	Oven Dry Mass			Percent Absorption
		Mass One (g)	Mass Two (g)	Mass Three (g)	
13.2mm (50%)	1052.65	1050.27	1050.25	1050.25	0.2%
9.5mm (30%)					
6.7mm (20%)					

3.3.9 Admixtures

A superplasticiser with high water reducing ratio was used as a water reducing admixture. The properties of the superplasticiser are outlined in Table 3-11. The superplasticiser datasheet provided by the supplier is attached in Annexure 9.

Table 3-11: Superplasticiser Properties (Sika, 2016)

Admixture	Properties	
Superplasticiser	Chemical Base	Aqueous Solution of Modified Polycarboxylates
	Density	1.07kg/l
	pH Value	5.5
	Chloride Ion Content	Chloride Free

3.3.10 Mixing Water

Normal tap water was utilised as the mixing water.

3.4 Concrete Mix Design

The study evaluated high strength concrete mixes which incorporate high volume fly ash contents. The concrete mixes investigated in this study were designed on the basis of high strength concrete. Numerous researchers have proposed mix proportions for high strength concrete with and without fly ash (Addis 1991, Mehta 2004). Owens (2009) defines high strength concrete as concrete having 28-day compressive strength higher than 60 MPa with binder contents ranging from 380 to 500kg/m^3. Addis (1991) investigated high strength concrete mixes and suggested that the w/c ratio of high strength concrete ranges between 0.25 to 0.45, coarse aggregates range between 1050 to 1250 kg/m^3 and water content ranges between 130L/m^3 and 160L/m^3 of concrete. Burg and Ost (1994) suggested that the typical mixture proportions of high strength concrete have coarse aggregate content of 1080kg/m^3, fine aggregate content of 650kg/m^3 and binder content of 500kg/m^3 of concrete. They stated that high performance concrete used in large projects in the USA, Canada and France had concrete mixes similar to the ones they proposed and the mixes had coarse aggregate content of 1080kg/m^3, fine aggregate content of 700kg/m^3 and binder content of 520kg/m^3. The concrete mixes had 28-day compressive strength ranging above 70MPa. Mehta (2004) suggests that high performance-HVFA concrete is characterised by fly ash content of 50%, with OPC content less than 200kg/m^3 and water content of 130kg/m^3. The mix proportions for high strength-high volume fly ash concrete proposed by Mehta (2004) are shown in Table 3-12.

Table 3-12: Typical Mix Proportions for high strength HVFA Concrete (Mehta, 2004)

Concrete Age	**Strength Level (MPa)**
28 Days	40 MPa
90 Days to 1 Year	60 MPa
Concrete Constituent	**Mix Proportions (kg/m^3)**
Water	100 – 120 l/m^3
OPC Cement	180 – 200kg/m^3
Fly Ash,	200 – 225kg/m^3
w/c ratio	0.3 – 0.32
Coarse Aggregates	1100 – 1200 kg/m^3
Fine Aggregates	800 – 900kg/m^3

Conventional concrete mix design methods could not be applied in developing concrete mixes for high strength concrete used in this study. The Cement and Concrete Institute (C&CI) method which is generally used for the design of conventional concrete mixes in South Africa could not be used in the design of high strength concrete with low water to cement ratio as it resulted in high cement contents. In this study, the high strength concrete mix incorporating OPC only was designed first and thereafter the cement was replaced with varying quantities of fly ash. The mass of cementitious material was kept constant at 400kg/m^3. The rationale of the mix design was to modify high strength concrete to high strength-high volume fly ash concrete. The fly ash contents used to substitute cement were 25%, 35% and 50% by mass of cementitious material. Mass substitution of cement with fly ash presents an easy and more practical method of producing fly ash concrete at construction sites. Mass substitution of cement with fly ash has been widely used by many other researchers in fly ash concrete (Ballim and Graham (2009); Poon et al., (2000); Kate and Thakare (2017)). In order to keep the concrete mixes consistent, no adjustments in water content and coarse aggregate content were made as a result of fly ash addition. Five percent calcium hydroxide by mass of cementitious material was added to some of the concrete mixes in order to activate fly ash pozzolanic reactions. Five percent $Ca(OH)_2$ was adopted on the basis of literature review findings, $Ca(OH)_2$ cost and water demand for $Ca(OH)_2$. Studies conducted on $Ca(OH)_2$ activated fly ash concrete established that 5% $Ca(OH)_2$ addition was effective in reversing the retardation effect of high volume fly ash concrete (Bentz, 2010; Davis 2012). $Ca(OH)_2$ has a high water demand, adopting a higher percentage of $Ca(OH)_2$ has a negative impact on the workability of concrete with low water to cement ratio (Looney and Pavia, 2014; Holland et. al. 2012).

Table 3-13 gives an outline of the 16 concrete mixes that were investigated in the study.

Table 3-13: Concrete Mix Proportions Investigated in the Study

Mix No.	Cementitious Material	W/C Ratio	Total Water (L/m^3)	OPC (kg/m^3)	FA (kg/m^3)	Coarse Aggregate (kg/m^3)	Fine Aggregate (kg/m^3)	Powder Calcium Hydroxide (% of OPC + FA)
1	OPC	0.35	140L	400kg	0kg	1200kg	895kg	5%
2	OPC	0.35	140L	400kg	0kg	1200kg	895kg	0%
3	OPC	0.45	180L	400kg	0kg	1200kg	895kg	5%
4	OPC	0.45	180L	400kg	0kg	1200kg	895kg	0%

Mix No.	Cementitious Material	W/C Ratio	Total Water (L/m^3)	OPC (kg/m^3)	FA (kg/m^3)	Coarse Aggregate (kg/m^3)	Fine Aggregate (kg/m^3)	Powder Calcium Hydroxide (% of OPC + FA)
5	OPC+25% FA	0.35	140L	300kg	100kg	1200kg	895kg	5%
6	OPC+25% FA	0.35	140L	300kg	100kg	1200kg	895kg	0%
7	OPC+25% FA	0.45	180L	300kg	100kg	1200kg	895kg	5%
8	OPC+25% FA	0.45	180L	300kg	100kg	1200kg	895kg	0%
9	OPC+35% FA	0.35	140L	260kg	140kg	1200kg	895kg	5%
10	OPC+35% FA	0.35	140L	260kg	140kg	1200kg	895kg	0%
11	OPC+35% FA	0.45	180L	260kg	140kg	1200kg	895kg	5%
12	OPC+35% FA	0.45	180L	260kg	140kg	1200kg	895kg	0%
13	OPC+50% FA	0.35	140L	200kg	200kg	1200kg	895kg	5%
14	OPC+50% FA	0.35	140L	200kg	200kg	1200kg	895kg	0%
15	OPC+50% FA	0.45	180L	200kg	200kg	1200kg	895kg	5%
16	OPC+50% FA	0.45	180L	200kg	200kg	1200kg	895kg	0%

3.5 Concrete Mix Design Trial Tests

The initial concrete mix designs were subjected to trial tests in order to ascertain the workability of the concrete mixes and also determine the effective superplasticiser to be utilised in the study. Trial tests were done on OPC concrete mixes with varying low water to cement ratios. Five commercially available superplasticisers were used during trial testing and one was adopted for use in this study.

3.6 Concrete Mixing

The study investigated sixteen concrete mix designs outlined in Table 3-14. The mix proportions per cubic metre of concrete are given in Table 3-13. Eight concrete mixes had a w/c ratio of 0.35 and the other eight mixes had a w/c ratio of 0.45. The total mass of cementitious material and aggregate contents were kept constant in all the sixteen concrete mixes. Calcium hydroxide was added to eight concrete mixes in order to activate the fly ash pozzolanic reactions. Two control mixes were prepared for each w/c ratio of 0.35 and 0.45. The control mixes had ordinary Portland cement as the sole cementitious material. The workability of the concrete mixes was controlled using slump tests. The w/c ratios used in the study were low and admixtures were used to improve the workability of concrete. The high range water reducing superplasticiser was added in varying dosages directly to the concrete during concrete mixing. Precaution was taken in order to ensure that there was no bleeding of concrete.

Table 3-14: Concrete Mixes Investigated in the Study

Mix No.	Cementitious	w/c	Calcium Hydroxide
1	OPC	0.35	5%
2	OPC	0.35	0%
3	OPC	0.45	5%
4	OPC	0.45	0%
5	OPC+25% FA	0.35	5%
6	OPC+25% FA	0.35	0%
7	OPC+25% FA	0.45	5%
8	OPC+25% FA	0.45	0%
9	OPC+35% FA	0.35	5%
10	OPC+35% FA	0.35	0%
11	OPC+35% FA	0.45	5%
12	OPC+35% FA	0.45	0%
13	OPC+50% FA	0.35	5%
14	OPC+50% FA	0.35	0%
15	OPC+50% FA	0.45	5%
16	OPC+50% FA	0.45	0%

3.6.1 Mixing of Concrete With w/c Ratio of 0.45

The workability of all concrete mixes with w/c ratio of 0.45 was improved with a superplasticiser which was dosed directly onto the concrete during mixing in order to attain a desired workability with slump value of 65mm±25mm.

Concrete Mix No. 3 and 4

Concrete mix 3 and 4 had the same quantities of concrete constituents with a w/c ratio of 0.45. The difference between the two concrete mixes was that $Ca(OH)_2$ content of 5% of cementitious mass was added to mix 3 whilst no $Ca(OH)_2$ was added to mix 4. The two mixes comprised of OPC as the sole cementitious material. Table 3-15 shows the quantities of the constituents for the two concrete mixes.

Table 3-15: Quantities for Concrete Mix 3 and 4: w/c ratio = 0.45

	OPC (100%)	FA (0%)	Water		Coarse Aggregate	Fine Aggregate	Calcium Hydroxide	Superplasticiser	
			Free Water	Absorption Water				Mass	Ratio to Cementitious Mass
Mix 3	20.4kg	0kg	9.18L	0.944L	61.2kg	45.65kg	1.02kg	124g	0.61%
Mix 4	20.4kg	0kg	9.18L	0.944L	61.2kg	45.65kg	0kg	99g	0.49%

Concrete mix 3 attained a slump of 51mm after adding 124 grams of superplasticiser whilst concrete mix 4 required 99 grams of the superplasticiser in order to achieve a slump of 60mm. Concrete mix 3 required more superplasticiser in order to attain desired workability compared to concrete mix 4. Considering that both concrete mixes had the same quantity of concrete constituents, the differences in superplasticiser requirement can be attributed to the addition of $Ca(OH)_2$. Calcium hydroxide increases the water requirement for concrete hence the higher superplasticiser dosage (Looney and Pavia, 2014; Holland et. al. 2012). Both concrete mixes were cohesive and there was no segregation of concrete. The appearance of the slump for concrete mix 3 is shown in Figure 3.9. The density of fresh concrete was measured and the results are shown in Table 3-16. The density of fresh concrete was measured by using a standard mould for casting concrete cylinders. Fresh concrete was placed in the mould in three layers which were tamped using a standard slump test tamping rod. The fresh concrete density was taken as the mass of fresh concrete divided by the volume of the steel mould.

Table 3-16: Wet Density for Concrete Mix 3 and 4

Concrete Parameter	Quantity	
	Concrete Mix 3	Concrete Mix 4
Wet Mass	13.32kg	13.15kg
Wet Volume	0.0053m^3	0.0053m^3
Wet Density	2509kg/m^3	2481kg/m^3



Figure 3.9: Slump for Concrete Mix 3 with Superplasticiser

Concrete Mix No. 7 and 8

Concrete mix 7 and 8 had similar concrete constituents with w/c ratio of 0.45. The difference between the two mixes was that $Ca(OH)_2$ was added to mix 7 whilst no $Ca(OH)_2$ was added to mix 8. The two mixes comprised of OPC and 25% FA as the binder material. Table 3-17 outlines the quantities of the constituents for Mix 7 and 8.

Table 3-17: Quantities for Concrete Mix 7 and 8: w/c ratio = 0.45

	OPC (75%)	FA (25%)	Water		Coarse Aggregate	Fine Aggregate	Calcium Hydroxide	Superplasticiser	
			Free Water	Absorption Water				Mass	Ratio to Cementitious Mass
Mix 7	15.3kg	5.1kg	9.18L	0.944L	61.2kg	45.65kg	1.02kg	112g	0.55%
Mix 8	15.3kg	5.1kg	9.18L	0.944L	61.2kg	45.65kg	0kg	91g	0.45%

During mixing, the superplasticiser was dosed directly onto the concrete. Concrete mix 7 required 112 grams of superplasticiser in order to attain workability with slump value of 70mm whilst concrete mix 8 required 91 grams of superplasticiser in order to attain workability with a slump value of 40mm. Concrete with $Ca(OH)_2$ required more superplasticiser dosage as a result of $Ca(OH)_2$ having a high-water demand. The concrete from both mixes was cohesive and it did not segregate. The appearance of the concrete slump for concrete mix 7 and 8 is shown in Figure 3.10. The concrete wet density measurements are shown in Table 3-18.

Table 3-18: Wet Density for Concrete Mix 7 and 8

Concrete Parameter	Quantity	
	Concrete Mix 7	**Concrete Mix 8**
Wet Mass	13.1kg	13.2kg
Wet Volume	0.0053m^3	0.0053m^3
Wet Density	2471kg/m^3	2490kg/m^3



Slump for Concrete Mix 7



Slump for Concrete Mix 8

Figure 3.10: Concrete Slump for Mix 7 and 8 With Superplasticiser

Concrete Mix No. 11 and 12

Concrete mix 11 and 12 comprised of OPC and 35% fly ash as the cementitious material. Both mixes had similar concrete constituents with a water to cement ratio of 0.45. The difference between the two mixes was that $Ca(OH)_2$ was added to mix 11 whilst no $Ca(OH)_2$ was added to mix 12. Table 3-19 outlines the quantities of the constituents for the two concrete mixes.

Table 3-19: Quantities for Concrete Mix 11 and 12: w/c ratio = 0.45

	OPC (65%)	FA (35%)	Water		Coarse Aggregate	Fine Aggregate	Calcium Hydroxide	Superplasticiser	
			Free Water	Absorption Water				Mass	Ratio to Cementitious Mass
Mix 11	13.26kg	7.14kg	9.18L	0.944L	61.2kg	45.65kg	1.02kg	97g	0.48%
Mix 12	13.26kg	7.14kg	9.18L	0.944L	61.2kg	45.65kg	0kg	58g	0.28%

Concrete mix 11 attained workability with slump value of 65mm after adding 97 grams of the superplasticiser whilst concrete mix 12 required 58 grams of superplasticiser to attain workability with slump value of 48mm. The concrete that had $Ca(OH)_2$ required higher superplasticiser dosage. The concrete from both mixes was cohesive and did not segregate. The appearance of the concrete slump for mix 11 and 12 is shown in Figure 3.11. The concrete wet density measurements are shown in Table 3-20.

Table 3-20: Wet Density for Concrete Mix 11 and 12

Concrete Parameter	**Quantity**	
	Mix 11	**Mix 12**
Wet Mass	13.30kg	13.34kg
Wet Volume	0.0053m^3	0.0053m^3
Wet Density	2509kg/m^3	2517kg/m^3



Figure 3.11: Slump for Concrete Mix 11 and 12 With Superplasticiser

Concrete Mix No. 15 and 16

Concrete mix 15 and 16 comprised of OPC and 50% fly ash as the cementitious material. Both mixes had similar concrete constituents with a water to cement ratio of 0.45. The difference between the two mixes was that $Ca(OH)_2$ was added to mix 15 whilst no $Ca(OH)_2$ was added to mix 16. Table 3-21 outlines the quantities of the constituents for the two concrete mixes.

Table 3-21: Quantities for Concrete Mix 15 and 16: w/c ratio = 0.45

	OPC (50%)	FA (50%)	Water		Coarse Aggregate	Fine Aggregate	Calcium Hydroxide	Superplasticiser	
			Free Water	Absorption Water				Mass	Ratio to Cementitious Mass
Mix 15	10.2kg	10.2kg	9.18L	0.944L	61.2kg	45.65kg	1.02kg	83g	0.41%
Mix 16	10.2kg	10.2kg	9.18L	0.944L	61.2kg	45.65kg	0kg	33g	0.16%

Concrete mix 15 attained workability with slump value of 58mm after adding 83 grams of the superplasticiser whilst concrete mix 16 required 33 grams of superplasticiser to attain workability with slump value of 57mm. Concrete with $Ca(OH)_2$ required more superplasticiser dosage. The concrete from both mixes was cohesive and it did not segregate. The appearance of the concrete slump for concrete mix 15 and 16 is shown in Figure 3.12. The concrete wet density measurements are shown in Table 3-22.

Table 3-22: Wet Density for Concrete Mix 15 and 16

Concrete Parameter	**Quantity**	
	Mix 15	**Mix 16**
Wet Mass	13.28kg	13.30kg
Wet Volume	0.0053m^3	0.0053m^3
Wet Density	2506kg/m^3	2509kg/m^3



Figure 3.12: Slump for Concrete Mix 15 and 16 with Superplasticiser

Table 3-23: Concrete Slump Values for Concrete with w/c ratio of 0.45

Concrete Mix	Slump Value
Mix 3	51mm
Mix 4	60mm
Mix 7	70mm
Mix 8	40mm
Mix 11	65mm
Mix 12	48mm
Mix 15	58mm
Mix 16	57mm

3.6.2 Mixing of Concrete With w/c Ratio of 0.35

During concrete mixing it was observed that concrete mixes with w/c ratio of 0.35 were dry compared to concrete mixes with w/c ratio of 0.45. Due to the lower water content in mixes with w/c ratio of 0.35, the superplasticiser dosage was high in particular for mixtures with $Ca(OH)_2$ and this resulted in concrete mixes with unrealistically high slump values despite the superplasticiser dosage being kept within the recommended dosage range of between 0.2% and 2% by mass of cementitious material (Sika, 2016).

Concrete Mix No. 1 and 2

Table 3-24 shows the quantities used to produce Concrete Mix 1 and 2. The two mixes had the same quantity of concrete constituents and a w/c ratio of 0.35. The two concrete mixes comprised of OPC as the sole cementitious material. The difference between the two mixes was that $Ca(OH)_2$ was added to concrete mix 1 whilst concrete mix 2 did not contain $Ca(OH)_2$. The content of $Ca(OH)_2$ added to concrete mix 1 was 5% of total mass of cementitious material.

Table 3-24: Quantities for Concrete Mix 1 and 2: w/c ratio = 0.35

	OPC (100%)	FA (0%)	Water		Coarse Aggregate	Fine Aggregate	Calcium Hydroxide	Superplasticiser	
			Free Water	Absorption Water				Mass	Ratio to Cementitious Mass
Mix 1	20.4kg	0kg	7.14L	0.944L	61.2kg	45.65kg	1.02kg	248g	1.22%
Mix 2	20.4kg	0kg	7.14L	0.944L	61.2kg	45.65kg	0 kg	198g	0.97%

During mixing, it was observed that both concrete mixes were dry before the addition of the superplasticiser. 248 grams of the superplasticiser was added to Concrete mix 1 and the slump value measured was 196mm. 198 grams of superplasticiser was added to Concrete mix 2 and the slump value measured was 200mm. The higher slump values for both mixes are attributed to the continuous flow of concrete after removal of slump cone. However, the concrete remained homogenous without any segregation. Figure 3.13 shows the appearance of the concrete slump for mix 1. The concrete wet density was measured and the results are shown in Table 3-25.

Table 3-25: Wet Density for Concrete Mix 1 and 2

Concrete Parameter	Concrete Mix 1	Concrete Mix 2
Wet Mass	13.68kg	13.67kg
Wet Volume	0.0053m^3	0.0053m^3
Wet Density	2581kg/m^3	2579kg/m^3



Figure 3.13: Slump for Concrete Mix 1 With Superplasticiser

Concrete Mix No. 5 and 6

Concrete mix 5 and 6 comprised of OPC and 25% fly ash as the cementitious material. Both mixes had similar concrete constituents with a water to cement ratio of 0.35. The difference between the two mixes was that $Ca(OH)_2$ was added to mix 5 whilst no $Ca(OH)_2$ was added to mix 6. Table 3-26 outlines the quantities of the constituents for both concrete Mix 5 and 6.

Table 3-26: Quantities for Concrete Mix 5 and 6: w/c ratio = 0.35

	OPC (75%)	FA (25%)	Water		Coarse Aggregate	Fine Aggregate	Calcium Hydroxide	Superplasticiser	
			Free Water	Absorption Water				Mass	Ratio to Cementitious Mass
Mix 5	15.3kg	5.1kg	7.14L	0.944L	61.2kg	45.65kg	1.02kg	231g	1.13%
Mix 6	15.3kg	5.1kg	7.14L	0.944L	61.2kg	45.65kg	0kg	124g	0.61%

During mixing, both concrete mixes were dry and the superplasticiser was gradually dosed directly onto the concrete mixes in order to attain workability with target slump value of 130mm±25mm. Concrete mix 5 attained workability with slump value of 105mm after adding 231 grams of the superplasticiser whilst concrete mix 6 required 124 grams of superplasticiser to attain workability with slump value of 126mm. The concrete mix with $Ca(OH)_2$ required more superplasticiser dosage due to the high-

water demand of $Ca(OH)_2$. The concrete slump for both mixes remained homogenous and there was no disintegration of concrete. The concrete wet density measurements are shown in Table 3-27.

Table 3-27: Wet Density for Concrete Mix 5 and 6

Concrete Parameter	Quantity	
	Mix 5	**Mix 6**
Wet Mass	13.36kg	13.20kg
Wet Volume	0.0053m^3	0.0053m^3
Wet Density	2520kg/m^3	2490kg/m^3

Concrete Mix No. 9 and 10

Concrete mix 9 and 10 comprised of OPC and 35% fly ash as the cementitious material. The two mixes had similar concrete constituents with a water to cement ratio of 0.35. The difference between the two mixes was that $Ca(OH)_2$ was added to mix 9 whilst no $Ca(OH)_2$ was added to mix 10. Table 3-28 gives an outline of the constituents for the two concrete mixes.

Table 3-28: Quantities for Concrete Mix 9 and 10: w/c ratio = 0.35

	OPC (65%)	FA (35%)	Water		Coarse Aggregate	Fine Aggregate	Calcium Hydroxide	Superplasticiser	
			Free Water	Absorption Water				Mass	Ratio to Cementitious Mass
Mix 9	13.26kg	7.14kg	7.14L	0.944L	61.2kg	45.65kg	1.02kg	149g	0.73%
Mix 10	13.26kg	7.14kg	7.14L	0.944L	61.2kg	45.65kg	0kg	99g	0.49%

During mixing, the concrete appeared dry and the superplasticiser was gradually dosed in order to attain workability with slump value within the target range. Concrete mix 9 attained workability with slump value of 130mm after adding 149 grams of the superplasticiser whilst concrete mix 10 required 99 grams of superplasticiser to attain workability with slump value of 119mm. The concrete that had $Ca(OH)_2$ required more superplasticiser dosage in order to improve workability. The concrete from both mixes was cohesive and it did not segregate. The concrete wet density measurements are shown in Table 3-29.

Table 3-29: Wet Density for Concrete Mix 9 and 10

Concrete Parameter	Quantity	
	Mix 9	Mix 10
Wet Mass	12.68kg	12.18kg
Wet Volume	0.0053m^3	0.0053m^3
Wet Density	2392kg/m^3	2298kg/m^3

Concrete Mix No. 13 and 14

Concrete mix 13 and 14 comprised of OPC and 50% FA as the cementitious material. Both concretes had similar concrete constituents with a water to cement ratio of 0.35. The difference between the two mixes was that $Ca(OH)_2$ was added to mix 13 whilst no $Ca(OH)_2$ was added to mix 14. Table 3-30 outlines the quantities of the constituents for the two concrete mixes.

Table 3-30: Quantities for Concrete Mix 13 and 14: w/c ratio = 0.35

	OPC (50%)	FA (50%)	Water		Coarse Aggregate	Fine Aggregate	Calcium Hydroxide	Superplasticiser	
			Free Water	Absorption Water				Mass	Ratio to Cementitious Mass
Mix 13	10.2kg	10.2kg	7.14L	0.944L	61.2kg	45.65kg	1.02kg	124g	0.61%
Mix 14	10.2kg	10.2kg	7.14L	0.944L	61.2kg	45.65kg	0kg	91g	0.45%

Concrete mix 13 attained workability with slump value of 199mm after adding 124 grams of the superplasticiser whilst concrete mix 14 required 91 grams of superplasticiser to attain workability with slump value of 151mm. The concrete mix that had $Ca(OH)_2$ required more superplasticiser dosage. The appearance of the concrete slump is shown in Figure 3.14. Table 3-31 shows the wet density measurements.

Table 3-31: Wet Density for Concrete Mix 13 and 14

Concrete Parameter	**Quantity**	
	Mix 13	**Mix 14**
Wet Mass	12.72kg	12.86kg
Wet Volume	0.0053m^3	0.0053m^3
Wet Density	2400kg/m^3	2426kg/m^3



Slump for Concrete Mix 13 Slump for Concrete Mix 14

Figure 3.14: Slump for Concrete Mix 13 and 14 With Superplasticiser

Table 3-32: Concrete Slump Values for Concrete with w/c ratio of 0.35

Concrete Mix	Slump Value
Mix 1	196
Mix 2	200
Mix 5	105
Mix 6	126
Mix 9	130
Mix 10	119
Mix 13	199
Mix 14	151

3.7 Superplasticizer Dosage

Table 3-33 and Figure 3.15 show a summary of the superplasticiser dosages for the 16 concrete mixes. The superplasticiser dosages indicate that OPC concrete required more superplasticiser dosage compared to fly ash concrete in order to achieve similar slump. The dosage of superplasticiser varied significantly with the content of fly ash used in the concrete. It can be observed that as fly ash content increased, the superplasticiser requirement decreased. This is attributed to the ball bearing effect of fly ash spherical shape in improving workability of concrete and resulting in reduced water requirement. The results also indicate that concrete with $Ca(OH)_2$ required more superplasticiser dosage compared to similar concrete without $Ca(OH)_2$. A comparison of the superplasticiser dosages is given in Figure 3.16 which shows line graphs for superplasticiser dosages for the two w/c ratios with and without $Ca(OH)_2$. The concrete with OPC and $Ca(OH)_2$ required a higher superplasticiser dosage in order to achieve similar target slump for each w/c ratio. The differences in superplasticiser dosages were mainly due to w/c ratio, fly ash and $Ca(OH)_2$ contents.

Table 3-33: Superplasticiser Dosage

FA Content	w/c=0.35		w/c=0.45	
	With $Ca(OH)_2$	Without $Ca(OH)_2$	With $Ca(OH)_2$	Without $Ca(OH)_2$
0%	248g	198g	124g	99g
25%	231g	124g	112g	91g
35%	149g	99g	97g	58g
50%	124g	91g	83g	33g

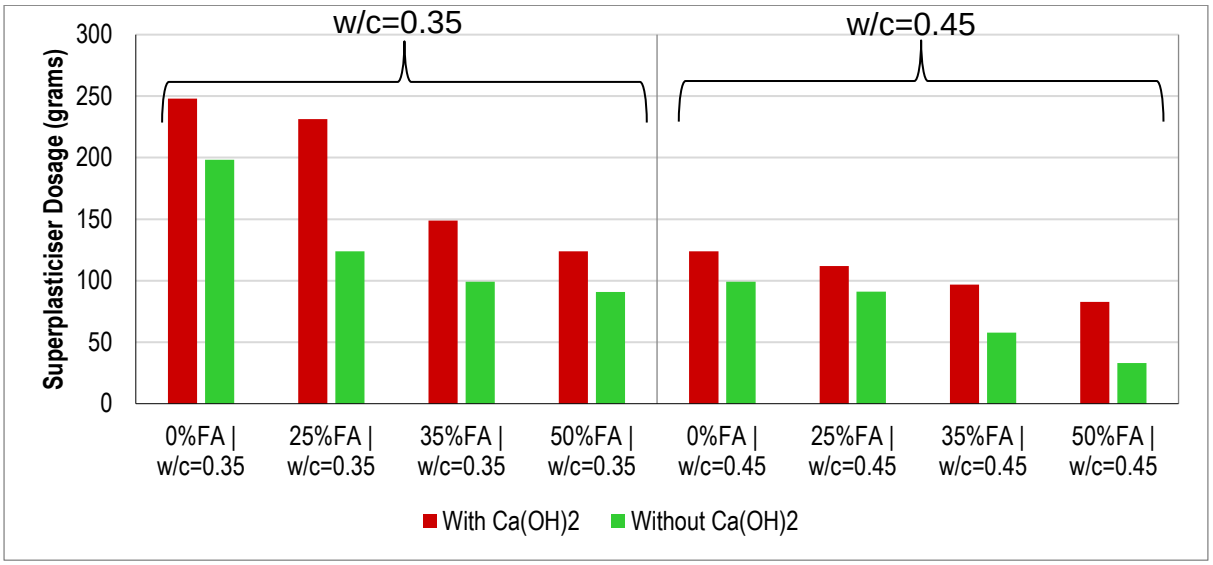

Figure 3.15: Superplasticiser Dosage

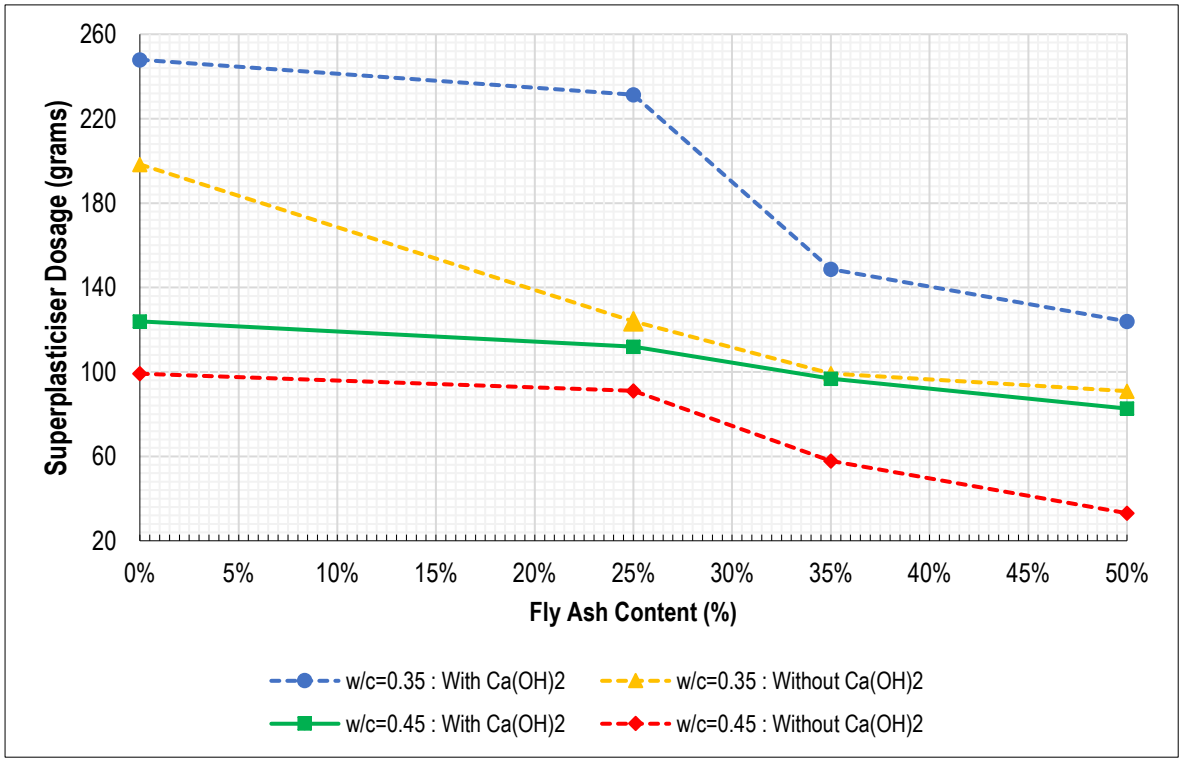

Figure 3.16: Comparison of superplasticiser dosages

3.8 Curing of Concrete

All concrete cubes were moist cured in water for the entire duration of the study. Half of the concrete cubes were cured in water at a temperature of (23±2)ºC and the other cubes were cured in water at a temperature of (40±2)ºC. The higher curing temperature of 40°C was adopted to represent conditions in hot climates. Concrete moulds were placed in air tight plastic bags just after casting the cubes as shown in Figure 3.17. Concrete moulds were then placed in each respective curing bath. Multiple layers of plastic bags were used for each concrete mould in order to stop water penetrating the plastic and getting to the concrete. The concrete cubes were demoulded after 24 hours of curing and they were immediately returned into the curing bath just after demoulding. Figure 3.18 shows the curing bath with concrete cubes.



Figure 3.17: Plastic Wrapped Concrete Moulds in Curing Bath



Figure 3.18: Concrete Cubes in Curing Water Bath

3.9 Hardened Concrete Testing

3.9.1 Compressive Strength Test

The study investigated the influence of high volume fly ash content, curing temperature, w/c ratio and $Ca(OH)_2$ activation on the compressive strength of concrete. Compressive strength tests were conducted on hardened concrete cubes at the ages of 1 day, 3 days, 7 days, 28 days, 90 days and 180 days. The compressive strength tests were conducted in terms of SANS 5863 (2006). A total of 576 concrete cubes of 100mm dimensions were tested for compressive strength. Three concrete cubes from each mix were tested at each age and the average of the three results was adopted as compressive strength. Table 3-34 gives a breakdown of the number of concrete cubes that were tested for compressive strength. Figure 3.19 shows the Amsler Universal Testing machine which was used for compressive strength testing.

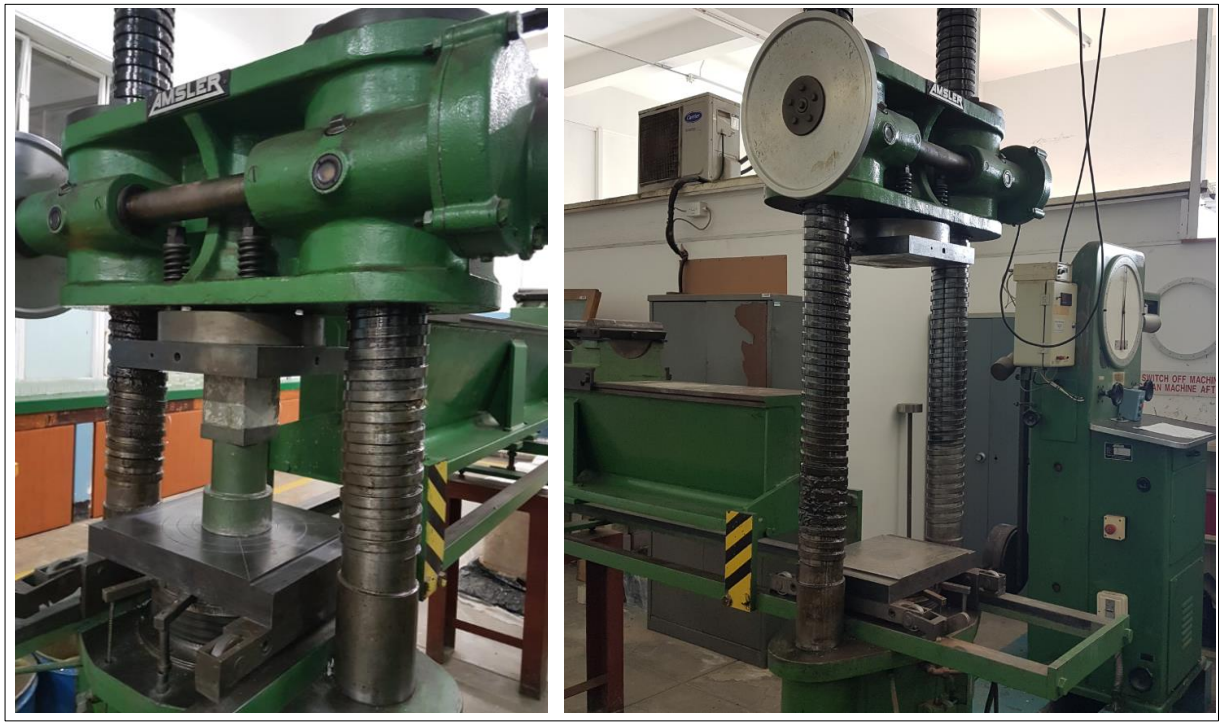

Figure 3.19: Amsler Compressive Strength Testing Machine

Table 3-34: Hardened Concrete Cubes Tested for Compressive Strength

				Number of Concrete Cubes Tested for Compressive Strength												
Mix No.	Cementitious Material	W/C Ratio	$Ca(OH)_2$	23°C Curing Temperature						40°C Curing Temperature						Total
				1 Day	3 Days	7 Days	28 Days	90 Days	180 Days	1 Day	3 Days	7 Days	28 Days	90 Days	180 Days	
1	OPC	0.35	5%	3	3	3	3	3	3	3	3	3	3	3	3	**36**
2	OPC	0.35	0%	3	3	3	3	3	3	3	3	3	3	3	3	**36**
3	OPC	0.45	5%	3	3	3	3	3	3	3	3	3	3	3	3	**36**
4	OPC	0.45	0%	3	3	3	3	3	3	3	3	3	3	3	3	**36**
5	OPC+25% FA	0.35	5%	3	3	3	3	3	3	3	3	3	3	3	3	**36**
6	OPC+25% FA	0.35	0%	3	3	3	3	3	3	3	3	3	3	3	3	**36**
7	OPC+25% FA	0.45	5%	3	3	3	3	3	3	3	3	3	3	3	3	**36**
8	OPC+25% FA	0.45	0%	3	3	3	3	3	3	3	3	3	3	3	3	**36**
9	OPC+35% FA	0.35	5%	3	3	3	3	3	3	3	3	3	3	3	3	**36**
10	OPC+35% FA	0.35	0%	3	3	3	3	3	3	3	3	3	3	3	3	**36**
11	OPC+35% FA	0.45	5%	3	3	3	3	3	3	3	3	3	3	3	3	**36**
12	OPC+35% FA	0.45	0%	3	3	3	3	3	3	3	3	3	3	3	3	**36**
13	OPC+50% FA	0.35	5%	3	3	3	3	3	3	3	3	3	3	3	3	**36**
14	OPC+50% FA	0.35	0%	3	3	3	3	3	3	3	3	3	3	3	3	**36**
15	OPC+50% FA	0.45	5%	3	3	3	3	3	3	3	3	3	3	3	3	**36**
16	OPC+50% FA	0.45	0%	3	3	3	3	3	3	3	3	3	3	3	3	**36**
Total Number of Cubes Cast				**48**	**48**	**48**	**48**	**48**	**48**	**48**	**48**	**48**	**48**	**48**	**48**	**576**

3.9.2 Durability Tests

The study determined the influence of high-volume fly ash content, curing temperature, w/c ratio and $Ca(OH)_2$ activation on the durability of concrete. The South African durability index test methods were used to evaluate the durability properties of concrete. The durability tests that were conducted on concrete specimens are the chloride conductivity index test, water sorptivity index test and the oxygen permeability index test. The tests were conducted in accordance with the South African National Standards and South African durability index testing manual.

Chloride Conductivity Index (CCI) Test

The chloride conductivity index test entails passing electrical current through a concrete specimen saturated with 5M NaCl solution and instantaneously measuring the corresponding voltage and current. The chloride conductivity index test was done in accordance with SANS 3001-CO3-3 (2015) standard. The test was used to determine the chloride conductivity index and porosity of concrete. The specimens for the CCI tests were prepared at the age of 28 days and they consisted of four 30mm thick concrete discs with a diameter of 70mm. The specimens were dried, measured, weighed, vacuum saturated and tested according to the procedure outlined in SANS 3001-CO3-3 (2015). Figure 3.20 shows the vacuum tank apparatus used to saturate the concrete specimens. Figure 3.21 shows the components of the chloride conductivity apparatus and how they are assembled. The chloride conductivity test setup is depicted by the circuit diagram in Figure 3.22. The CCI for each specimen was determined using the relationship between current, voltage and specimen geometry in accordance with SANS 3001-CO3-3 (2015). The Chloride Conductivity Index was taken as the average index of four specimens. The results of the chloride conductivity index tests are presented in Annexure 4. The breakdown of the number of concrete specimens that were tested for chloride conductivity index is shown in Table 3-35



Figure 3.20: Vacuum Saturation Tank Apparatus

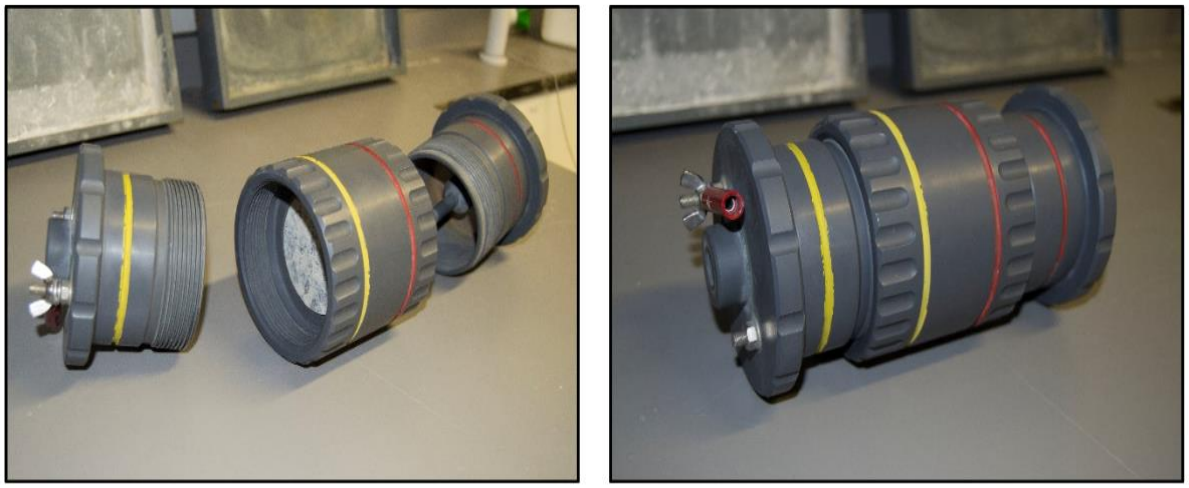

Figure 3.21: Chloride Conductivity Cell (Durability Index Testing Procedure Manual, 2018)

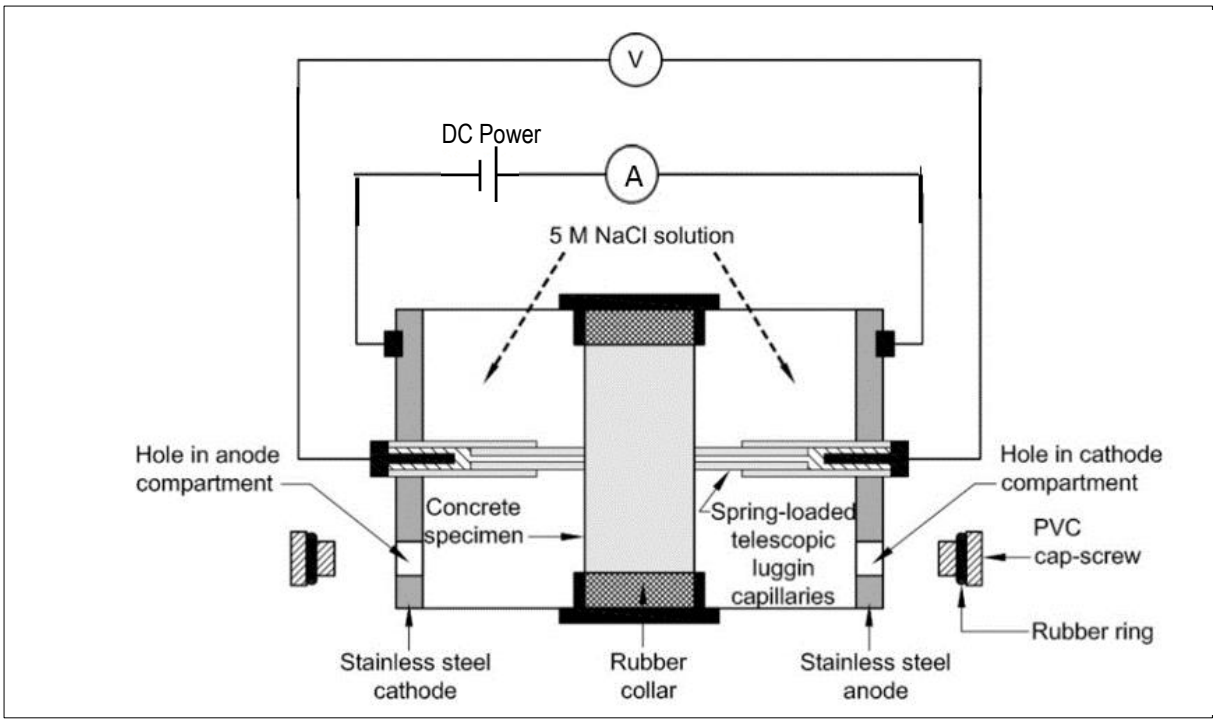

Figure 3.22: Chloride Conductivity Test Circuit Arrangement (SANS 3001-CO3-3:2015)

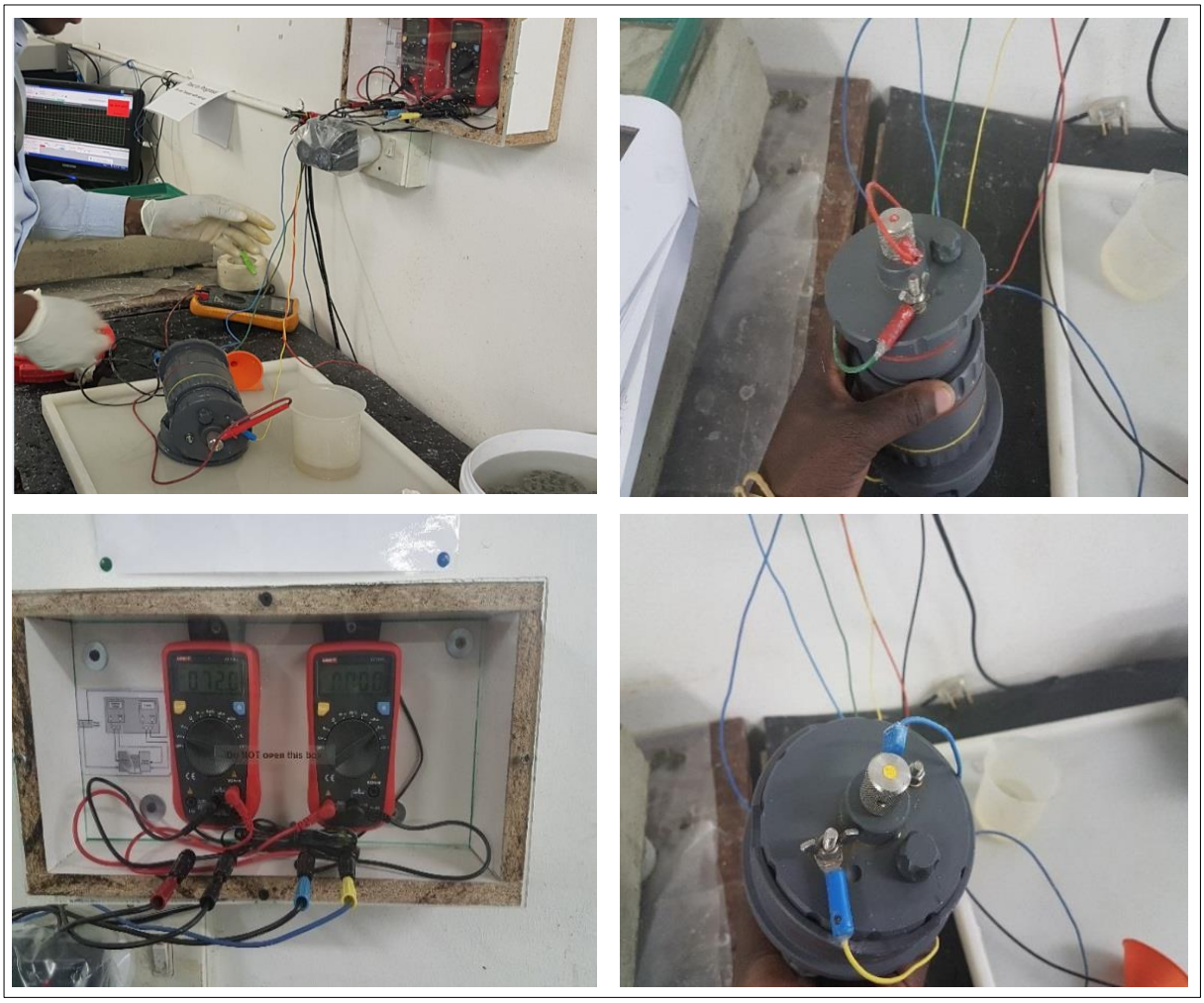

Figure 3.23: Chloride Conductivity Test Apparatus

Table 3-35: Concrete Samples Tested for Chloride Conductivity

						Number of Specimens Tested for CHLORIDE CONDUCTIVITY	
Specimen	**Mix**		**Cementitious Material**	**Activator**	**W/C Ratio**	**23ºC Curing Temperature**	**40ºC Curing Temperature**
OPC Concrete	1		OPC	$CA(OH)_2$	0.35	4	**4**
	2		OPC	None	0.35	4	**4**
	3		OPC	$CA(OH)_2$	0.45	4	**4**
	4		OPC	None	0.45	4	**4**
Fly Ash Concrete	5		OPC + 25% Fly Ash	$CA(OH)_2$	0.35	4	4
	6		OPC + 25% Fly Ash	None	0.35	4	4
	7		OPC + 25% Fly Ash	$CA(OH)_2$	0.45	4	4
	8		OPC + 25% Fly Ash	None	0.45	4	4
	9		OPC + 35% Fly Ash	$CA(OH)_2$	0.35	4	4
	10		OPC + 35% Fly Ash	None	0.35	4	4
	11		OPC + 35% Fly Ash	$CA(OH)_2$	0.45	4	4
	12		OPC + 35% Fly Ash	None	0.45	4	4
	13		OPC + 50% Fly Ash	$CA(OH)_2$	0.35	4	4
	14		OPC + 50% Fly Ash	None	0.35	4	4
	15		OPC + 50% Fly Ash	$CA(OH)_2$	0.45	4	4
	16		OPC + 50% Fly Ash	None	0.45	4	4
Total Number of Concrete Specimens						**64**	**64**
						128	

Oxygen Permeability Index (OPI) Test

The oxygen permeability index test is used to determine the permeability of concrete specimens by measuring the pressure of oxygen passing through a concrete specimen. The OPI test was conducted in accordance with the South African National Standard SANS 3001-CO3-2:2015. The specimens for the OPI tests were prepared at the age of 28 days and they consisted of four 30mm thick concrete discs with a diameter of 70mm. The specimens were dried, measured, weighed, vacuum saturated and tested according to the procedure outlined in SANS 3001-CO3-2 (2015). Figure 3.24 shows the appearance of the oxygen permeability index test specimens. Table 3-36 gives an outline of the quantity of concrete specimens that were tested for oxygen permeability.



Figure 3.24: Oxygen Permeability Index Test Specimens

The oxygen permeability index test apparatus comprises of a pressure vessel, compressible rubber collar, metal sleeve, pressure gauges, transducers, oxygen gas supply and data logger (SANS 3001-CO3-2:2015). The setup of the oxygen permeability test apparatus is shown in Figure 3.25.

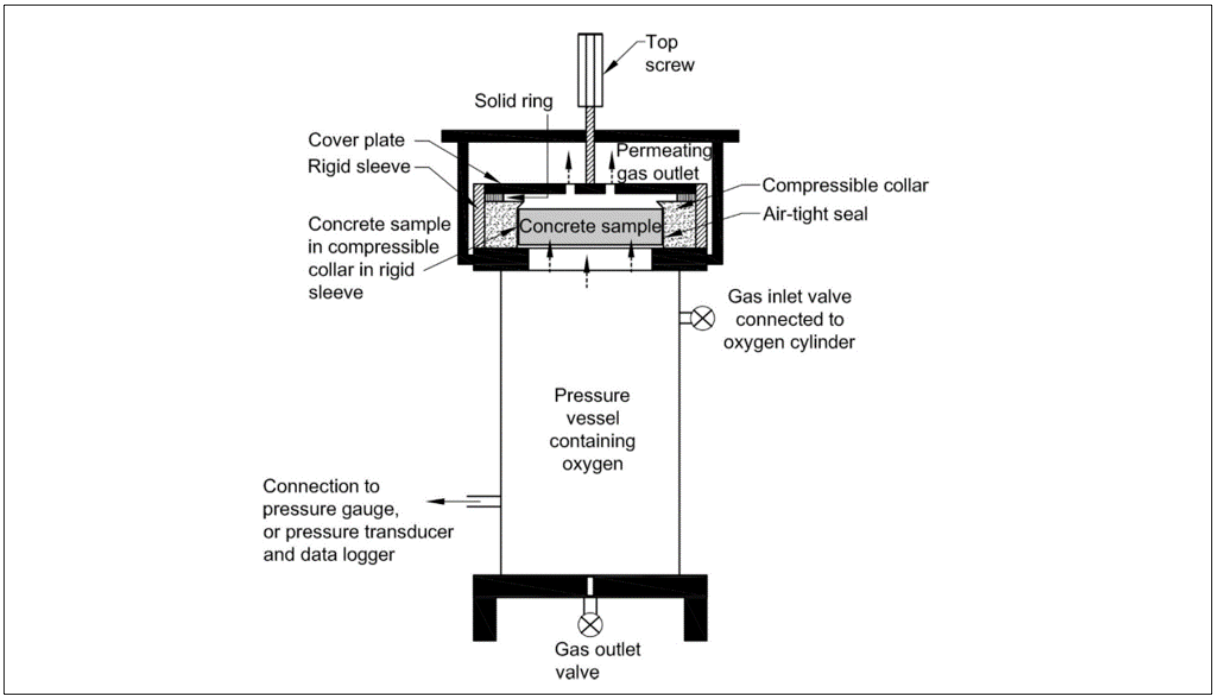

Figure 3.25: Oxygen Permeability Test Setup (Durability Index Testing Procedure Manual, 2018)

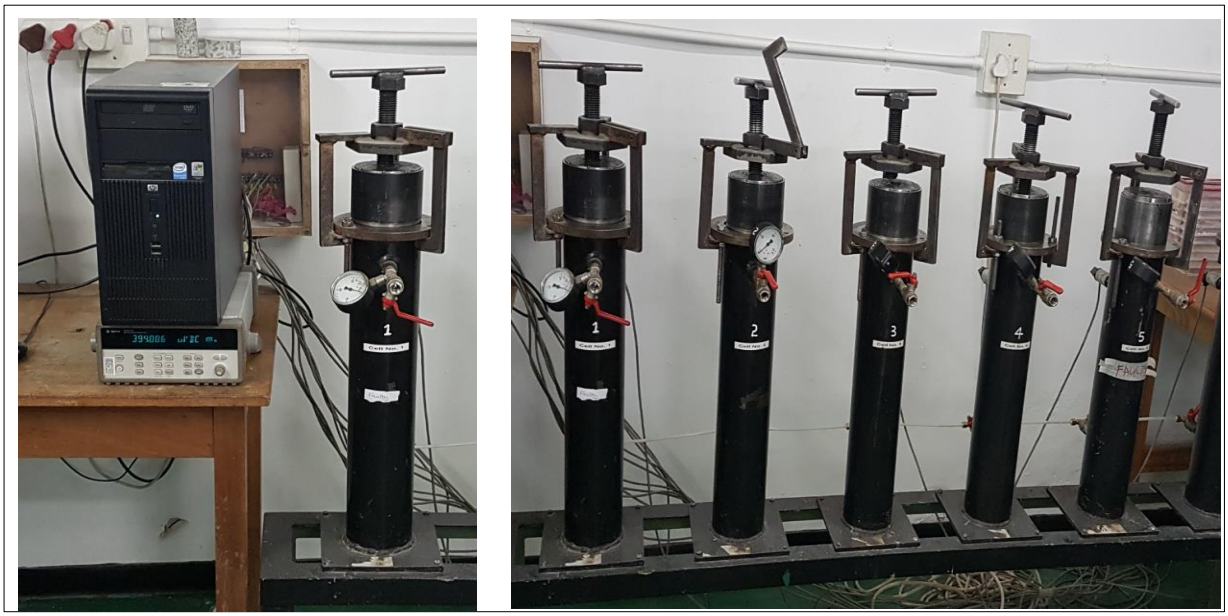

Figure 3.26: Oxygen Permeability Index Test Apparatus

The OPI test entails measuring pressure drop at 15-minute intervals over a period of 6 hours. The results of the OPI tests are shown in detail in Annexure 5. The results of the OPI test were processed using the equations provided in SANS 3001-CO3-2 (2015). The oxygen permeability index is taken as the negative log of the Darcy coefficient of permeability (SANS 3001-CO3-2:2015). The chloride conductivity index is taken as the average OPI of four specimens.

Table 3-36: Concrete Samples for Oxygen Permeability Test

						Number of Specimens Tested for OXYGEN PERMEABILITY	
Specimen	**Mix**		**Cementitious Material**	**Activator**	**W/C Ratio**	**23ºC Curing Temperature**	**40ºC Curing Temperature**
OPC Concrete	1		OPC	$CA(OH)_2$	0.35	4	**4**
	2		OPC	None	0.35	4	**4**
	3		OPC	$CA(OH)_2$	0.45	4	**4**
	4		OPC	None	0.45	4	**4**
Fly Ash Concrete	7		OPC + 25% Fly Ash	$CA(OH)_2$	0.45	4	4
	8		OPC + 25% Fly Ash	None	0.45	4	4
	11		OPC + 35% Fly Ash	$CA(OH)_2$	0.45	4	4
	12		OPC + 35% Fly Ash	None	0.45	4	4
	13		OPC + 50% Fly Ash	$CA(OH)_2$	0.35	4	4
	14		OPC + 50% Fly Ash	None	0.35	4	4
	15		OPC + 50% Fly Ash	$CA(OH)_2$	0.45	4	4
	16		OPC + 50% Fly Ash	None	0.45	4	4
Total Number of Concrete Specimens						**48**	**48**
						96	

Water Sorptivity Index (WSI) Test

The water sorptivity index test was done according to the South African Durability Index Testing Procedure Manual (2018). The test was used to determine the water sorptivity index and porosity of concrete. The test entails placing one flat surface of dry concrete specimens in a calcium hydroxide solution and measuring the mass gain. The specimens were prepared, measured, weighed and vacuum saturated according to the procedure outlined in South African durability index testing procedure manual (2018). Figure 3.27 shows the water sorptivity test setup. The results for the water sorptivity index test are outlined in Annexure 5. The final water sorptivity index is taken as the average water sorptivity index of four specimens. Table 3-37 gives an outline of the quantity of concrete specimens that were tested for water sorptivity.



Figure 3.27: Water Sorptivity Test Setup

Table 3-37: Concrete Samples for Water Sorptivity Test

						Number of Specimens Tested for Water Sorptivity Test	
Specimen	**Mix**		**Cementitious Material**	**Activator**	**W/C Ratio**	**23ºC Curing Temperature**	**40ºC Curing Temperature**
OPC Concrete	1		OPC	$CA(OH)_2$	0.35	4	**4**
	2		OPC	None	0.35	4	**4**
	3		OPC	$CA(OH)_2$	0.45	4	**4**
	4		OPC	None	0.45	4	**4**
Fly Ash Concrete	5		OPC + 25% Fly Ash	$CA(OH)_2$	0.35	4	4
	6		OPC + 25% Fly Ash	None	0.35	4	4
	7		OPC + 25% Fly Ash	$CA(OH)_2$	0.45	4	4
	8		OPC + 25% Fly Ash	None	0.45	4	4
	9		OPC + 35% Fly Ash	$CA(OH)_2$	0.35	4	4
	10		OPC + 35% Fly Ash	None	0.35	4	4
	11		OPC + 35% Fly Ash	$CA(OH)_2$	0.45	4	4
	12		OPC + 35% Fly Ash	None	0.45	4	4
	13		OPC + 50% Fly Ash	$CA(OH)_2$	0.35	4	4
	14		OPC + 50% Fly Ash	None	0.35	4	4
	15		OPC + 50% Fly Ash	$CA(OH)_2$	0.45	4	4
	16		OPC + 50% Fly Ash	None	0.45	4	4
Total Number of Concrete Discs						**64**	**64**
						128	

4. RESULTS AND DISCUSIONS

4.1 Compressive Strength Test Results

Compressive strength is one of the most important properties of concrete. It is usualy used as a concrete specification and often viewed as a measure of the competence of concrete. This section gives a comprehensive discussion on the compressive strength results of concrete. The section presents a comparison of the compressive strength results of fly ash concrete with the results of OPC concrete which was used as the control. The discussion gives more emphasis on the comparison of strength results of 50%FA concrete with those of OPC concrete. The compressive strength tests were conducted at the ages of 1 day, 3 days, 7 days, 28 days, 90 days and 180 days. The concrete cubes were cured in water for the entire duration of the study. The results presented in this section are the average of three compressive strength results as shown by

Equation 4-1.

$$f_{cm} = \frac{\sum_{i=1}^{i=3} f_{ci}}{3} \qquad \text{Equation 4-1}$$

4.1.1 Influence of Fly Ash Content on Compressive Strength

This section focuses on the influence of fly ash content on compressive strength of concrete. The section presents a discussion on the compressive strength results of concrete that had the same w/c ratio and cured at the same temperature. The main variable that forms the basis of discussion in this section is the fly ash content.

Results for Concrete Cured at 23^{0}C without Ca(OH)$_2$ Activator (w/c = 0.45)

Table 4-1 and Figure 4.1 shows the compressive strength results of concrete cubes that were cast without Ca(OH)$_2$ and cured at 23^{0}C. The concrete cubes had a w/c ratio of 0.45 and FA contents of 0%, 25%, 35% and 50% by mass of cementitious material. The results are also presented as line graphs in Figure 9.1 which depicts a comparison of the compressive strength results of concrete with varying amounts of FA.

Table 4-1: Compressive Strength for Concrete Cured at 23^{0}C without Ca(OH)$_2$ Activator (w/c = 0.45)

Age (Days)	Compressive Strength (MPa)			
	0%FA	25%FA	35%FA	50%FA
1	19	16	13	7
3	57	45	27	17
7	69	59	39	25
28	**77**	**85**	**62**	**42**
90	88	107	79	62
180	90	109	89	75

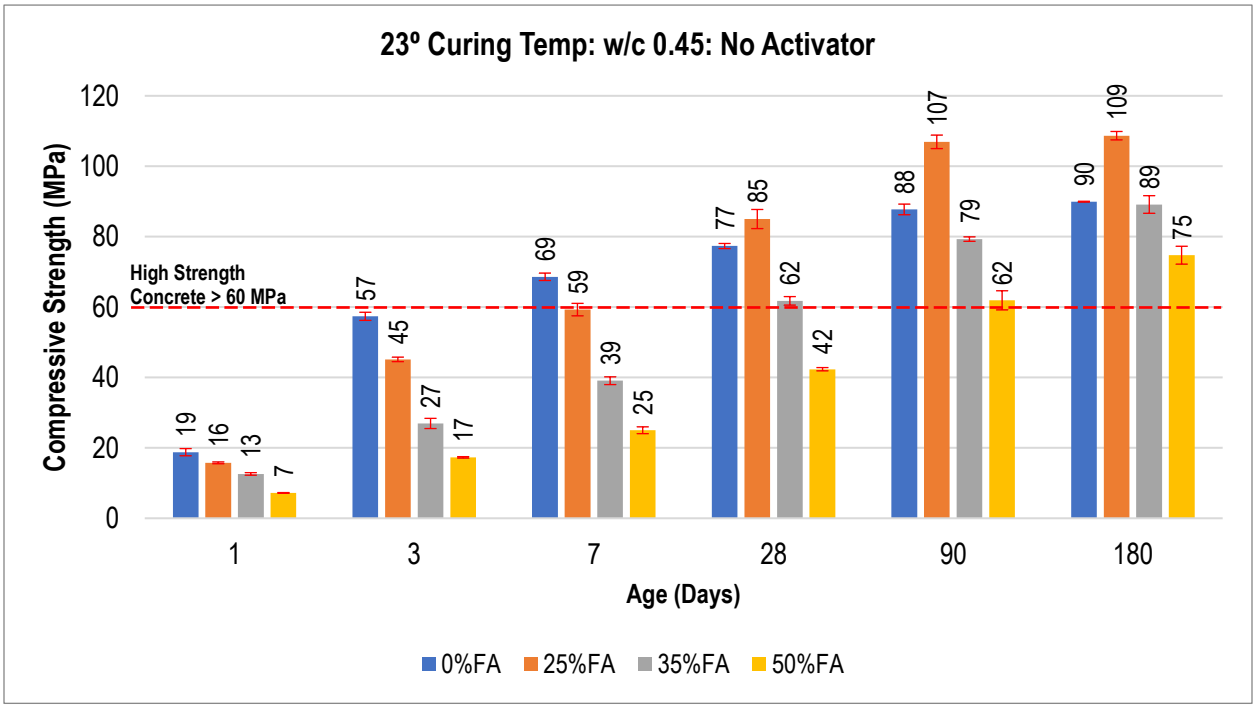

Figure 4.1: Compressive Strength for Concrete Cured at 23^{0}C without Ca(OH)$_2$ Activator (w/c = 0.45)

The compressive strength results indicate that at the early ages of 1 day, 3 days and 7 days the concrete with FA contents of 0% and 25% yielded higher strength. OPC concrete had the highest strength upto the age of 7 days. At later ages of 28 days, 90 days and 180 days the results indicate that the concrete with 25% fly ash content surpassed OPC concrete and yielded the highest compressive strength. The rate of strength gain of FA concrete improved at the age of 28 days and beyond. This can be attributed to the acceleration of pozzolanic reactions resulting from the increased amount of $Ca(OH)_2$ produced by the hydration reaction. Concrete with 50% FA content had the lowest strength at all ages. A comparison of the strength of 50% FA concrete with that of OPC concrete indicates that at early ages of 1 day, 3 days and 7 days, the strength of 50% FA concrete was approximately 34% of the concrete strength of the OPC concrete. Significant strength gain of 50%FA concrete was observed at the age of 28 days, where the strength of 50%FA concrete was 55% of the strength of OPC concrete. At the age of 90 days, the strength of 50%FA concrete increased to approximately 70% of the OPC concrete strength. At the age of 180 days, the 50% FA concrete strength increased to 83% of OPC concrete strength. The strength gain trend indicates that OPC concrete gained the bulk of its strength at early ages owing to the rapid hydration reaction whereas the FA concrete gained the bulk of its strength at later ages of 28 days and beyond due to the delayed pozzolanic reactions which accelerate when more $Ca(OH)_2$ is produced by the hydration reaction. The discussion above is summarised in Table 4-2 which gives an outline of the relative strength of fly ash concrete as a percentage of OPC concrete. Figure 4.2 shows a graphical presentation of the reduction or increase in compressive strength of fly ash concrete as a percentage of OPC concrete compressive strength.

Table 4-2: Relative Strength of Concrete as a Percentage of OPC Concrete Strength (23^oC : Without $Ca(OH)_2$: w/c = 0.45)

Age	**Relative Strength of Concrete as a Percentage of OPC Concrete Strength (%)**			
(Days)	**0%FA**	**25%FA**	**35%FA**	**50%FA**
1	100%	84%	68%	37%
3	100%	79%	47%	30%
7	100%	86%	57%	36%
28	**100%**	**110%**	**81%**	**55%**
90	100%	122%	90%	70%
180	100%	121%	99%	83%

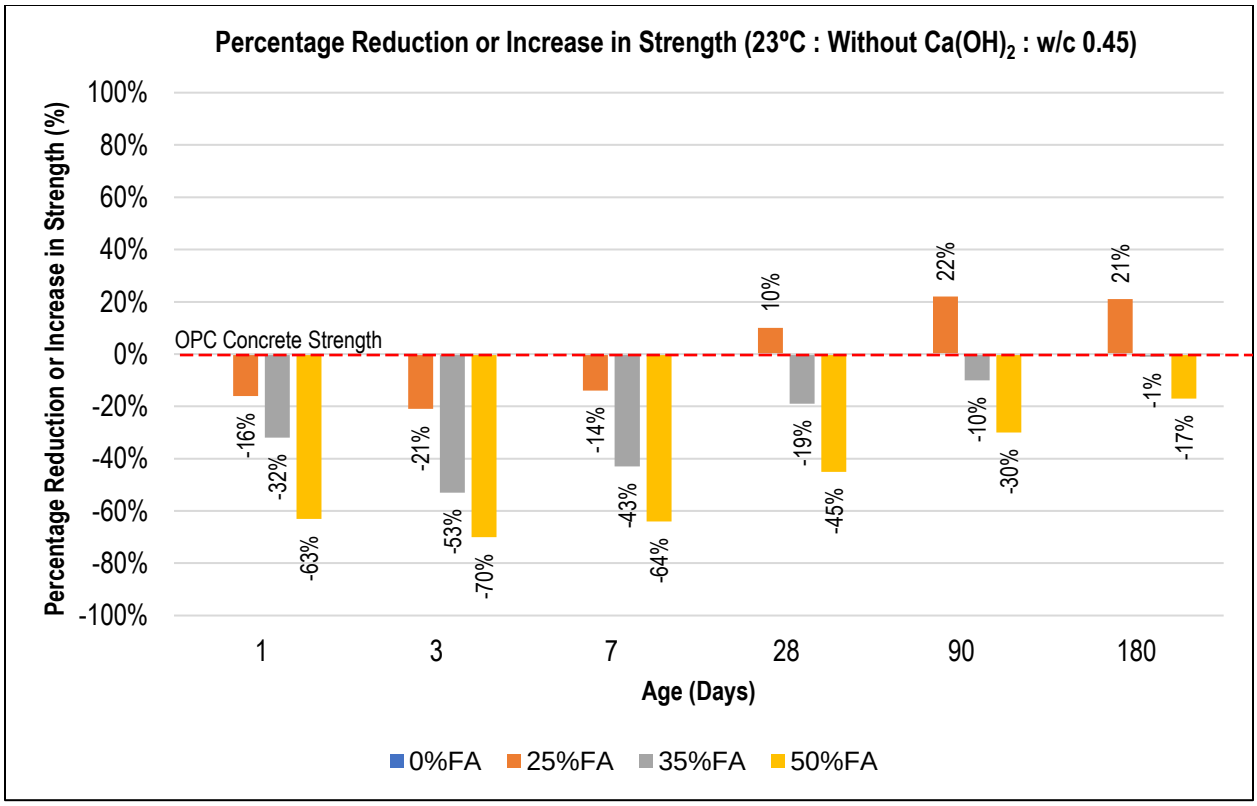

Figure 4.2: Reduction or Increase in Strength as a Percentage of OPC Concrete Strength (23^{0}C : No Activator: w/c = 0.45)

Results for Concrete Cured at 23^{0}C with $Ca(OH)_2$ Activator (w/c = 0.45)

Table 4-3 and Figure 4.3 outline the compressive strength results of concrete cubes that were cured at 23ºC. Calcium hydroxide was added to the concrete in order to activate the fly ash. The concrete had a w/c ratio of 0.45 and varying FA contents of 0%, 25%, 35% and 50% by mass of cementitious material. The results are also presented as line graphs in Figure 9.2 which depicts a comparison of the compressive strength results of concrete with varying amounts of FA.

Table 4-3: Compressive Strength for Concrete Cured at 23^{0}C with $Ca(OH)_2$ Activator (w/c = 0.45)

Age (Days	Compressive Strength (MPa)			
	0%FA	25%FA	35%FA	50%FA
1	24	18	14	9
3	59	44	37	23
7	70	58	48	30
28	**87**	**81**	**70**	**51**
90	92	105	94	71
180	95	109	103	83

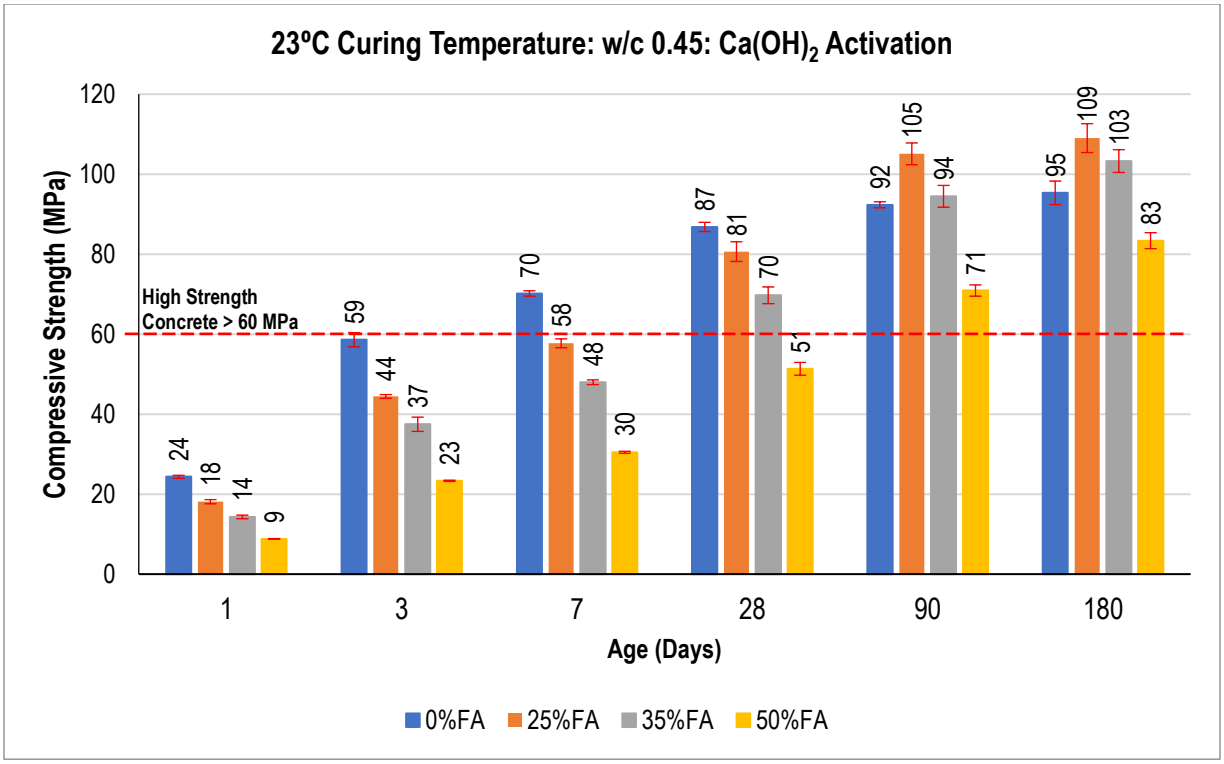

Figure 4.3: Compressive Strength for Cubes Cured at 23°C with $Ca(OH)_2$ Activation (w/c = 0.45)

The results show that during the early ages at 1 day, 3 days, 7 days and 28 days the OPC concrete and 25%FA concrete had higher strength. The OPC concrete had the highest strength upto the age of 28 days. However at the age of 90 days it can be noted that the concrete cubes with 25% and 35% fly ash content yielded higher strength than OPC concrete. When a comparison is made between the results of concrete activated with $Ca(OH)_2$ and the results of concrete without $Ca(OH)_2$ activation, it can be noted that adding $Ca(OH)_2$ to fly ash concrete improves early age strength of fly ash concrete. The strength of concrete with 50%FA was low at the early ages of 1 day, 3 days and 7 days. A comparison of the strength of 50%FA concrete with that of OPC concrete shows that the strength of 50%FA concrete was approximately 40% of the OPC concrete strength during the early ages up-to 7 days. However at 28 days the strength of 50%FA concrete increased to approximately 59% of the 28 day strength of OPC concrete. At the age of 90 days the 50%FA concrete strength was 77% of the OPC concrete strength. Strength gain improvements of 50% FA were also noted at 180 days where the strength of 50% FA concrete was 87% of the OPC concrete strength. The results show that the rate of strength development of 50%FA concrete increased rapidly at 28 days and beyond. This

is an indication of the acceleration of pozzolanic reactions following the precipitation of additional $Ca(OH)_2$ from the hydration reaction. The results indicate that 50%FA concrete activated by $Ca(OH)_2$ gained strength faster than 50%FA concrete without $Ca(OH)_2$ activation. It can also be noted that OPC concrete gained the bulk of its strength at early ages owing to the rapid hydration reaction whereas the 50%FA concrete gained the bulk of its strength at later ages as a result of pozzolanic reactions which accelerated at later ages. This analysis is summarised in Table 4-4 which outlines the relative strength of FA concrete as a percentage of OPC concrete. Figure 4.4 shows the reduction or increase in compressive strength of FA concrete as a percentage of OPC concrete strength.

Table 4-4: Relative Strength of Concrete as a Percentage of OPC Concrete Strength (23^oC : $Ca(OH)_2$ Activator : w/c = 0.45)

Age	Relative Strength as a Percentage of OPC Concrete Strength (%)			
(Days)	0%FA	25%FA	35%FA	50%FA
1	100%	75%	58%	38%
3	100%	75%	63%	39%
7	100%	83%	69%	43%
28	**100%**	**93%**	**80%**	**59%**
90	100%	114%	102%	77%
180	100%	115%	108%	87%

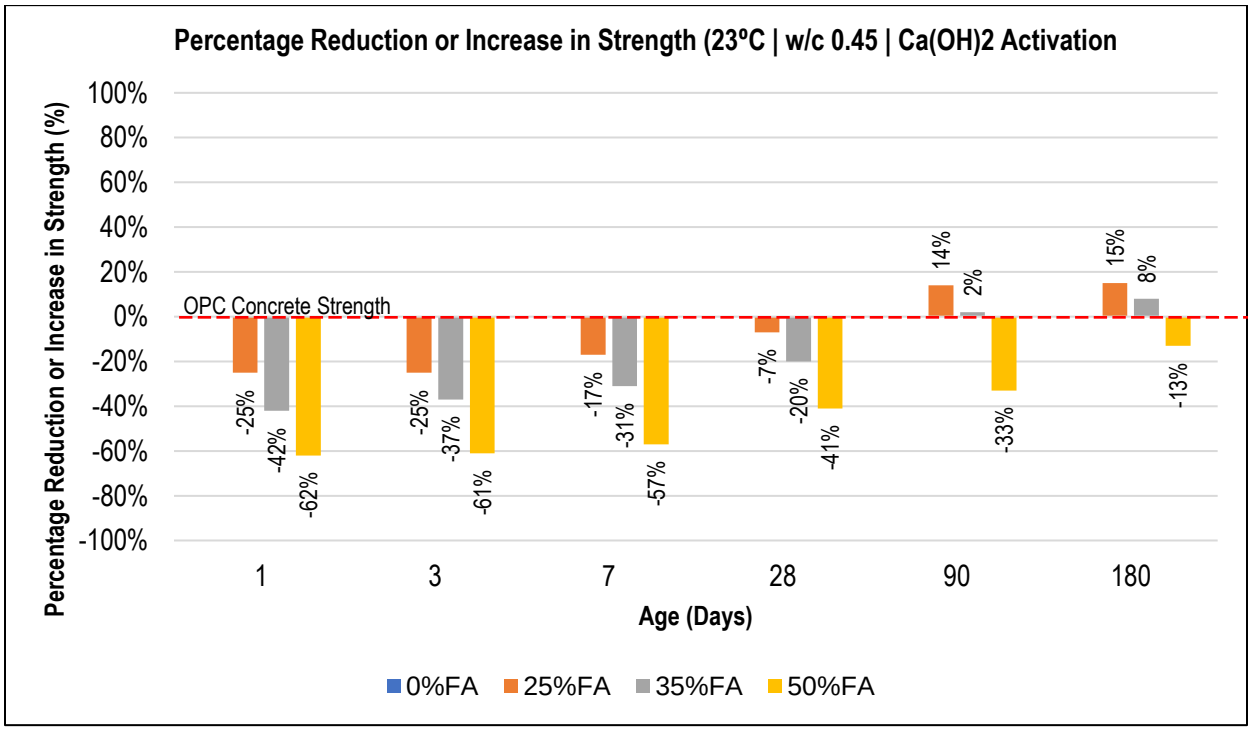

Figure 4.4: Reduction or Increase in Strength as a Percentage of OPC Concrete Strength (23^oC : With $Ca(OH)_2$: w/c = 0.45)

Results for Concrete Cured at 40^{0}C without $Ca(OH)_2$ Activator (w/c = 0.45)

Table 4-5 and Figure 4.5 outline the compressive strength results of concrete cubes that were cast without adding $Ca(OH)_2$ and cured at 40ºC. The cubes were cast using concrete which had a w/c ratio of 0.45 and FA contents of 0%, 25%, 35% and 50% by mass of cementitious material. The results are also presented as line graphs in Figure 9.3 which depicts a comparison of the compressive strength results of concrete with varying amounts of FA.

Table 4-5: Compressive Strength for Concrete Cured at 40^{0}C without $Ca(OH)_2$ Activator (w/c = 0.45)

Age (Days)	Compressive Strength (MPa)			
	0%FA	25%FA	35%FA	50%FA
1	31	25	20	11
3	55	51	38	24
7	63	70	54	36
28	**71**	**98**	**79**	**61**
90	74	105	91	71
180	78	107	94	73

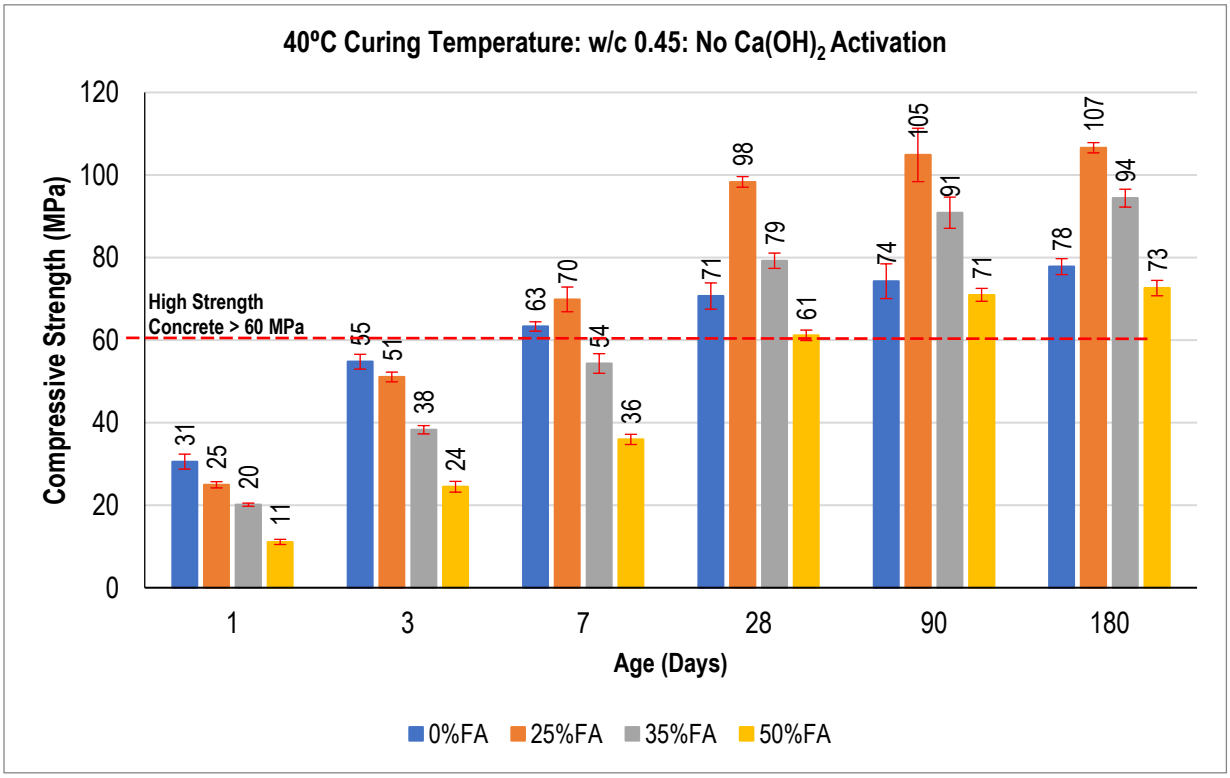

Figure 4.5: Compressive Strength for Concrete Cured at 40^{0}C without $Ca(OH)_2$ Activator (w/c = 0.45)

The results indicate that during the early ages at 1 day and 3 days the OPC concrete and 25%FA concrete had the highest strength. The control OPC concrete had the highest strength at the age of 1 day and 3 days, however at the age of 7 days and beyond, it can be noted that the concrete with 25%FA and 35%FA yielded higher strength than OPC concrete. A comparison of the results of OPC concrete cured at 23^0C to the results of OPC concrete cured at 40ºC indicates that late age strength of OPC concrete is reduced when concrete is cured at high temperature. Comparison of fly ash concrete results indicates that the rate of strength development of FA concrete is accelerated when the concrete is cured at a higher temperature. These results indicate the beneficial effects of heat activation in accelerating pozzolanic reactions between FA and $Ca(OH)_2$. Based on these observations, it can be concluded that high temperature curing reduces late age strength of OPC concrete whilst improving strength of fly ash concrete by accelerating pozzolanic reactions.

When comparing the results of 50% FA concrete with the results of OPC concrete, it can be noted that the strength of 50% FA concrete was approximately 35% of the strength of OPC concrete at the age of 1 day. At the ages of 3 days the relative strength of 50%FA concrete increased to approximately 44% of the strength of OPC concrete. At 28 days the strength of 50% OPC concrete was 86% of the strength of OPC concrete. Significant strength improvements of 50% FA concrete were noted at the ages of 90 days and 180 days where the strength of 50%FA concrete was approximately 94% of the OPC concrete strength. The results indicate that 50% FA concrete gained strength rapidly when it was cured at a high temperature of 40ºC. This observation confirms that pozzolanic reactions between FA and $Ca(OH)_2$ are accelerated by high temperature curing. The discussion above is summarized in Table 4-6 which outlines the relative strength of fly ash concrete as a percentage of OPC concrete. Figure 4.6 shows the reduction or increase in compressive strength of fly ash concrete as a percentage of OPC concrete strength.

Table 4-6: Relative Strength of Concrete as a Percentage of OPC Concrete Strength (40^0C : No Activator : w/c = 0.45)

Age (Days)	Relative Strength as a Percentage of OPC Concrete Strength (%)			
	0%FA	25%FA	35%FA	50%FA
1	100%	81%	65%	35%
3	100%	93%	69%	44%
7	100%	111%	86%	57%
28	**100%**	**138%**	**111%**	**86%**
90	100%	142%	123%	96%
180	100%	137%	121%	94%

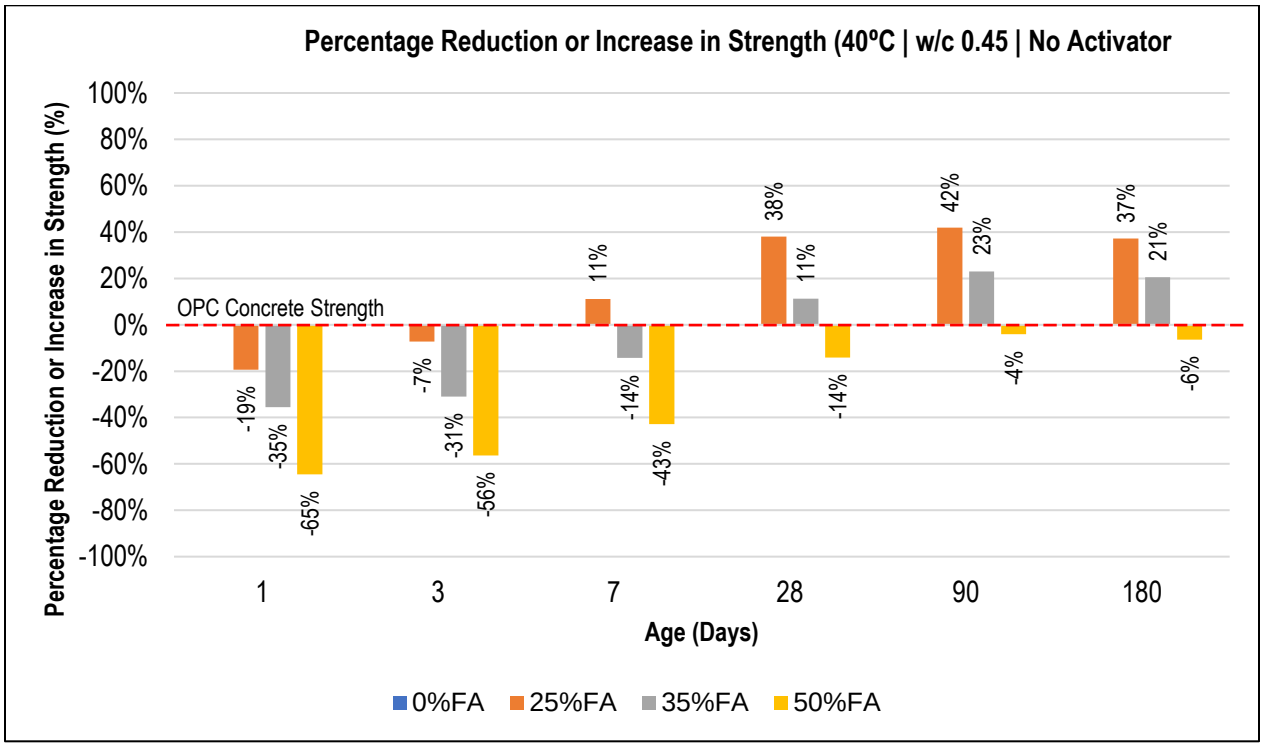

Figure 4.6: Reduction or Increase in Strength as a Percentage of OPC Concrete Strength (40^0C:Without $Ca(OH)_2$:w/c = 0.45)

Results for Concrete Cured at 40^0C with $Ca(OH)_2$ Activator (w/c = 0.45)

Table 4-7 and Figure 4.7 outline the compressive strength results of concrete activated with $Ca(OH)_2$ and cured at 40^0C. The concrete cubes were cast using concrete which had a w/c ratio of 0.45 and FA contents of 0%, 25%, 35% and 50% by mass of cementitious material. The results are also presented as line graphs in Figure 9.4 which depicts a comparison of the compressive strength results of concrete with varying amounts of FA.

Table 4-7: Compressive Strength for Cubes Cured at 40^{0}C with $Ca(OH)_2$ Activator (w/c = 0.45)

Age (Days)	Compressive Strength (MPa)			
	0%FA	25%FA	35%FA	50%FA
1	33	31	21	13
3	58	52	43	32
7	68	73	61	47
28	**76**	**97**	**88**	**70**
90	78	106	102	84
180	82	108	107	86

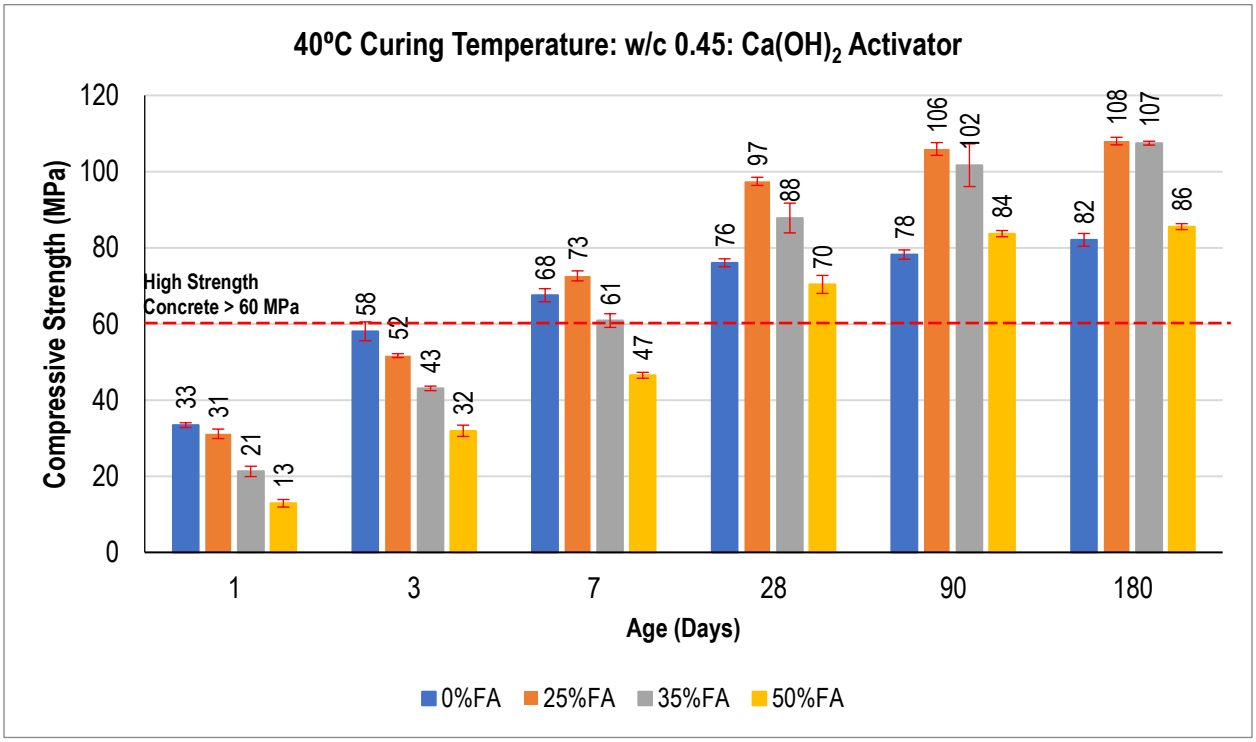

Figure 4.7: Compressive Strength for Concrete Cured at 40^{0}C with $Ca(OH)_2$ Activator (w/c = 0.45)

The results indicate that at the ages of 1 day and 3 days, OPC concrete and 25%FA concrete had higher strength. The control OPC concrete had the highest strength at the ages of 1 day and 3 days. However, at the age of 28 days it can be noted that the concrete with 25% and 35% fly ash content yielded higher strength than the OPC concrete. At the ages of 90 days and 180 days the strength of all concretes cubes with fly ash surpassed the strength of OPC concrete. The strength development pattern of $Ca(OH)_2$ activated concrete cured at 40ºC indicates that late age strength gain of OPC concrete is reduced when concrete is cured at high temperature. However, the strength development patterns

of FA concrete indicate that the rate of strength gain of FA concrete is accelerated when the concrete is cured at a higher temperature and activated with $Ca(OH)_2$. This indicates the influence of $Ca(OH)_2$ activation and high temperature curing on accelerating pozzolanic reactions in fly ash concrete.

A comparison of the compressive strength results of 50% FA concrete with that of OPC concrete indicates that the strength of 50% FA concrete was approximately 40% of the OPC concrete strength at the age of 1 day. At the age of 3 days the strength of 50% FA concrete increased to 55% of the 3-day strength of OPC concrete. At the age of 7 days the strength of 50% FA concrete was approximately 70% of the strength of OPC concrete. At 28 days the strength of 50% OPC concrete increased to 92% of the strength of OPC concrete. It can be observed that at 90 days and 180 days the strength of 50%FA concrete exceeded the strength of OPC concrete. The results indicate that the 50%FA concrete gained strength rapidly when it was subjected to high temperature curing and $Ca(OH)_2$ activation. The results show the effect of high temperature curing and $Ca(OH)_2$ activation on pozzolanic reaction between FA and $Ca(OH)_2$. The discussion above is summarised in Table 4-8 which outlines the relative strength of fly ash concrete as a percentage of OPC concrete. Figure 4.8 shows the reduction or increase in compressive strength of fly ash concrete as a percentage of OPC concrete strength.

Table 4-8: Relative Strength of Concrete as a Percentage of OPC Concrete Strength (40^oC : $Ca(OH)_2$ Activator : w/c = 0.45)

Age	**Relative Strength as a Percentage of OPC Concrete Strength (%)**			
(Days)	**0%FA**	**25%FA**	**35%FA**	**50%FA**
1	100%	94%	64%	39%
3	100%	90%	74%	55%
7	100%	107%	90%	69%
28	**100%**	**128%**	**116%**	**92%**
90	100%	136%	131%	108%
180	100%	132%	132%	105%

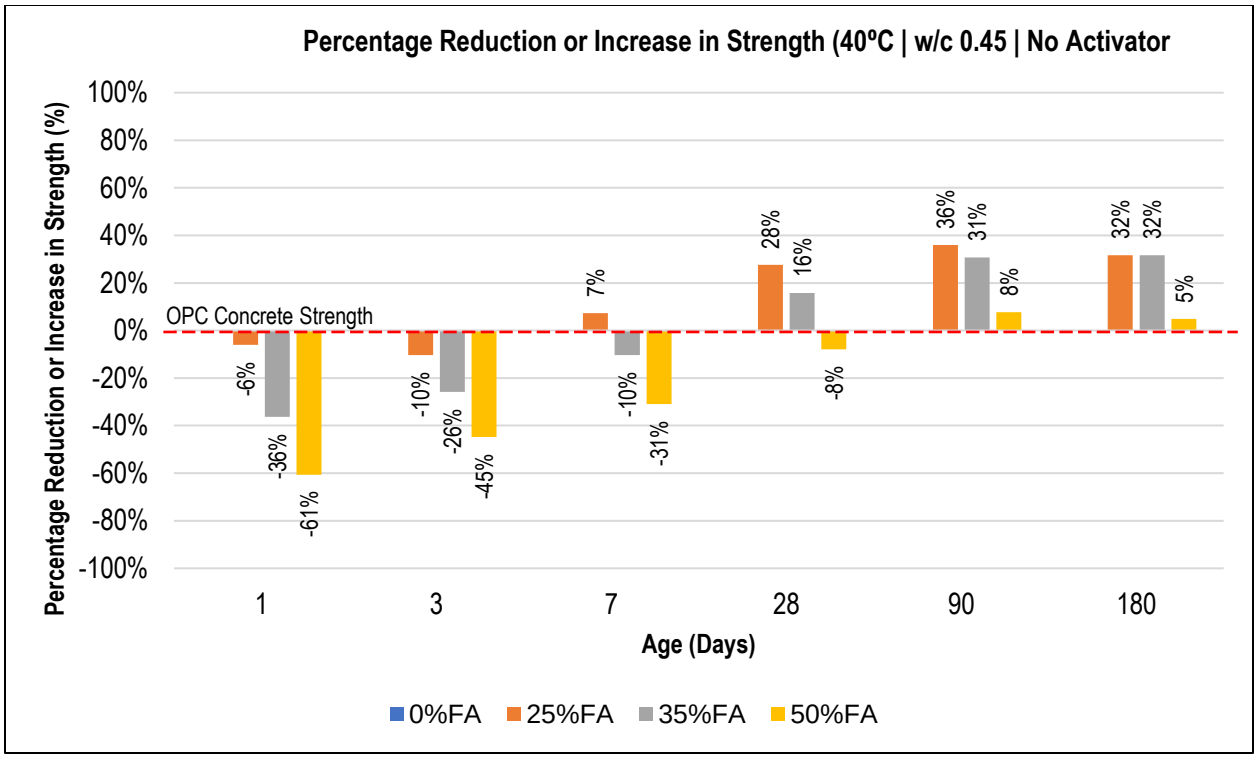

Figure 4.8: Reduction or Increase in Strength as a Percentage of OPC Concrete Strength (40^{0}C : With $Ca(OH)_2$: w/c = 0.45)

Results for Concrete Cured at 23^{0}C without $Ca(OH)_2$ Activation (w/c = 0.35)

Table 4-9 and Figure 4.9 outline the compressive strength results of concrete cubes that were cast without adding $Ca(OH)_2$ and cured at 23^{0}C. The cubes were cast using concrete with a w/c ratio of 0.35 and FA content of 0%, 25%, 35% and 50% by mass of cementitious material. The results are also presented as line graphs in Figure 9.5 which depicts a comparison of the compressive strength results of concrete with varying amounts of FA.

Table 4-9: Compressive Strength for Concrete Cured at 23^{0}C without $Ca(OH)_2$ Activator (w/c = 0.35)

Age (Days)	Compressive Strength (MPa)			
	0%FA	25%FA	35%FA	50%FA
1	55	31	28	21
3	90	58	51	34
7	98	75	64	44
28	**120**	**101**	**90**	**67**
90	124	126	100	89
180	126	128	104	105

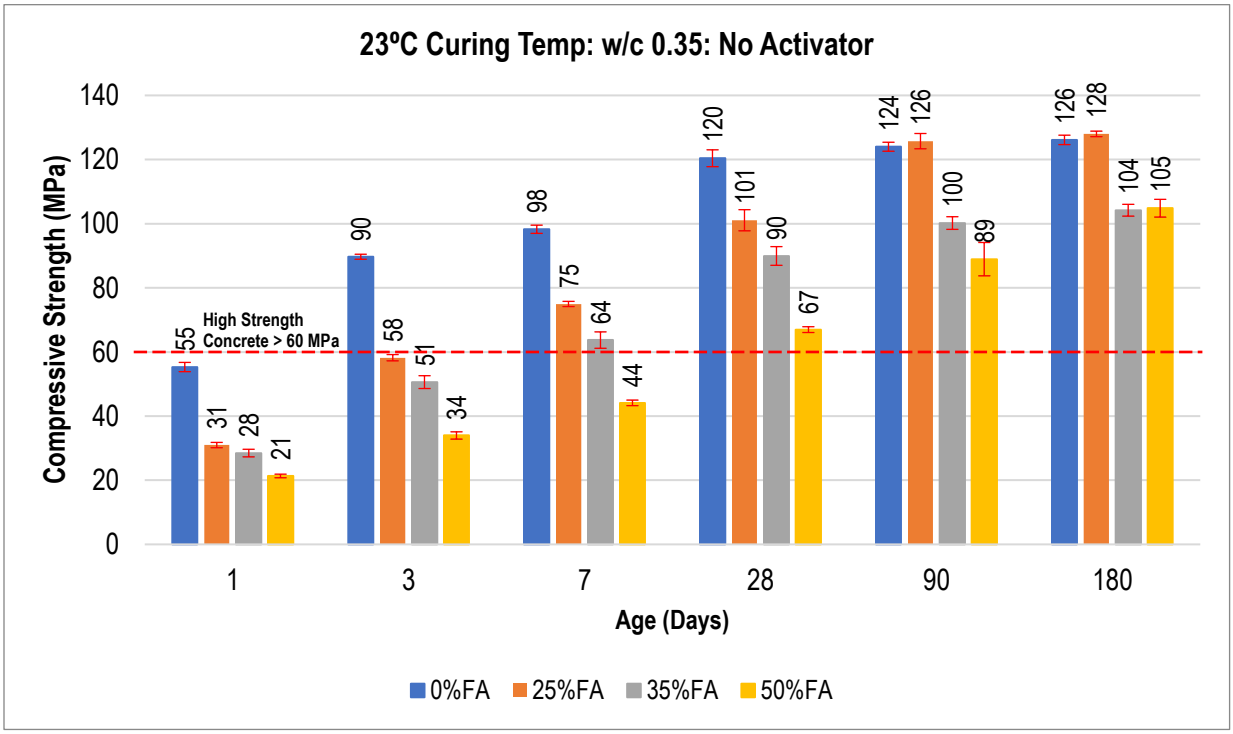

Figure 4.9: Compressive Strength for Concrete Cured at 23^{0}C without $Ca(OH)_2$ Activator (w/c = 0.35)

The compressive strength results indicate that OPC concrete had the highest strength at early ages upto 28 days. At 90 days and 180 days, the strength of OPC concrete was surpassed by the compressive strength of 25%FA concrete. It can be observed that the rate of strength gain of FA concrete increased at later ages. A comparison of the strength of 50% FA concrete with that of OPC concrete indicates that at early ages of 1 and 3 days, the strength of 50% FA concrete was approximately 38% of the concrete strength of the OPC concrete. Significant strength gain of 50%FA concrete was observed at the age of 28 days, where the strength of 50% FA concrete was 56% of the 28 day strength of OPC concrete. At the age of 90 days the 50% FA concrete strength was 72% of the 90 day strength of OPC concrete. At the age of 180 days the strength of 50% OPC concrete increased to 83% of the OPC concrete strength. The results indicate that 50% FA concrete gained strength significantly at later ages of 28 days and beyond. This points to the delayed pozzolanic reactions which accelerate with concrete age as more $Ca(OH)_2$ is produced during the hydration process. The discussion above is summarised in Table 4-10 which outlines the relative strength of fly ash concrete as a percentage of OPC

concrete. Figure 4.10 shows the change in compressive strength of fly ash concrete as a percentage of OPC concrete strength.

Table 4-10: Relative Strength of Concrete as a Percentage of OPC Concrete Strength (23^{0}C : No Activator : w/c = 0.35)

Age (Days)	Relative Strength as a Percentage of OPC Concrete Strentgh (%)			
	0%FA	25%FA	35%FA	50%FA
1	100%	56%	51%	38%
3	100%	64%	57%	38%
7	100%	77%	65%	45%
28	**100%**	**84%**	**75%**	**56%**
90	100%	102%	81%	72%
180	100%	102%	83%	83%

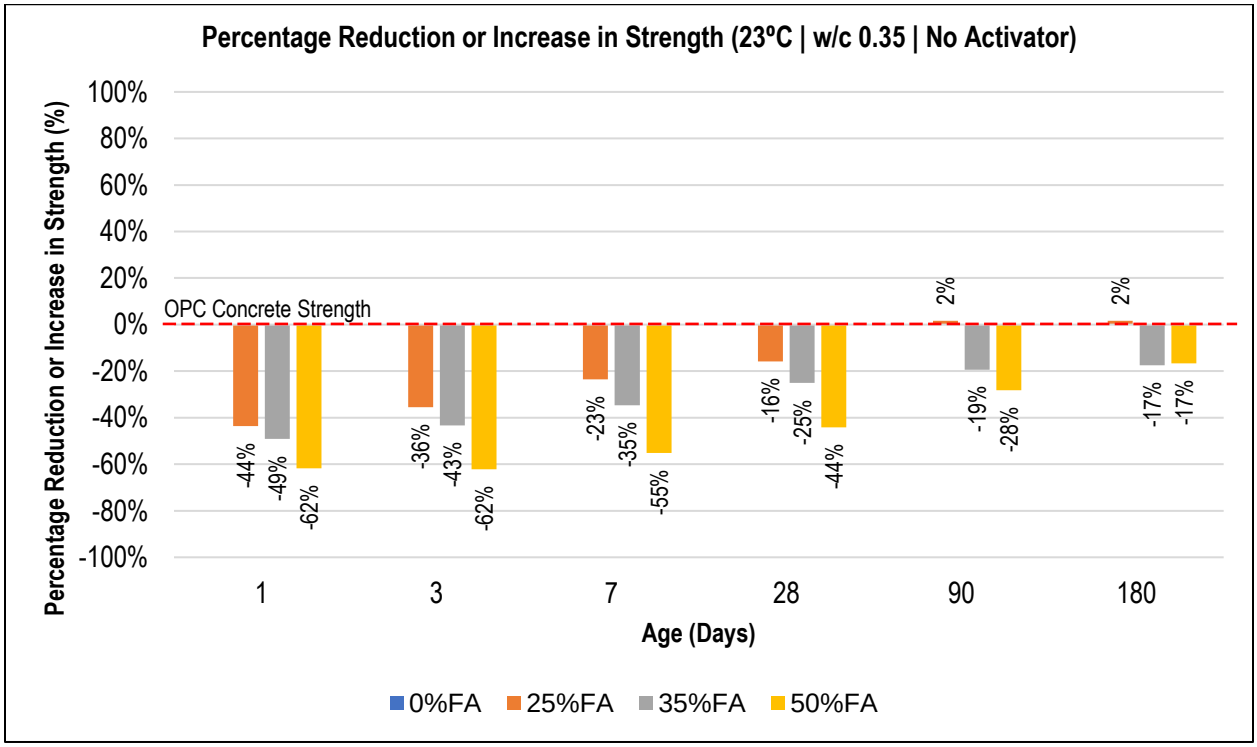

Figure 4.10: Reduction or Increase in Strength as a Percentage of OPC Concrete Strength (23^{0}C : No Activator : w/c = 0.35)

Results for Concrete Cured at 23^{0}C with $Ca(OH)_2$ Activation (w/c = 0.35)

Table 4-11 and Figure 4.11 outline the compressive strength results of concrete cubes that were cast using concrete which was activated by $Ca(OH)_2$ and cured at 23^{0}C. The concrete used to cast the cubes had a w/c ratio of 0.35 and FA contents of 0%, 25%, 35%

and 50% by mass of cementitious material. The results are also presented as line graphs in Figure 9.6 which depicts a comparison of the compressive strength results of concrete with varying amounts of FA.

Table 4-11: Compressive Strength for Concrete Cured at 23^{0}C with $Ca(OH)_2$ Activation (w/c = 0.35)

Age (Days)	Compressive Strength (MPa)			
	0%FA	25%FA	35%FA	50%FA
1	59	35	32	22
3	81	62	50	38
7	95	82	69	49
28	**115**	**108**	**96**	**77**
90	120	121	105	105
180	122	124	113	115

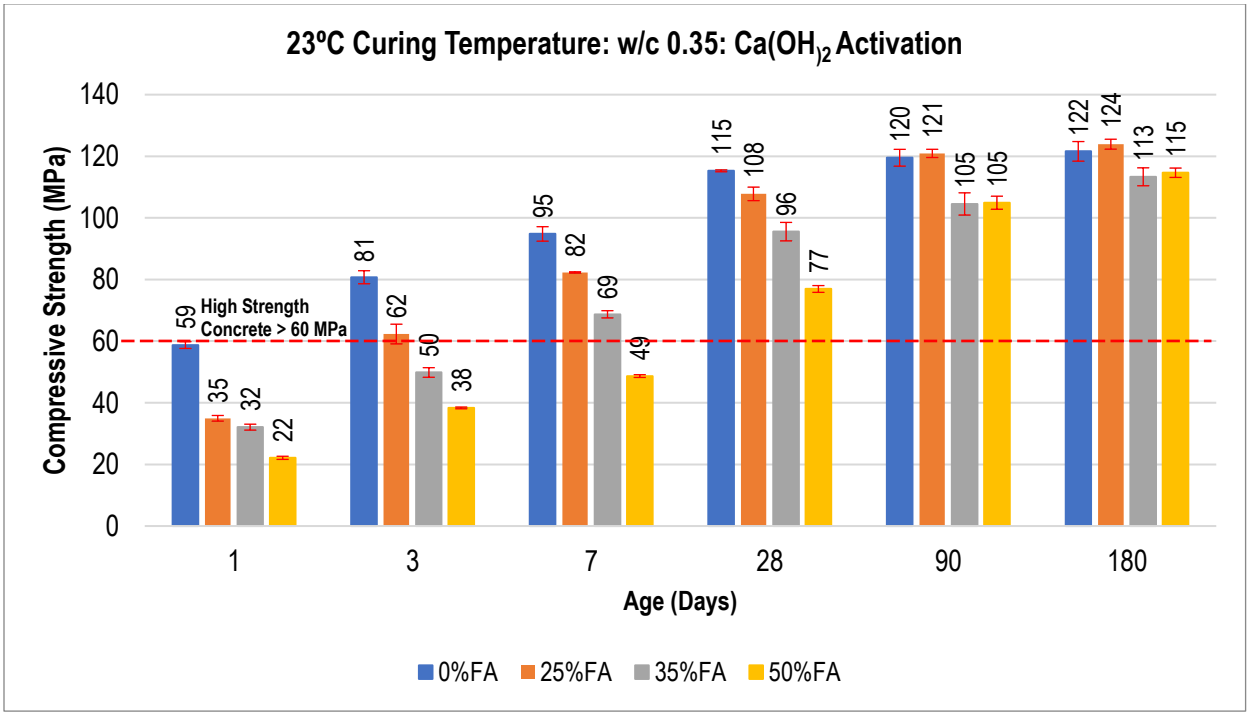

Figure 4.11: Compressive Strength for Concrete Cured at 23^{0}C with $Ca(OH)_2$ Activation (w/c = 0.35)

The compressive strength results show that during the early ages of 1 day, 3 days, 7 days and 28 days the OPC concrete and 25%FA concrete had higher strength. The OPC concrete had the highest strength upto 28 days. However at the age of 90 days and 180 days it can be noted that concrete with 25% fly ash concrete yielded slightly higher

strength than OPC concrete. When the results of concrete activated with $Ca(OH)_2$ are compared to the results of concrete without $Ca(OH)_2$, it can be established that adding $Ca(OH)_2$ improves early age strength of FA concrete. A comparison of the strength of 50%FA concrete with that of OPC concrete indicates that the strength of 50% FA concrete was approximately 37% of the concrete strength of OPC concrete at the age of 1 day. However at the ages of 3 days and 7 days the strength of 50%FA concrete increased to approximately half the 28 day strength of OPC concrete. At the age of 28 days the strength of 50%FA concrete was 67% of the 28 day strength of OPC concrete. At the age of 90 days the 50%FA concrete strength was 88% of the OPC concrete strength. Further improvement of the strength of 50%FA concrete was noted at 180 days where the strength was 94% of the OPC concrete strength. The results show that the strength of 50%FA concrete increased rapidly at 28 days and beyond. The results indicate that the 50%FA concrete activated by $Ca(OH)_2$ gained strength faster that 50%FA concrete without $Ca(OH)_2$ activation. The discussion above is summarised in Table 4-12 which outlines the relative strength of fly ash concrete as a percentage of OPC concrete. Figure 4.12 shows the reduction or increase in compressive strength of fly ash concrete as a percentage of OPC concrete strength.

Table 4-12: Relative Strength of Concrete as a Percentage of OPC Concrete Strength (23^oC : $Ca(OH)_2$ Activator : w/c = 0.35)

Age (Days)	Relative Strength as a Percentage of OPC Concrete Strength (%)			
	0%FA	25%FA	35%FA	50%FA
1	100%	59%	54%	37%
3	100%	77%	62%	47%
7	100%	86%	73%	52%
28	**100%**	**94%**	**83%**	**67%**
90	100%	101%	88%	88%
180	100%	102%	93%	94%

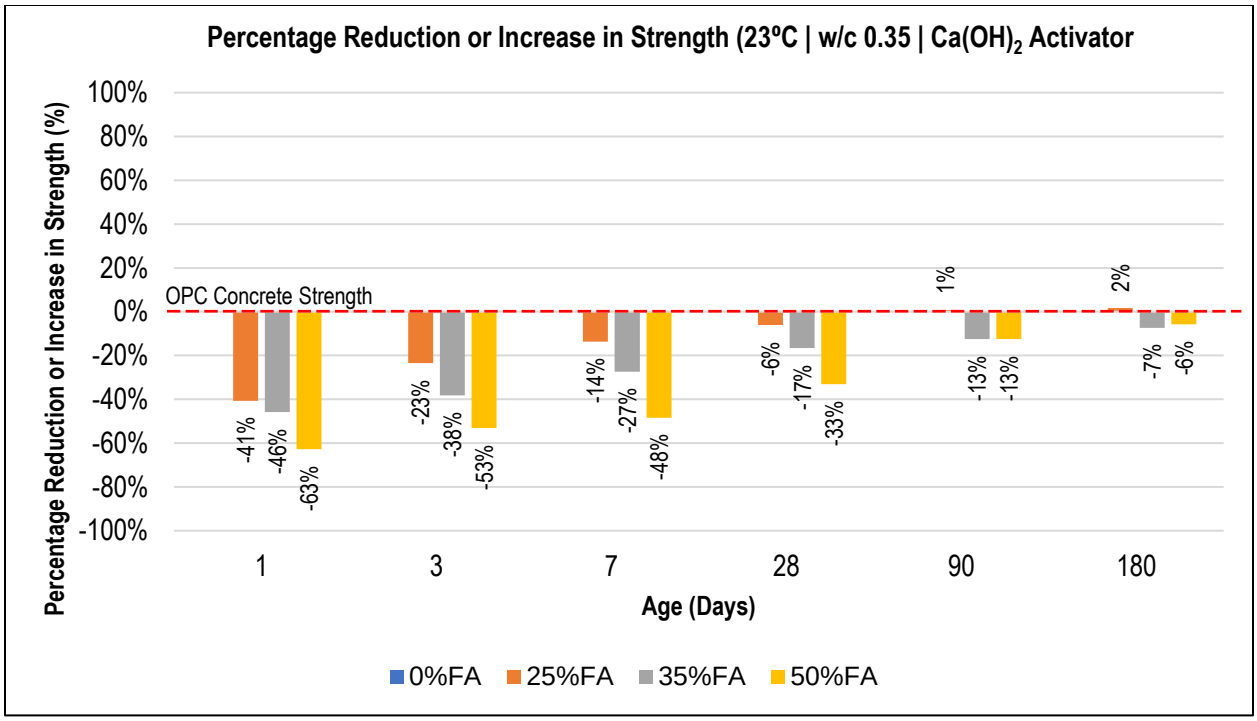

Figure 4.12: Reduction or Increase in Strength as a Percentage of OPC Concrete Strength (23^0C : $Ca(OH)_2$: w/c= 0.35)

Results for Concrete Cured at 40^0C without $Ca(OH)_2$ Activator (w/c = 0.35)

Table 4-13 and Figure 4.13 outline the compressive strength results of concrete cubes that were cast without $Ca(OH)_2$ and cured at 40^0C. The cubes were cast using concrete which had a w/c ratio of 0.35 and FA contents of 0%, 25%, 35% and 50% by mass of cementitious material. The results are also presented as line graphs in Figure 9.7 which depicts a comparison of the compressive strength results of concrete with varying amounts of fly ash.

Table 4-13: Compressive Strength for Concrete Cured at 40^0C without $Ca(OH)_2$ Activator (w/c = 0.35)

Age (Days)	Compressive Strength (MPa)			
	0%FA	25%FA	35%FA	50%FA
1	69	41	38	27
3	81	62	58	43
7	86	80	80	62
28	**105**	**107**	**102**	**87**
90	110	116	106	97
180	114	118	109	103

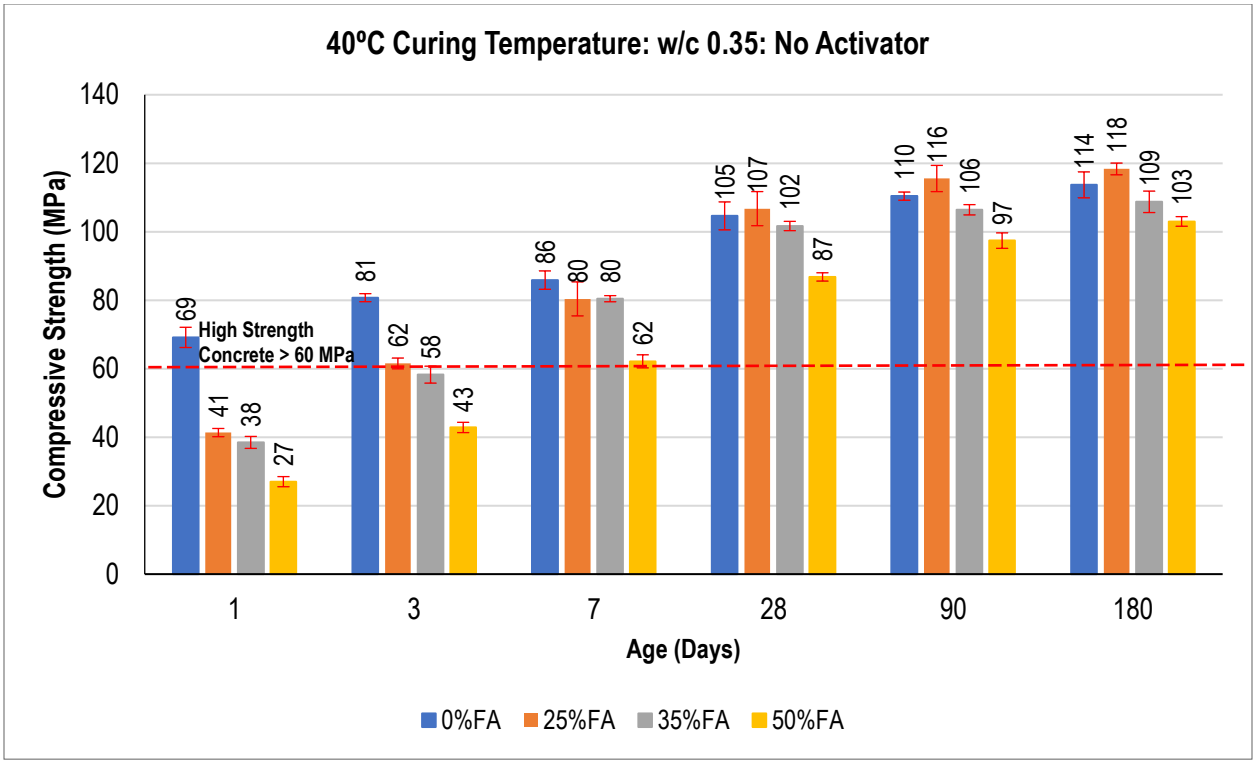

Figure 4.13: Compressive Strength for Concrete Cured at 40^{0}C without Activator (w/c = 0.35)

The results indicate that during the early ages of 1 day, 3 days and 7 days the OPC concrete had the highest strength. However, at the ages of 28 days and beyond, it can be noted that the concrete with 25% fly ash yielded higher strength than OPC concrete. The strength development pattern of OPC concrete cured at 40^{0}C indicates that the late age strength gain of OPC concrete is reduced when concrete is cured at high temperature. However, the strength development patterns of fly ash concrete indicate that the rate of strength gain of FA concrete is accelerated when the concrete is cured at a higher temperature. These results confirm that pozzolanic reactions between FA and $Ca(OH)_2$ are accelerated when fly ash concrete is subjected to heat activation. Based on the results of fly ash concrete cured at 40 degrees, it can be concluded that high temperature curing improves the strength of fly ash concrete. When the results of 50%FA concrete are compared with the results of OPC concrete, it can be noted that the strength of 50%FA concrete was approximately 40% of the strength of OPC concrete at the age of 1 day. At the age of 3 days the strength of 50%FA concrete increased to approximately 53% of the strength of OPC concrete. At 28 days the strength of 50%FA concrete

increased to 83% of the 28-day strength of OPC concrete. At 90 days and 180 days, the 50%FA concrete strength was approximately 90% of the OPC concrete strength. These results indicate that 50%FA concrete gained strength rapidly when it was cured at a high temperature of 40^{0}C. These results are further confirmation that the pozzolanic reactions between FA and $Ca(OH)_2$ are accelerated by high temperature curing. The comparison outlined above is summarised in Table 4-14 which outlines the relative strength of fly ash concrete as a percentage of OPC concrete. Figure 4.14 shows the reduction or increase in compressive strength of fly ash concrete as a percentage of OPC concrete strength.

Table 4-14: Relative Strength of Concrete as a Percentage of OPC Concrete Strength (40^{0}C : No Activator : w/c = 0.35)

Age (Days)	Relative Strength as a Percentage of OPC Concrete Strentgh (%)			
	0%FA	25%FA	35%FA	50%FA
1	100%	59%	55%	39%
3	100%	77%	72%	53%
7	100%	93%	93%	72%
28	**100%**	**102%**	**97%**	**83%**
90	100%	105%	96%	88%
180	100%	104%	96%	90%

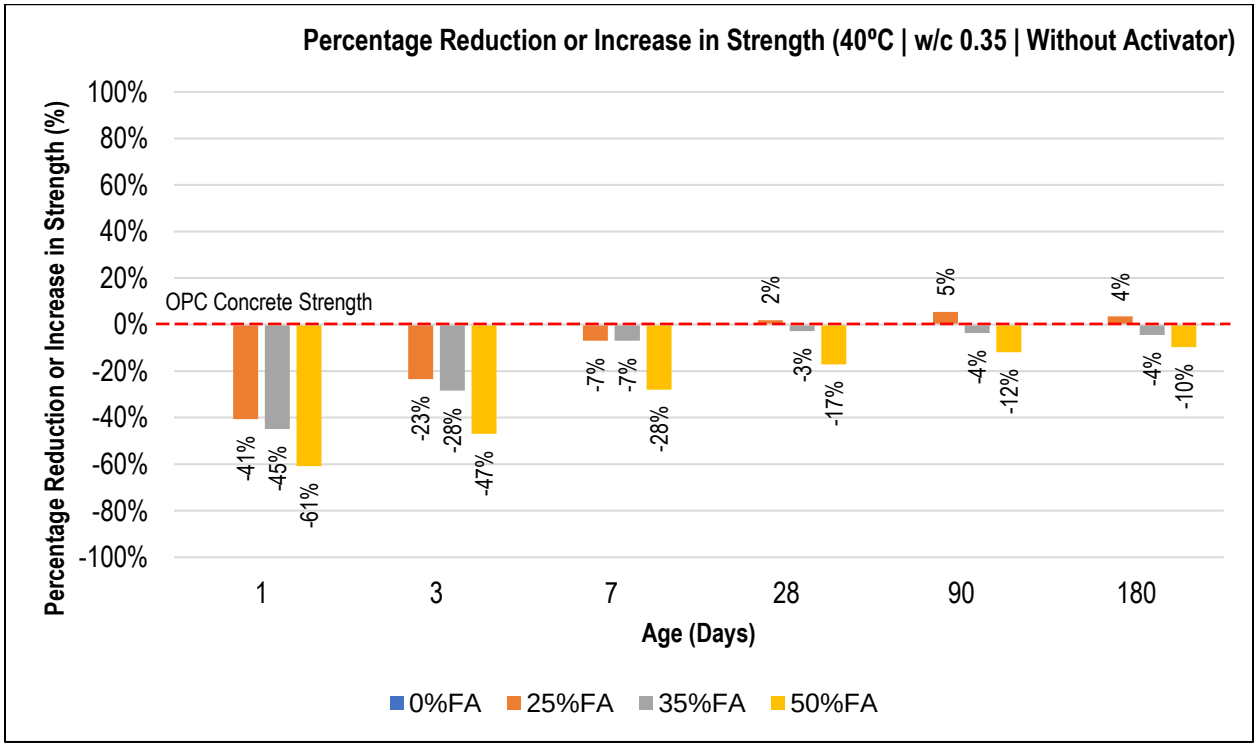

Figure 4.14: Reduction or Increase in Strength as a Percentage of OPC Concrete Strength (40^{0}C : No Activator : w/c = 0.35)

Results for Concrete Cured at 40^0C with $Ca(OH)_2$ Activator (w/c = 0.35)

Table 4-15 and Figure 4.15 outline the compressive strength results of concrete cubes that were cast using concrete which was activated by $Ca(OH)_2$ and cured at 40^0C. The concrete had a w/c ratio of 0.35 and FA contents of 0%, 25%, 35% and 50% by mass of cementitious material. $Ca(OH)_2$ was added to the concrete mixes in order to activate the FA reactions. The results are also presented as line graphs in Figure 9.8 which depicts a comparison of the compressive strength results of concrete with varying amounts of FA.

Table 4-15: Compressive Strength for Concrete Cured at 40^0C with $Ca(OH)_2$ Activator (w/c = 0.35)

Age (Days)	Compressive Strength (MPa)			
	0%FA	25%FA	35%FA	50%FA
1	73	46	41	31
3	85	73	58	51
7	92	87	80	73
28	**110**	**117**	**114**	**95**
90	112	119	116	108
180	114	121	119	114

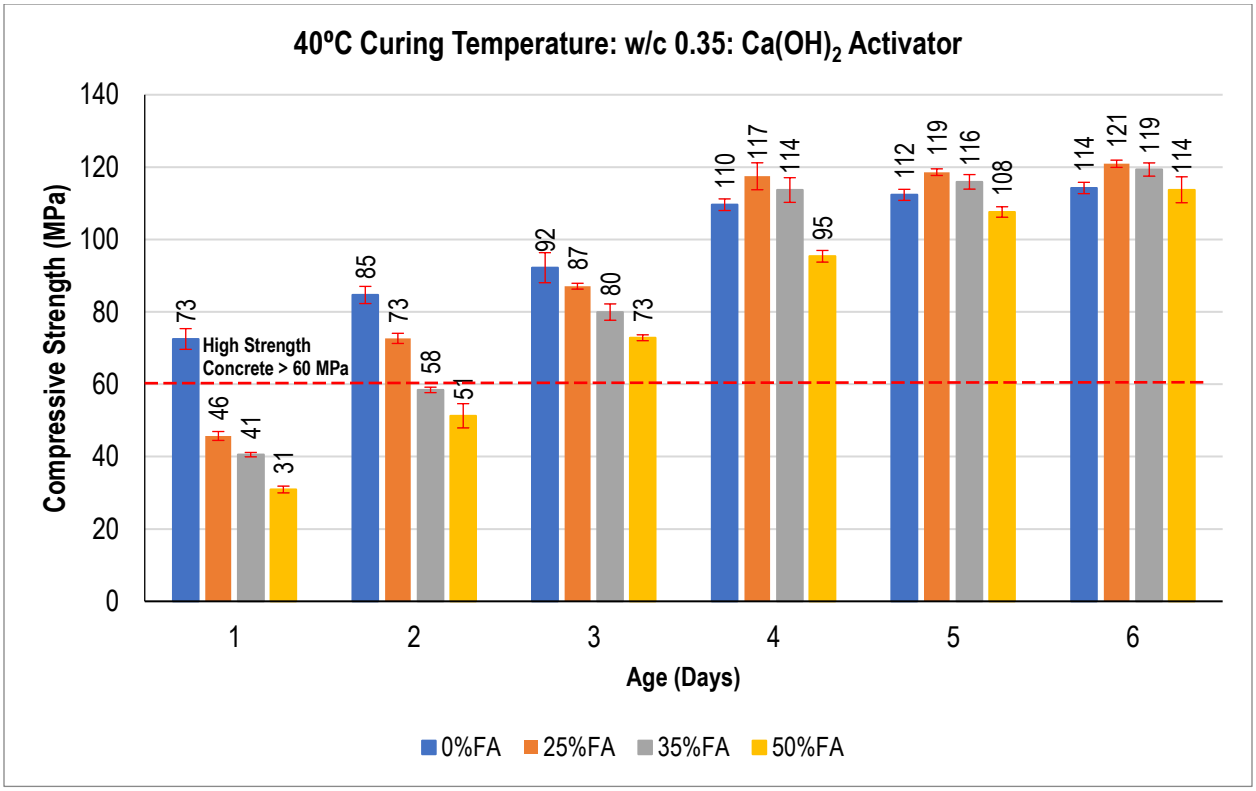

Figure 4.15: Compressive Strength for Concrete Cured at 40^{0}C with $Ca(OH)_2$ Activator (w/c = 0.35)

The results indicate that during the early ages of 1 day, 3 days and 7 days, OPC concrete had the highest strength. However, at the ages of 28 days, 90 days and 180 days it can be noted that the concrete with 25% and 35% fly ash yielded strength higher than the OPC concrete strength. The strength development patterns of $Ca(OH)_2$ activated concrete cured at 40^{0}C indicate that late age strength gain of OPC concrete is reduced when concrete is cured at high temperature. On the contrary, the strength development patterns of FA concrete indicate that the rate of strength gain of FA concrete is accelerated when the concrete is cured at a higher temperature and also when the FA is activated by $Ca(OH)_2$. The results confirm that high temperature curing and addition of $Ca(OH)_2$ significantly improves the strength development of fly ash concrete. A comparison of the compressive strength results of 50%FA concrete with those of OPC concrete indicates that the strength of 50%FA concrete was approximately 42% of the concrete strength of the OPC concrete during the early age of 1 day. At the age of 3 days the strength of 50% FA concrete was approximately 60% of the 3-day strength of OPC concrete. At the age of 7 days the strength of 50% FA concrete was approximately 80%

of the strength of OPC concrete. At 28 days the strength of 50% OPC concrete increased to 86% of the strength of OPC concrete. At 90 days the 50% FA concrete strength was 96% of the strength of OPC concrete. At the age of 180 days the strength of 50% FA concrete was equal to the strength of OPC concrete. The results indicate that the 50% FA concrete gained strength rapidly when it was subjected to high temperature curing and $Ca(OH)_2$ activation. These results are further confirmation that the pozzolanic reactions between FA and $Ca(OH)_2$ are accelerated by high temperature curing and $Ca(OH)_2$ activation. The comparison outlined above is summarised in Table 4-16 which outlines the strength of FA concrete as a percentage of OPC concrete strength. Figure 4.16 shows the reduction or increase in compressive strength of fly ash concrete as a percentage of OPC concrete strength.

Table 4-16: Relative Strength of Concrete as a Percentage of OPC Concrete Strength (40^oC : $Ca(OH)_2$ Activator : w/c = 0.35)

Age	Relative Strength as a Percentage of OPC Concrete Strentgh (%)			
(Days)	0%FA	25%FA	35%FA	50%FA
1	100%	63%	56%	42%
3	100%	86%	68%	60%
7	100%	95%	87%	79%
28	**100%**	**106%**	**104%**	**86%**
90	100%	106%	104%	96%
180	100%	106%	104%	100%

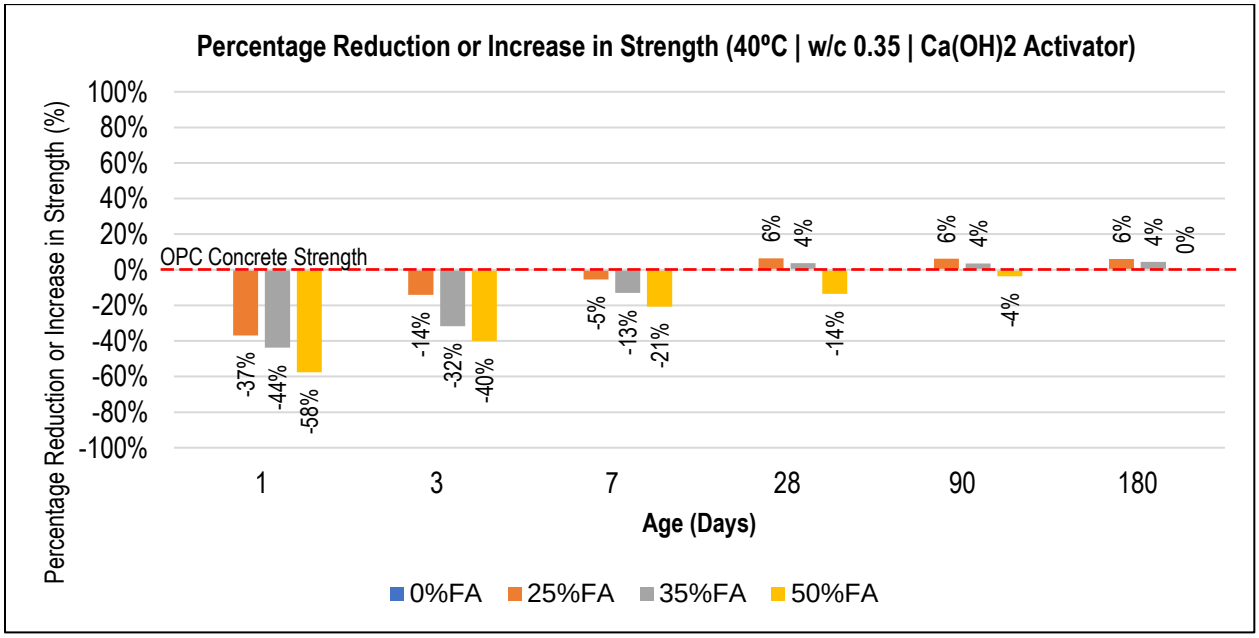

Figure 4.16: Reduction or Increase in Strength as a Percentage of OPC Concrete Strength (40^oC:$Ca(OH)_2$: w/c = 0.35)

4.1.2 Influence of Curing Temperature and $Ca(OH)_2$ Activation

This section discusses the influence of curing temperature and $Ca(OH)_2$ activation on compressive strength development of concrete. The section presents a comparison between the compressive strength results of concrete with $Ca(OH)_2$ activator and those of concrete without activator. The comparison is based on strength results of concrete which had the same w/c ratio and same fly ash content. The study variables that form the basis of discussion in this section are the curing temperature and $Ca(OH)_2$ content.

Compressive Strength Results for OPC concrete with w/c ratio of 0.45

Figure 4.17 and Figure 4.18 show a comparison of compressive strength results of OPC concrete with w/c ratio of 0.45.

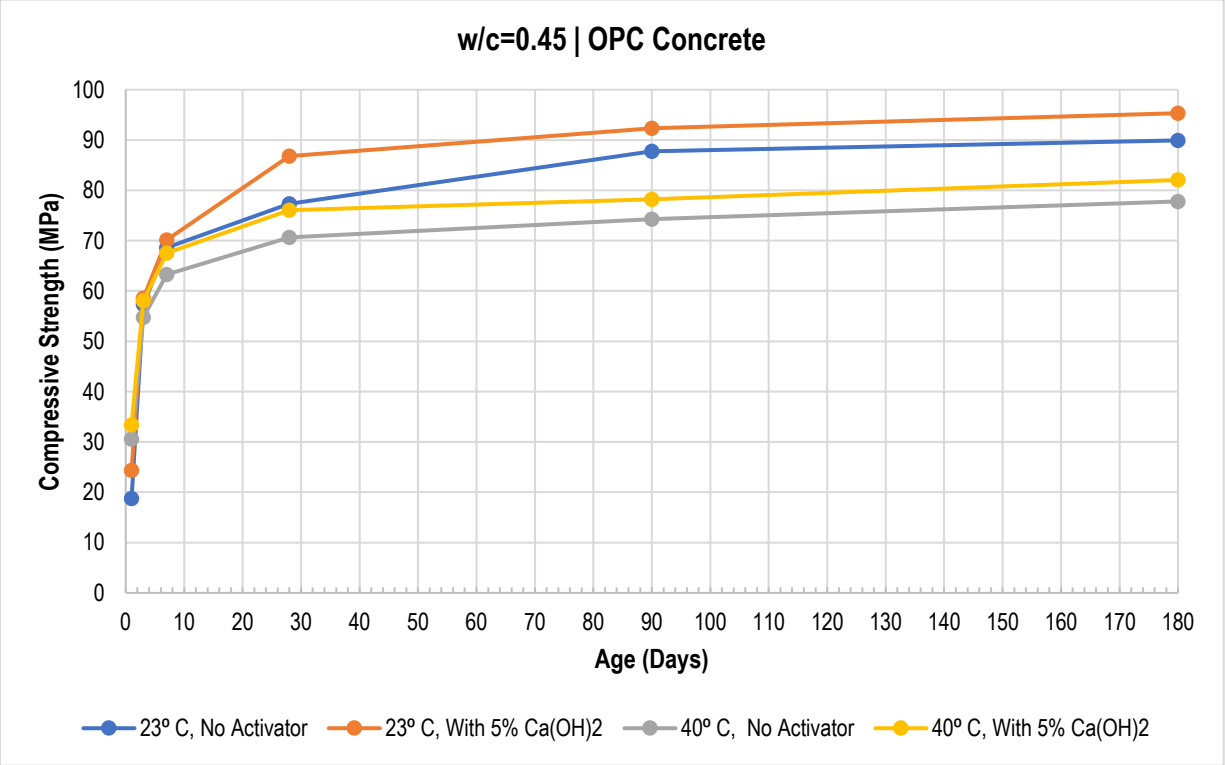

Figure 4.17: Compressive Strength Results of OPC Concrete with w/c ratio of 0.45

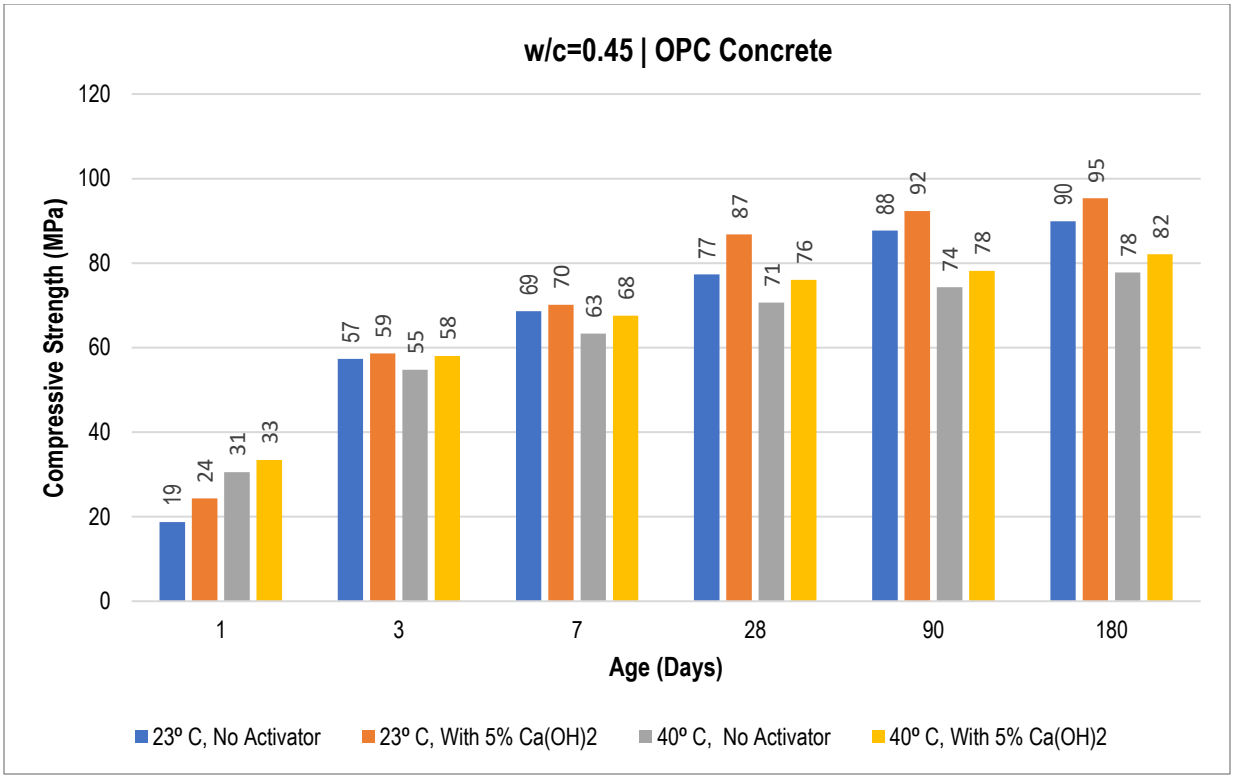

Figure 4.18: Compressive Strength Results of OPC Concrete with w/c ratio of 0.45

The results indicate that at the age of 1-day concrete cubes that were cured at 40^{0}C had higher compressive strength than cubes that were cured at 23ºC. However, it can be noted that at the ages of 7 days and beyond, the compressive strength of OPC concrete cured at 40^{0}C was lower than the strength of OPC concrete cured at 23ºC. Based on this observation, it can be concluded that continuous high temperature curing results in the reduction of strength of OPC concrete at the ages of 7 days and beyond. This conclusion is confirmed by Zemajtis (2014) who states that high curing temperature increase early age strength however it results in the decrease of concrete strength at 28-days and beyond. Figure 4.19 shows a model presented by Zemajtis (2014) where he illustrates the effect of high temperature curing on compressive strength of concrete. The OPC concrete strength reduction can be attributed to the quality of the hydration products formed when concrete is cured at high temperature. Cabrera and Nwaubani (1998) investigated the microstructure of concrete and reported that OPC concrete cured at high temperature had less late age compressive strength owing to the rapid formation of hydration products around cement particles. They state that this affects the diffusion of

water required for the progression of hydration. They concluded that this phenomenon is the cause of the coarser pore structure in OPC pastes cured at high temperature. They further pointed out that high temperature curing results in conversion, a process where unstable reaction products with high volume convert to stable products with low volume. They attribute the coarsening of the pore structure to the conversion of unstable reaction products. Their conclusion is complimented by the results of a study conducted by Elsageer et. al. (2009) on the influence of curing temperature on OPC concrete strength. Elsageer et. al. (2009) observed that at later ages there was significant reduction in the compressive strength of OPC concrete cured at higher temperature. They also attributed this to the rapid formation of hydration products and non-uniform distribution of hydration products which creates large pores. Wajahat et al. (1991) investigated the temperature effect on strength of mortars and concrete. They reported that concrete containing OPC yielded low compressive strength when it was exposed to temperatures above 25°C. High temperature curing of OPC concrete also presents challenges such as delayed ettringite formation which leads to expansion and cracking of concrete (Acquaye, 2006).

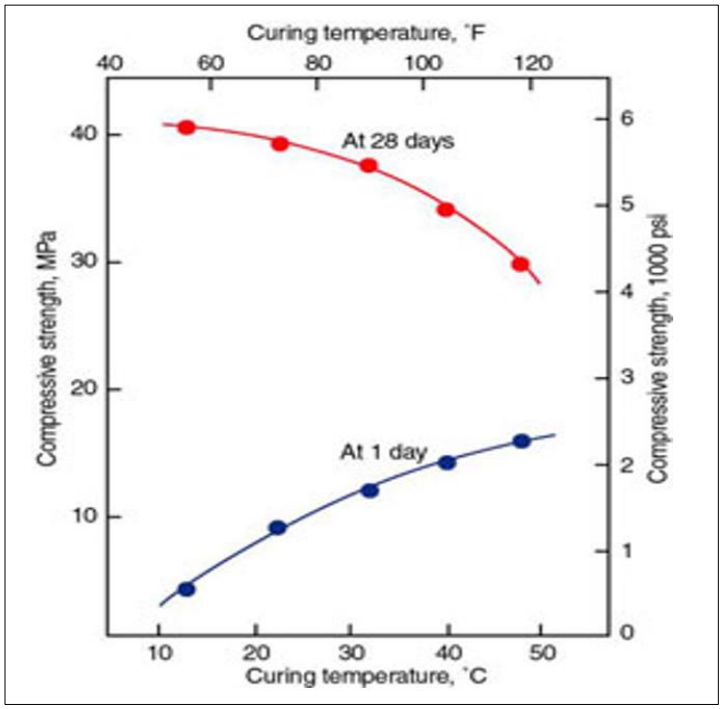

Figure 4.19: Effect of Curing Temperature on Compressive Strength (Zemajtis, 2014)

The effect of $Ca(OH)_2$ activation on OPC concrete was only noticeable at the age of 1 day. The results show that at the age of 1 day, concrete cubes that had $Ca(OH)_2$ activation yielded higher compressive strength when compared to concrete cubes that did not have $Ca(OH)_2$. At the age of 3 days and beyond, there was no significant effect of $Ca(OH)_2$ activation on OPC concrete. The OPC concrete cubes had similar strength despite having differing $Ca(OH)_2$ contents.

Compressive Strength Results for OPC Concrete with w/c ratio of 0.35

Figure 4.20 and Figure 4.21 show a comparison of results of OPC concrete with w/c ratio of 0.35. The results indicate that at the early age of 1-day, concrete cubes that were cured at 40^0C had higher strength that those that were cured at 23^0C. At the ages of 7 days and beyond, it can be noted that OPC concrete cured at 40^0C yielded lower compressive strength compared to OPC concrete cured at 23^0C. This trend is similar to the trend observed in the results of OPC concrete with w/c ratio of 0.45. It can be noted that the effect of $CA(OH)_2$ activation was noticeable only at the age of 1 day, where concrete cubes with $Ca(OH)_2$ activation yielded higher strength compared to those that did not have $Ca(OH)_2$. At the age of 3 days and beyond it can be observed that concrete cubes that were cured at 23^0C without $Ca(OH)_2$ addition yielded higher strength than concrete cubes cured at similar temperature with $Ca(OH)_2$ activation. This trend is different in OPC concrete cured at 40^0C. It can be noted that OPC concrete cured at 40^0C with $Ca(OH)_2$ yielded slightly higher compressive strength results compared to OPC concrete cured at 40^0C without Ca(OH) activation. In general, the results indicate that high temperature curing reduces strength of OPC concrete at the ages of 3 days and beyond. This is consistent with the findings of a study conducted by Acquaye (2006) which concluded that there was significant reduction in late age compressive strength of OPC concrete cured at high temperature. A comparison of the results of OPC concrete with w/c ratios of 0.45 and 0.35 indicates that OPC concrete with w/c ratio of 0.35 yielded higher strength than OPC concrete with a w/c ratio of 0.45.

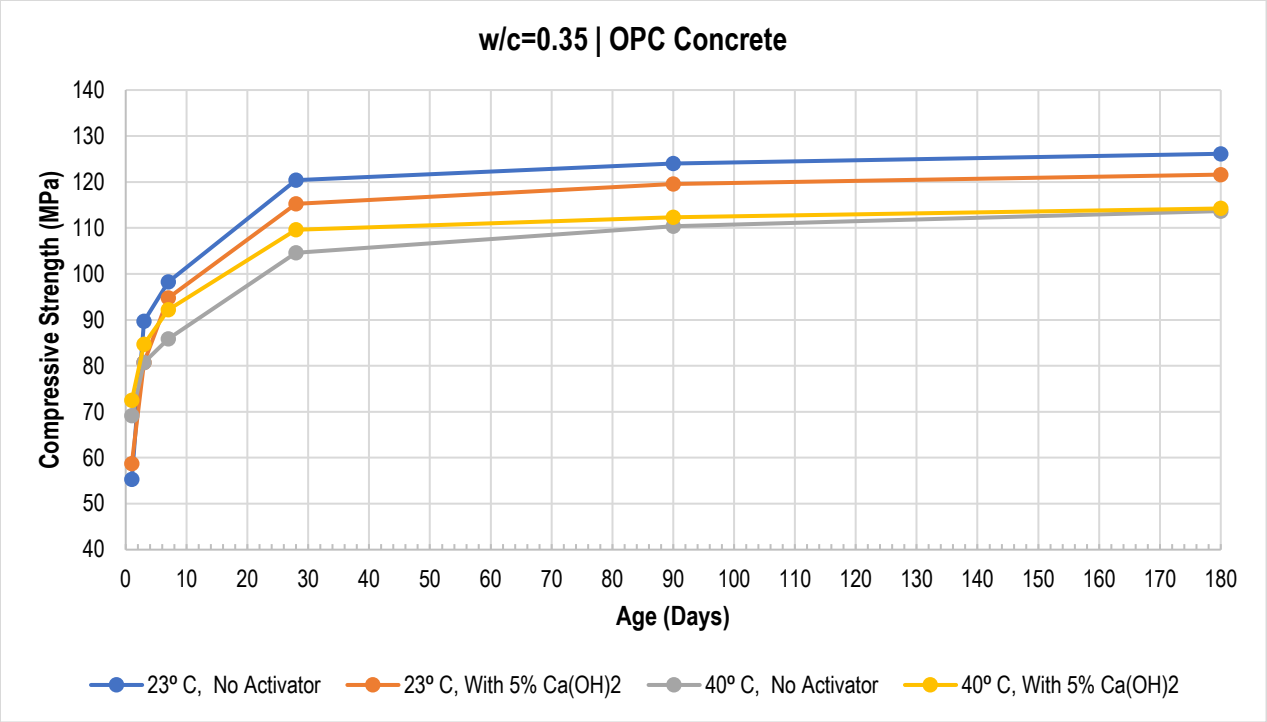

Figure 4.20: Compressive Strength Results for OPC Concrete with w/c ratio of 0.35

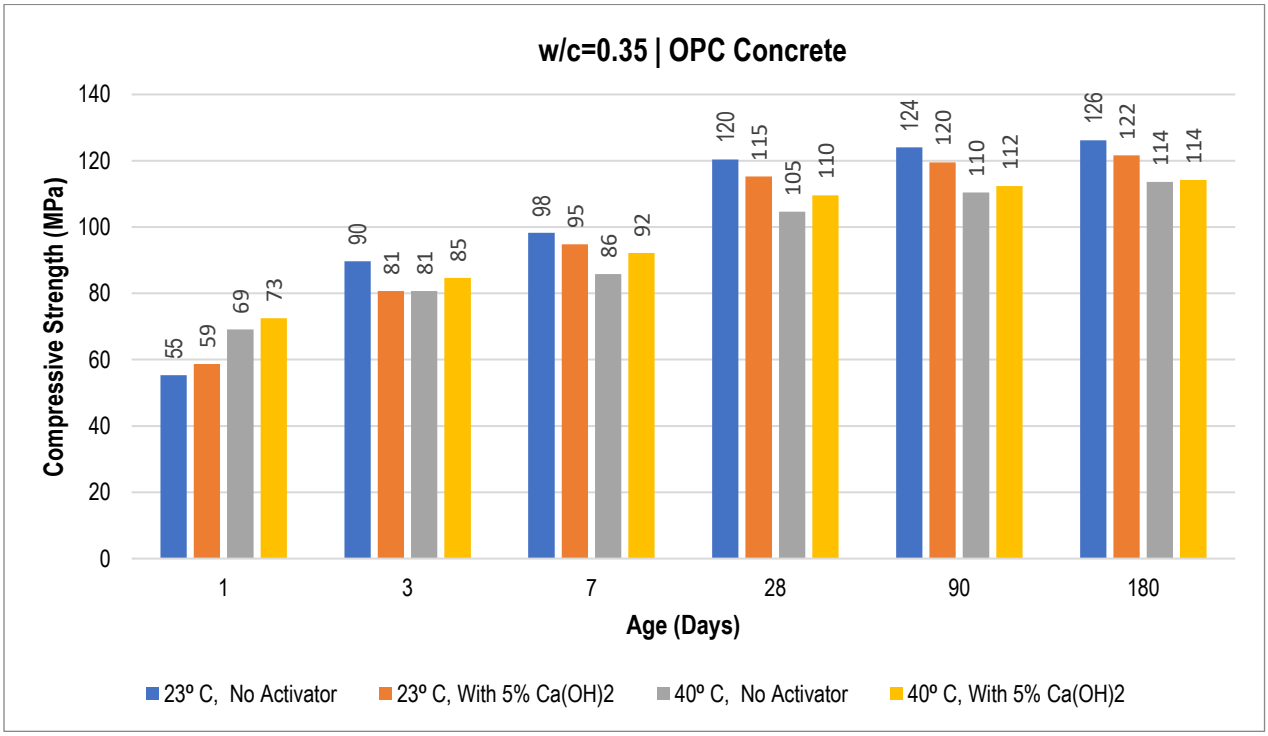

Figure 4.21: Compressive Strength Results for OPC Concrete with w/c of 0.35

Compressive Strength Results for 25%FA Concrete with w/c ratio of 0.45

Figure 4.22 and Figure 4.23 present a comparison of compressive strength results for 25%FA concrete with w/c ratio of 0.45. The results show that at the ages of 1 day, 3 days, 7 days and 28 days, concrete cured at 40^0C yielded higher strength than similar concrete cured at 23^0C. This is contrary to what was observed with OPC concrete, where OPC concrete cured at 23^0C yielded higher strength than OPC concrete cured at 40^0C at the ages of 7 days and beyond. It can be observed that at later ages of 90 days and 180 days, the compressive strength of 25%FA concrete cured at 23^0C catches up with the strength of 25%FA concrete cured at 40^0C. The effect of $Ca(OH)_2$ activation on 25%FA concrete is only significant at the age of 1 day. At all other ages of 3 days and beyond the effect of $Ca(OH)_2$ activation was not significant. The effect of high temperature curing was noticeable up-to the age of 28 days. At the ages of 90 days and 180 days, the concrete had approximately the same strength despite being cured at different temperatures and having different contents of $Ca(OH)_2$. The rate of concrete strength development beyond the age of 90 days was very low and the compressive strength results for 180 days were similar to the 90 days strength results. Based on these results it can be concluded that the influence of $Ca(OH)_2$ activation on 25%FA concrete is insignificant.

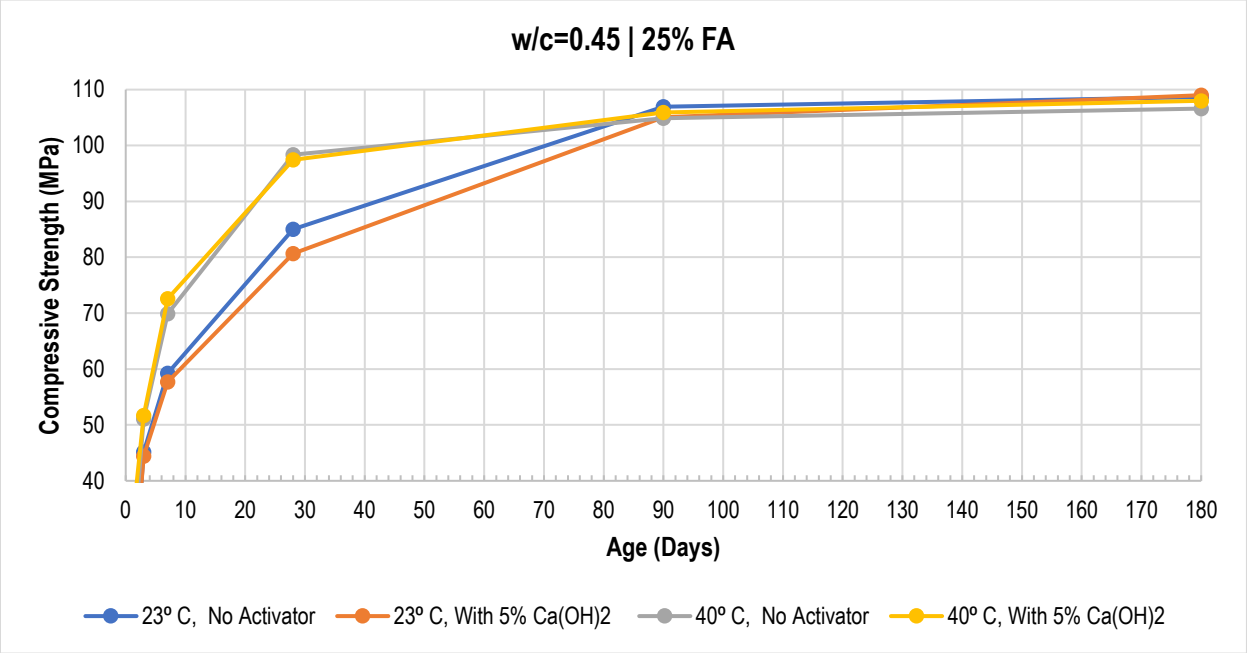

Figure 4.22: Compressive Strength Results for 25%FA Concrete with w/c ratio of 0.45

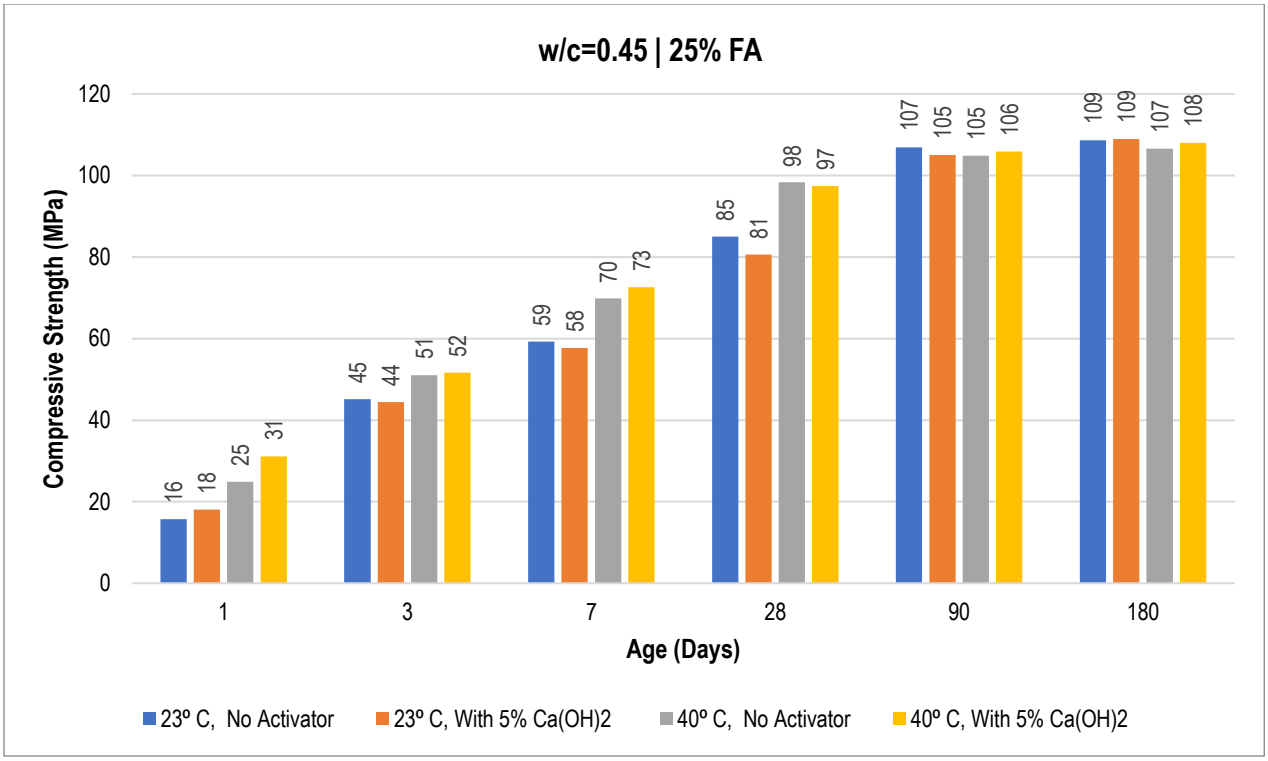

Figure 4.23: Compressive Strength Results for 25%FA Concrete with w/c ratio of 0.45

Compressive Strength Results for 25%FA Concrete with a w/c ratio of 0.35

Figure 4.24 and Figure 4.25 show a comparison of compressive strength results of 25%FA concrete with w/c ratio of 0.35. The results indicate that at the ages of 1 day, 3 days, 7 days and 28 days, concrete cured at 40^0C had higher strength than similar concrete cured at 23^0C. Also it can be noted that the influence of adding $Ca(OH)_2$ was noticeable at the ages of 1 day up to 28 days. Beyond the age of 28 days, the effect of $Ca(OH)_2$ activation was only noticeable in concrete cured at 40^0C, where $Ca(OH)_2$ activated concrete yielded higher strength than concrete without activation. This is attributed to the role of high temperature in accelerating the pozzolanic reactions between fly ash and $Ca(OH)_2$. At the ages of 90 days and 180 days, it is observed that concrete cured at 23^0C without activation yielded higher strength than concrete cured at 23^0C with activation. It can also be noted that concrete cured at 23^0C had lower strength at early ages upto the age of 28 days, however beyond 28 days it surpassed the strength of concrete cured at 40^0C.

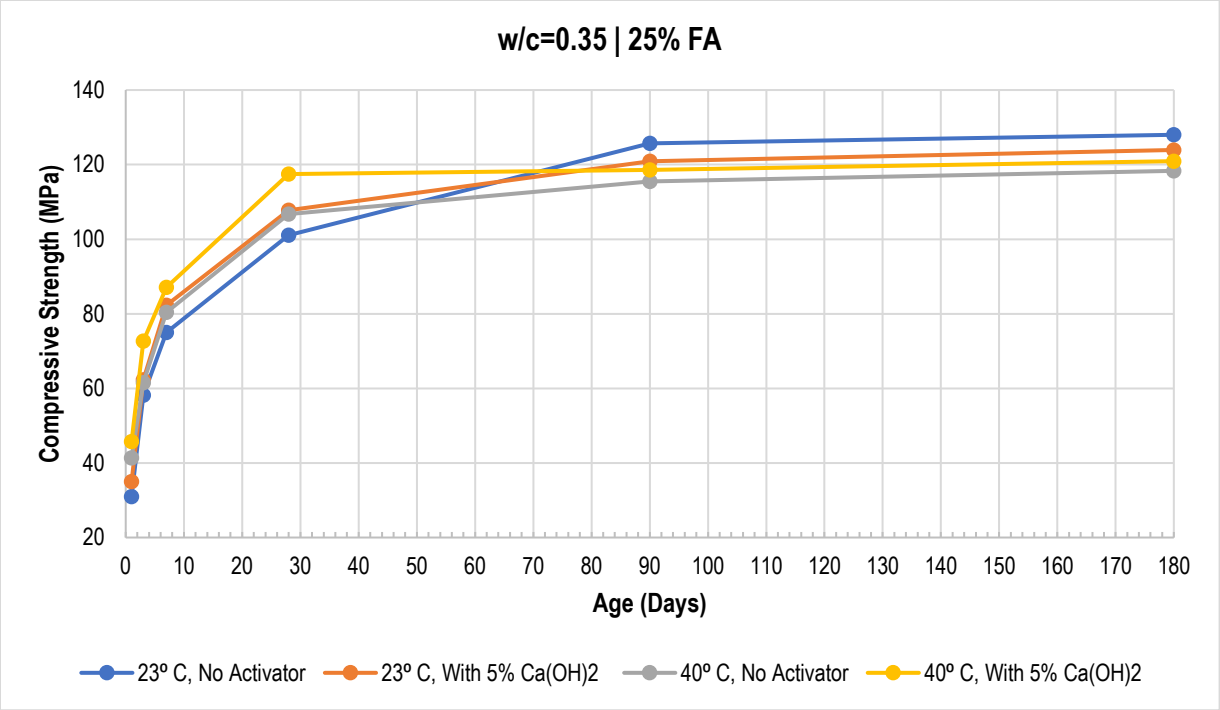

Figure 4.24: Compressive Strength Results for 25%FA Concrete with w/c ratio of 0.35

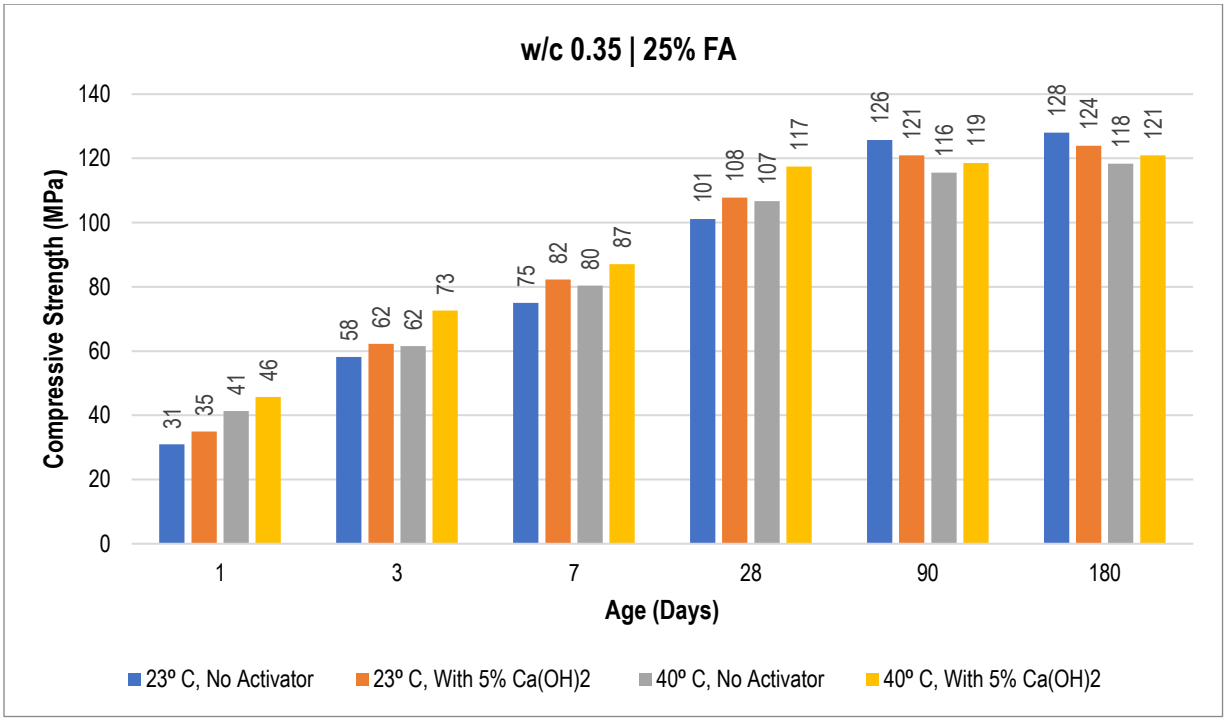

Figure 4.25: Compressive Strength Results for 25%FA Concrete with w/c ratio of 0.35

Compressive Strength Results for Concrete with 35% FA and a w/c ratio of 0.45

Figure 4.26 and Figure 4.27 show the results for 35%FA concrete with w/c ratio of 0.45. The results show that at all ages the effect of high temperature curing and $Ca(OH)_2$ activation is significant. This is contrary to the observation made on the compressive strength results of OPC concrete and 25%FA concrete where at some ages the effect of high temperature curing and $Ca(OH)_2$ addition was not noticeable. It can be noted that at all ages concrete cured at 40^0C yielded higher strength compared to similar concrete cured at 23^0C. It is also observed that at all ages, concrete with $Ca(OH)_2$ activation yielded higher strength compared to similar concrete without $Ca(OH)_2$ activation which was cured under same conditions. These results give an indication that addition of $Ca(OH)_2$ and heat activation accelerates fly ash pozzolanic reactions. Based on the results of 35% FA concrete, it can be concluded that heat curing yields higher compressive strength benefits compared to $Ca(OH)_2$ activation. However, the combined effect of both high temperature curing and $Ca(OH)_2$ activation significantly increases the compressive strength of 35%FA concrete.

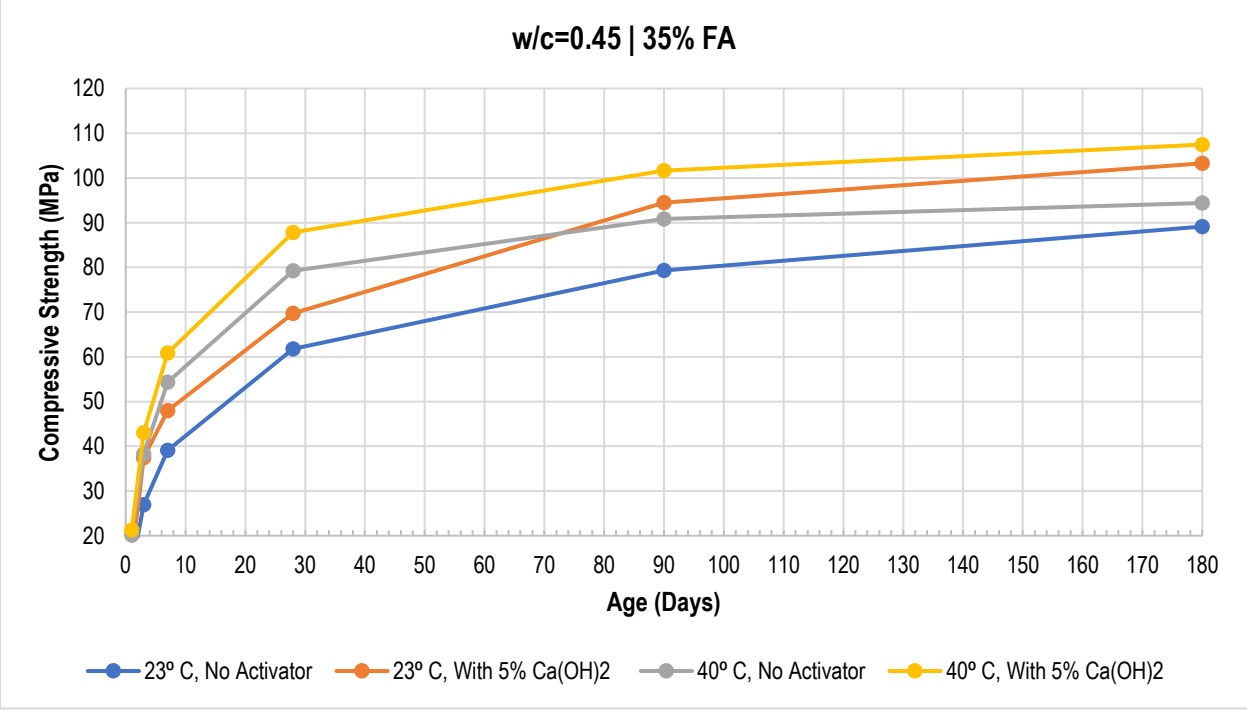

Figure 4.26: Compressive Strength Results for 35%FA Concrete with w/c ratio of 0.45

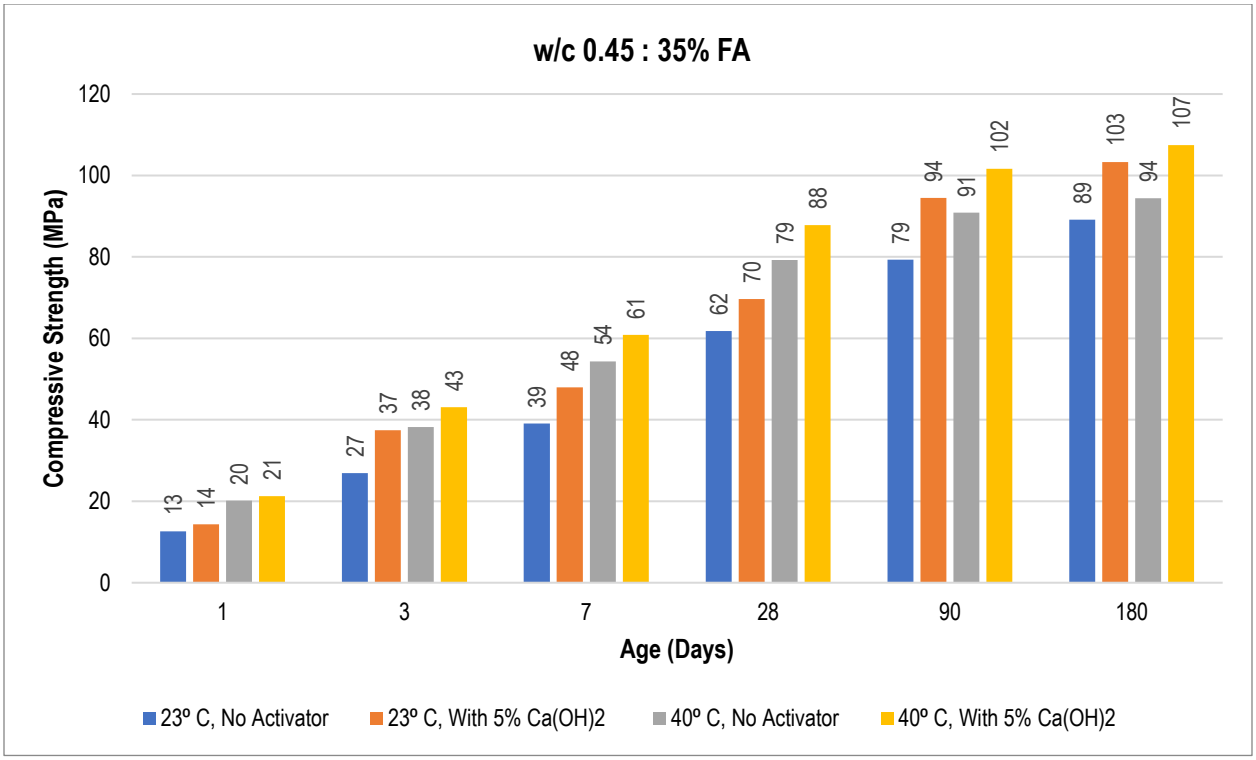

Figure 4.27: Compressive Strength Results for 35% FA Concrete with w/c ratio of 0.45

Compressive Strength Results for Concrete with 35% FA and a w/c ratio of 0.35

Figure 4.28 and Figure 4.29 show a comparison of compressive strength results for 35%FA concrete with a w/c ratio of 0.35. The results show a similar trend to 35%FA concrete with a w/c ratio of 0.45. The results indicate that at the ages of 1 day, 3 days and 7 days, the effect of $Ca(OH)_2$ addition is not significant but the effect of high temperature curing is more defined with concrete cured at 40^0C having higher strength than concrete cured at 23^0C. At the age of 28 days the effect of both $Ca(OH)_2$ addition and high temperature curing is significant, the cubes that had $Ca(OH)_2$ activation and cured at high temperature yielded higher results. Similar results were observed at 90 days and 180 days where concrete with $Ca(OH)_2$ cured at high temperature yielded the highest strength.

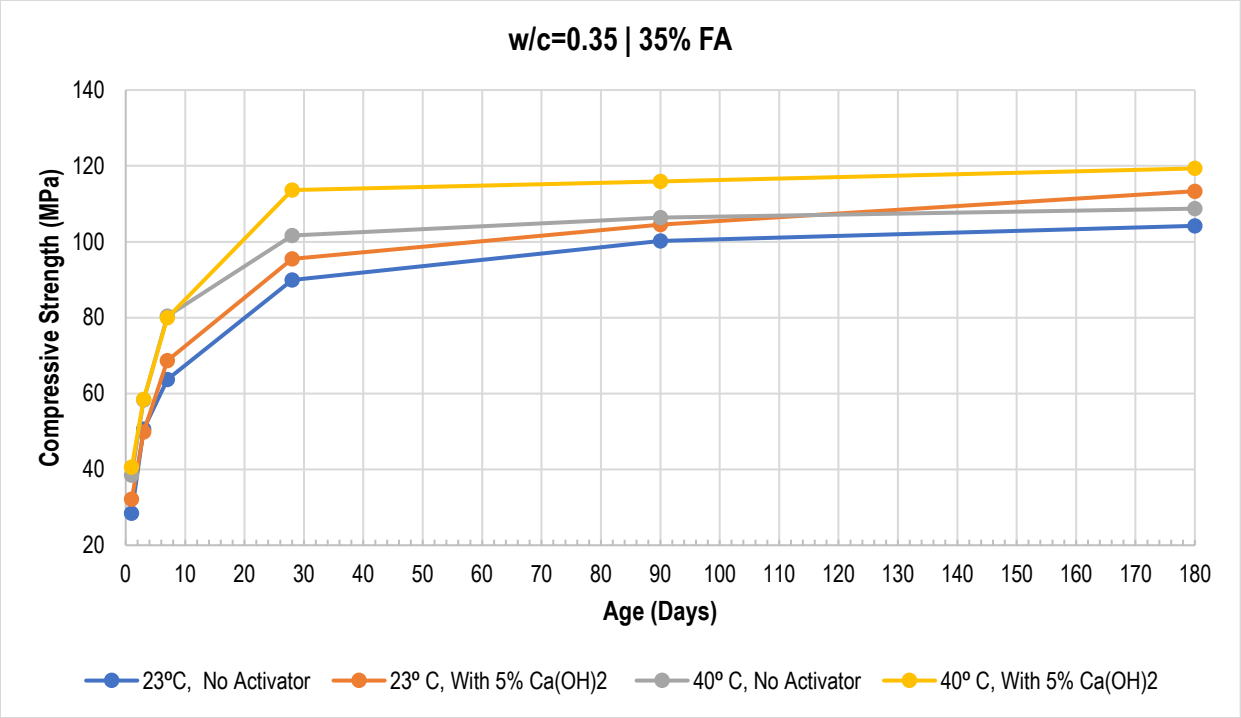

Figure 4.28: Compressive Strength Results for 35%FA Concrete with w/c ratio of 0.35

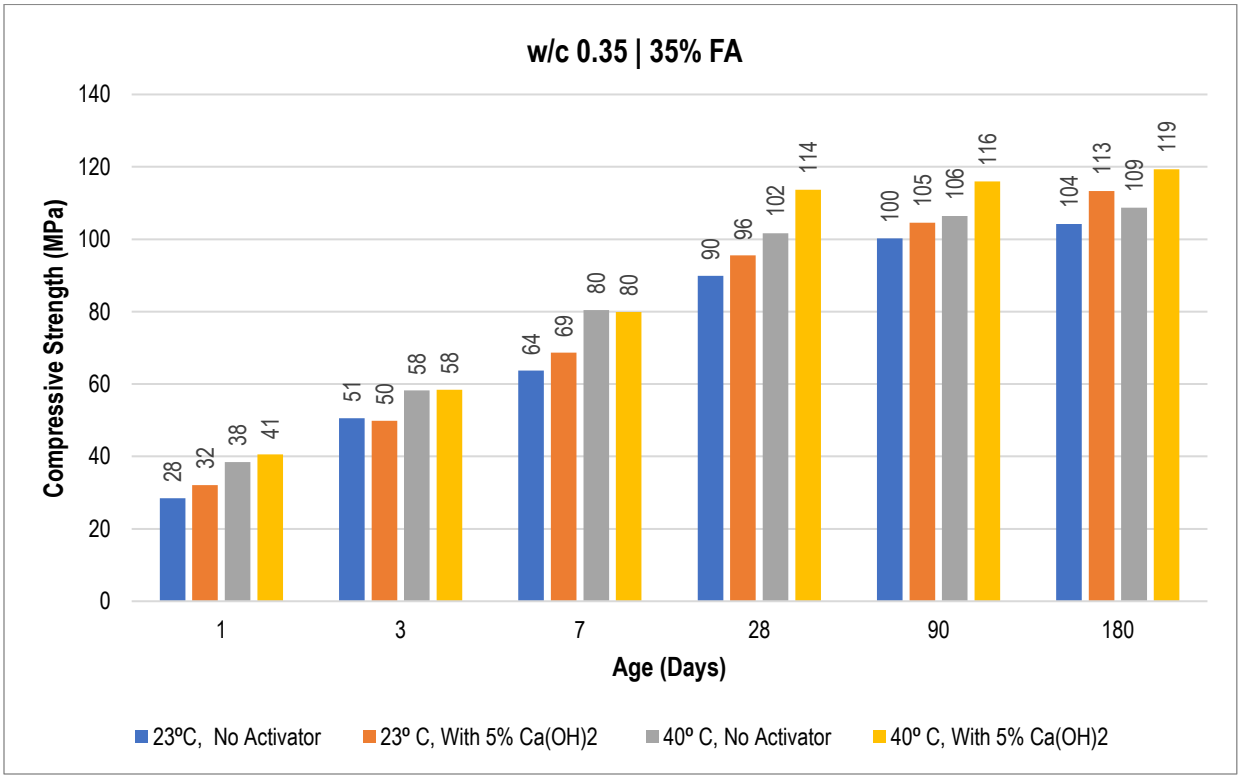

Figure 4.29: Compressive Strength Results for 35%FA Concrete with w/c ratio of 0.35

Compressive Strength Results for 50%FA Concrete with w/c ratio of 0.45

Figure 4.30 and Figure 4.31 present a comparison of results for 50%FA concrete with w/c ratio of 0.45. It can be noted that at all ages the effect of high temperature curing and $Ca(OH)_2$ addition is more significant. This is contrary to the results of OPC concrete and 25%FA concrete which didn't show significant effect of high temperature curing and $Ca(OH)_2$ activation. Concrete cured at 40^0C yielded much higher strength compared to concrete cured at 23^0C. Also, it can be observed that 50%FA concrete with $Ca(OH)_2$ activation yielded higher strength than similar concrete without $Ca(OH)_2$ which was cured under similar conditions. These results clearly indicate the influence of curing temperature and $Ca(OH)_2$ activation on high volume fly ash concrete. It is noted that concrete cured at normal temperature of 23^0C without $Ca(OH)_2$ activation had the least strength. Based on the results of 50%FA concrete, it can be concluded that the combined effect of high temperature curing and $Ca(OH)_2$ activation significantly increases the early age strength of concrete with high volume fly ash content. When the results of 50%FA content are compared with the results of OPC concrete, it can be observed that 50%FA concrete responded positively to high temperature curing and $Ca(OH)_2$ activation whereas OPC concrete had reduced late age strength when it was subjected to high temperature curing.

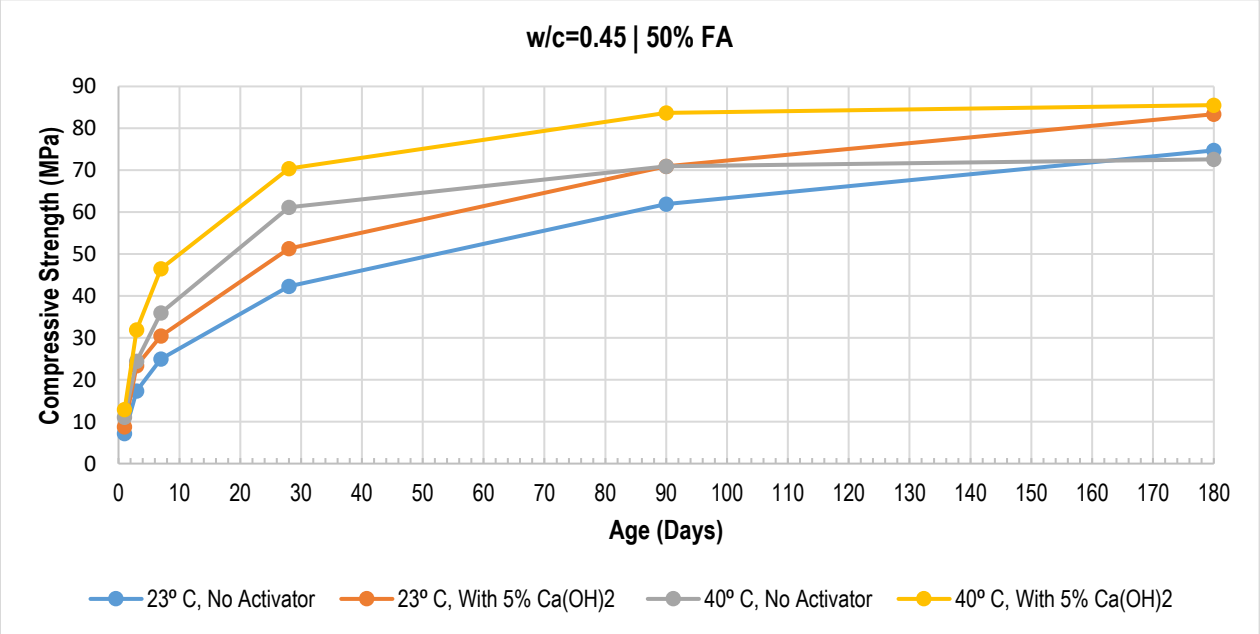

Figure 4.30: Compressive Strength Results for 50%FA Concrete with w/c ratio of 0.45

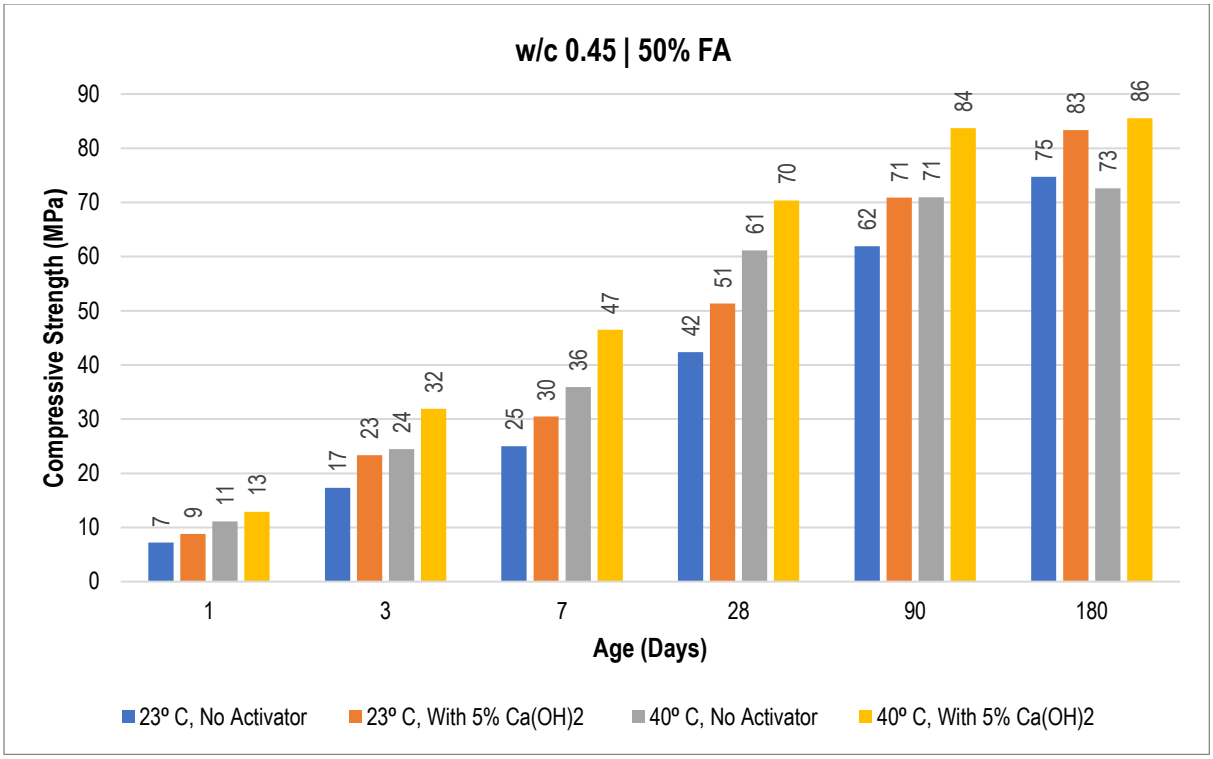

Figure 4.31: Compressive Strength Results for 50%FA Concrete with w/c ratio of 0.45

Compressive Strength Results for 50%FA Concrete with w/c ratio of 0.35

Figure 4.32 and Figure 4.33 show a comparison of compressive strength results for 50%FA concrete with w/c ratio of 0.35. The results show that at all ages the effect of high temperature curing and $Ca(OH)_2$ addition is clearly noticeable. This trend is similar to the trend observed in the results of 50%FA concrete with w/c ratio of 0.45. Concrete cured at 40^0C yielded higher compressive strength than concrete cured at 23^0C. It can also be noted that concrete with $Ca(OH)_2$ activation yielded higher strength than similar concrete without $Ca(OH)_2$. Concrete cured at 23^0C without $Ca(OH)_2$ activation yielded the least strength at all ages. The combined effect of high temperature curing and $Ca(OH)_2$ activation significantly increased the strength of 50%FA concrete. A comparison of results of 50%FA content to the results of OPC concrete shows that 50%FA concrete strength is significantly improved by high temperature curing and $Ca(OH)_2$ activation compared to OPC concrete.

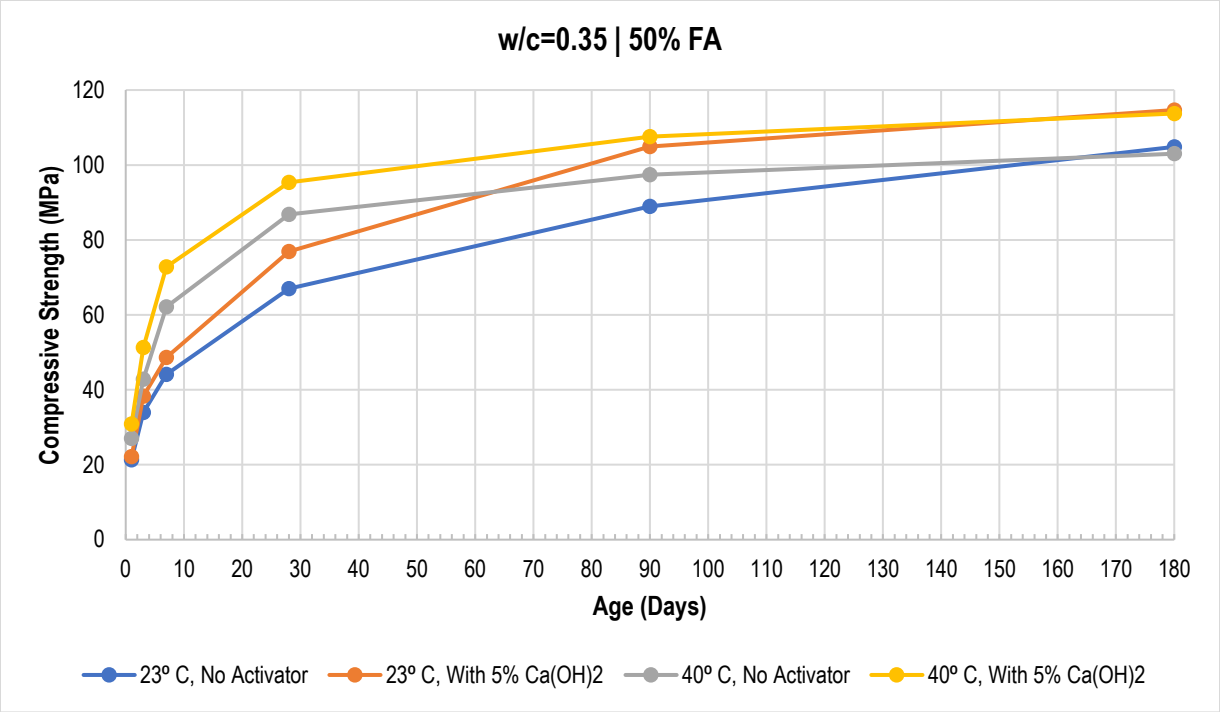

Figure 4.32: Compressive Strength Results for 50%FA Concrete with w/c ratio of 0.35

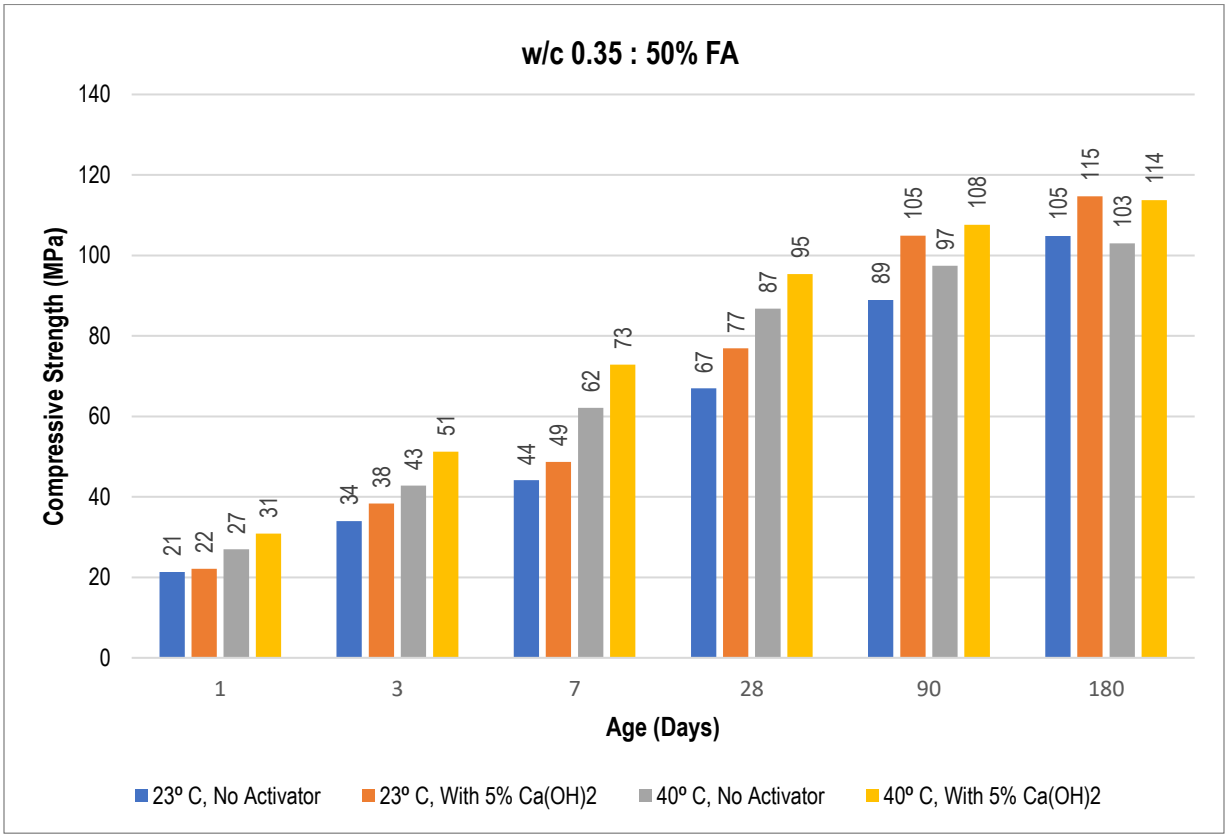

Figure 4.33: Compressive Strength Results for 50%FA Concrete with w/c ratio of 0.35

4.1.3 Influence Of Water To Cement Ratio on Compressive Strength

The compressive strength of concrete is highly influenced by the size of pores in cement paste. The water to cement ratio generally exhibits an inverse relationship with concrete compressive strength. As the w/c ratio of concrete increases, the compressive strength decreases. Concrete with a high w/c ratio has high volume of capillary pores which are formed when the mixing water is consumed leaving behind pores (Owens, 2009). High volume of capillary pores results in reduced compressive strength of concrete. Figure 4.34 and Figure 4.35 show a comparison of the compressive strength results on the basis of w/c ratio. It can be observed in all the graphs that concrete with w/c ratio of 0.35 always yielded significantly higher compressive strength results compared to similar concrete with w/c ratio of 0.45. The results indicate the significant influence of water to cement ratio on the compressive strength of concrete. The inverse relationship between w/c ratio and compressive strength is best described by Abrams' law which is expressed by Equation 4-2.

$$\sigma_c = \frac{A}{B^{\frac{W}{C_{eq}}}} \qquad \text{Equation 4-2} \qquad \text{(Rao, 2001)}$$

Where: σ_c - is compressive strength
W – water content
C_{eq} –Cementitious Material
A and B are constants

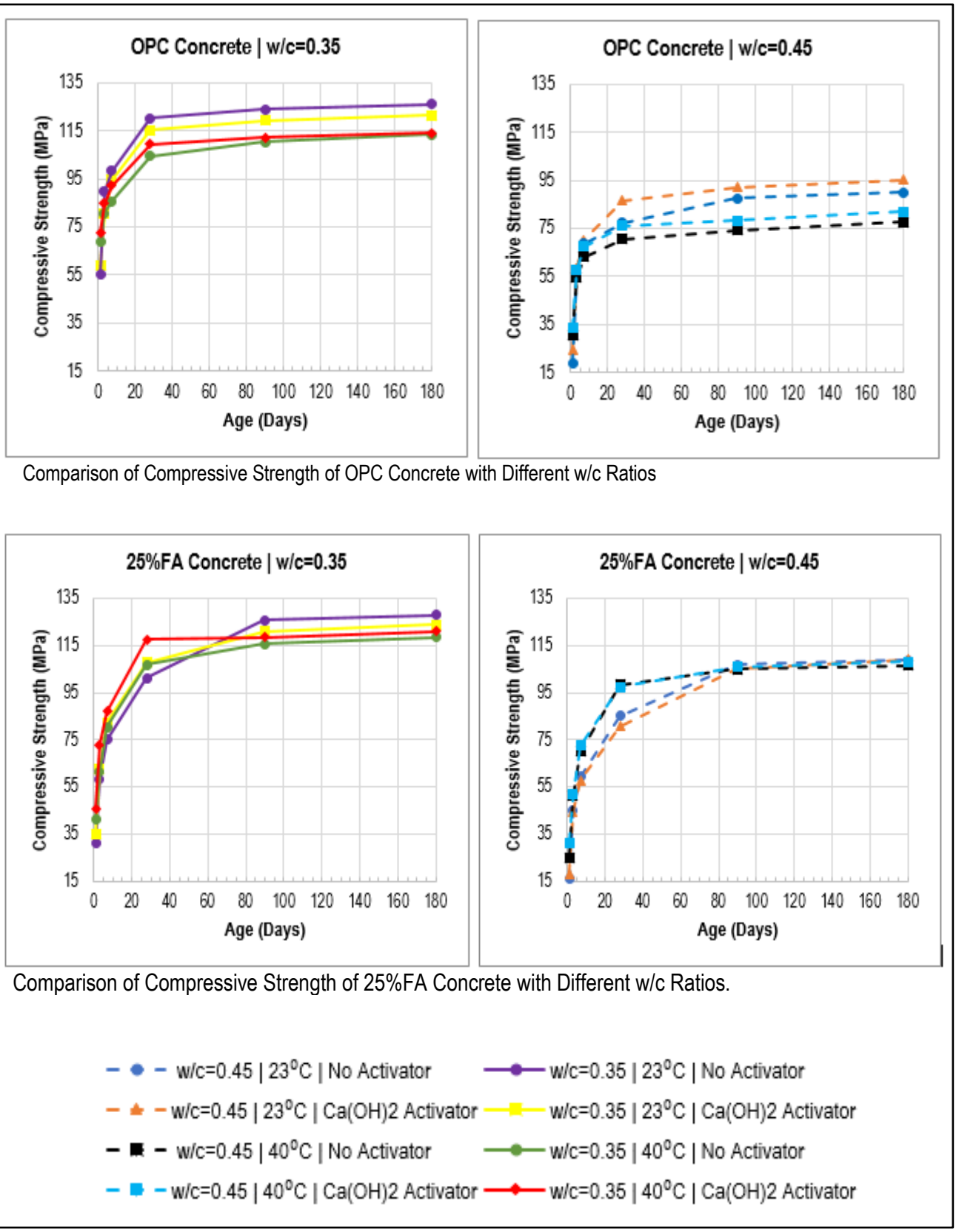

Comparison of Compressive Strength of OPC Concrete with Different w/c Ratios

Comparison of Compressive Strength of 25%FA Concrete with Different w/c Ratios.

Figure 4.34: Comparison of Compressive Strength of Concrete with Different w/c Ratios

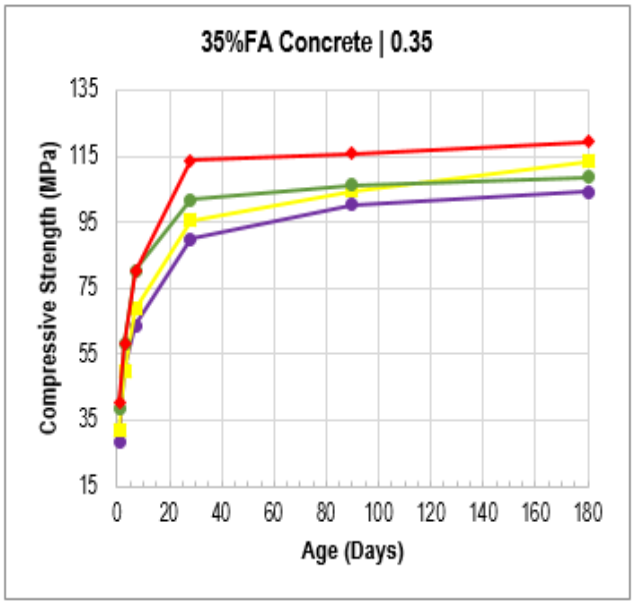

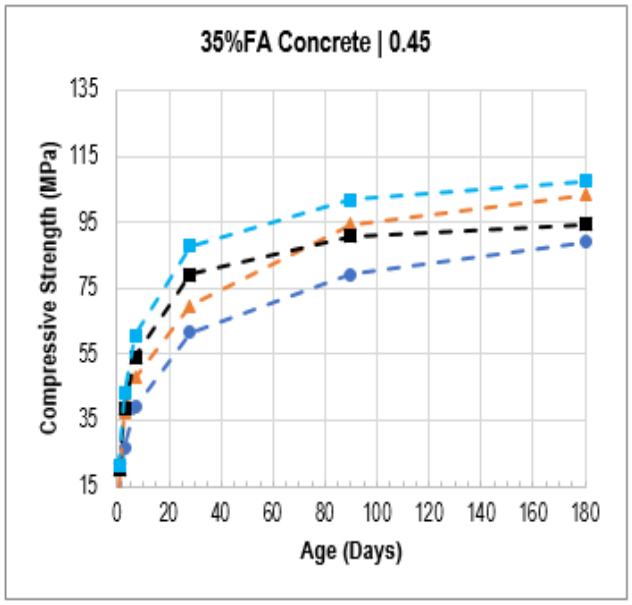

Comparison of Compressive Strength of 35%FA Concrete with Different w/c Ratios.

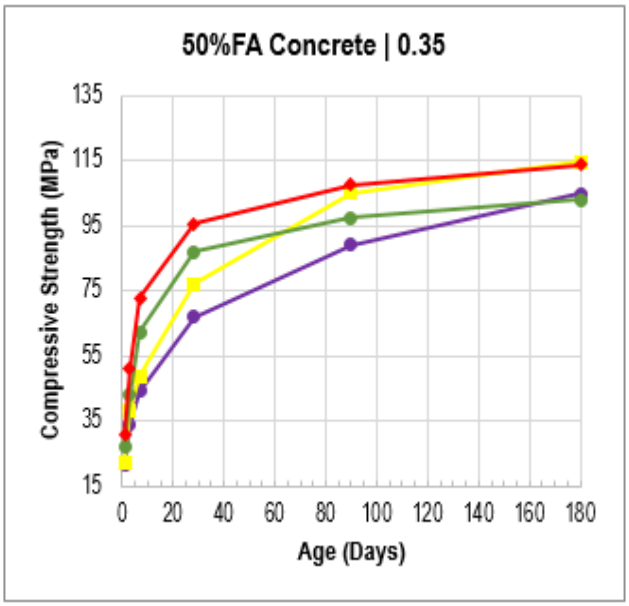

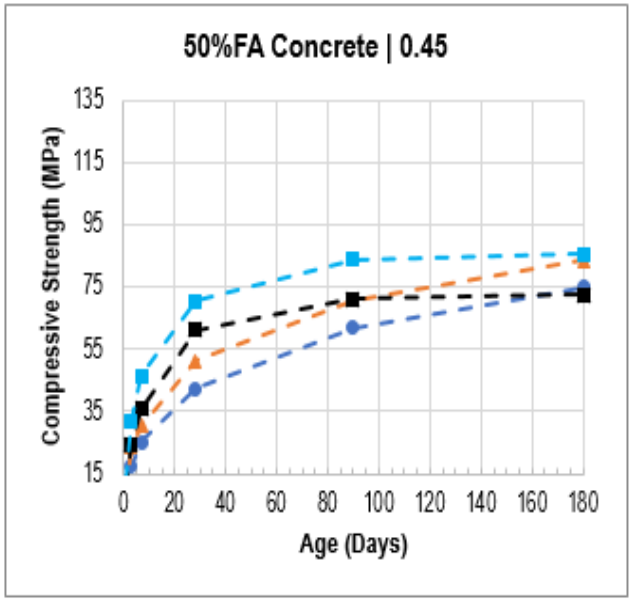

Comparison of Compressive Strength of 50%FA Concrete with Different w/c Ratios.



Figure 4.35: Comparison of Compressive Strength of Concrete with Different w/c Ratios

4.1.4 Comparison of compressive strength Results with Published Data

The strength development patterns of all concrete mixes investigated in this study are comparable to trends reported by other researchers in similar studies. In this study, the bulk of the 28-day compressive strength results are well over the 60MPa mark which depicts high strength concrete. The majority of 28-day compressive strength results for 50%FA concrete are in the high strength concrete range with the exception of compressive strength results for 50%FA concrete with w/c ratio of 0.45 which was cured at 23ºC. The compressive strength results are consistent with the findings of similar published research on high strength HVFA concrete (Poon et al, 2000; Elsageer et al., 2009; Solikin et al., 2013). Poon et al., (2000) investigated high strength concrete using 45% fly ash and developed high volume fly ash concrete with 28-day compressive strength higher than 80MPa using w/c ratio of 0.24. Elsageer et. al. (2009) achieved 32-day compressive strength of approximately 70MPa in their investigation of strength development of 45%FA concrete using cementitious material of 367kg/m^3 of concrete and w/c ratio of 0.3. Solikin et. al. (2013) investigated HVFA concrete using 50% fly ash and developed concrete with 28-day compressive strength of 71MPa using cementitious material of 450kg/m^3 and w/c ratio of 0.31. Nath and Sarker (2011) investigated the effect of fly ash on the durability of high strength concrete using a w/c ratio of 0.31 and 40% fly ash content. They produced high strength concrete with 28-day cylinder compressive strength of 60 MPa and the compressive strength was more than 70 MPa at 56 days. They also reported that the 56 day strength of 40% FA concrete with w/c ratio of 0.29 yielded relative strength of 92% of OPC concrete. Owens et al. (2010) investigated activation of 50%FA pastes using chemical activators and achieved 7-day compressive strength of approximately 50MPa in specimens cured at 20ºC. In specimens cured at 60ºC for one day, the 7-day compressive strength was approximately 60MPa. The results obtained by Owens et al. (2010) compare well with the compressive strength results achieved in this study. Bilodeau and Malhotra (1995) achieved 28-day cylinder compressive strength of approximately 47MPa using 50% fly ash content. Table 4-17 outlines the compressive strength results reported in similar studies on HVFA concrete.

Table 4-17: Compressive Strength of High Volume Fly Ash Concrete Mixes

		Kate & Thakare, 2017	Elsageer et. al., 2009	Solikin et. al. 2013	Nath and Sarker (2011)	Results Obtained in This Study (23°C | No Activator)	
Cementitious material (kg/m^3)		478kg	367kg	450kg	440kg	400kg	400kg
OPC Content (kg/m^3)		263kg	202kg	225kg	264kg	200kg	200kg
Fly Ash Content (kg/m^3)		215kg	165kg	225kg	176kg	200kg	200kg
Fly Ash Content (%)		45%	45%	50%	40%	50%	50%
w/c Ratio		0.33	0.3	0.31	0.31	0.35	0.45
Sample Type		-	100 mm cubes	100mm Diameter Cylinders	100mm Diameter Cylinders	100-mm cubes	100-mm cubes
Curing Temperature		-	20^oC	24^oC	23^oC	23^oC	23^oC
Cement (Major Oxides)	SiO_2	-	20.6%	-	21.1%	21.15%	21.15%
	CaO	-	63.4%	-	63.6%	61.41%	61.41%
Fly Ash (Major Oxides)	SiO_2	-	45-51%	65.9%	50.5%	53.98%	53.98%
	Al_2O_3	-	27-32%	28.89%	26.6%	32.55%	32.55%
Curing Age (Days)		**Compressive Strength (MPa)**					
1 Day		-	20 MPa	-	-	21 MPa	7 MPa
3 Days		-	40 MPa	-	-	34 MPa	17 MPa
7 Days		38 MPa	60 MPa	-	-	44 MPa	25 MPa
28 Days		39 MPa	70 MPa	71 MPa	60 MPa	67 MPa	42 MPa
56 Days		46 MPa	-	75 MPa	75 MPa	-	-
90 Days		68 MPa	-	-	-	89 MPa	62 MPa
180 Days		-	-	-	-	105 MPa	75 MPa
Study Location		India	University of Liverpool	Melbourne, Australia	Australia	South Africa	

The compressive strength results obtained in this study indicate that the rate of strength development of fly ash concrete increased when it was subjected to high temperature curing whereas the late age strength development of OPC concrete reduced when it was subjected to high temperature curing. This observation is consistent with findings of similar studies on the influence of curing temperature on OPC concrete and high-volume fly ash concrete (Elsageer et. al., 2009; Owens et al., 2010; Wajahat et al. (1991)). The reduction in late age strength of OPC concrete due to high temperature curing is consistent with the model developed by Berry and Malhotra (1987), presented in Figure 4.36 which shows the relationship between compressive strength factor and curing temperature rise.

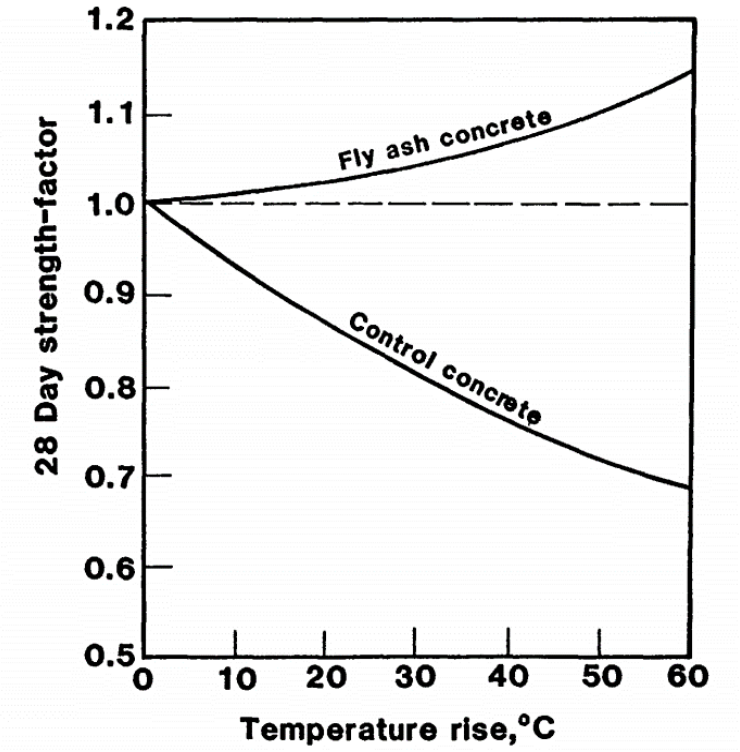

Figure 4.36: Effect of curing temperature rise on compressive strength development (Berry and Malhotra, 1987)

The compressive strength results of fly ash concrete are also comparable with the results of a study conducted by Seedat (2003) using the same type of fly ash that was used in this study. Seedat (2003) achieved 28-day compressive strength of 84MPa with OPC concrete and 83MPa with 20% fly ash concrete using a w/c ratio of 0.38 and binder content of 400kg/m^3 of concrete. The compressive strength that he achieved with 20% fly ash concrete in all the concrete mixes was similar to or higher than the strength of OPC concrete. There was no compressive strength reduction as a result of incorporating 20% fly ash in concrete. In this study it was observed that the majority of the 25% fly ash concrete mixes yielded higher 28-day compressive strength than OPC concrete mixes. The compressive strength results obtained in this study are also comparable to the typical 28-day compressive strength values shown in Table 4-18 which were suggested by the supplier of fly ash that was utilised in this study.

Table 4-18: Compressive Strength Values Suggested by Fly Ash Supplier (Ash Resources)

	OPC Concrete	**10% FA Concrete**
CEM 1	400kg	360kg
Ultra-Fine Fly Ash	-	40kg
w/c ratio	0.41	0.35
Compressive Strength		
1 day	15MPa	20MPa
7 Days	52MPa	58MPa
28 Days	70MPa	82MPa
90 Days	70MPa	91MPa

The high compressive strength results obtained in this study are consistent with the results achieved in other similar studies alluded to in this section. Ekolu and Murugan (2012) evaluated high strength concrete mixes and achieved 28-day compressive strength of 87MPa using blended cement with up to 20% fly ash and a w/c ratio of 0.4.

4.1.5 Relationship Between Compressive Strength, Age and Fly Ash Content

Relationship Between Compressive Strength and Age of Concrete

Regression analysis was used to correlate the compressive strength and concrete age for each concrete mix. It was established that the logarithmic regression was the most applicable in correlating the relationship between compressive strength (f_c) and concrete age (t). The relationships between compressive strength and concrete age follow the regression analysis functions shown in Figure 4.37 with correlation (R^2) values ranging between 0.85 and 0.99. The typical regression trend lines correlating compressive strength to concrete age are shown in Figure 4.37.

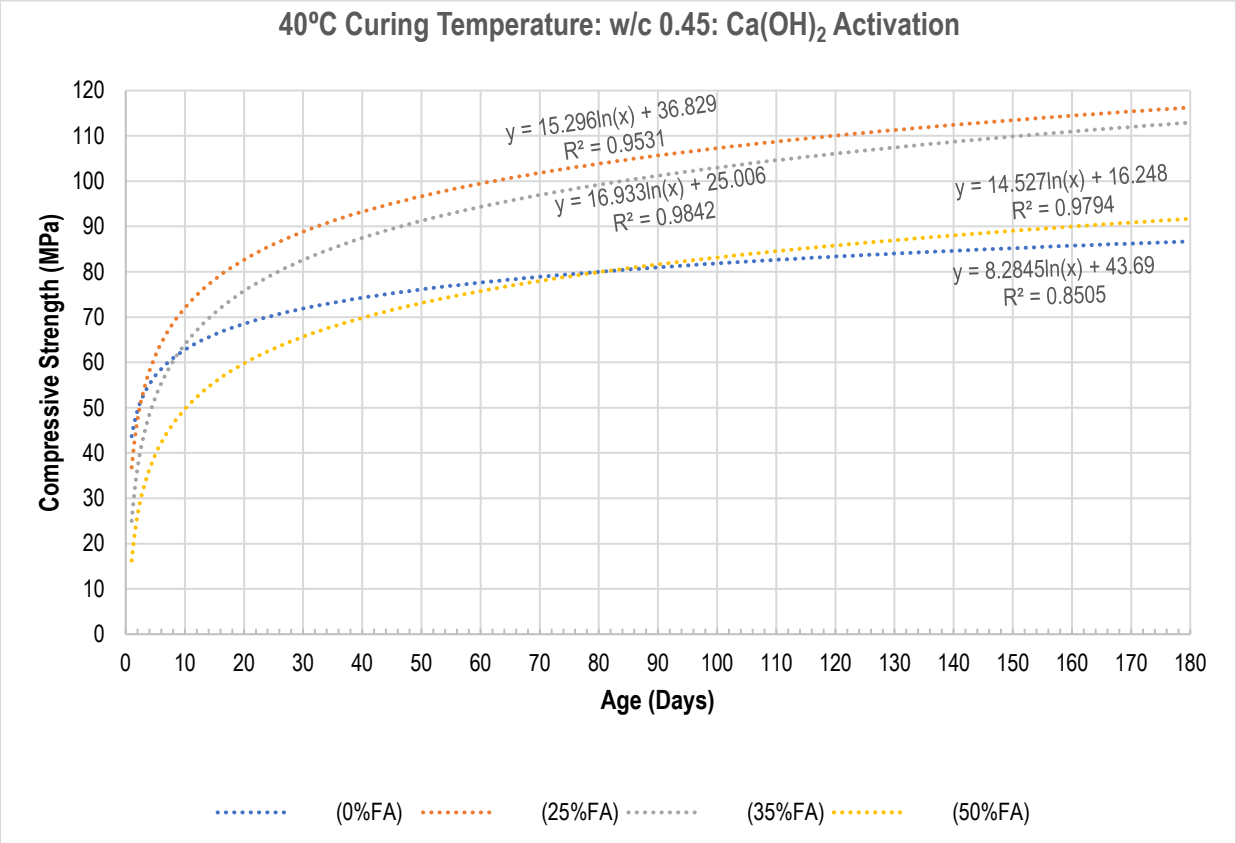

Figure 4.37: Typical Regression Lines for The Relationship Between Compressive Strength and Concrete Age

The regression functions for each particular concrete mix showed a high correlation between concrete compressive strength and concrete age. The regression functions can be reliably used to develop prediction models for compressive strength at any age of concrete.

Relationship Between Compressive Strength and Fly Ash Content

The graphs in Annexure A3 outline the relationship between compressive strength and FA content for concrete at the ages of 1 day, 3 days, 7 days, 28 days, 90 days and 180 days. Figure 4.38 shows the typical regression trendline graphs outlining the relationship between compressive strength and FA content at each specific concrete age. It was established that the relationship between compressive strength and FA content can be best described by a polynomial regression function of the form shown in Equation 4-3.

$$f_c = Ax^2 + Bx + C \qquad \text{Equation 4-3}$$

Where : f_c is compressive strength, MPa
A, B and C are constants
x is fly ash content (%)

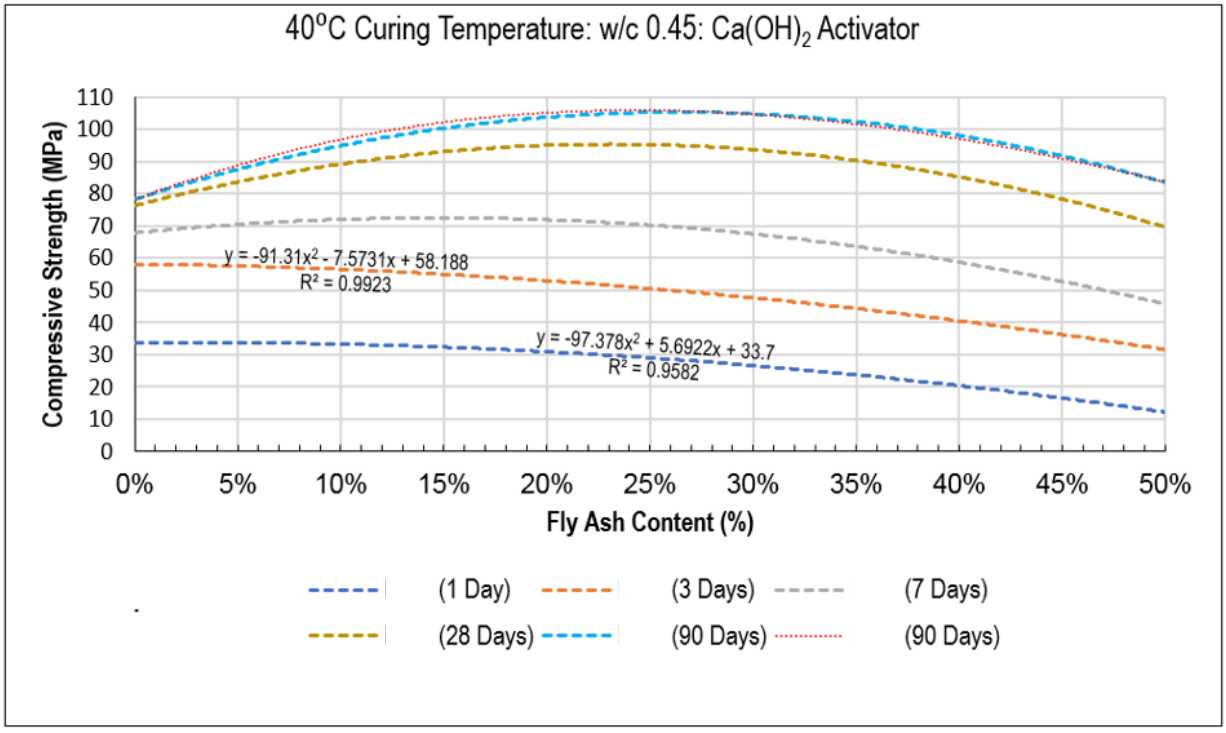

Figure 4.38: Typical Regression Lines for Relationship Between Compressive Strength and FA Content

4.2 X-Ray Diffraction Analysis

X-ray diffraction (XRD) technique was used to identify the hydrated crystalline phases and monitor the consumption of portlandite in the fly ash concrete. A qualitative XRD analysis of milled concrete samples was done at the ages of 28 days and 90 days. The analysis was done on concrete with water to cement ratio of 0.45 which was cured in water at either 23^0C or 40ºC. The concrete cubes were crushed into small particles and thereafter saturated in isopropanol liquid. The isopropanol liquid was used as a drying agent in order to stop the hydration process by removing and replacing water molecules in the pores through a process of solvent exchange. The Isopropanol liquid was then allowed to evaporate leaving dry samples. Kowalczyk et al. (2014) state that solvents such as methanol, isopropanol and acetone are effective in the removal of water from concrete in order to halt the hydration reaction. However, they state that isopropanol is a better solvent because it does not alter the properties of the cement paste during solvent exchange. The crushed concrete samples were milled to a powder using a pneumatic milling machine. Isopropanol liquid was added again to the powder samples in order to extract any water still present. The powder samples were allowed to dry and thereafter they were examined with a Bruker D2 Phaser X-ray diffractometer using scan radiation wavelength of 1.54060 and diffraction angle of $2\boldsymbol{\theta}$. The phases were identified by comparing with known XRD patterns for fly ash concrete hydration products. The key objective of qualitative XRD analysis was to track the consumption of $Ca(OH)_2$ in concrete samples. Figure 4.39 up to Figure 4.42 show a comparison of the diffractograms of OPC and 50%FA concrete at the ages of 28 days and 90 days.

Figure 4.39 shows the XRD patterns for OPC and 50%FA concrete samples cured at 40^0C with $Ca(OH)_2$ Activator. The diffractograms show the existence of hydration products of OPC and 50%FA concrete and they also indicate the presence of Quartz, which is derived from the fine and coarse aggregates. A comparison of the diffractograms in Figure 4.39 indicates that the intensity of the portlandite peaks was significantly higher in OPC concrete mixes compared to 50%FA concrete mixes at both 28 days and 90 days. This notable difference in portlandite peaks gives an indication of significant $Ca(OH)_2$

depletion in high volume fly ash concrete compared to OPC concrete. Hung (1997) reported that the portlandite peaks for high volume fly ash concrete completely disappeared at the age of 90 days. The depletion of $Ca(OH)_2$ in 50%FA mixes confirms the existence of fly ash pozzolanic activity. It can be noted that there is not much difference in the portlandite peaks of 50%FA concrete at the ages of 28 days and 90 days. This can be attributed to the fact that the bulk of $Ca(OH)_2$ was consumed by the pozzolanic reaction within the first 28 days and not much pozzolanic activity took place after the 28 days. This could be the justification for the high 28-day compressive strength of 50%FA concrete cured at 40ºC. In OPC concrete the portlandite peaks are high and they also appear to be equally high at both 28 days and 90 days. This gives an indication that there was no consumption of portlandite in OPC concrete.

Figure 4.40 shows the XRD patterns for OPC and 50%FA concrete samples cured at 40^0C without calcium hydroxide activator. The diffractograms indicate a similar pattern to those shown in Figure 4.39 for concrete cured at 40ºC with calcium hydroxide activator. It can be observed that the intensity of the portlandite peaks is significantly higher in OPC concrete mixes compared to 50%FA concrete mixes at 28 days. This difference in portlandite peaks gives an indication of $Ca(OH)_2$ depletion in high volume fly ash concrete compared to OPC concrete. It can also be noted that there is not much difference in the portlandite peaks of 50%FA concrete at the ages of 28 days and 90 days.

Figure 4.41 shows XRD patterns for OPC and 50%FA concrete samples cured at 23^0C with $Ca(OH)_2$ activator. The diffractograms show that the intensity of the portlandite peaks is significantly higher in OPC concrete mixes compared to 50%FA concrete mixes at 28 days and 90 days. It can be noted that there is a difference in the portlandite peaks of 50%FA concrete at the ages of 28 days and 90 days. The portlandite peak for 50%FA concrete samples cured at 23ºC is higher at 28 days compared to the peak at 90 days. This is in contrast to the observation made in concrete samples cured at 40ºC where the 28 day portlandite peaks for 50%FA concrete were low and similar at both 28 days and 90 days. The higher 28-day portlandite peak in 50%FA concrete cured at 23ºC signals a

slower rate of pozzolanic activity compared to concrete samples cured at 40ºC. Figure 4.42 shows XRD patterns for OPC and 50%FA concrete samples cured at 23^0C without calcium hydroxide activator. The diffractograms also indicate that the intensity of the portlandite peaks is significantly higher in OPC concrete mixes compared to 50%FA concrete mixes at 28 days. It can also be noted that the portlandite peak for 50%FA concrete samples cured at 23^0C is higher at 28 days compared to the peak at 90 days. This gives an indication of slower rate of pozzolanic activity in samples cured at 23ºC.

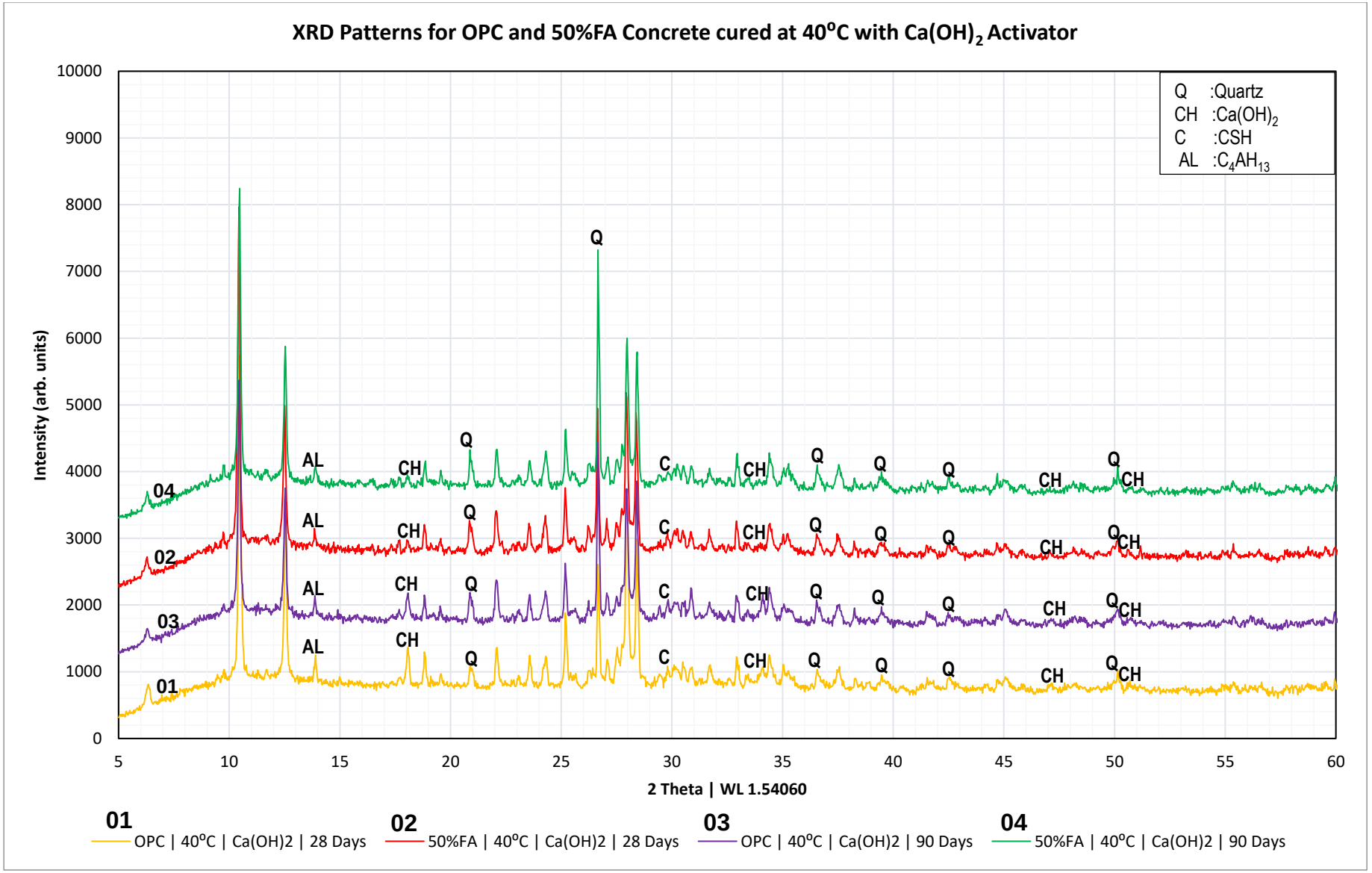

Figure 4.39: XRD Patterns for OPC and 50%FA Concrete cured at 40°C with $Ca(OH)_2$ Activator

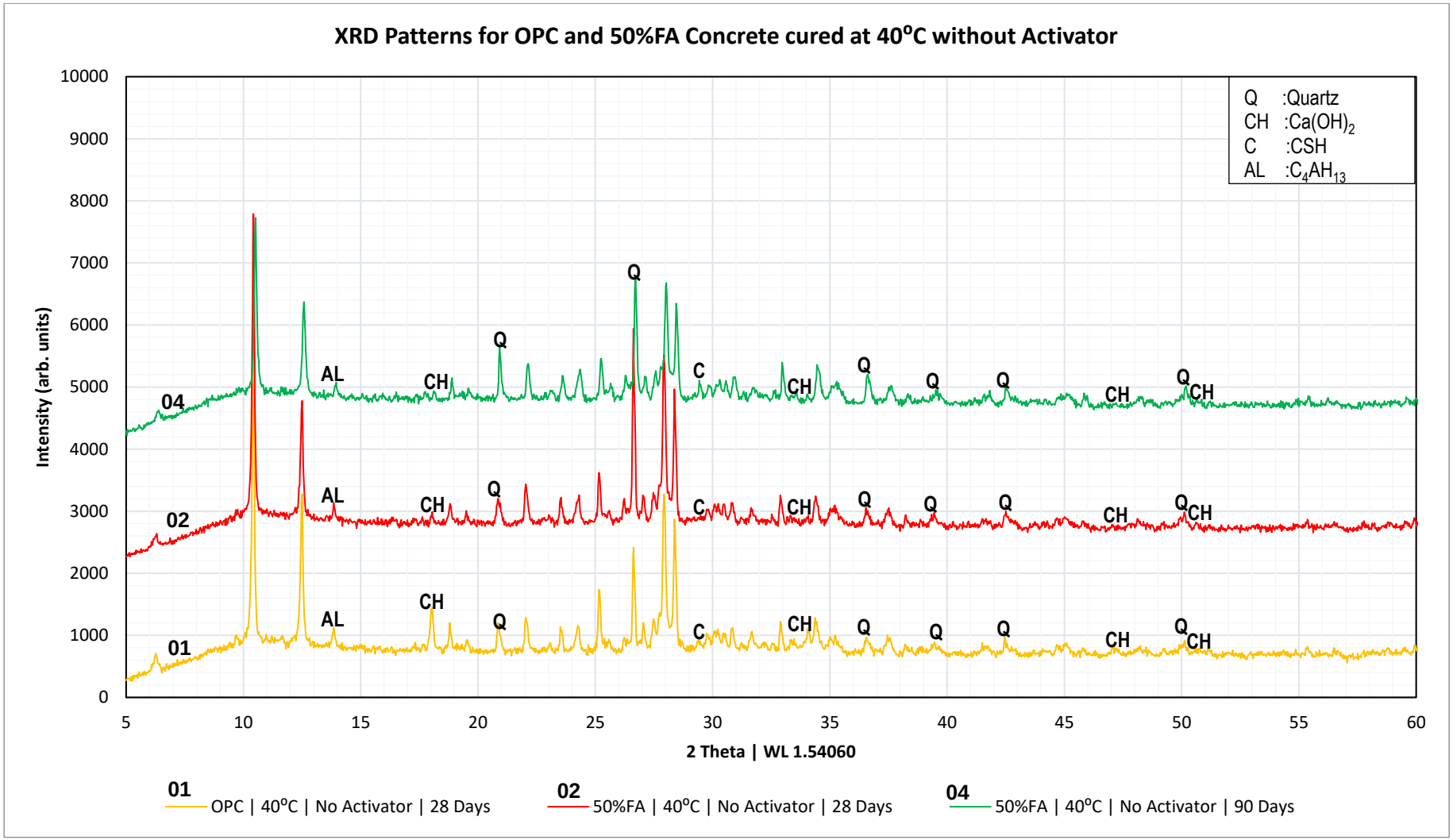

Figure 4.40: XRD Patterns for OPC and 50%FA Concrete cured at 40°C without Activator

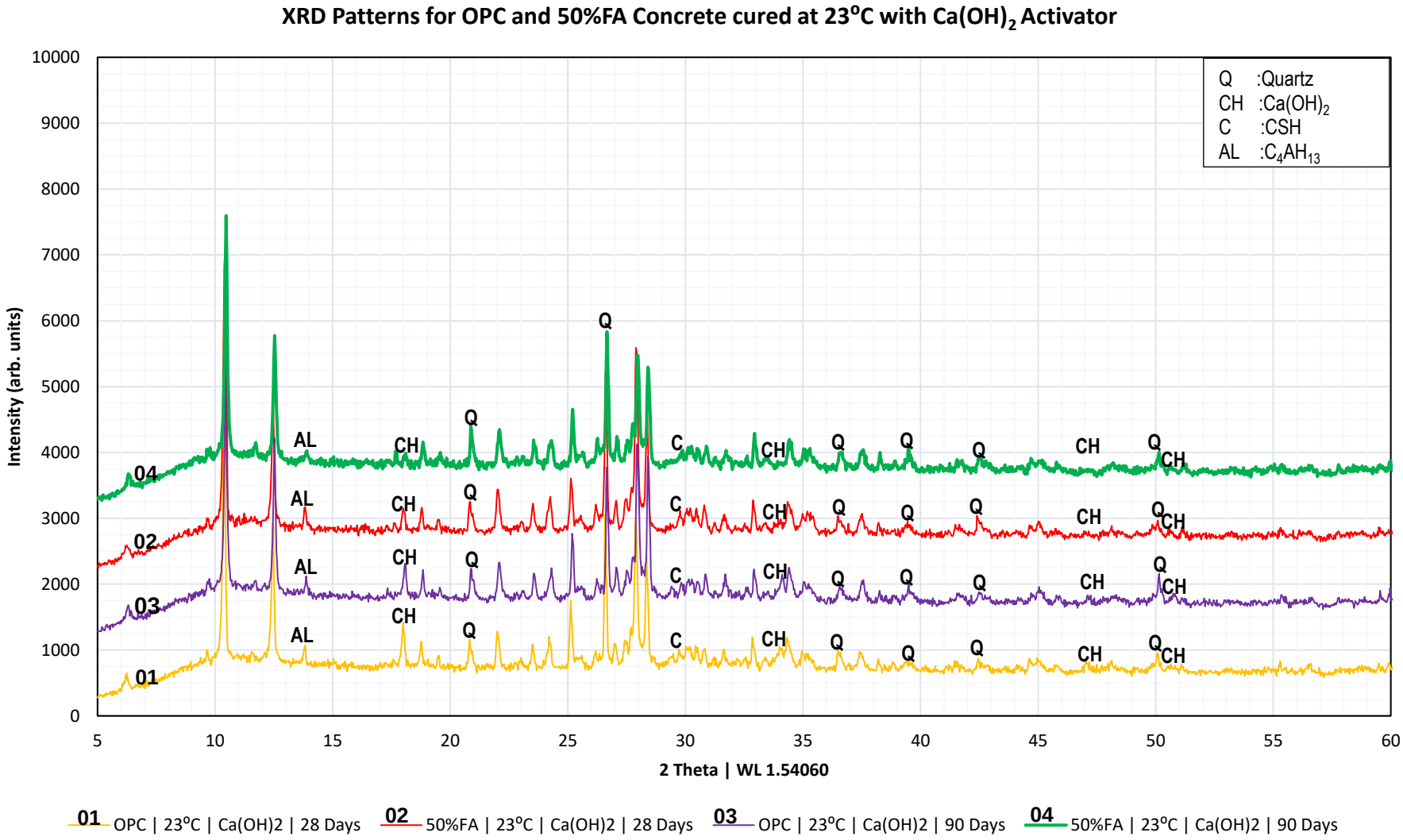

Figure 4.41: XRD Patterns for OPC and 50%FA Concrete cured at 23°C with $Ca(OH)_2$ Activator

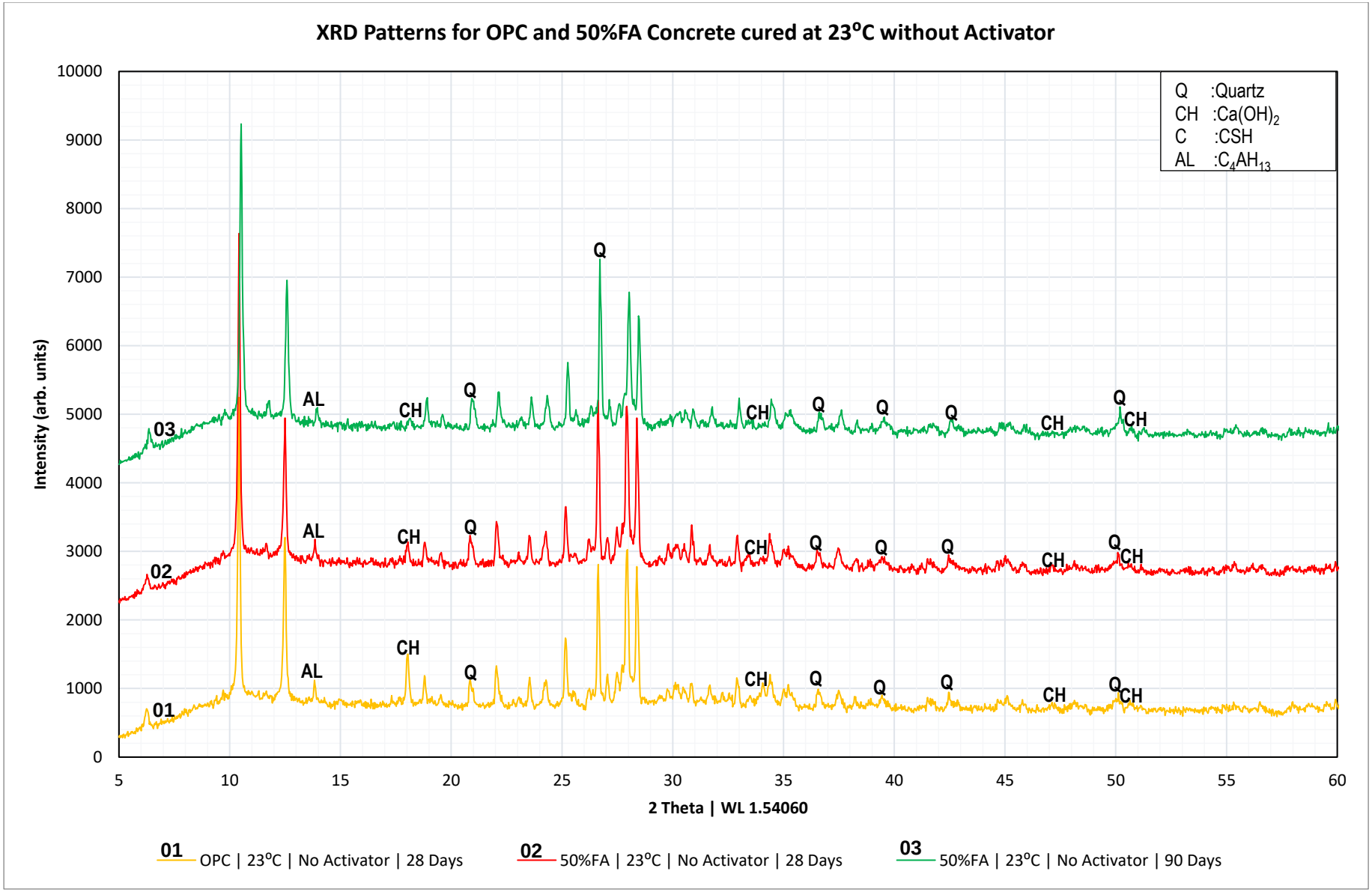

Figure 4.42: XRD Patterns for OPC and 50%FA Concrete cured at 23°C without Activator

4.3 Durability Index Test Results

The South African durability index testing methods were used to examine the durability properties of concrete. The durability properties that were investigated are water sorptivity index, oxygen permeability index and chloride conductivity index of concrete. The durability index tests evaluate the fluid transport mechanisms of concrete such as permeation, diffusion and absorption. The durability index values can be used to predict service life of concrete structures and they can also be used for specifying concrete quality (Beushausen and Alexander, 2008). Alexander (2004) states that the durability indexes can be used for classifying materials and specifying the performance of concrete. The objective of durability index testing in this study was to determine the influence of high volume fly ash, w/c ratio, curing temperature and $Ca(OH)_2$ activation on the microstructure of concrete.

The durability index tests were also used to determine the porosity of concrete specimens with differing w/c ratio, FA content and $Ca(OH)_2$ content. Porosity is an important property in the discussion pertaining to concrete durability. Concrete properties such as strength and durability are highly influenced by the porosity of the hardened cement paste. Porous concrete has low compressive strength and poor durability. Concrete strength exhibits an inverse relationship with porosity of the cement paste. An increase in porosity results in a corresponding decrease in concrete strength. Similarly, the durability of concrete exhibits an inverse relationship with concrete porosity. Porous concrete is prone to high rates of ingress of harmful substances which lead to the deterioration of concrete. The hardened cement paste pore structure consists of gel and capillary pores. Capillary pore volume is highly dependent on the w/c ratio (Owens, 2009). A high w/c ratio results in a high volume of capillary pores. Hydration products such as Calcium Silicate Hydrate have a pore filler effect and can alter the network of capillary pores resulting in concrete with low porosity. In high volume fly ash concrete, the continued pozzolanic reactions between fly ash and $Ca(OH)_2$ greatly contribute towards the reduction of capillary pores by producing more cementing compounds that act as filler for the pores. Owens (2009) alludes to the weakness of the interfacial transition zone (ITZ) caused by the thin water

film on the surfaces of aggregates which tends to increase the water content on the aggregate surfaces. He further states that fly ash has a filler effect which reduces the porosity of the ITZ. The durability tests investigated the porosity of the concrete specimens through water sorptivity index and chloride conductivity index tests.

4.3.1 Chloride Conductivity Index (CCI) Test Results

Otieno and Alexander (2015) define chloride conductivity index (CCI) as a quality control parameter used to measure the resistance of concrete to chloride penetration. The chloride conductivity tests were used to determine two parameters namely chloride conductivity index and porosity of concrete specimens. The discussion on chloride conductivity index test results focuses on the relationship between fly ash content, chloride conductivity index and porosity. These relationships are analysed in order to establish the influence of FA, curing temperature and $Ca(OH)_2$ addition on chloride conductivity and porosity of concrete. The chloride conductivity index values range from below 0.5 mS/cm for concrete with high chloride resistance to above 0.5 mS/cm porous concrete susceptible to chloride penetration (Otieno and Alexander (2015). Concrete with good durability has a low chloride conductivity index value whereas concrete with poor durability has a high value of chloride conductivity index (Alexander, 2004).

Chloride Conductivity Test: Conductivity Index Results

Table 4-19 and Figure 4.43 shows the chloride conductivity test results for concrete specimens with a w/c ratio of 0.35.

Table 4-19: Chloride Conductivity Index for Samples with w/c = 0.35

FA content	Chloride Conductivity Index (mS/cm)			
	40^oC / $Ca(OH)_2$	40^oC / No Activator	23^oC / $Ca(OH)_2$	23^oC / No Activator
0%	0.24	0.28	0.28	0.28
25%	0.04	0.05	0.15	0.18
35%	0.04	0.04	0.12	0.12
50%	0.06	0.06	0.24	0.22

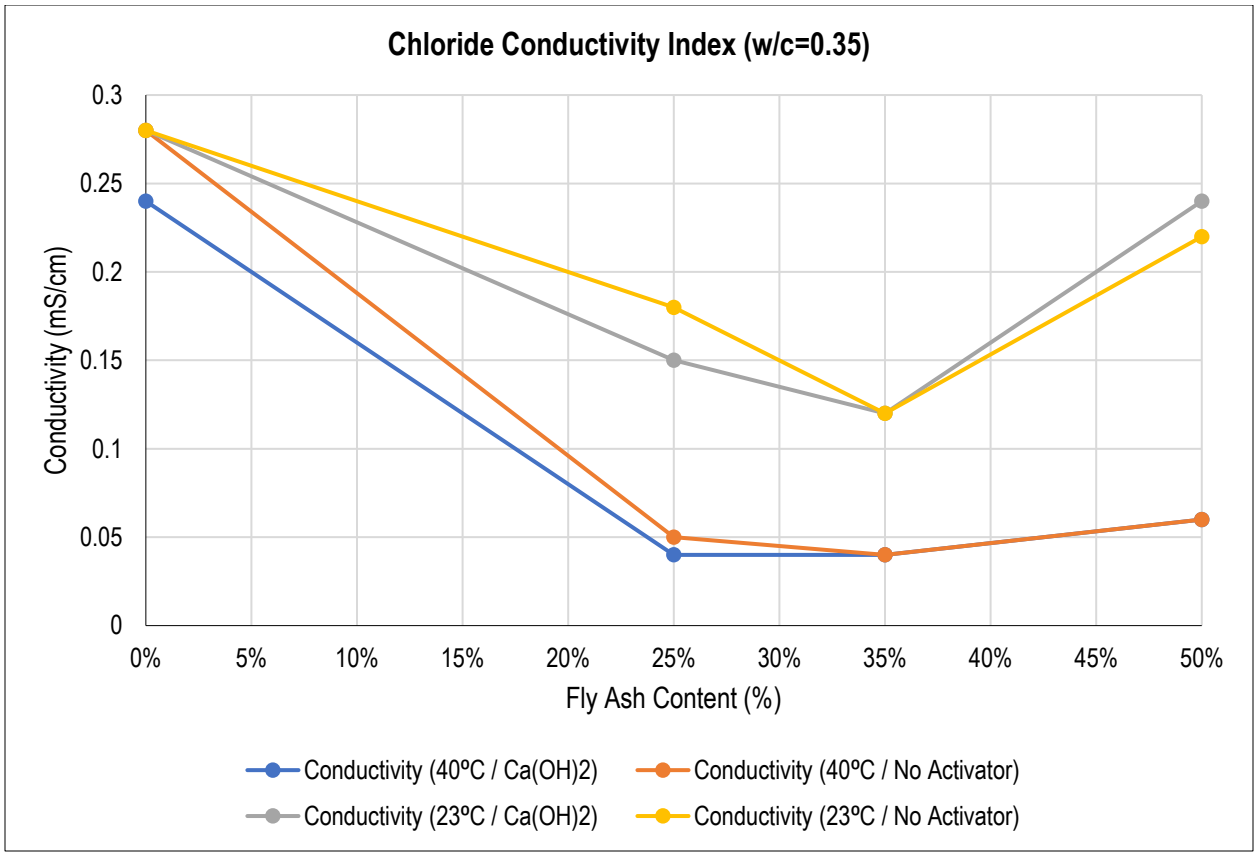

Figure 4.43: Relationship between FA content and Chloride Conductivity Index for Samples with w/c = 0.35

Table 4-20 and Figure 4.44 shows the chloride conductivity test results for concrete specimens with a w/c ratio of 0.45.

Table 4-20: Chloride Conductivity Index for Samples with w/c = 0.45

FA content	Chloride Conductivity Index (mS/cm)			
	40^oC / $Ca(OH)_2$	40^oC / No Activator	23^oC / $Ca(OH)_2$	23^oC / No Activator
0%	0.74	0.77	0.76	0.85
25%	0.09	0.13	0.38	0.45
35%	0.06	0.07	0.27	0.29
50%	0.08	0.07	0.37	0.39

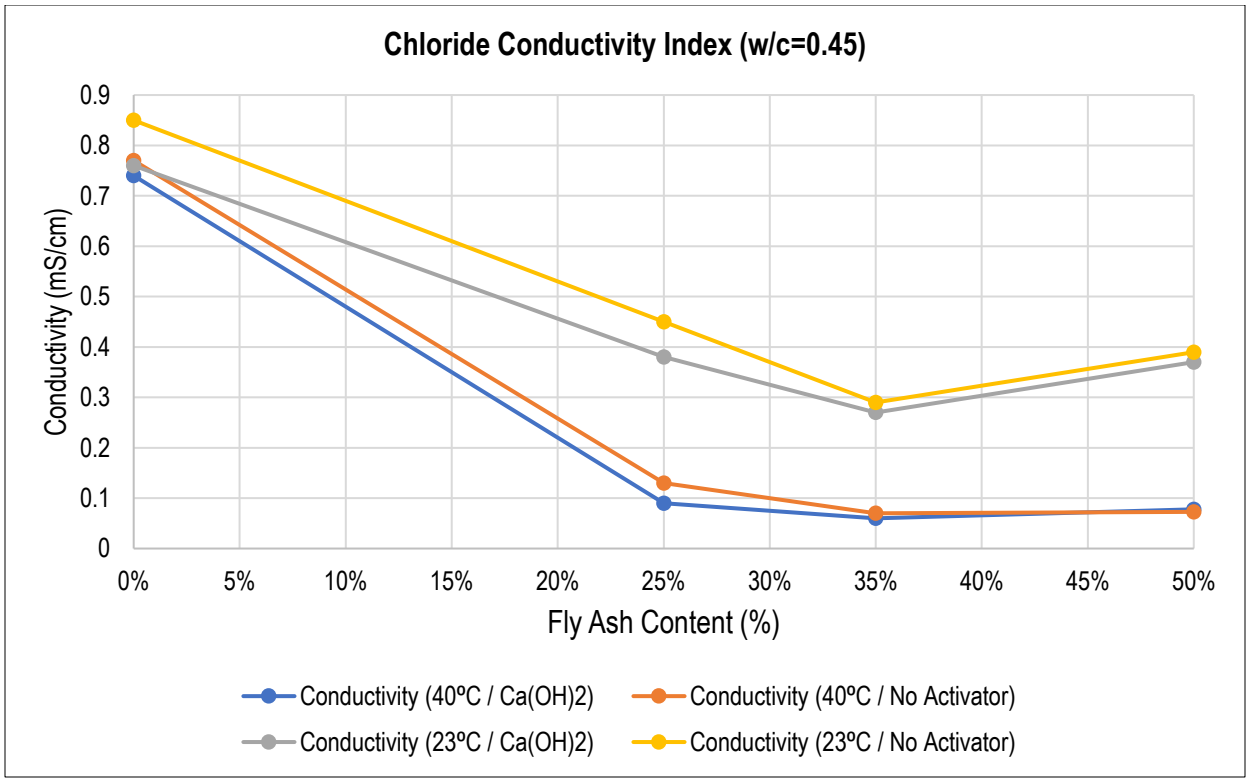

Figure 4.44: Relationship between FA content and Chloride Conductivity Index for Samples with w/c = 0.45

Table 4-19 and Table 4-20 show the results of the chloride conductivity index tests for concrete specimens with w/c ratio of 0.35 and 0.45 respectively. The relationship between chloride conductivity index and fly ash content is shown by graphs in Figure 4.43 and Figure 4.44. It can be observed from the graphs that the chloride conductivity index results for both w/c ratios exhibit identical trends. The results clearly indicate that OPC concrete had the highest chloride conductivity index for concrete with w/c ratios of 0.35 and 0.45. This result is consistent with the findings of the study conducted by Nath and Sarker (2011) in which they investigated the effect of fly ash on the durability properties of high strength concrete and reported that fly ash concrete had better resistance to chloride ion penetration compared to OPC concrete. They concluded that the resistance to chloride penetration increased with the increase in fly ash content. It can also be observed from the graphs that there was a significant reduction in chloride conductivity for concrete specimens with 25% FA and 35% FA across both w/c ratios of 0.35 and 0.45. The reduction in chloride conductivity index is consistent with the findings of a study conducted by Alexander et al. (2001) on fly ash and GGBS concretes which reported that there was

a reduction in chloride conductivity index in concrete incorporating FA and GGBS. Gardner et al. (2006) states that materials like fly ash can change the microstructure of cement paste resulting low permeability and increased chloride binding capacity. Saha (2017) investigated the effect of fly ash on the durability properties of concrete and reported that fly ash concrete had lower chloride permeability. He attributed this to alkali binding and discontinuous pore network of fly ash concrete. Alkali binding is the uptake of alkali ions by hydrates such as Calcium Silicate Hydrates (C-S-H) through surface adsorption and structural incorporation (Ye and Radlinska, 2017).

The results indicate that the chloride conductivity index was lowest in concrete with 35% fly ash content. The influence of curing temperature on chloride conductivity index was distinct and significant. It was observed that concrete cured at 40^0C had significantly lower chloride conductivity index compared to the concrete cured at 23^0C. This was observed across all concrete specimens with w/c ratios of 0.35 and 0.45. This reduction in chloride conductivity index can be attributed to the role played by heat in accelerating pozzolanic reactions that increase the quantity of cementing compounds which fill the pore spaces and lead to the reduction of capillary pore sizes in the hardened cement paste. Based on these observations, it can be concluded that curing temperature regimes have a significant influence in the durability of concrete with respect to the chloride ion diffusion. The results also indicate that the chloride conductivity index of 50%FA concrete slightly increased when compared to the chloride conductivity index of 25%FA and 35%FA concrete. This observation is consistent with the findings made by Dhir et al., (1997) in a study on chloride binding capacity of FA pastes. The study reported that up to 33% FA content, the chloride binding capacity was effective in improving chloride resistance, however at fly ash levels above 33%, they reported a decline in chloride binding capacity and an increase in chloride penetration. The increase in chloride conductivity index for concrete with 50% FA can also be attributed to the fact that at the 28-day age of testing concrete with 50% FA, the quantity of pozzolanic reaction products had not yet risen to levels that could start impacting on the porosity of concrete. A comparison of the results of concrete with $Ca(OH)_2$ activation and those of concrete without $Ca(OH)_2$ indicates that concrete with $Ca(OH)_2$ activation had slightly lower chloride conductivity index.

Figure 4.45 outlines the relationship between FA content, w/c ratio, $Ca(OH)_2$, curing temperature and chloride conductivity index. The bar graphs indicate the trends discussed above. It can be noted that concrete with w/c ratio of 0.35 had significantly lower chloride conductivity index compared to specimens with w/c ratio of 0.45. This confirms the fact that water to cement ratio plays a pivotal role in the porosity of concrete. A lower w/c ratio yields concrete with low porosity. Ekolua and Murugan (2012) investigated durability index performance of high strength concretes and reported that concrete with low w/c ratio of 0.4 yielded results that fall under the good durability class (CCI range: 0.75-1.5mS/cm) while higher w/c ratios gave poorer chloride conductivity indexes (CCI range: 1.5-2.5mS/cm). Similar findings were observed by McCarthy and Dhir (2005) in their investigation of chloride diffusion in HVFA mixes. They observed that the chloride diffusion decreased with increasing compressive strength. Table 4-21 outlines the suggested durability index values developed by Alexander et al., (1999). The durability classes outlined in Table 4-21 are qualitative and they provide a general framework for performance specifications (Alexander et al., 2010). Each durability class represents the applicability of the durability indexes. “Excellent” category is applicable when durability considerations are of utmost importance such as in very severe exposure conditions, “Good” category is acceptable durability for most exposure conditions, “Poor” category is applicable in mildly aggressive conditions and “Very Poor” category is applicable only in non-aggressive environments (Du-Preez and Alexander, 2004).

A comparison of the CCI results with these suggested durability index values indicates that the bulk of the CCI results fall in the “Excellent” category (CCI<0.75mS/cm). Only CCI results for OPC concrete with w/c ratio of 0.45 fall in the “Good” category (CCI range: 0.75-1.5mS/cm). A similar comparison of the CCI results with the acceptance criterion detailed in Table 4-22 shows that the bulk of the CCI results fall within the acceptable criterion for laboratory concrete. Table 4-23 shows a comparison of CCI results with values suggested by Alexander et al, (1999).

Table 4-21: Suggested Ranges for Durability Classification Index Values (Alexander et al., 1999)

Durability Class	OPI (Log Scale)	Sorptivity ($mm/hr^{0.5}$)	Chloride Conductivity (mS/cm)
Excellent	> 10	< 6	< 0.75
Good	9.5 - 10	6 – 10	0.75 – 1.5
Poor	9 – 9.5	10 – 15	1.5 – 2.5
Very Poor	< 9	> 15	> 2.5

Table 4-22: Acceptance Limits for Durability Indexes (Alexander et al., 2001)

Acceptance Criterion		OPI (Log Scale)	Sorptivity ($mm/hr^{0.5}$)	Chloride Conductivity (mS/cm)
Laboratory Concrete		> 10	< 6	< 0.75
Concrete from As-built Structures	Full Acceptance	> 9.4	< 9	< 1
	Conditional Acceptance	9 – 9.4	9 - 12	1 – 1.5
	Remedial Measures	8.75 - 9	12 - 15	1.5 - 2.5
	Rejection	< 8.75	> 15	> 2.5

Table 4-23: Comparison of Chloride Conductivity Index Results with values suggested by Alexander et al, 1999

FA content	w/c Ratio	Chloride Conductivity Index (mS/cm)			
		40^oC / $Ca(OH)_2$	40^oC / No Activator	23^oC / $Ca(OH)_2$	23^oC / No Activator
0%	0.45	0.74 < 0.75:Excellent	0.77 < 1.5:Good	0.76 < 1.5:Good	0.85 < 1.5:Good
25%		0.09 < 0.75:Excellent	0.13 < 0.75:Excellent	0.38 < 0.75:Excellent	0.45 < 0.75:Excellent
35%		0.06 < 0.75:Excellent	0.07 < 0.75:Excellent	0.27 < 0.75:Excellent	0.29 < 0.75:Excellent
50%		0.08 < 0.75:Excellent	0.07 < 0.75:Excellent	0.37 < 0.75:Excellent	0.39 < 0.75:Excellent
0%	0.35	0.24 < 0.75:Excellent	0.28 < 0.75:Excellent	0.28 < 0.75:Excellent	0.28 < 0.75:Excellent
25%		0.04 < 0.75:Excellent	0.05 < 0.75:Excellent	0.15 < 0.75:Excellent	0.18 < 0.75:Excellent
35%		0.04 < 0.75:Excellent	0.04 < 0.75:Excellent	0.12 < 0.75:Excellent	0.12 < 0.75:Excellent
50%		0.06 < 0.75:Excellent	0.06 < 0.75:Excellent	0.24 < 0.75:Excellent	0.22 < 0.75:Excellent

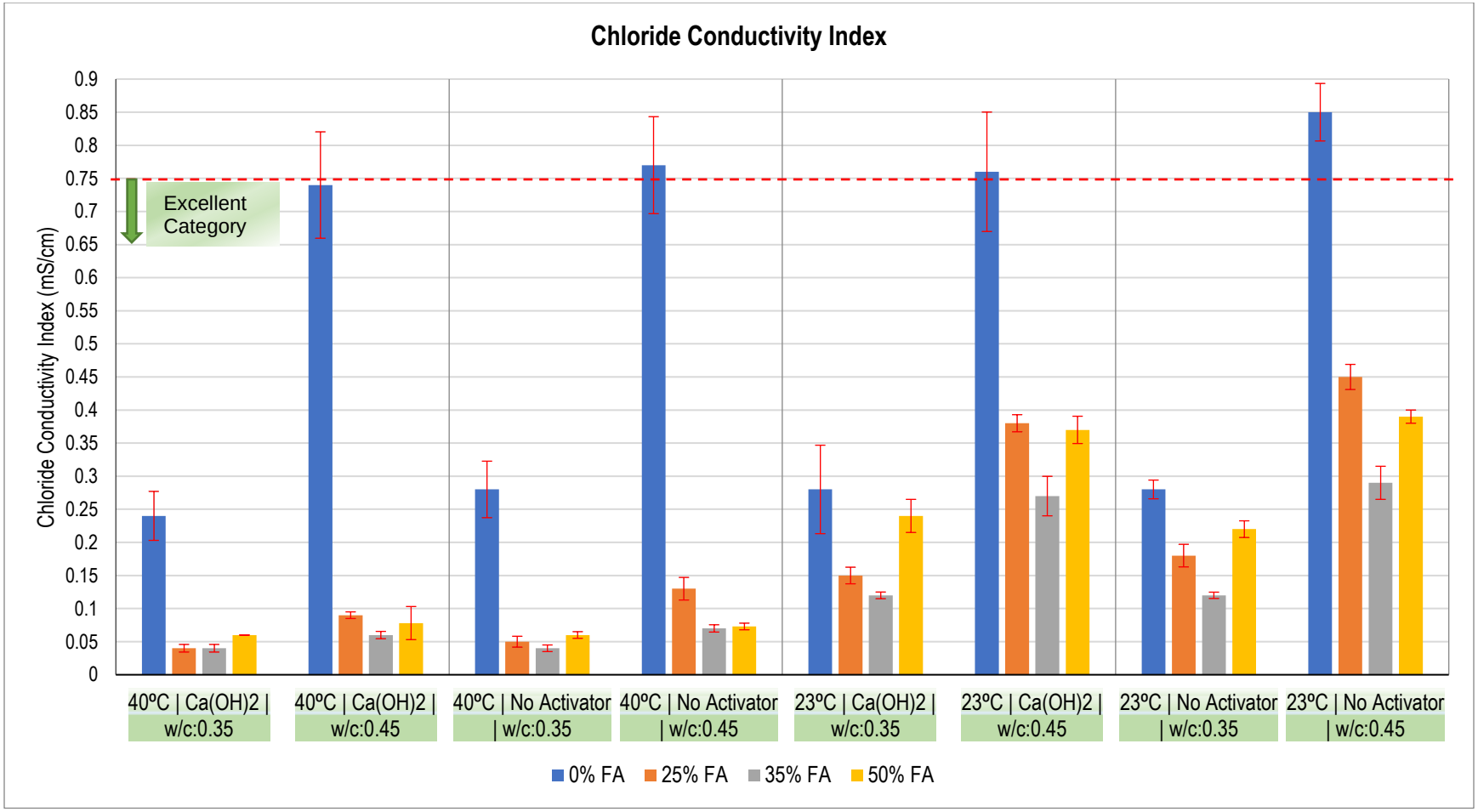

Figure 4.45: Chloride Conductivity Index Results for Specimens with w/c of 0.35 and 0.45

Chloride Conductivity Test: Porosity Results

Table 4-24 and Table 4-25 show the results of the concrete porosity determined using the chloride conductivity index test method. The porosity was determined by vacuum saturating concrete specimens in a 5M Sodium Chloride solution for a period of eighteen hours. The test procedure is outlined in Section 3.9.2.

Table 4-24: Porosity Results from CCI Tests (w/c = 0.35)

FA content	POROSITY (%)			
	40°C / $Ca(OH)_2$	40°C / No Activator	23°C / $Ca(OH)_2$	23°C / No Activator
0%	1.43	2.48	1.4	2.13
25%	0.79	1.12	1.96	2.16
35%	0.72	0.73	2.05	2.29
50%	0.95	1.03	2.36	2.73

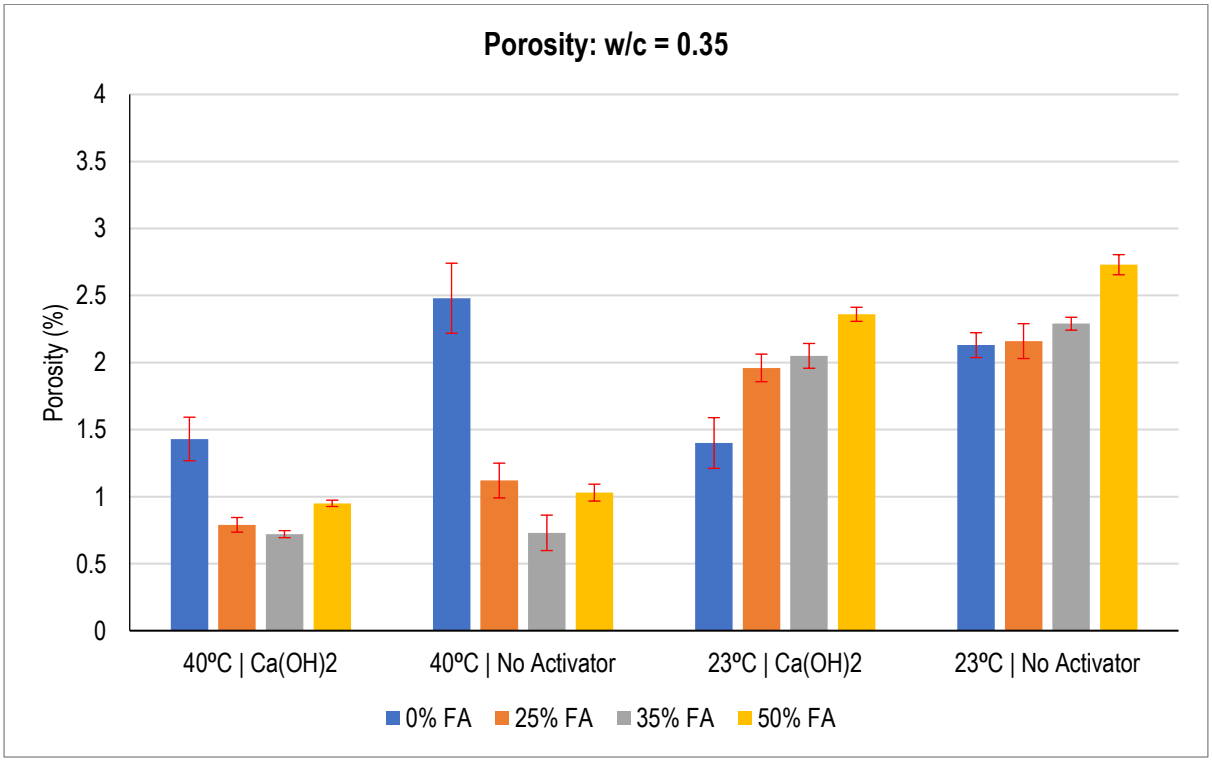

Figure 4.46: Porosity Results from CCI Tests (w/c = 0.35)

Table 4-25: Porosity Results from CCI Tests (w/c = 0.45)

FA content	POROSITY (%)			
	40°C / $Ca(OH)_2$	40°C / No Activator	23°C / $Ca(OH)_2$	23°C / No Activator
0%	3.27	3.43	3.28	3.47
25%	1.69	2.34	3.37	3.78
35%	1.31	1.51	3.45	3.82
50%	1.49	1.58	3.37	3.55

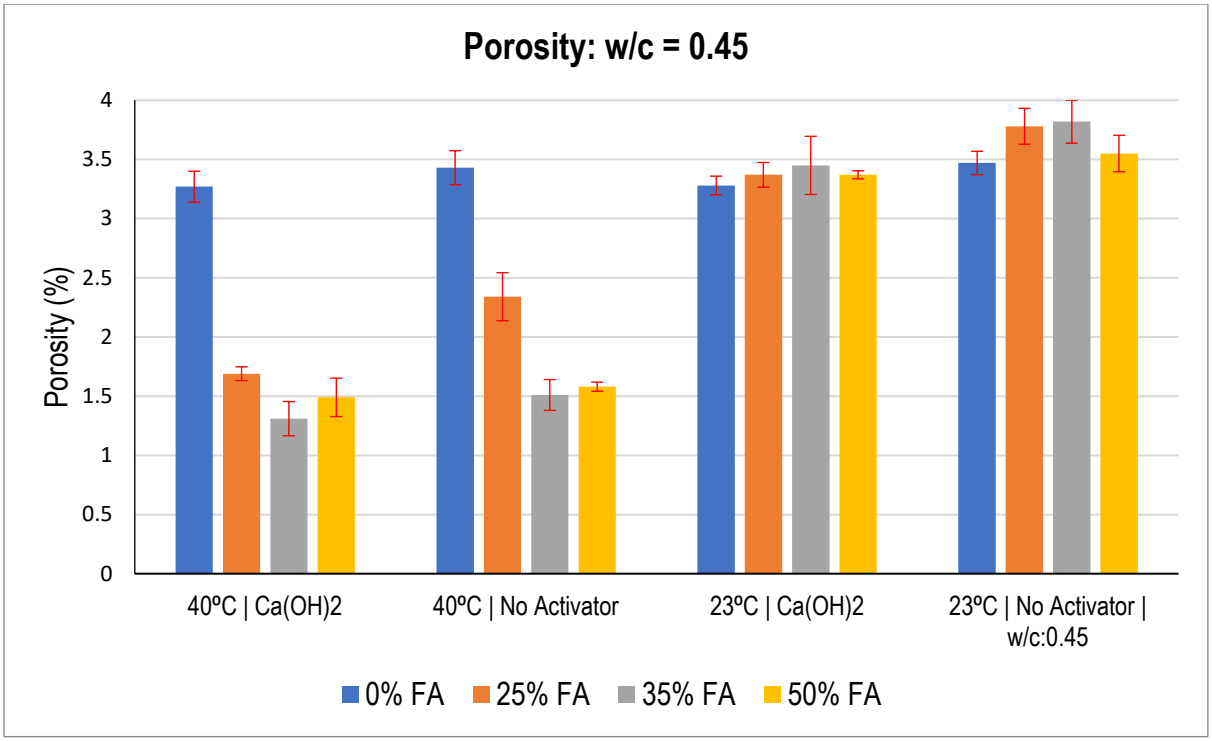

Figure 4.47: Porosity Results from CCI Tests (w/c = 0.45)

The porosity results display a trend similar to the chloride conductivity index results. Figure 4.46 and Figure 4.47 show the relationship between porosity and FA content. It can be observed that the porosity of fly ash concrete cured at high temperature is much lower than the porosity of fly ash concrete cured at 23°C. It can be noted that in concrete specimens cured at 40^0C, there was a reduction in porosity as fly ash content increased. A comparison between $Ca(OH)_2$ activated concrete and concrete without activation shows that concrete activated with $Ca(OH)_2$ yielded lower porosity at 25%FA, 35%FA and 50%FA replacement levels. However, the effect of $Ca(OH)_2$ activation was not noticeable on OPC concrete. The porosity of OPC concrete appeared to be generally the same for concrete with $Ca(OH)_2$ and for concrete without $Ca(OH)_2$ activation. This trend is observed across both curing temperature regimes and across the two w/c ratios of 0.35 and 0.45. The porosity results indicate that adding $Ca(OH)_2$ to FA concrete, curing at high temperature and reducing the w/c ratio reduces the porosity of concrete. Figure 4.48 shows the relationship between fly ash content, w/c ratio, $Ca(OH)_2$ content, curing temperature and concrete porosity.

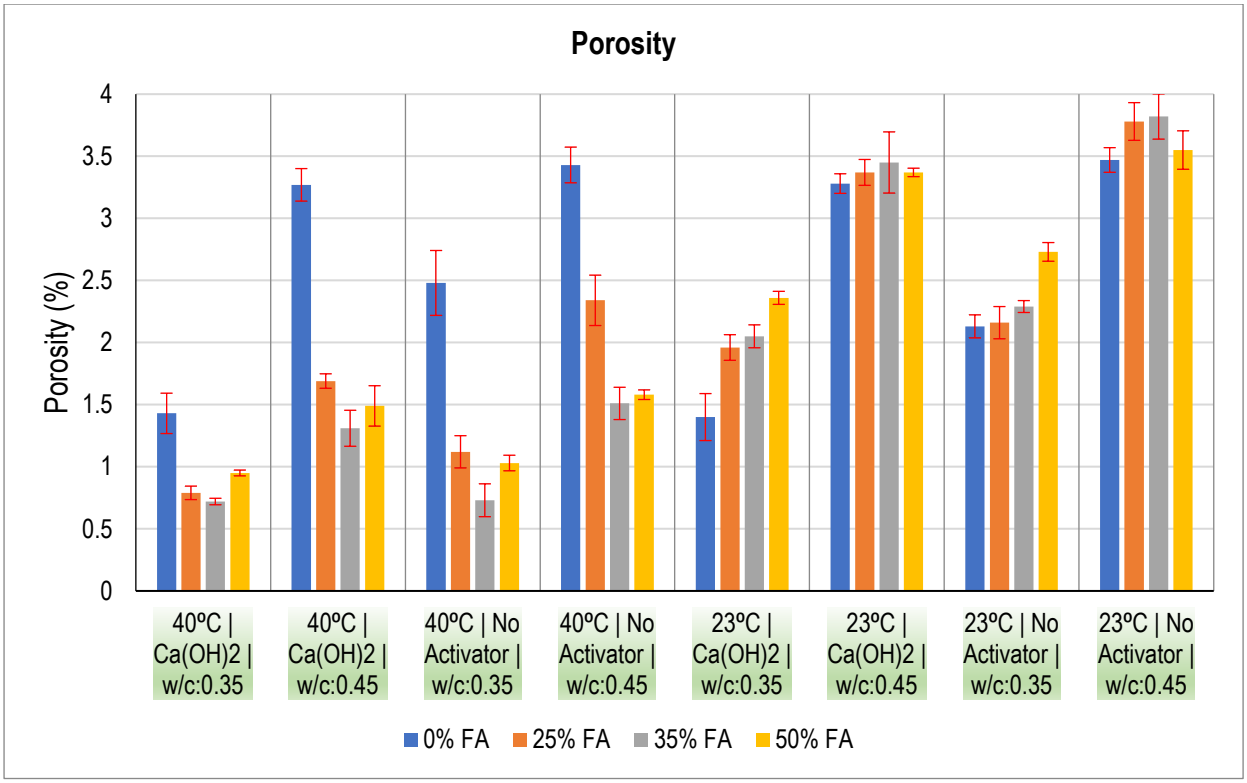

Figure 4.48: Porosity Results for Specimens with w/c of 0.35 and 0.45 based on CCI Test.

4.3.2 Water Sorptivity Test

Water Sorptivity Index (WSI) Test Results

This section gives a comprehensive discussion of the results of water sorptivity index tests. The discussion focuses on the effect of varying FA content, curing temperature and w/c ratio on water absorption of concrete. The water sorptivity tests were used to determine the water sorptivity index and effective porosity of concrete specimens. The relationships between these parameters and fly ash content were investigated in order to establish the influence of fly ash on sorptivity and porosity of concrete. Sorptivity, often reffered to as surface absorption is the rate at which water moves through a concrete medium under capillary action. The movement of water through the concrete specimen is in one direction. Sorptivity is highly influenced by the pore structure of concrete, in particular the extent of capillary pores. Concrete with a bigger and continuous network of capillary pores absorbs water at a faster rate than concrete with smaller and less interconnected capillary pores. A low water sorptivity index value depicts durable concrete whereas a high water sorptivity index value depicts concrete with poor durability. Sorptivity index values generally range from 5 $mm/h^{0.5}$ for high durability concrete to 20 $mm/h^{0.5}$ for low durability concrete (Alexander et al., 2008). The results shown in Table 4-26 and Table 4-27 were obtained from water sorptivity tests carried out on the concrete specimens. The results are an average of the output of four specimens, however in cases where some specimens exhibited huge variation, the average of three results was adopted as the final result. The outlier results were not considered in calculating the final average.

Table 4-26: Sorptivity Test Results for Specimens with w/c = 0.45

Fly Ash Content	SORPTIVITY INDEX ($mm/hr^{0.5}$)			
	40^oC / $Ca(OH)_2$	40^oC / No Activator	23^oC / $Ca(OH)_2$	23^oC / No Activator
0%	4.55	4.58	5.69	6.55
25%	5.13	5.55	5.14	5.42
35%	6.18	5.97	5.63	5.44
50%	5.53	4.95	5.28	5.96

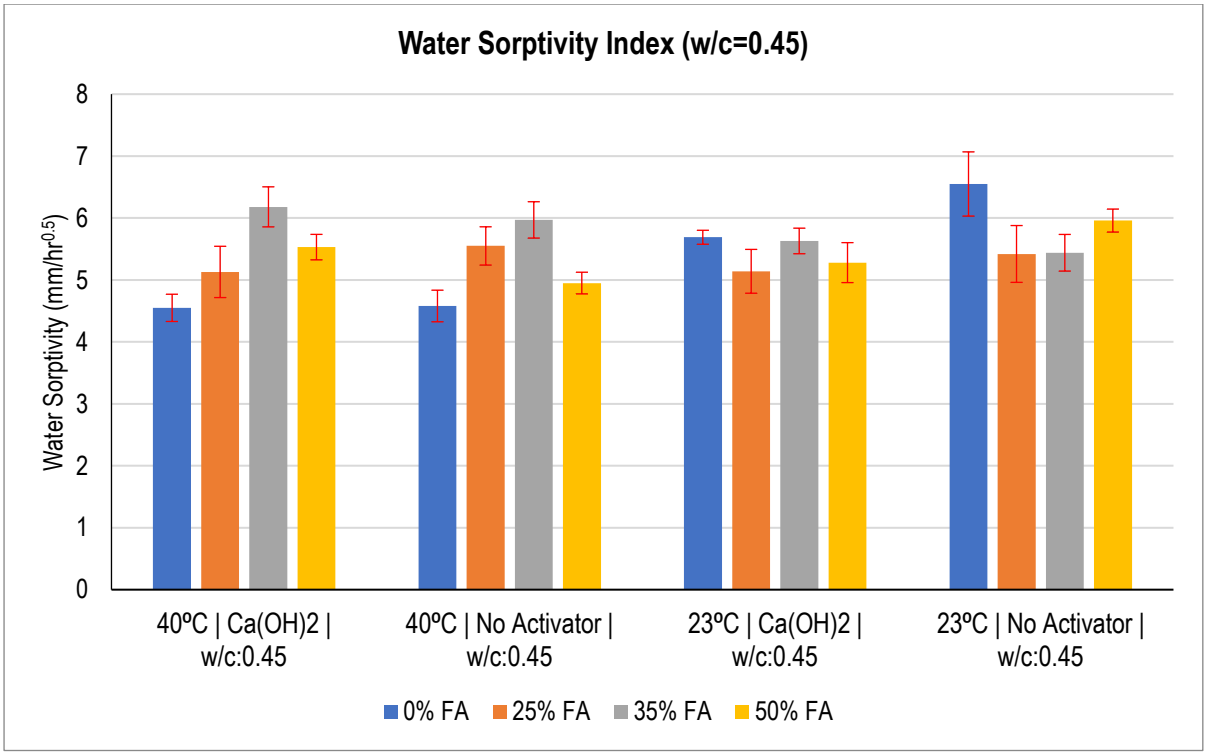

Figure 4.49: Water Sorptivity Index Results for Specimens with w/c of 0.45

Table 4-26 and Figure 4.49 show water sorptivity index results of concrete specimens with w/c ratio of 0.45. It can be observed that all the concrete specimens yielded similar sorptivity results and there were no significant differences in sorptivity results as a result of varying fly ash content, curing temperature and $Ca(OH)_2$ addition.

Table 4-27: Sorptivity Test Results for Specimens with w/c = 0.35

Fly Ash Content	SORPTIVITY INDEX ($mm/hr^{0.5}$)			
	40^oC / $Ca(OH)_2$	40^oC / No Activator	23^oC / $Ca(OH)_2$	23^oC / No Activator
0%	4.28	4.54	5.64	5.69
25%	3.63	4.55	6.04	6.43
35%	3.17	4.30	6.66	5.16
50%	4.36	3.55	4.85	5.06

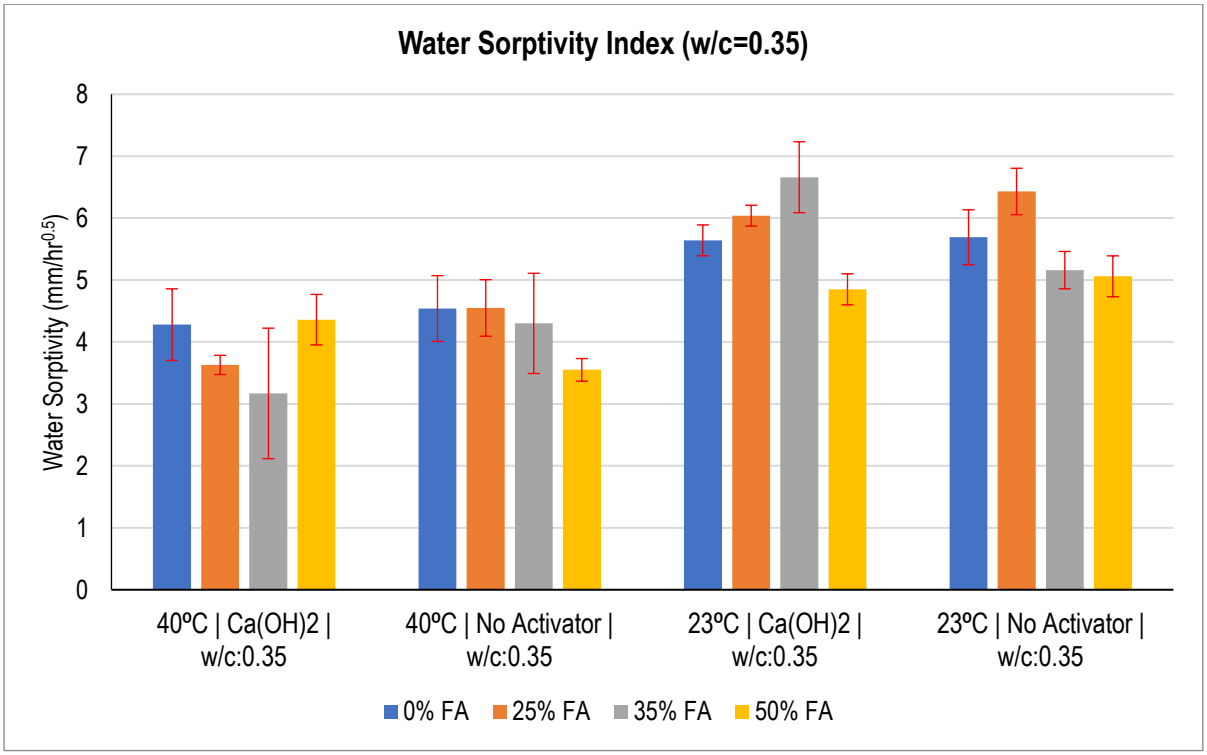

Figure 4.50: Water Sorptivity Index Results for Specimens with w/c of 0.35

Table 4-27 and Figure 4.50 show the results of water sorptivity tests for concrete specimens with w/c ratio of 0.35. The results indicate that concrete specimens that were cured at 40ºC recorded slightly lower water sorptivity results compared to specimens cured at 23ºC. It can also be observed that there are no notable differences in the water sorptivity results as a result of adding $Ca(OH)_2$ to some concrete mixes. Table 4-28 shows a comparison of Water Sorptivity Index results with values suggested by Alexander et al, (1999).

Table 4-28: Comparison of Water Sorptivity Index Results with values suggested by Alexander et al, (1999)

Fly Ash Content	w/c Ratio	SORPTIVITY INDEX (mm/hr$^{0.5}$)			
		40°C / $Ca(OH)_2$	40°C / No Activator	23°C / $Ca(OH)_2$	23°C / No Activator
0%	0.45	4.55 < 6: Excellent	4.58 < 6: Excellent	5.69 < 6: Excellent	6.55 < 10: Good
25%		5.13 < 6: Excellent	5.55 < 6: Excellent	5.14 < 6: Excellent	5.42 < 6: Excellent
35%		6.18 < 10: Good	5.97 < 6: Excellent	5.63 < 6: Excellent	5.44 < 6: Excellent
50%		5.53 < 6: Excellent	4.95 < 6: Excellent	5.28 < 6: Excellent	5.96 < 6: Excellent
0%	0.35	4.28 < 6: Excellent	4.54 < 6: Excellent	5.64 < 6: Excellent	5.69 < 6: Excellent
25%		3.63 < 6: Excellent	4.55 < 6: Excellent	6.04 < 10: Good	6.43 < 10: Good
35%		3.17 < 6: Excellent	4.30 < 6: Excellent	6.66 < 10: Good	5.16 < 6: Excellent
50%		4.36 < 6: Excellent	3.55 < 6: Excellent	4.85 < 6: Excellent	5.06 < 6: Excellent

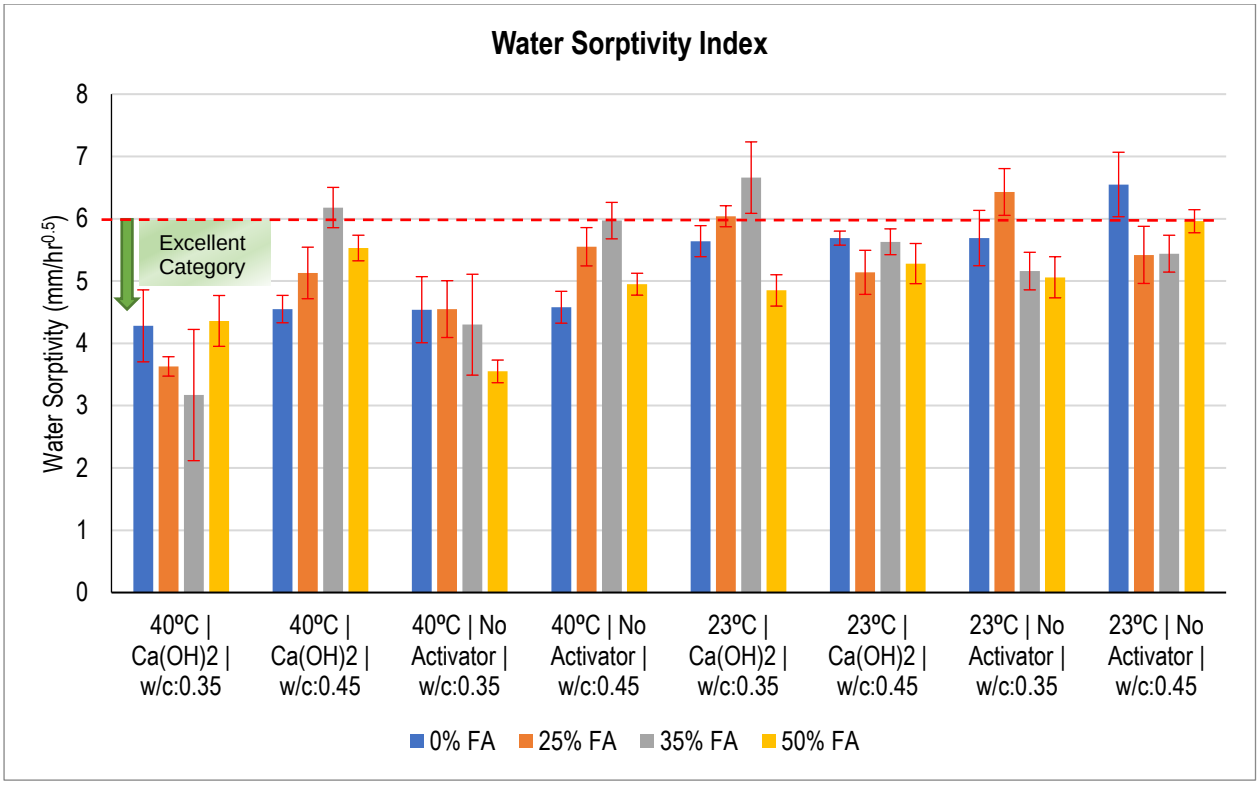

Figure 4.51: Water Sorptivity Index Results for Specimens with w/c of 0.35 and 0.45

Figure 4.51 shows a graphical comparison of all the water sorptivity index results. The results display differing trends for both w/c ratios of 0.35 and 0.45. A comparison of the results for all concrete specimens cured at 40ºC indicates that concrete with w/c ratio of 0.35 yielded slightly lower sorptivity index results compared to concrete with w/c ratio of 0.45. The lower water sorptivity index of concrete with w/c ratio of 0.35 can be attributed to the reduced density of capillary pores in concrete with lower w/c ratio. This observation is consistent with the findings of Ekolu and Murugan (2012) who investigated durability index performance of high strength concretes and reported that increasing w/c ratio resulted in corresponding increase in water sorptivity index. The results for concrete cured at 23ºC do not show any significant differences as a result of varying w/c ratio and $Ca(OH)_2$ addition. Generally, the specimens cured at 23ºC yielded higher sorptivity results when compared to concrete specimens cured at 40ºC. This can be attributed to the influence of high temperature curing. The water sorptivity index results are too close to make any conclusive remarks regarding the influence of fly ash content, curing temperature and $Ca(OH)_2$ addition. Table 4-21 shows the suggested water sorptivity index values developed by Alexander et al., (1999). A comparison of the water sorptivity index results with the suggested durability index

values indicates that the bulk of the water sorptivity index results fall in the excellent category (WSI<6). A similar comparison of the water sorptivity index results with the acceptance criterion detailed in Table 4-22 shows that the bulk of the water sorptivity results fall within the acceptable criterion for laboratory concrete.

Water Sorptivity Test: Porosity Results

Table 4-29 and Table 4-30 show the results of concrete porosity determined using the water sorptivity index test. The porosity was determined by vacuum saturating concrete specimens in a $Ca(OH)_2$ solution for a period of eighteen hours. Table 4-29 and Figure 4.52 show the results for concrete specimens with w/c ratio of 0.45.

Table 4-29: Porosity Results from Water Sorptivity Tests (w/c = 0.45)

FA content	POROSITY (%)			
	40°C / Ca(OH)2	40°C / No Activator	23°C / Ca(OH)2	23°C / No Activator
0%	6.78	7.58	7.37	7.84
25%	4.66	5.94	8.64	9.37
35%	4.47	4.4	9.67	9.71
50%	4.08	4.43	8.9	9.78

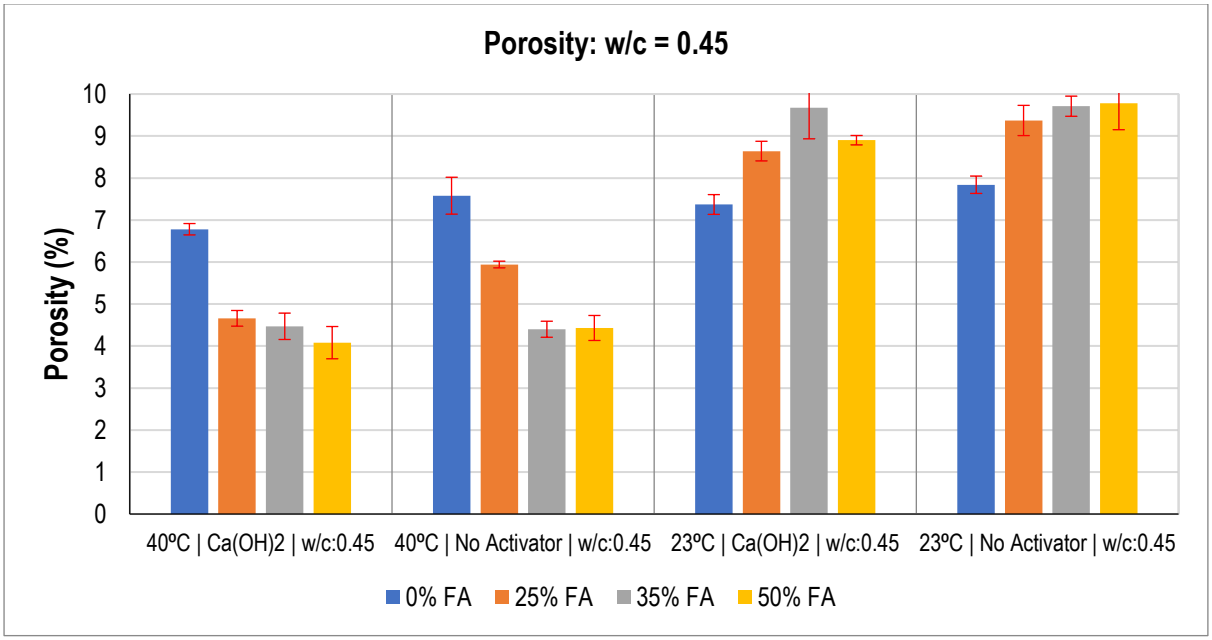

Figure 4.52: Porosity Results for Specimens with w/c of 0.45

The results presented in Figure 4.52 indicate the significant influence of high temperature curing on the porosity of fly ash concrete. The porosity results for OPC concrete are similar for concrete cured at both curing temperatures of 23ºC and 40ºC. Figure 4.52 shows that the porosity of concrete specimens cured at 23ºC increased

slightly as the FA content was increased whereas the porosity of concrete cured at 40ºC decreased as the FA content increased. The reduction in porosity of concrete cured at 40ºC is an indication of improved concrete pore structure due to the acceleration of pozzolanic reactions by heat activation. It can also be observed that under both curing temperatures, the concrete specimens with $Ca(OH)_2$ addition yielded slightly lower porosity results when compared to specimens without $Ca(OH)_2$. Table 4-30 and Figure 4.53 show the results for specimens with w/c ratio of 0.35.

Table 4-30: Porosity Results from Water Sorptivity Tests (w/c = 0.35)

Fly Ash Content	POROSITY (%)			
	40°C / Ca(OH)2	40°C / No Activator	23°C / Ca(OH)2	23°C / No Activator
0%	2.75	4.46	3.44	5.24
25%	2.25	2.15	3.86	4.02
35%	2.00	1.75	3.99	4.75
50%	2.54	2.84	6.03	6.92

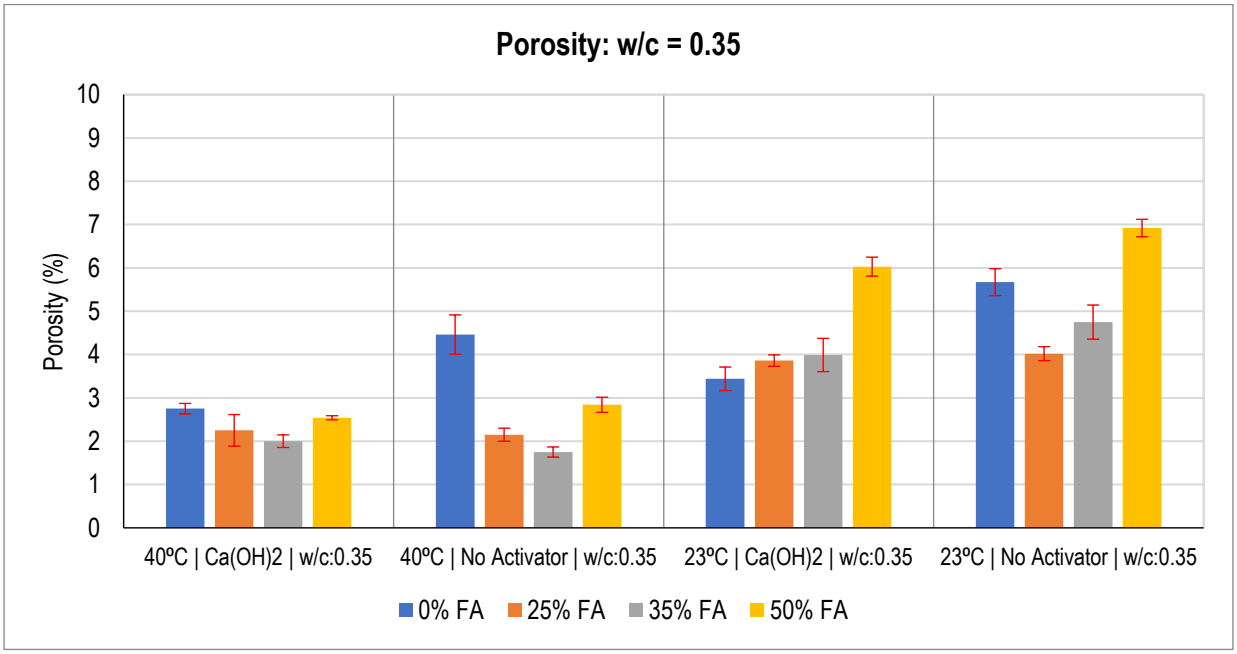

Figure 4.53: Porosity Results for Specimens with w/c of 0.35

Figure 4.53 shows a graphical presentation of porosity results for concrete with w/c ratio of 0.35. The results display a trend similar to the results of concrete specimens with a w/c ratio of 0.45. It can be noted that specimens cured at 40ºC yielded significantly lower porosity results when compared to specimens cured at 23ºC. A comparison of concrete specimens cured at 23ºC shows that specimens with $Ca(OH)_2$ activation had lower porosity results compared to those that did not have $Ca(OH)_2$

addition. A comparison of concrete specimens cured at 40ºC shows that specimens with 25% FA and 35% FA which were activated with $Ca(OH)_2$ yielded slightly lower porosity results compared to the specimens without $Ca(OH)_2$ addition. There is a trend showing that concrete with $Ca(OH)_2$ activation yielded lower porosity results compared to concrete without $Ca(OH)_2$ activation. However, this trend is not quite distinct due to the close similarities of the results. In general, the results don't display significant influence of $Ca(OH)_2$ addition on concrete porosity determined using the water sorptivity index test. 50%FA concrete specimens with $Ca(OH)_2$ addition had slightly lower porosity when compared with 50%FA specimens without $Ca(OH)_2$ activation.

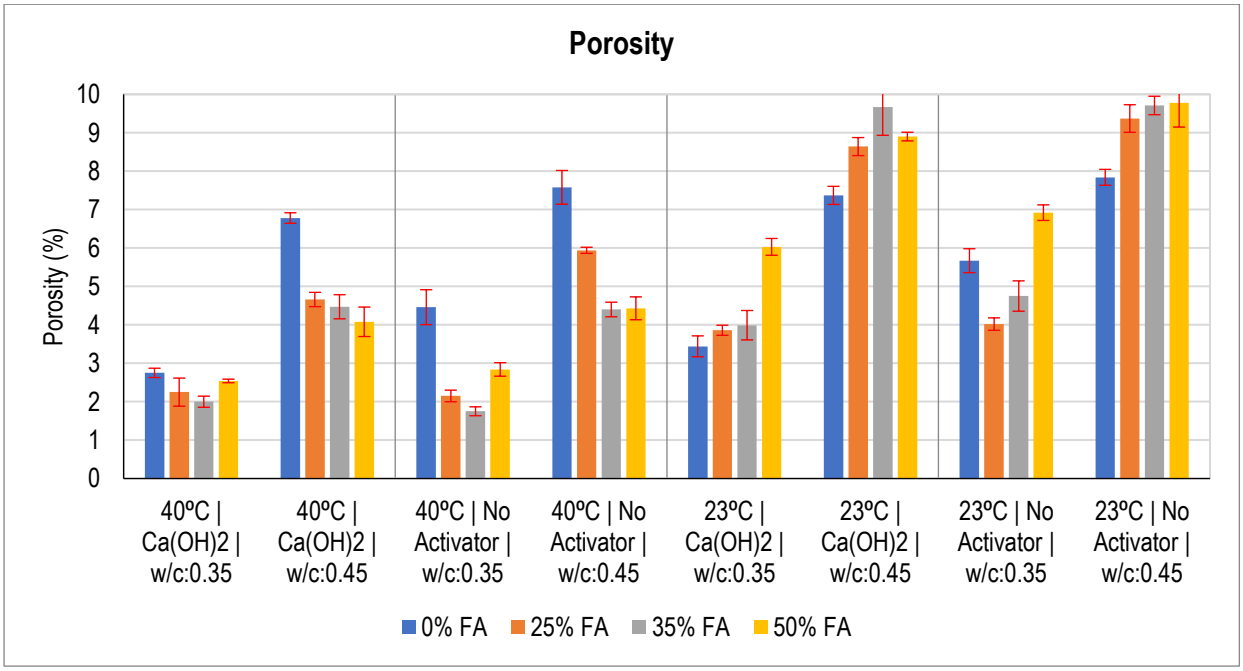

Figure 4.54: Porosity Results for Specimens with w/c of 0.35 and 0.45

Figure 4.54 shows a graphical comparison of the porosity results for concrete specimens with w/c ratio of 0.35 and 0.45. The bar graphs display a consistent trend which indicates that all the specimens with w/c ratio of 0.35 yielded lower porosity compared to specimens with w/c ratio of 0.45. This shows the influence of w/c ratio on porosity of concrete and it indicates that low w/c ratio results in reduced concrete porosity. It can be noted that adding $Ca(OH)_2$ to specimens cured at 40ºC and 23ºC did not result in significant changes of porosity. OPC concrete specimens don't show any notable changes in porosity when cured at 40ºC and 23ºC. However, fly ash concrete specimens cured at 40ºC yielded significantly lower porosity when compared

to fly ash concrete specimens cured at 23ºC. This can be attributed to the influence of fly ash as a fine filler and also the role played by high temperature curing on accelerating pozzolanic reactions. Based on these observations coupled with the sorptivity index results, it can be concluded that lower w/c ratio, high temperature curing and $Ca(OH)_2$ activation reduces the porosity of concrete and greatly contributes to the durability of concrete.

4.3.3 Oxygen Permeability Index (OPI) Test

Permeability is an important durability property of concrete. Permeable concrete is prone to ingress of deleterious substances such as carbon dioxide. The oxygen permeability index (OPI) test evaluates the extent of voids and pores in concrete and it is highly sensitive to voids and cracks in the concrete.

Permeation is another transport mechanism responsible for the movement of deleterious substances through concrete pores and cracks. The oxygen permeability index (OPI) test models the movement of fluids through concrete under a pressure gradient. The OPI test consists of a falling head permeameter in which oxygen under pressure is passed through concrete over a period of time and the Darcy coefficient of permeability (k) for the concrete is determined. The oxygen permeability index value gives a measure of the concrete permeability. High oxygen permeability index values signify concrete that is less permeable whereas low oxygen permeability index values indicate more permeable concrete. The oxygen permeability index values normally range between 8 and 11 (Alexander et al., 2008). Table 4-31 shows the oxygen permeability index results for concrete with w/c ratio of 0.45. A graphical comparison of the OPI results for concrete with w/c ratio of 0.45 is shown in Figure 4.55. It can be noted that the OPI results for all the specimens are similar such that it is not possible to determine the influence of curing temperature or $Ca(OH)_2$ addition on the oxygen permeability index. During OPI testing, it was observed that the rate of oxygen pressure decay was very slow such that some consecutive readings from the data logger were the same instead of reducing. The slow rate of oxygen pressure decay can be attributed to the dense microstructure of the concrete specimens.

Table 4-31: Oxygen Permeability Index Results for Specimens with w/c ratio of 0.45

Fly Ash Content	Oxygen Permeability Index : w/c = 0.45			
	40°C / $Ca(OH)_2$	40°C / No Activator	23°C / $Ca(OH)_2$	23°C / No Activator
0%	11.71	11.49	11.58	11.44
25%	11.49	11.24	11.09	10.97
35%	11.30	11.56	10.99	11.01
50%	11.26	10.97	11.26	10.83

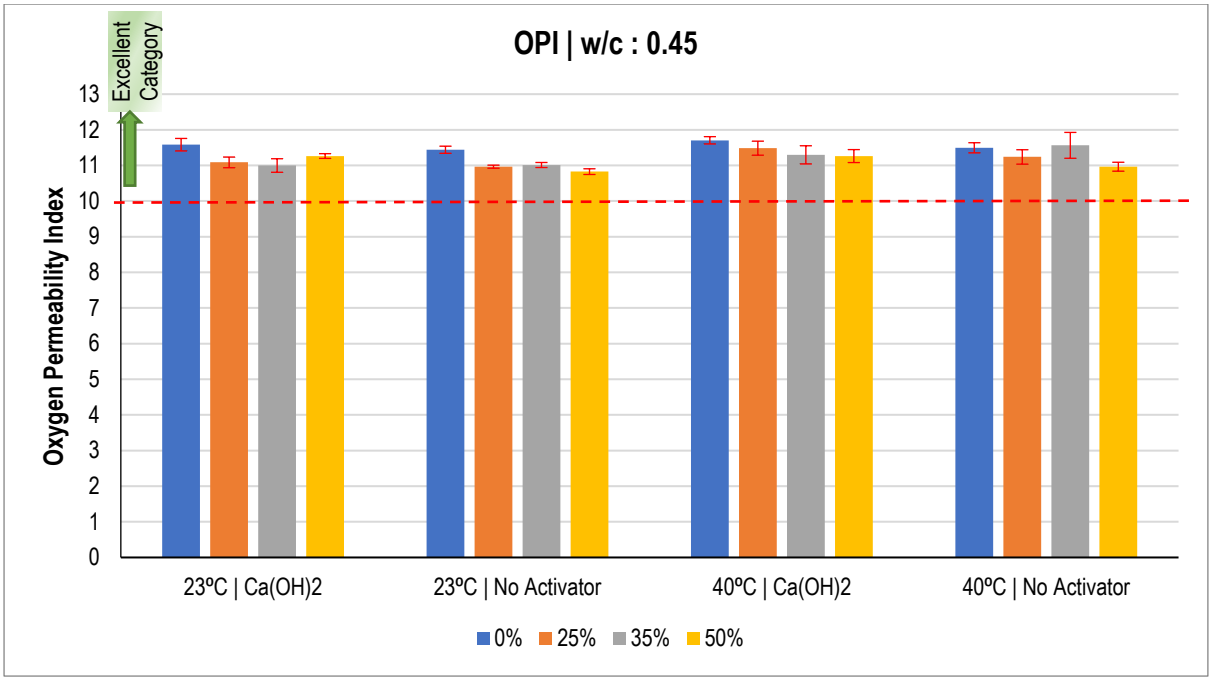

Figure 4.55: Oxygen Permeability Index Results for Specimens with w/c ratio of 0.45

Table 4-32: Oxygen Permeability Index Results for Specimens with w/c ratio of 0.35

Fly Ash Content	Oxygen Permeability Index: w/c = 0.35			
	40°C / $Ca(OH)_2$	40°C / No Activator	23°C / $Ca(OH)_2$	23°C / No Activator
0%	11.25	11.09	11.48	11.16
50%	11.23	11.50	11.14	11.25

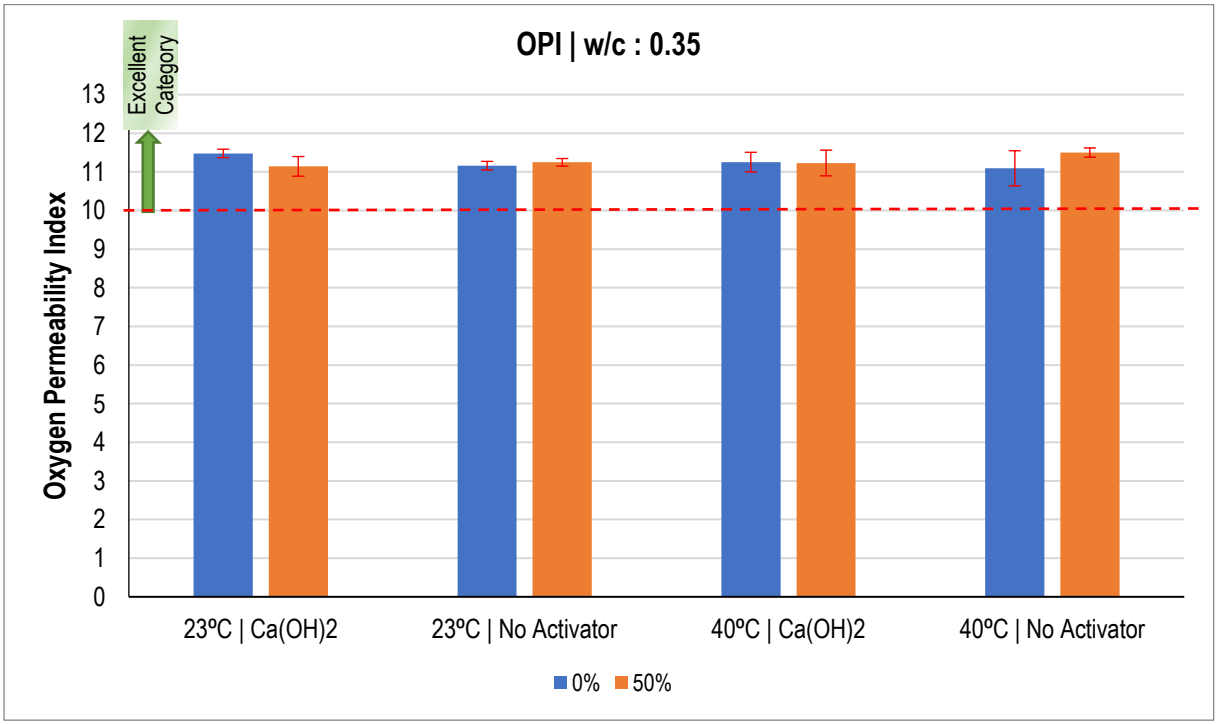

Figure 4.56: Oxygen Permeability Index Results for Specimens with w/c ratio of 0.35

Table 4-32 and Figure 4.56 show the results of OPC concrete specimens and 50% FA concrete specimens with a w/c ratio of 0.35. It can be observed that the results are similar and there is no notable difference between the OPI results for OPC concrete specimens and those of 50% FA concrete specimens. The similarity of these results indicates that varying curing temperature, $Ca(OH)_2$ addition and 50% FA replacement did not yield any notable influence on the oxygen permeability index of concrete investigated in this study.

Table 4-21 shows the suggested oxygen permeability Index values developed by Alexander et al., (1999). A comparison of the OPI results with these suggested OPI values indicates that all the OPI test results fall in the excellent category (OPI > 10). Similarly, comparing the OPI results with the acceptance criterion detailed in Table 4-22 shows that all the OPI results fall within the acceptable criterion for laboratory concrete and that of concrete in as-built structures. Table 4-33 shows a comparison of the Oxygen Permeability Index results with values suggested by Alexander et al, (1999)

Table 4-33: Comparison of Oxygen Permeability Index results with values suggested by Alexander et al, (1999)

Fly Ash Content	w/c Ratio	Oxygen Permeability Index			
		40^oC / $Ca(OH)_2$	40^oC / No Activator	23^oC / $Ca(OH)_2$	23^oC / No Activator
0%	0.45	11.71	11.49	11.58	11.44
25%		11.49	11.24	11.09	10.97
35%		11.30	11.56	10.99	11.01
50%		11.26	10.97	11.26	10.83
0%	0.35	11.25	11.09	11.48	11.16
50%		11.23	11.50	11.14	11.25

4.3.4 Summary of durability Index Tests

The durability index results indicate that all the concrete mixes examined in this study were of superior quality. The influence of a number of factors such as fly ash content, w/c ratio, curing temperature and $Ca(OH)_2$ addition was established. In some cases, the influence of some of the factors was not significant. The results indicated that adding fly ash improved the durability of concrete with respect to chloride ion diffusion and water sorptivity. The durability parameter that was significantly improved by adding fly ash was the chloride conductivity index. The influence of adding $Ca(OH)_2$ to the concrete yielded slightly better results compared to concrete without $Ca(OH)_2$ activation. High temperature curing improved the durability of fly ash concrete as evidenced by the results of chloride conductivity index and water sorptivity index. A study conducted by Cabrera and Nwaubani (1998) on the microstructure of cements containing metakaolin and fly ash reported that high temperature curing accelerates the pozzolanic reactions and results in the rapid filling of capillary pores with reaction products. The fly ash fine filler effect can also be attributed to the improved durability of fly ash concrete. Superplasticizers also have the potential of improving the durability of concrete. Investigations conducted by Ekolu (2014) on the effects of superplasticizers on durability indexes established that superplasticizers can influence the durability indexes of concrete. They reported that some superplasticizers improved durability indexes whilst some resulted in lower durability index performance.

The concrete porosity values obtained from Chloride conductivity test are lower than the porosity values obtained from the Sorptivity test. This can be attributed to chloride binding which results in the formation of Friedel's salt that lessen the porous structure of the paste (Gardner et. al., 2006; Shen et. al., 2019; Yuan et. al., 2009). The Chloride conductivity test is carried out after the chloride binding has taken place on samples that have been saturated in a highly concentrated sodium chloride solution.

4.3.5 Regression Analysis of Durability and Compressive Strength Results

Regression analysis was used to relate the chloride conductivity index to fly ash content. It was established that a polynomial regression function of order two can best describe the relationship between chloride conductivity index and fly ash content. The relationship was best described by the regression analysis function of the form shown in Equation 4-4 with an average correlation (R^2) value of 0.97. The regression functions for each graph showed a high correlation and they can be used to develop prediction models of chloride conductivity index in concrete with varying fly ash contents. The typical regression trendlines depicting the relationship between chloride conductivity index and fly ash content are shown in Figure 4.57.

$$y = Ax^2 - Bx + C \qquad \text{Equation 4-4}$$

Where: y is the Chloride Conductivity Index
A, B and C are constants
x is fly ash content as a percentage

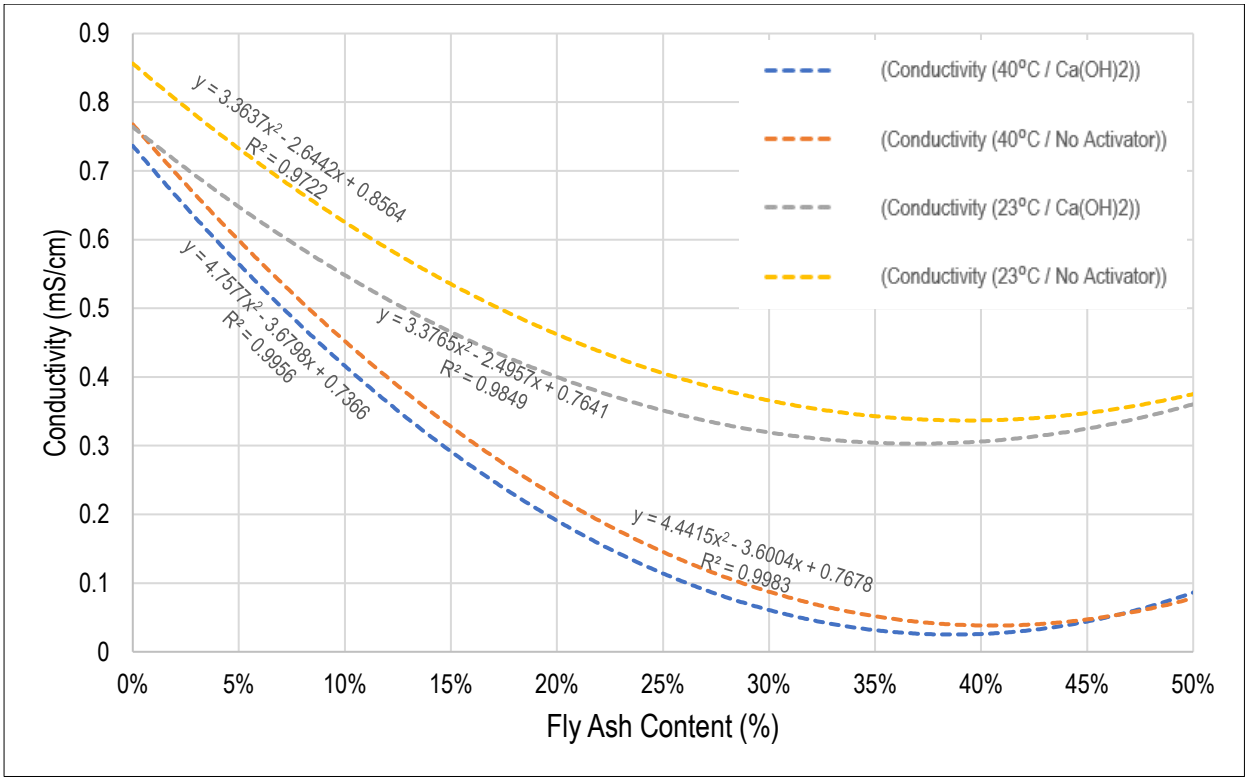

Figure 4.57: Typical Regression Trendlines for the Relationship between FA content and Chloride Conductivity Index

Figure 4.58 outlines the relationship between chloride conductivity index and porosity of concrete determined using the chloride conductivity index test. It can be noted that there is good correlation between chloride conductivity index and porosity of concrete. An increase in concrete porosity results in a corresponding increase in chloride conductivity. This relationship can be observed across all the concrete specimens. The relationship between chloride conductivity index and porosity is best described by the regression function of the form shown in Equation 4-5.

$$y = Ax^B \qquad \text{Equation 4-5}$$

Where: y is the Chloride Conductivity Index
A and B are constants
x is concrete porosity

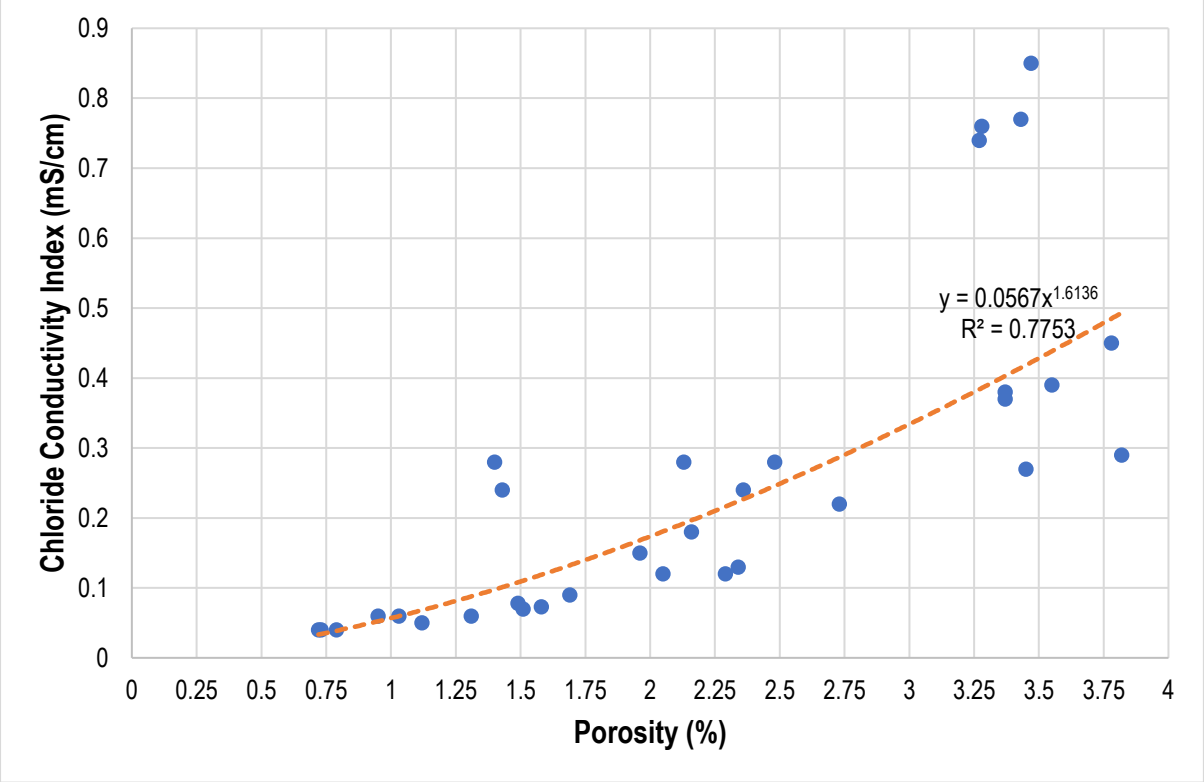

Figure 4.58: Relationship between Chloride Conductivity Index and Porosity Determined Using CCI Test

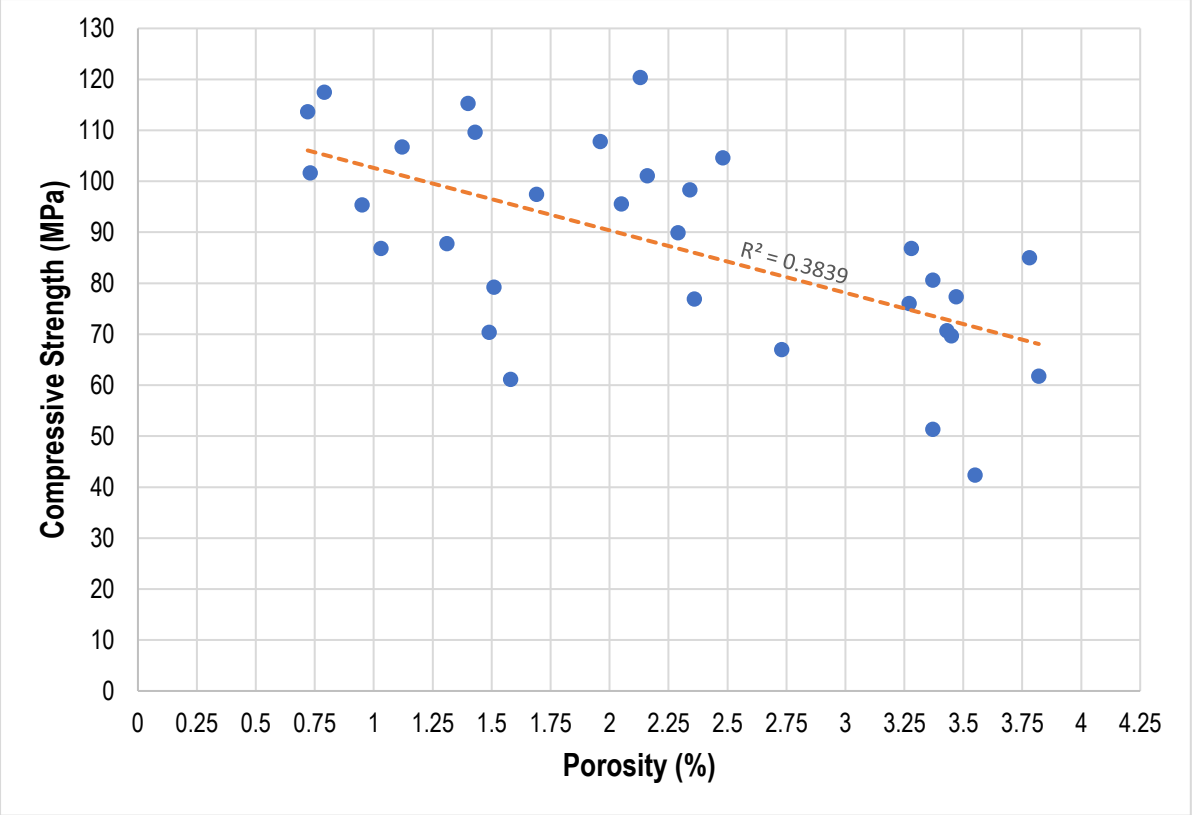

Figure 4.59: Relationship between Compressive Strength and Porosity Determined Using **Chloride Conductivity Index** Test

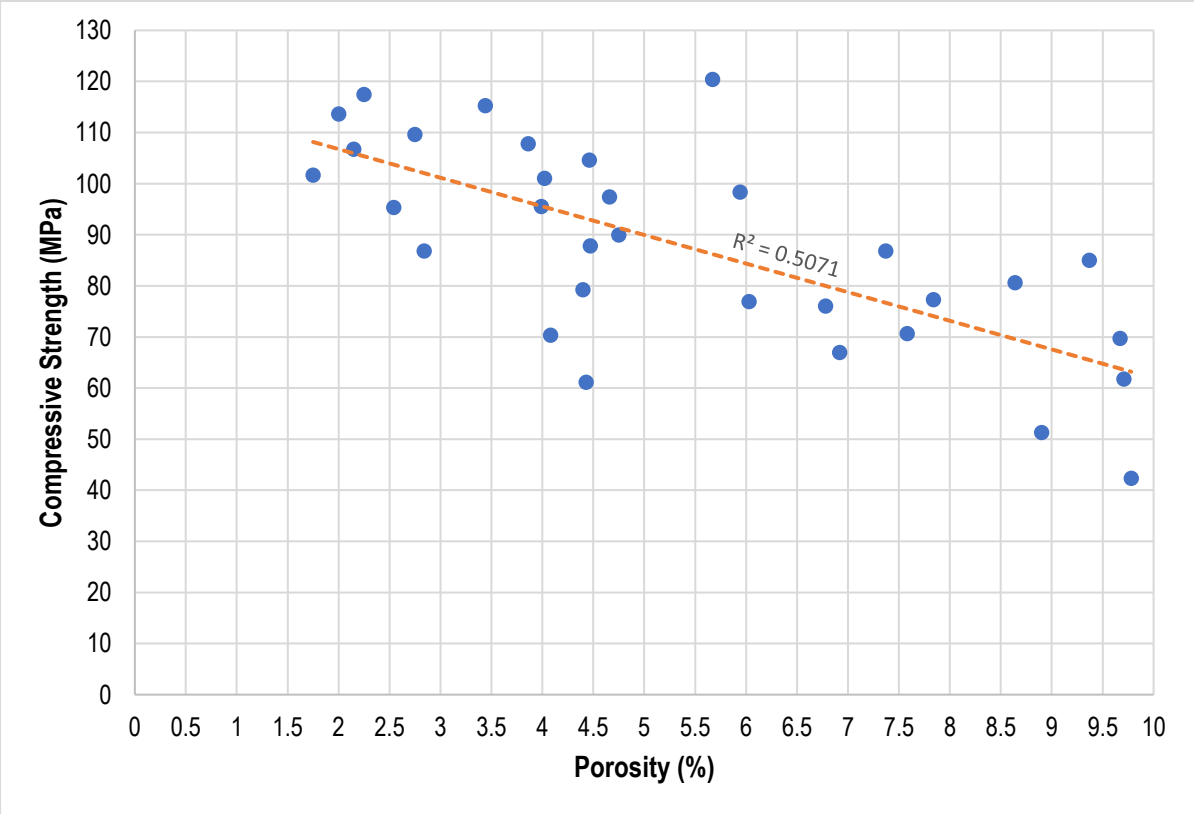

Figure 4.60: Relationship between Compressive Strength and Porosity Determined Using **Water Sorptivity Index** Test

Figure 4.59 and Figure 4.60 shows the relationship between compressive strength and porosity determined using the chloride conductivity index test and water sorptivity index test respectively. It can be noted in both graphs that the correlation between compressive strength and porosity is low. However, it can be established in both graphs that an increase in concrete porosity resulted in a corresponding decrease in compressive strength. Figure 4.61 shows the relationship between compressive strength and water sorptivity index. The graph indicates that there is no correlation between compressive strength and water sorptivity index, however it can be noted that when the water sorptivity index increases the compressive strength of concrete reduces. The discussion on the regression analysis of the relationship between durability indexes, porosity and compressive strength indicates that when porosity increases there is a corresponding reduction in compressive strength. Similarly, an increase in porosity results in a corresponding increase in chloride conductivity.

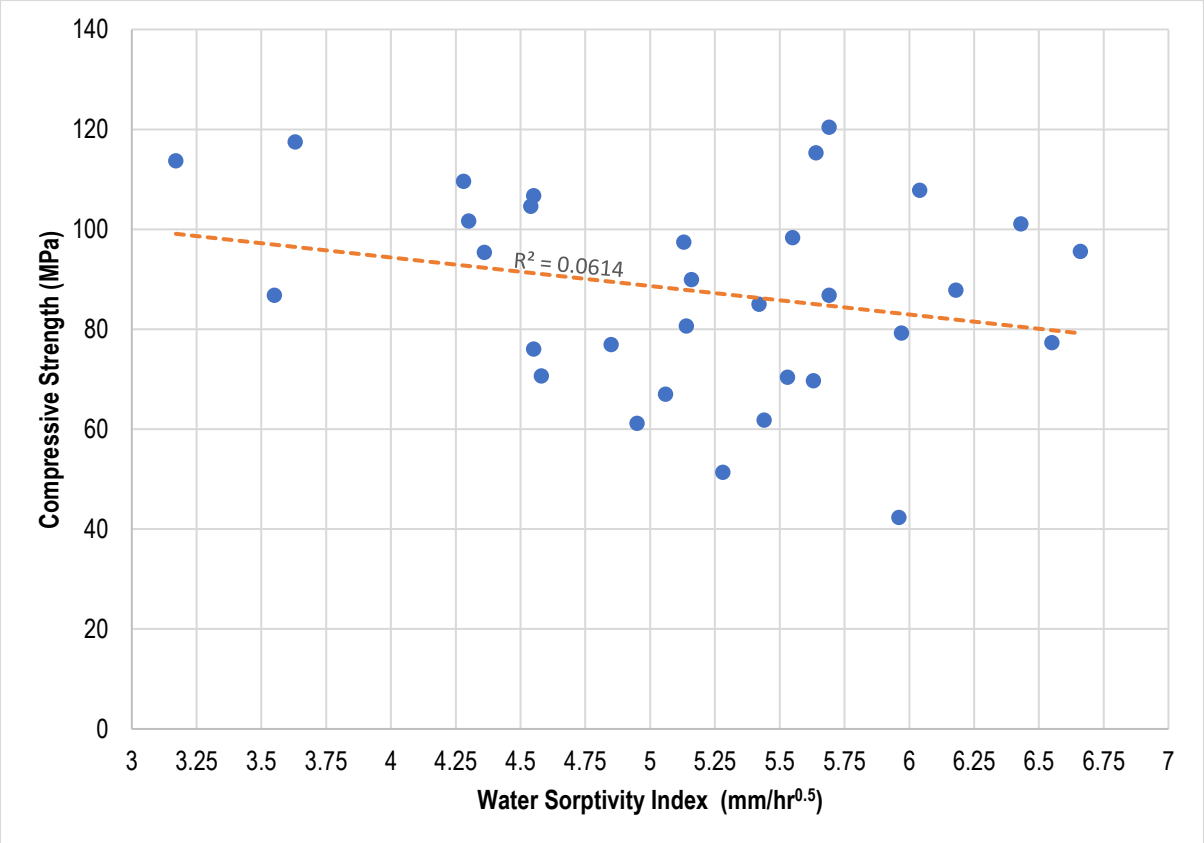

Figure 4.61: Relationship between Compressive Strength and Water Sorptivity Index

5. Economic Analysis of High Strength High Volume Fly Ash Concrete

The compressive strength and durability results of high-volume fly ash concrete obtained in this study indicate that it is beneficial to utilize higher quantities of fly ash in concrete. The benefits of increased fly ash utilisation range from improved concrete properties to significant cost reduction in concrete material cost. This section gives an overview of the economic benefits of incorporating fly ash in concrete based on the results obtained during the laboratory testing of concrete samples.

5.1 Engineering Benefits

High volume fly ash improves the workability of concrete. This presents significant cost savings as a result of reduced demand for high range water reducing admixtures. The superplasticiser dosage results presented in Figure 3.15 indicate that 50% fly ash concrete utilised the least amount of superplasticiser when compared to the other concrete mixes. The durability results indicate that incorporating high volume fly ash improved the durability properties of concrete. The improved durability prolongs the life span of a concrete structure and this presents a possible cost saving on the future maintenance cost of a concrete structure.

5.2 Environmental Benefits

The economic benefits of high-volume fly ash utilisation are not only limited to direct cost saving due to the reduction in cement content in concrete. The economic benefits also include reduction in costs associated with environmental factors such as carbon emissions, extraction of cement raw material and fly ash disposal. The cement manufacture process is an energy intensive process which emits significant amounts of carbon dioxide (Duda et al., 2016). Therefore, reducing the demand of cement by incorporating high volume fly ash results in corresponding reduction in energy costs associated with cement manufacture. The costs associated with cement raw material extraction and the resulting environmental degradation can be reduced when significant quantities of cement are replaced with fly ash. Duda et al. (2016) state that the production of 1 kg of cement emits 0.86 kg of carbon dioxide. With such high carbon emissions, cement manufacturing is likely to be affected by carbon emissions penalties such as statutory carbon taxes. The South African government has introduced the Carbon Tax Bill (2018) which proposes a tax rate of R120 per tonne of

carbon dioxide emitted. This carbon tax burden can be lessened through increased use of fly ash in cement and concrete. Table 5-5 gives an overview of the possible carbon tax costs for 60MPa concrete incorporating high volume fly ash. The other significant benefit of high-volume fly ash utilisation is the reduction in the cost of fly ash disposal in compliance with environmental laws.

5.3 Cost Benefits

An economic analysis of high-volume fly ash concrete is essential in promoting higher levels of cement substitution with fly ash. Figure 5.1 presents the graphical relationship between the 28-day compressive strength results and fly ash content. It can be noted that most of the concrete samples yielded compressive strength above 60MPa with fly ash contents of up to 50%. A regression analysis of the 28-day compressive strength graphs shown in Figure 5.1 indicates that it is possible to achieve 28-day compressive strength of 60MPa with FA contents in excess of 50%. Table 5-1 shows the regression functions for each of the 28-day compressive strength graphs presented in Figure 5.1.

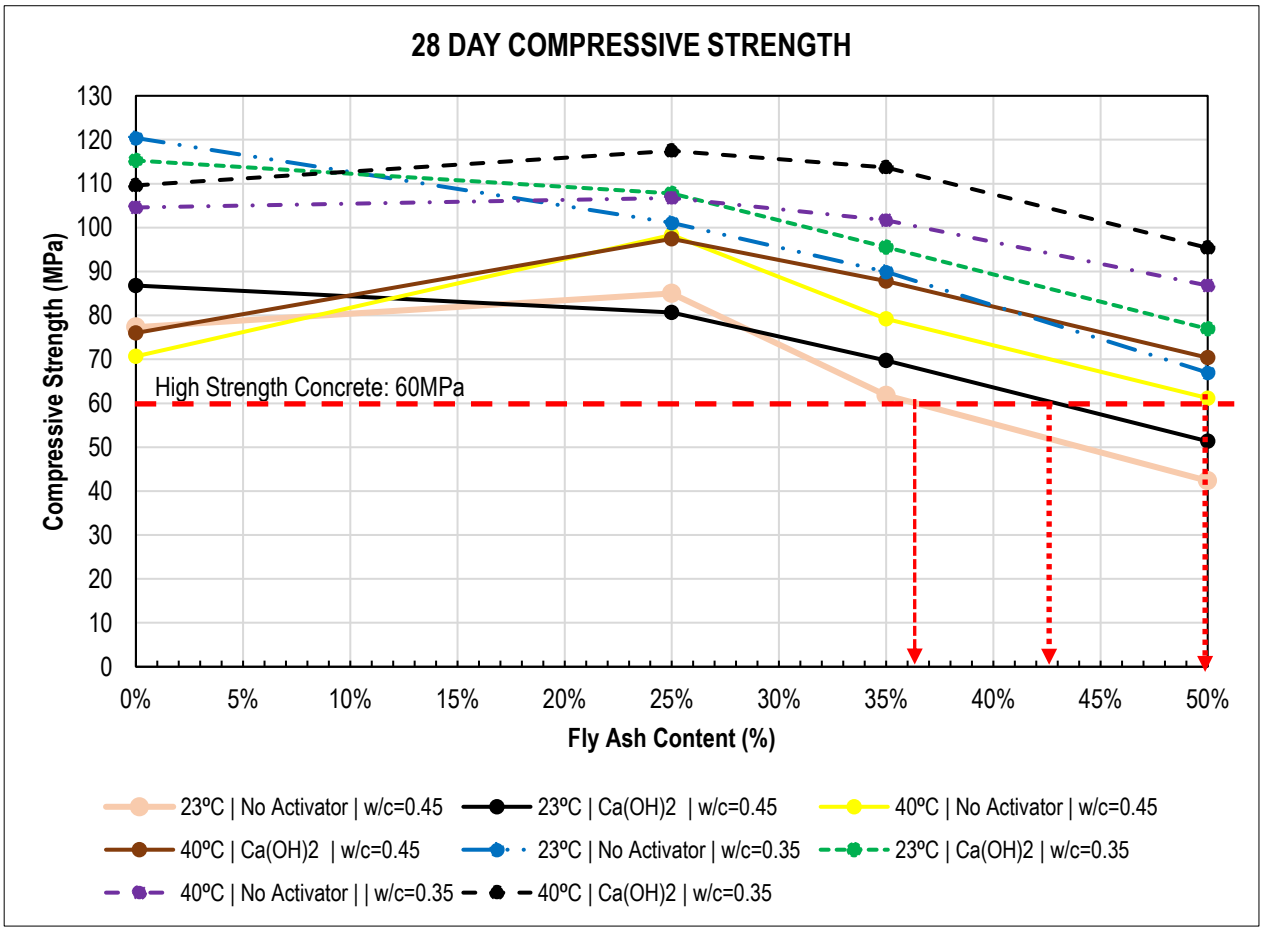

Figure 5.1: Relationship between 28 Day Compressive Strength and Fly Ash Content

Table 5-1: Regression Functions for 28 Day Compressive Strength Graphs

w/c Ratio	Curing Temperature | Chemical Activator	Regression Function	Correlation Factor
w/c=0.35	40ºC | $Ca(OH)_2$	$y = -249.5x^2 + 96.924x + 109.5$	$R^2 = 0.9959$
	40ºC | No Activator	$y = -178.28x^2 + 53.656x + 104.58$	$R^2 = 0.9998$
	23ºC | $Ca(OH)_2$	$y = -168.75x^2 + 6.497x + 115.45$	$R^2 = 0.9951$
	23ºC | No Activator	$y = -123.1x2 - 44.989x + 120.35$	$R^2 = 0.9998$
w/c=0.45	40ºC | $Ca(OH)_2$	$y = -356.48x^2 + 164.85x + 76.342$	$R^2 = 0.9730$
	40ºC | No Activator	$y = -437.44x^2 + 194.37x + 71.468$	$R^2 = 0.8931$
	23ºC | $Ca(OH)_2$	$y = -171.62x^2 + 13.99x + 86.933$	$R^2 = 0.9970$
	23ºC | No Activator	$y = -320.13x^2 + 84.635x + 78.148$	$R^2 = 0.9223$

Where: y is Compressive Strength (MPa)
X is Fly Ash Content (%)

Plotting the regression functions presented in Table 5-1 for fly ash contents ranging between 0% and 90% yields compressive strength-fly ash content trendlines shown in Figure 5.2.

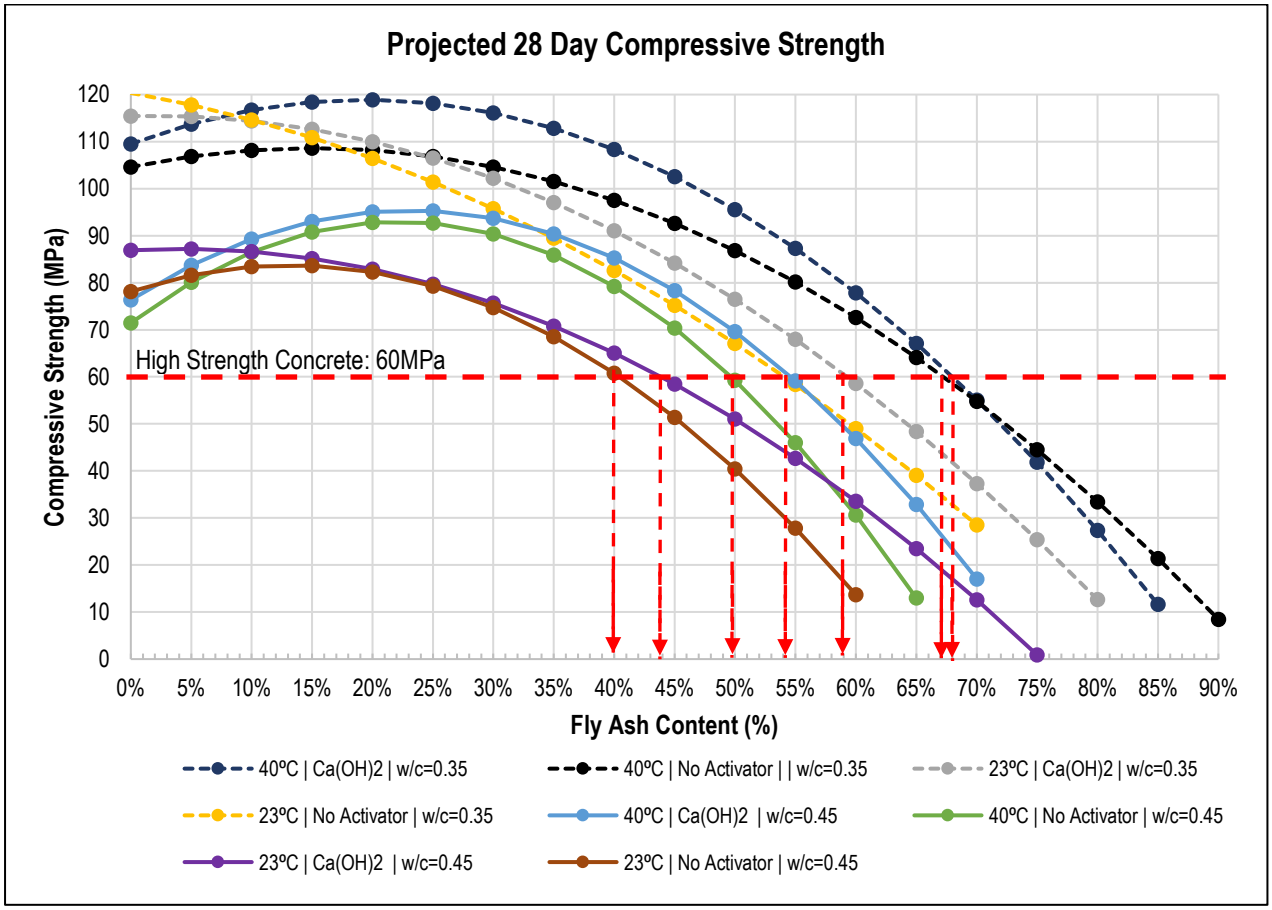

Figure 5.2: Trendlines for the Relationship Between 28 Day Compressive Strength and Fly Ash Content based on Regression Functions Presented in Table 5-1.

The regression trendlines in Figure 5.2 indicate that it is possible to achieve 28-day compressive strength of 60MPa with fly ash content of up-to 68% for concrete cured at 40°C with w/c ratio of 0.35. Table 5-2 shows eight concrete mixes which can be developed by incorporating fly ash contents derived from regression trendlines in Figure 5.2. The eight concrete mixes can attain 28-day compressive strength of 60MPa for each particular w/c ratio, curing temperature and activation method. It can be observed in Figure 5.2 that there is a general trend of decreasing 28-day compressive strength with increasing fly ash content. This trend can be reversed by using a combination of fly ash activation techniques. The 28-day compressive strength of concrete can be increased through the use of alkali activators such as $Ca(OH)_2$ in combination with heat activation and fine fly ash or fly ash blended with active components.

Table 5-2: Eight 60MPa Concrete Mixes Incorporating Fly Ash Contents Derived from Regression Trendlines

Mix	w/c Ratio	Curing Temperature | Chemical Activator	Projected Fly Ash Content	Projected 28 Day Compressive Strength
P01	w/c=0.35	40ºC | $Ca(OH)_2$	68%	60MPa
P02		40ºC | No Activator	67%	60MPa
P03		23ºC | $Ca(OH)_2$	59%	60MPa
P04		23ºC | No Activator	54%	60MPa
P05	w/c=0.45	40ºC | $Ca(OH)_2$	54%	60MPa
P06		40ºC | No Activator	50%	60MPa
P07		23ºC | $Ca(OH)_2$	44%	60MPa
P08		23ºC | No Activator	40%	60MPa

The cost analysis was done for the binder material due to its significant contribution on the cost of concrete. The cost of other concrete constituents such as aggregates was not considered in the analysis due to the fact that their contents were kept constant in all the concrete mixes and their influence on the overall cost of concrete is much lower compared to the cost of binder material. A cost analysis of the binder material was done in order to ascertain the cost effectiveness of utilising high-volume fly ash and activation methods. The analysis was based on the cost of binder material per cubic metre of concrete. The cost of cement and fly ash was obtained from commercial retailers. The cost of a 50kg bag of OPC CEM 1 52.5N cement was R105.00 inclusive of VAT. The cost of a 40kg bag of ultra-fine fly ash was R62.10 inclusive of VAT. The cost of ultra-fine fly ash is equal to 74% of the cost of OPC. Table 5-3 presents an outline of the cost of the binder materials used in the study. It can be noted that replacement of cement with fly ash yielded a corresponding binder cost reduction ranging between 6 and 13%. Table 5-4 shows the estimated binder costs based on the projections of fly ash binder materials which yield equal 28-day

compressive strength of 60MPa as outlined in Figure 5.2. The projected binder material costs shown in Table 5-4 indicate that high temperature curing and $Ca(OH)_2$ activation yield the highest binder material cost reduction for both w/c ratios.

Table 5-3: Cost Comparison Between OPC and Fly Ash Binder Material

Concrete Mix	Cement		Fly Ash		Total Cost of Binder Material *(R/m³ of Concrete)*	Binder Cost Reduction	
	Quantity *(kg/m³ of Concrete)*	**Cement Cost** *(R/m³ of Concrete)*	**Quantity** *(kg/m³ of Concrete)*	**FA Cost** *(R/m³ of Concrete)*		*(R/m³ of Concrete)*	*Percentage Cost Reduction (%)*
OPC	400	R 840	0	R 0.00	R 840.00	R 0.00	0%
25% FA	300	R 630	100	R 153.90	R 783.90	R 56.10	6.7%
35% FA	260	R 546	140	R 215.46	R 761.46	R 78.54	9.35%
50% FA	200	R 420	200	R 310.50	R 730.50	R 109.50	13%

Table 5-4: Projected Cost of Binder Material Which Yields 28 Day Compressive Strength of 60MPa

Mix	Projected Fly Ash Content	w/c Ratio	Curing Temperature | Chemical Activator	Cement		Fly Ash		Total Cost of Binder Material *(R/m³ of Concrete)*
				Quantity *(kg/m³ of Concrete)*	**Cost** *(R/m³ of Concrete)*	**Quantity** *(kg/m³ of Concrete)*	**FA Cost** *(R/m³ of Concrete)*	
P01	68%	w/c=0.35	40ºC | $Ca(OH)_2$	128	R268.80	272	R422.28	R691.08
P02	67%		40ºC | No Activator	132	R277.20	268	R416.07	R693.27
P03	59%		23ºC | $Ca(OH)_2$	164	R344.40	236	R366.39	R710.79
P04	54%		23ºC | No Activator	184	R386.40	216	R335.34	R721.74
P05	54%	w/c=0.45	40ºC | $Ca(OH)_2$	184	R386.40	216	R335.34	R721.74
P06	50%		40ºC | No Activator	200	R420.00	200	R310.50	R730.50
P07	44%		23ºC | $Ca(OH)_2$	224	R470.40	176	R273.24	R743.64
P08	40%		23ºC | No Activator	240	R504.00	160	R248.40	R752.40

Table 5-5: Carbon Tax Cost Per Cubic Metre of Concrete with Projected 28 Day Strength of 60MPa

Mix	Projected Fly Ash Content	w/c Ratio	Curing Temperature | Chemical Activator	Cement *(kg/m³ of Concrete)*	Fly Ash *(kg/m³ of Concrete)*	Carbon Emissions** *(kg/m³ of Concrete)*	Carbon Tax *(R/m³ of Concrete)*
P01	68%	w/c=0.35	40ºC | $Ca(OH)_2$	128kg	272kg	110.08kg	R13.21
P02	67%		40ºC | No Activator	132kg	268kg	113.52kg	R13.62
P03	59%		23ºC | $Ca(OH)_2$	164kg	236kg	141.04kg	R16.92
P04	54%		23ºC | No Activator	184kg	216kg	158.24kg	R18.99
P05	54%	w/c=0.45	40ºC | $Ca(OH)_2$	184kg	216kg	158.24kg	R18.99
P06	50%		40ºC | No Activator	200kg	200kg	172.00kg	R20.64
P07	44%		23ºC | $Ca(OH)_2$	224kg	176kg	192.64kg	R23.12
P08	40%		23ºC | No Activator	240kg	160kg	206.40kg	R24.77

**Carbon emissions calculated based on the emission of 0.86kg of CO_2 for every kilogram of cement produced (Duda et al, 2016)

A cost analysis to evaluate the possible cost savings of using high volume fly ash was done using the total cost of binder material outlined in Table 5-4 and carbon tax costs outlined in Table 5-5. The binder content used in a study conducted by Angelucci (2013) was used to estimate the binder cost of OPC only concrete with 28-day compressive strength of 60MPa. Angelucci (2013) achieved 28 days compressive strength of 61MPa using OPC content of 388kg/m^3 of concrete. Based on the OPC cement prices obtained in this study, the cost of OPC binder material used by Angelucci (2013) is R814.80 per cubic metre of concrete. The carbon tax cost for binder material with OPC content of 388kg/m^3 is R46.56 per cubic metre of concrete. The cost of OPC only binder and carbon tax costs of OPC only concrete was used to compare with those of projected HVFA concrete mixes in order to determine the possible cost savings. Table 5.6 and Table 5.7 show the possible binder material and carbon tax cost savings respectively.

Table 5-6: Possible binder material cost savings

Mix	Projected Fly Ash Content	w/c Ratio	Curing Temperature | Chemical Activator	Total Cost of Binder Material *(R/m^3 of Concrete)*	Binder Cost Saving *(R/m^3 of Concrete)*
P01	68%	w/c=0.35	40^{0}C | $Ca(OH)_2$	R 691.08	R 123.72
P02	67%		40^{0}C | No Activator	R 693.27	R 121.53
P03	59%		23^{0}C | $Ca(OH)_2$	R 710.79	R 104.01
P04	54%		23^{0}C | No Activator	R 721.74	R 93.06
P05	54%	w/c=0.45	40^{0}C | $Ca(OH)_2$	R 721.74	R 93.06
P06	50%		40^{0}C | No Activator	R 730.50	R 84.30
P07	44%		23^{0}C | $Ca(OH)_2$	R 743.64	R 71.16
P08	40%		23^{0}C | No Activator	R 752.40	R 62.40

Table 5-7: Possible Carbon Tax Cost Savings

Mix	Projected Fly Ash Content	w/c Ratio	Curing Temperature | Chemical Activator	Carbon Tax Cost *(R/m^3 of Concrete)*	Carbon Tax Saving *(R/m3 of Concrete)*
P01	68%	w/c=0.35	40^{0}C | $Ca(OH)_2$	R 13.21	R 33.35
P02	67%		40^{0}C | No Activator	R 13.62	R 32.94
P03	59%		23^{0}C | $Ca(OH)_2$	R 16.92	R 29.64
P04	54%		23^{0}C | No Activator	R 18.99	R 27.57
P05	54%	w/c=0.45	40^{0}C | $Ca(OH)_2$	R 18.99	R 27.57
P06	50%		40^{0}C | No Activator	R 20.64	R 25.92
P07	44%		23^{0}C | $Ca(OH)_2$	R 23.12	R 23.44
P08	40%		23^{0}C | No Activator	R 24.77	R 21.79

Table 5-8 outlines the increase or decrease in 28-day compressive strength of concrete due to fly ash addition. A comparison between increase or decrease in 28-day compressive strength and reduction in binder cost is presented in Figure 5.3. It can be noted that in concrete cured at 40ºC, the binder cost reduction of up to 11% had a corresponding increase in 28-day compressive strength. It can also be observed that concrete cured at 23ºC exhibited significant decrease in 28-day compressive strength due to fly ash addition. Binder cost reduction of 13% had a corresponding 28-day compressive strength decrease of approximately 40%. The binder cost and change in compressive strength comparisons are detailed in Figure 5.3 and Figure 5.4.

Table 5-8: Increase or decrease in 28 Day Compressive Strength Compared to OPC Concrete Strength: w/c=0.45

Concrete Mix	**Total Cost of Cementitious Material** *(R/m³ of Concrete)*	**Cost Reduction** *(R/m³ of Concrete)*	**Increase or Decrease in 28 Day Compressive Strength Compared to OPC Concrete Strength**			
			23 ºC | No Activator | w/c=0.45	*23 ºC | Ca(OH)₂ | w/c=0.45*	*40 ºC | No Activator | w/c=0.45*	*40 ºC | Ca(OH)₂ | w/c=0.45*
OPC	R 840.00	R 0.00	0 MPa	0 MPa	0 MPa	0 MPa
25% FA	R 783.90	R 56.10	+7.67 MPa	-6.17 MPa	+27.67 MPa	+21.4 MPa
35% FA	R 761.46	R 78.54	-15.57 MPa	-17.1 MPa	+8.57 MPa	+11.77 MPa
50% FA	R 730.50	R 109.50	-35 MPa	-35.47 MPa	-9.5 MPa	-5.67 MPa

Table 5-9: Increase or Decrease in 28 Day Compressive Strength Compared to OPC Concrete Strength: w/c=0.35

Concrete Mix	**Total Cost of Cementitious Material** *(R/m³ of Concrete)*	**Cost Reduction** *(R/m³ of Concrete)*	**Increase or decrease in 28 Day Compressive Strength Compared to OPC Concrete Strength**			
			23 ºC | No Activator | w/c=0.35	*23 ºC | Ca(OH)2 | w/c=0.35*	*40 ºC | No Activator | w/c=0.35*	*40 ºC | Ca(OH)2 | w/c=0.35*
OPC	R 840.00	R 0.00	0 MPa	0 MPa	0 MPa	0 MPa
25% FA	R 783.90	R 56.10	-19.33 MPa	-7.47 MPa	+2.13 MPa	+7.87 MPa
35% FA	R 761.46	R 78.54	-30.47 MPa	-19.73 MPa	-2.93 MPa	+4.07 MPa
50% FA	R 730.50	R 109.50	-53.43 MPa	-38.33 MPa	-17.8 MPa	-14.23 MPa

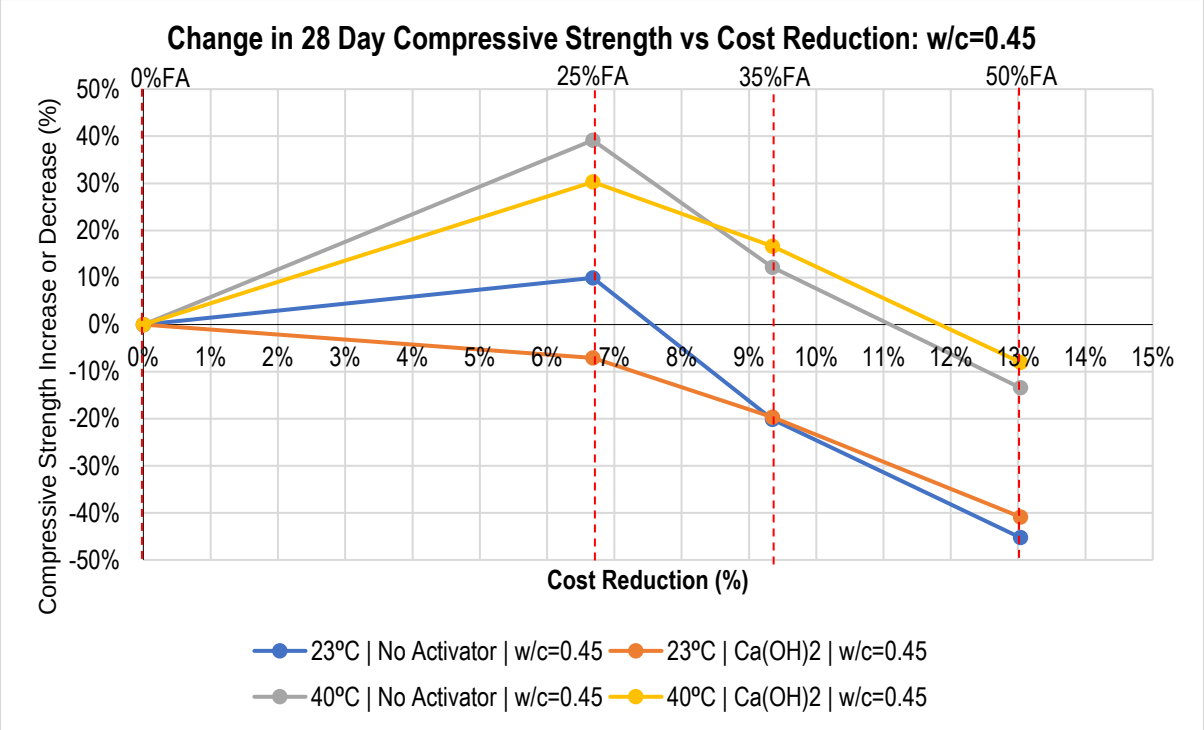

Figure 5.3: Increase or Decrease in 28 Day Compressive Strength vs Cost Reduction (w/c=0.45)

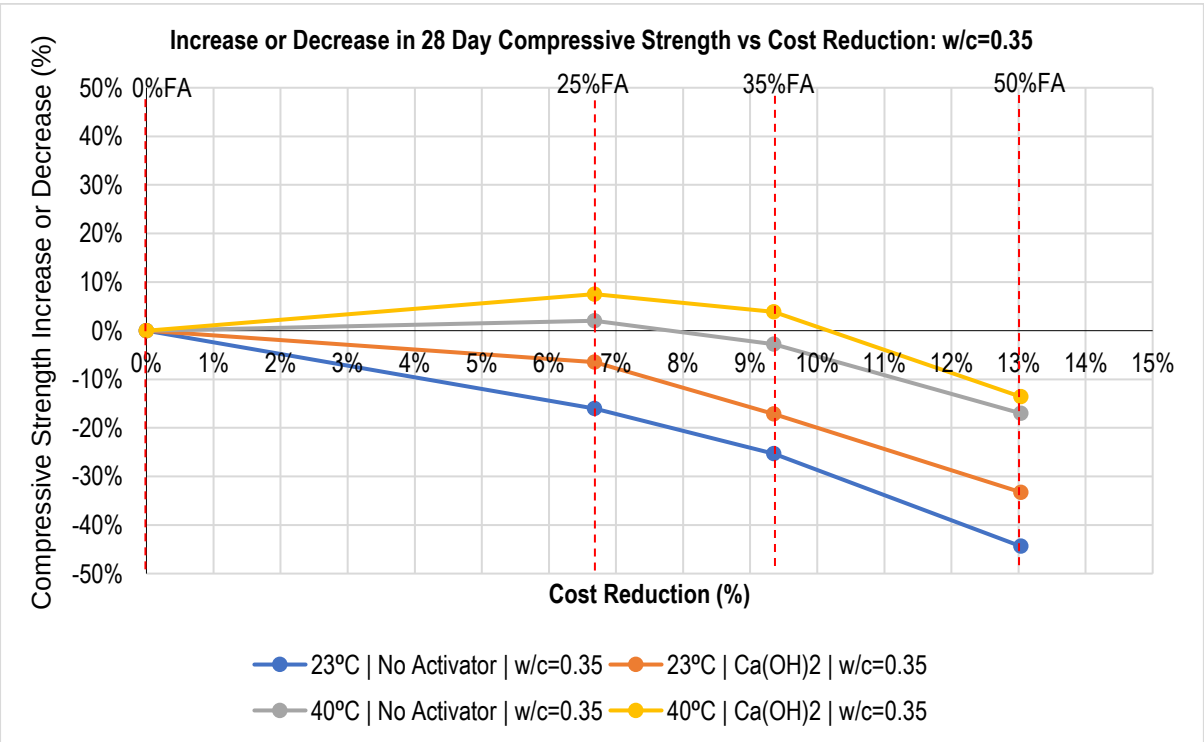

Figure 5.4: Increase or Decrease in 28 Day Compressive Strength vs Cost Reduction (w/c=0.35)

5.4 Conclusion

High volume fly ash concrete has significant economic benefits. Apart from the direct cost savings resulting from cement substitution, high volume fly ash has proven that it has good compressive strength and durability properties. The results obtained in this

study indicate that HVFA concrete is less permeable and has excellent resistance chloride resistance. This translates into significant cost savings as a result of reduced maintenance costs and prolonged life span of a concrete structure. The literature review on the ecological benefits of high-volume fly ash indicates that its utilisation contributes to sustainability development and environmental preservation. This will help to mitigate against the costly effects of climate change. The cost analysis has shown that utilisation of high-volume fly ash is a worthwhile initiative that can be embraced in the quest to reduce the cost of concrete materials.

6. CONCLUSIONS

The objectives of this study were to investigate the influence of high volume fly ash content, curing temperature, $Ca(OH)_2$ activation and water to cement ratio on compressive strength development and durability of concrete. The following conclusions were made based on the findings of this investigation.

1. Effect of high-volume fly ash content on compressive strength and durability of concrete

- The results indicate that partial replacement of cement with 25% fly ash produces concrete with compressive strength higher than that of OPC concrete, 35%FA concrete and 50%FA concrete at the ages of 28 days and beyond. This is notable at both curing temperature conditions and across both w/c ratios of 0.35 and 0. 45. Therefore, it can be concluded that the optimum fly ash content for concrete evaluated in this study is 25%.

- Substituting cement with 50% fly ash results in reduced early age compressive strength development when concrete is cured at normal temperature without chemical activation. However, subjecting 50%FA concrete to high temperature curing and $Ca(OH)_2$ activation improves early age strength of concrete.

- The regression analysis of compressive strength development trends indicates that it is possible to develop high strength-high volume fly ash concrete with 28-day compressive strength of 60MPa using fly ash content of between 40% and 68% depending on the fly ash activation methods adopted.

- Fly ash concrete has better resistance to chloride penetration compared to OPC concrete. Increasing fly ash content in concrete improves the concrete resistance to chloride ingress. Improvements in chloride resistance were significant at 25%, 35% and 50% fly ash replacement levels. It can be concluded that the optimum fly ash replacement level for improved chloride resistance is 35%.

- Substituting cement with high volume fly ash content improves the workability of concrete. The results indicate that OPC concrete requires higher superplasticiser dosage compared to fly ash concrete in order to achieve workability within the desired slump range. The workability of concrete improves with increase in fly ash content. High volume fly ash concrete with 50% FA content had the most significant reduction in the water requirement. The reduction in the water demand for high-volume fly ash concrete results in cost saving owing to reduced use of superplasticisers.

- High strength concrete with 28 day compressive strength of 60MPa can be achieved with high volume fly ash content.

2. Effect of curing temperature on compressive strength of concrete and durability of concrete

- High temperature curing increases the rate of strength development of fly ash concrete. The increase in the rate of strength development is more significant in high volume fly ash concrete with 35%FA and 50%.

- Pozzolanic reactions between fly ash and $Ca(OH)_2$ are accelerated by high temperature curing. The results indicate that 50% FA concrete gained strength rapidly when it was cured at a high temperature of 40^0C compared to curing at 23ºC.

- The late age strength of OPC concrete is reduced when concrete is cured at high temperature. The results indicate that the late age compressive strength of OPC concrete cured at high temperature was lower than that of concrete cured at 23ºC. This was noted at both w/c ratios of 0.35 and 0.45. Therefore, it can be concluded that high temperature curing impacts on late age compressive strength development for OPC concrete.

- Curing fly ash concrete at high temperature results in concrete with improved resistance to chloride penetration. This effect is more significant in high volume fly ash concrete.

- High temperature curing improves the resistance of concrete to water penetration through capillary action.

- High temperature curing results in higher compressive strength and durability improvements compared to Calcium Hydroxide activation.

- The porosity of concrete cured at high temperature is lower that the porosity of concrete cured at 23°C.

- Concrete porosity determined using chloride conductivity index test is significantly lower than porosity determined using the water sorptivity index test.

3. Effect of Calcium Hydroxide Activation on compressive strength and durability of concrete

- $Ca(OH)_2$ activation improves the compressive strength of high volume fly ash concrete. The results indicate that there was no notable improvement in compressive strength of OPC concrete and 25% FA concrete as a result of $Ca(OH)_2$ activation. The effect of $Ca(OH)_2$ activation was significant in concrete with high volume fly ash contents of 35% and 50%.

- Calcium Hydroxide has a high-water demand. Addition of $Ca(OH)_2$ to concrete increases the water requirement of concrete. The superplasticiser dosage results indicate that concrete mixes with calcium hydroxide required more superplasticiser compared to similar concrete mixes without calcium hydroxide.

- Combination of high temperature curing and $Ca(OH)_2$ activation significantly improves strength of HVFA concrete.

4. Effect of water content on compressive strength and durability of concrete

- Low w/c ratio reduces the chloride conductivity index of concrete. The results indicate that concrete with w/c ratio of 0.35 had more resistance to chloride penetration compared to concrete with w/c ratio of 0.45.

- Low w/c ratio increases the compressive strength of concrete with varying amounts of fly ash content.

5. X-Ray diffraction Analysis

- The early age compressive strength of fly ash concrete can be improved by addition of Calcium Hydroxide. The X-ray diffraction analysis indicates that there was significant calcium hydroxide depletion in fly ash concrete compared to OPC concrete. The calcium hydroxide peaks for fly ash concrete were much smaller at 90 days compared to 28 days. However, in OPC concrete, the calcium hydroxide peaks at 90 days were the same as the peaks at 28 days.

6. Economic Analysis

- High volume fly ash concrete yields significant cost savings. The economic analysis indicates that replacing cement with FA can reduce the cost of concrete binder material.

7. RECOMMENDATIONS FOR FUTURE RESEARCH

The following research areas are recommended for future research in order to expand knowledge pertaining to development of high strength-high volume fly ash concrete subjected to high temperature and chemical activation.

- Influence of $Ca(OH)_2$ addition on water demand and workability of high volume fly ash concrete.

- Influence of $Ca(OH)_2$ addition on the heat of hydration of high volume fly ash concrete.

- Optimum Duration of high temperature curing of high-volume fly ash concrete

- Pore size distribution of high-volume fly ash concrete paste

- Reliability of Oxygen Permeability Index Test in the evaluation of high-strength concrete.

8. REFERENCES

Abualrous, Y., Panesar, D. K., Hooton, R. D., and Singh, D., 2016, Particle Size Analysis As A Means To Better Understand The Influence Of Fly Ash Variability In Concrete, Resilient Infrastructure, June 1–4, 2016

ACI Committee 363 (2010) Report on High-Strength Concrete. ACI 363R-10, American Concrete Institute Committee 363, Farmington Hills, MI.

Acquaye, L., 2006, Effect of High Curing Temperatures on The Strength, Durability and Potential of Delayed Ettringite Formation in Mass Concrete Structures, Phd Thesis, University of Florida

Addis, B. J., 1991, Properties of High Strength Concrete Made with South African Materials, PhD thesis, Johannesburg: University of the Witwatersrand

AfriSam, 2014, AfriSam Aggregate, Product Datasheet, retrieved, April, 2017, from https://www.afrisam.co.za /uploads/documents/afrisam-aggregate.pdf

Alexander, M. G., Santhanam, M. and Ballim, Y., 2010, Durability design and specification for concrete structures - The way forward, Int J Adv Eng Sci Appl Math (September 2010) 2(3):95–105

Alexander, M. G., Ballim, Y. and Stanish, K., 2008, A framework for use of durability indexes in performance-based design and specifications for reinforced concrete structures, Materials and Structures (2008) 41:921–936

Alexander, M. G., 2004, Durability indexes and their use in concrete engineering. In: Kovler K, Marchand J, Mindess S, Weiss J. (Eds.), Proceedings of the International RILEM Symposium on Concrete Science and Engineering – A Tribute to Arnon Bentur, Evanston, Illinois, USA. March 21–24, 2004. p. 9–22 retrieved, November, 14, 2017, from demo.webdefy.com

Alexander, M.G., Mackechnie, J.R., Ballim. Y., 1999, Research Monograph 2: Guide to the use of durability indexes for achieving durability in concrete structures, Department of Civil Engineering, University of Cape Town

Alexander, M.G., Mackechnie, J.R., Ballim. Y., 2001, Use of durability indexes to achieve durable cover concrete in reinforced concrete structures. Materials Science of Concrete. J.P.Skalny & S.Mindess, Ed. Westerville: American Ceramic Soceity. 483-511.

Alonso, S and Palomo, A, 2001, Alkaline activation of metakaolin and calcium hydroxide mixtures: Influence of temperature, activator concentration and solids ratio. Materials Letters. 47. 55-62.

American Coal Ash Association Educational Foundation, 2015, Sustainable Construction with Coal Combustion Products, Publication, retrieved January 25 2017 from https://www.acaa-usa.org.

American Coal Ash Association, 2003, Fly Ash Facts for Highway Engineers, Technical Report No. FHWA-IF-03-019, retrieved, December, 06, 2017 from https://www.fhwa.dot.gov/Pavement/recycling/fafacts.pdf

Angelucci, M., 2013, The Influence Of Mix Design Parameters And Compressive Strength On Durability Indices, MSc Thesis, Department of Civil Engineering, University of Cape Town.

Arezoumandi, M., Volz, J. S., Myers, J. J., Ortega, C. A. 2013, Shear Behaviour of High-Volume Fly Ash Concrete versus Conventional Concrete: Experimental Study, Journal of Structural Engineering, Volume 141 Issue 3 - March 2015

Arjunan P., Silsbee M. R., and Roy D. M., 2001, Chemical activation of low calcium fly ash. Part 1: Identification of suitable activators and their dosage, Proceedings of 2001 International Ash Utilisation Symposium, Vol. 105, Center for Applied Energy Research, University of Kentucky, Lexington, KY

ASTM C618-05, Standard Specification for Coal Fly Ash and Raw or Calcined Natural Pozzolan for Use in Concrete, ASTM International, West Conshohocken, PA, 2005, www.astm.org

Ballim, Y., 2015, Concrete Durability: Fundamentals and Transport Mechanisms, Lecture Notes, university of Witwatersrand.

Ballim, Y. and Graham, P. C., 2009. The effects of supplementary cementing materials in modifying the heat of hydration of concrete. Materials and Structures, Volume 42, p. 803–811, DOI 10.1617/s11527-008-9425-3

Ballim, Y. and Graham, P. C., 2003, A Maturity Approach to the Rate of Heat Evolution in Concrete, Magazine of Concrete Research vol. 55, No. 3, June 2003. pp. 249-256

Balakrishnan, B., Awal, A.S.M., Shehu, I.A., 2013, Influence of High Volume Fly Ash in Controlling Heat of Hydration of Concrete, International Journal of Engineering Research and Applications, Vol. 3, Issue 2, March - April 2013, pp.932-936

Balakrishnan B., Awal A. S. M., 2014, The durability properties of concrete containing high volume Malaysian fly ash, International Journal of Research in Engineering and Technology, Volume: 03 Issue: 04 | Apr-2014, retrieved from http://www.ijret.org

Bao-min W. and Li-jiu W. 2004, Development of studies and applications of activation techniques of fly ash, Proceedings of the International Workshop on Sustainable Development and Concrete Technology, May 2004, Beijing, China, 159-169.

Barough, A. S., Shoubi, M. V., Kiani, I., and Amini, Z., Advantages Of Using Fly Ash In Concrete Industry For Achieving Sustainable Development, Technical Paper, Management In Construction Research Association (MiCRA) Postgraduate Conference

Benaicha, M., Burtschell, Y., Alaoui, A. H., 2016, Prediction of compressive strength at early age of concrete – Application of maturity, Journal of Building Engineering 6 (2016)119–125

Bentz D. P., 2010, Powder Additions to Mitigate Retardation in High-Volume Fly Ash Mixtures, ACI Materials Journal, 107-M58

Bentz, D. P. and Ferraris, C. F. 2010, Rheology and setting of high volume fly ash mixtures, Cement and Concrete Composites Journal 32 (2010) 265–270

Berry, E.E. and Malhotra, V.M. 1987, Fly Ash in Concrete, Supplementary Cementing materials for Concrete, edited by Malhotra, V.M., Energy, Mines and resources Canada, Minister of Supply and Services Canada, CANMET.

Beushausen, H. and Luco, L. F., 2016, Performance-Based Specifications and Control of Concrete Durability – 2016, State-of-the-Art Report RILEM TC 230-PSC available online at https://www.rilem.net

Beushausen, H. D. and Alexander, M. G., 2008, The South African durability index tests in an international comparison, Technical Paper, Journal of The South African Institution of Civil Engineering, Vol 50 No 1, 2008, Pages 25–31, Paper 671

Bhattacharjee, B., Video Lecture, Building Materials and Construction, Indian Institute of Technology, Delhi, India

Bilodeau, A. and Malhotra, V M. 1995, Properties of High-Volume Fly Ash Concrete Made with High Early- Strength ASTM Type III Cement, ACI Publication, Volume 153, pages 1-24

Bold KK, 2013, http://flyash.com/about-fly-ash/

Bouzoubaa, N., Bilodeau, A., Sivasundaram, V., Chakraborty, A., 2007, Mechanical Properties and Durability Characteristics of High-Volume Fly Ash Concrete Made with Ordinary Portland Cement and Blended Portland Fly Ash Cement. 9th CANMET/ACI Fly Ash Conference (pp. 303-320), ACI.

Burg, R. G., and Ost, B. W. 1994, Engineering Properties of Commercially Available High-Strength Concretes, Research and Development Bulletin RD104, Portland Cement Association

Burke, F. D., 2012, Development of Concrete Mixtures with High-Volume Fly Ash Cement Replacement, NAVFAC Engineering Service Center Publication,2012 International Concrete Sustainability Conference

Brooks, A. G., Schindler, A. K., and Barnes, R. W., 2007, Maturity Method Evaluated for Various Cementitious Materials, Journal of Materials in Civil Engineering

Cabrera, J.G. and Nwaubani, S.O. 1998, The Microstructure and Chloride Ion Diffusion Characteristics of Cements Containing Metakaolin and Fly Ash, Technical Paper

Cai, Wenjing, 2017, Effect of Particle Packing on Flow Property and Strength of Concrete Mortar, Graduate Theses and Dissertations. 15271, available online at https://lib.dr.iastate.edu/etd/15271

Camoes, A., Aguiar, B. and Jalali, S., 2003, Durability of Low-Cost High-Performance Fly Ash Concrete, Technical Paper, 2003 International Ash Utilisation Symposium, Centre for Applied Research, University of Kentucky, Paper No. 43

Carbon Tax Bill, 2018, B 46 of 2018, 2018, Republic Of South Africa

Carino, N.J., 1991, "The Maturity Method," in Handbook on Nondestructive Testing of Concrete, Eds. V.M. Malhotra and N.J. Carino, CRC Press, Boca Raton, FL, pp. 101-146.

Chidiac, S. E., Moutassem, F., and Mahmoodzadem, F., 2013, Compressive strength model for concrete, Magazine of Concrete Research, Volume 65 Issue 9.

Concrete NZ, Curing Methods, available online at https://concretenz.org.nz/page/Curing

Cross, D., Stephens, J., Vollmar, J., 2005, Structural applications of 100% fly ash concrete, Publication, retrieved January 20 2017 from http://www.flyash.info/2005

Crouch, L. K., Hewitt, R., Byard, B., 2007, High Volume Fly Ash Concrete, World of Coal Ash (WOCA) Covington Publication, Kentucky, USA (2007) retrieved from www.flyash.info

Dhir, R. K., Byars, E. A., 1993, PFA Concrete: Chloride Diffusion Rates, Magazine of Concrete Research, 1993, 45, No. 162, Mar., 1-9

Dhir, R. K., El-Mohr, M. A. K., Dyer, T. D., 1997, Developing Chloride Resisting Concrete Using PFA, Cement and Concrete Research Journal, Vol 27, No. 11, pp 1633 -1639 1997.

Durability Index Testing Procedure Manual, Version 4.5.1, Department of Civil Engineering, University of Cape Town, 2018. Available online at, http://www.theconcreteinstitute.org.za/durability, 43 pp.

Duda, J., Kolosowski, M., Tomasiak, J., 2016, Methods for the Reduction of CO2 Emissions in the Cement Industry, Proceedings of the 27th DAAAM International Symposium, pp.0122-0130, B. Katalinic (Ed.), Published by DAAAM International, ISBN 978-3-902734-08-2, Vienna, Austria, DOI: 10.2507/27th.daaam.proceedings.018

Du-Preez, A. A. and Alexander, M. G., 2004, A site study of durability indexes for concrete in marine conditions, Materials and Structures Journal, Vol. 37, April 2004, pp 146-154

Dustan E. R., 2011, How Does Pozzolanic Reaction Make Concrete 'Green', World Coal Ash (WOCA) Conference (2011) Denver, CO, USA.

Duxson, P, Fernández-Jiménez, A, Provis, JL, Lukey, GC, Palomo, A, and Deventer, J.S.J., 2007, Geopolymer Technology: the Current State of the Art. Journal of Materials Science 42, no. 9 (2007): 2917–2933. doi:10.1007/S10853-006-0637-Z retrieved May 12, 2017 from www.springer.com

ESKOM, 2016, Ash Management in Eskom, Generation Communication CO 0004 Revision 12, Retrieved, January 28 2017 from www.eskom.co.za

Ekolu, S. O. and Murugan, S. 2012, Durability index performance of high strength concretes made basing on different standard Portland cements, University of the Witwatersrand, Technical Paper, retrieved February 12, 2018 from https://ujcontent.uj.ac.za/

Ekolu, O. S. 2014, Effect of superplasticizers on concrete durability indexes, University of Johannesburg, Technical Paper, retrieved July 2, 2018 from https://ujcontent.uj.ac.za/

Ekolu S.O, 2006, Heat curing practice in concrete precasting technology - problems and future directions. Concrete Beton, Jour. Concrete Society of Southern Africa, Dec 2006, 114: 5-10.

Elkhadiri, I., Palacios, M. and Puertas, F., 2009, Effect of curing temperature on cement hydration Ceramics-Silikáty, 53 (2) (2009), pp. 65-75

Elsageer, A. M., Millard, S. G. and Barnett, J. S. 2009, Strength Development of Concrete Containing Coal Fly Ash Under Different Curing Temperature Conditions, Proceedings of 2009 World of Coal Ash (WOCA) Conference – May 4-7, 2009 in Lexington, KY, USA

Fernández-Jiménez, A. and Palomo, A. 2005, Composition and Microstructure of Alkali Activated Fly Ash Binder: Effect of the Activator. Cement and Concrete Research, 35, 1984-1992.

Fernández-Jiménez, A. Palomo, A. and Revuelta, D. 2009, Alkali Activation Of Industrial By-Products To Develop New Earth-Friendly Cements, Proceeding of the 11th International Conference on Non-Conventional Materials And Technologies (NOMAT 2009) 6-9 September 2009, Bath, UK

Filho, J. H., Medeiros, M. H. F., Pereira, E., Helene, P. and Isaia, G. C., 2013, High-Volume Fly Ash Concrete with and without Hydrated Lime: Chloride Diffusion Coefficient from Accelerated Test, Journal of Materials in Civil Engineering, vol. 25. p. 411-418. 2013

Fraay, A.L.A., Bejen, J.M., de Haan Y.M. 1989, The reaction of fly ash in concrete: A critical examination, Cement and Concrete Research, 19 (1989) 235-246 retrieved May 15, 2018, from www.sciencedirect.com

Gardner, T., Stanish, K. and Alexander, M., 2006, Critical Review of Rapid Chloride Test Methods for Concrete, Technical Paper, Concrete Beton, Volume 113, pp 11-17, September 2006

Giatec Scientific Inc, 2019, An Overview of the Concrete Maturity Method, available online at https://www.giatecscientific.com/strength-maturity/

Gjorv, O. E., 2011, Durability of Concrete Structures, Arabian Journal for Science and Engineering, 36:151–172

Grieve, G.R.H., 1991, The influence of two South African fly ashes on the engineering properties of concrete, PhD thesis, Johannesburg: University of the Witwatersrand.

Grieve, G. R. H., and Kruger, R. A., 1990, The setting of fly ash cement mixes, SACAA first national symposium, Pretoria.

Hasanbeigi, A., Price, L., Lin, E. 2012, Emerging energy-efficiency and CO2 emission-reduction technologies for cement and concrete production: A technical review, Renewable and Sustainable Energy Reviews, Volume 16, Issue 8, Pages 6220-6238 retrieved March, 06, 2017 from www.sciencedirect.com

Hasheela, P.F. and Ekolu, S.O., 2010, Effect Of Fly Ash And Slag On The Cost Of Concrete, Technical Paper, available online at https://core.ac.uk/download/pdf/54200377.pdf

Helmuth, R., 1987, Fly Ash in Cement and Concrete, Portland Cement Association, USA.

Heyns, M. W., Hassan, M. M., 2014, South Africa Class F Fly Ash for Roads: Physical and Chemical Analysis, 2014, Interdisciplinary Journal, Vol. 12, No. 3, pp 28-41, 2013

Holland, N. L., Nichols, A. B. and Nichols, J. M., The Use of Hydrated Lime in Concrete as A Cement Replacement: Effect on Compressive Strength, Technical Paper, available online at https://www.researchgate.net

Hung, H. H., 1997, Properties of High-Volume Fly Ash Concrete, PhD Thesis, University of Shefield, UK

Hwang, S. D., Khatib, R., Lee, H. K., Lee, S. H., and Khayat, K. H., 2012, Optimization of steam-curing regime for high-strength, self-consolidating concrete for precast, prestressed concrete applications, PCI Journal . Summer2012, Vol. 57 Issue 3, p48-62. 15p.

Joshi, R.C., 2010, Fly Ash – Production, Variability and Possible Complete Utilization, Indian Geotechnical Conference – 2010, GEOtrendz December 16–18, 2010

Kate, G. K. and Thakare, S. B., 2017, An Experimental Study of High Strength-High Volume Fly Ash Concrete for Sustainable Construction Industry, IOP Conference Series: Materials Science and Engineering, 225 012247 doi:10.1088/1757-899X/225/1/012247

Kawai, T., 2002, State-of-the-art report on high-strength concrete in Japan – Recent developments and applications, Technical Department of Civil Engineering, Shimizu Corporation, Japan 105-8007, pp. 87-107

Kosmatka, S. H. and Wilson, M. L. 2011, Design and Control of Concrete Mixtures, Engineering Bulletin 001, 15th edition, Portland Cement Association, Skokie, Illinois, USA

Kovacevic, I. and Dzidic, S., 2018, High-Strength Concrete (HSC) Material For High-Rise Buildings, Metallic and Non-metallic Materials, B&H, 12th Scientific/Research Symposium with International Participation 19th-20th April 2018

Kowalczyk R. M., Gajewicz A. M. and McDonald P.J., 2014, The mechanism of water–isopropanol exchange in cement pastes evidenced by NMR relaxometry, Technical Paper, Royal Society of Chemistry, RSC Adv., 2014, 4, 20709

Kruse, K., Jasso, A., Folliard, K., Ferron, R., Juenger, M., and Drimalas, T., 2013, Characterizing Fly Ash, Center for Transportation Research, The University of Texas at Austin, Austin, USA

Kruger, J. E., 2003, South African Fly Ash: A Cement Extender, South African Coal Ash Association Publication, Johannesburg.

Looney, D. O. and Pavia, S., 2014, A Study of the Functionality of Hydrated Lime as an Admixture, Journal of Materials Science Research; Vol. 4, No. 1; 2015

Malhotra, M. V. 2004, Properties of high-volume fly ash concrete and its role in sustainability of cement and concrete, CANMET, Canada, Presentation, retrieved February 6, 2018, from http://www4.uwm.edu/cbu/Aci/Malhotra.HVFA.March2004.pdf

Malvern Instruments, 2007, Mastersizer 2000 User Manual, retrived, January, 30, 2019, from https://www.labmakelaar.com/fjc_documents/mastersizer-2000-2000e-manual-eng1.pdf

Manz, E., Worldwide production of coal ash and utilization in concrete and other products, Fuel, Volume 76, Issue 8, 1997, Pages 691-696

McCarthy, M. J., and Dhir, R. K. 2005, Development of high volume fly ash cements for use in concrete construction, Fuel Journal 84 (2005) 1423–1432

Mehta P. K., 2004, High-Performance, High-Volume Fly Ash Concrete For Sustainable Development, Proceedings of the International Workshop on Sustainable Development and Concrete Technology, Beijing, China, retrieved June 22, 2017 from researchgate.com

Moutassem, F. and Chidiac, S. E., 2016, Assessment of Concrete Compressive Strength Prediction Models, KSCE Journal of Civil Engineering (2016) 20(1):343-358

Mukadam, Z., 2014, Critical review of the South African durability index tests, with possible improvements. MSc dissertation, University of Cape Town, Department of Civil Engineering.

Mukheibir, P.V., 1990, The deformation properties of concrete with classified Lethabo fly ash, MSc Engineering Thesis, University of Cape Town.

Myadraboina H., Setunge S., Patnaikuni I., 2017, Pozzolanic Index and lime requirement of low calcium fly ashes in high volume fly ash mortar, Journal Paper, Construction and Building Materials 131 (2017) 690-695 retrieved April 25, 2018 from sciencedirect.com

Nassifa, A. Y. and Petrou, M. F., 2013, Influence of cold weather during casting and curing on the stiffness and strength of concrete, Construction and Building Materials, Volume 44, July 2013, Pages 161-167

Nath P., Sarker P., 2011, Effect of Fly Ash on the Durability Properties of High Strength Concrete, Science Direct Journal, Procedia Engineering 14 (2011) 1149–1156

National Ready Mix Concrete Association CIP 39, 2006, Maturity Methods to Estimate Concrete Strength,

Obla, H.K., Hill, R.L., Thomas, M.D.A., Shashiprakash, S.G. and Perebatova, O., 2003, Properties of Concrete Containing Ultra-Fine Fly Ash, ACI Materials Journal. 100. 426-433.

Obla, H. K., Lobo, C. L. and Kim, H. 2012, Greatly Increased Use of Fly Ash in Hydraulic Cement Concrete (HCC) for Pavement Layers and Transportation Structures - Volume I,

Otieno, M., 2018, Sensitivity of the rapid chloride conductivity index test to concrete quality and changes in various test parameters, Cement and Concrete Composites, Volume 86 (2018), 110-116

Otieno M., Alexander M., 2015, Chloride conductivity testing of concrete: Past and Recent Developments, Technical Paper, Journal of the South African Institution of Civil Engineering, Vol 57 No 4, December 2015, Pages 55–64, Paper 1306, Retrieved March 16, 2018 from http://www.scielo.org.za

Owens, G., 2009, Fulton's Concrete Technology, 9th Edition, Cement and Concrete Institute, Midrand, South Africa

Owens K. J., Bai Y., Cleland D., Basheer P.A.M., Kwasny J., Sonebi M., Taylor S., and Gupta A., 2010, Activation of High-Volume Fly Ash Pastes Using Chemical Activators, In. Proceedings of Second International Conference on Sustainable Construction Materials and Technologies, Ancona, Italy, 28–30 Jun 2010,

Özturan, M., Birgül Kutlu, B. and Özturan, T., 2008, Comparison Of Concrete Strength Prediction Techniques with Artificial Neural Network Approach, Building Research Journal, Volume 56, 2008

Pacheco-Torgal, F, Castro-Gomes, J, Jalali, S 2008, Alkali-activated binders: A review Part 1. Historical background, terminology, reaction mechanisms and hydration products, Journal Paper, Construction and Building Materials 22 (2008) 1305–1314

Palomo, A., Fernández-Jiménez, A, 2011, Alkaline activation, procedure for transforming fly ash into new materials. Part 1: Applications, Proceedings of the 2011 World of Coal Ash (WOCA) Conference in Denver, CO, USA, May 9-12, 2011

Patnaikuni, I., Setunge, S. and Solikin, M., Ling, X. and Boina, B., 2013, High Strength High Volume Fly Ash Concrete. In. Proceedings of The Seventh International Structural Engineering and Construction Conference, June 18-23, 2013 Honolulu, Hawaii, USA, retrieved February 20, from researchgate.com

Poon, C.S., Lam, L. and Wong, Y. L. 2000, A study on high strength concrete prepared with large volumes of low calcium fly ash, Cement and Concrete Research Journal 30 (2000) 447 ± 455

Popovics, S., 1998, History of a mathematical model for strength development of portland cement concrete. ACI Materials Journal Volume 95, Issue 5: 593–600.

PPC, 2014, Product Datasheet, retrieved July 21, 2017 from https://www.ppc.co.za/media/76879/OPC-datasheet-WEB-2014-1.pdf

Provis, JL, Duxson, P, Deventer, JSJ, and Lukey, G 2005, The Role of Mathematical Modelling And Gel Chemistry In Advancing Geopolymer Technology, Journal Paper, Chemical Engineering Research and Design. 83 (2005) 853-860 retrieved, January 18, 2018 from www.sciencedirect.com

Rangaraju, P., Use of Concrete Maturity For Measuring In-Place Strength of Concrete, Department of Civil Engineering, Clemson University

Rao, A. and Ramanjaneyulu, K., 2018, Recent Advances in Structural Engineering, Vol. 1; Springer Publication in Lecture Series in Civil Engineering ISBN 978-981-13-0362-3,(2018).

Rao, G. A., 2001, Generalization of Abrams' law for cement mortars, Cement and Concrete Research Journal 31 (2001) 495 ± 502, retrieved 26 May 2018 from ScienceDirect.

Rashid, M. A. and Mansur, M. A., 2009, Considerations in producing high strength concrete, Journal of Civil Engineering (IEB), 37(1) (2009) 53-63

Saha, A. K. 2017, Effect of class F fly ash on the durability properties of concrete, Sustainable Environment Research Journal 28 (2018) 25-31, retrieved July, 06, 2018 from www.elsevier.com

Seedat, E. Y., 2003, Super-Pozz: The New Generation Pozzolan for Superior Concrete, Technical Paper, Presented at the 11th International Congress on the Chemistry of Cement, Durban, South Africa, 11-16 May, 2003, retrieved 08 May 2018, from http://www.superpozz.com/

Shekhovtsova J., 2015, Using South African Fly Ashes as a Component of Alkali Activated Binders, PhD thesis, University of Pretoria, South Africa.

Shen, X., Jiang, W., Hou, D., Hu, Z., Yang, J. and Liu, Q., 2019, Numerical study of carbonation and its effect on chloride binding in concrete, Cement and Concrete Composites

Shi C., Krivenco P. V., Roy D., 2006, Alkali Activated Cements and Concretes, Ed. Taylor & Francis, New York, USA

Skvarla 1, J., Sisol, M., Botula, J., Kolesárová, M., And Krinická, I., 2011, The Potential Use of Fly Ash with a High Content of Unburned Carbon in Geopolymers, Acta Geodyn. Geomater., Vol. 8, No. 2 (162), 123–132, 2011

Solikin, M., Setunge, S. and Patnaikuni, I. 2013, Experimental design analysis of ultra fine fly ash, lime water, and basalt fibre in mix proportion of high volume fly ash concrete, Pertanika Journal of Science and Technology, vol. 21, no. 2, pp. 589-600, 2013.

South African Government, 2018, Treasury tables Carbon Tax Bill in Parliament, 18 November 2018. [Online]. Available at: https://www.gov.za/speeches/media-statement-tabling-carbon-tax-bill-21-nov-2018-0000 [Accessed 26 February 2019]

South African National Standard, 2013. Cement: Part 1: Composition, specifications and conformity criteria for common cements. (SANS 50197-1:2013). Pretoria: 2013

South African National Standard, 2006. Concrete tests Part 3: Making and curing of test specimens. (SANS 5861-3:2006). Pretoria: 2006

South African National Standard, 2015. Civil engineering test methods: Part CO3-3: Concrete durability index testing - Chloride conductivity test. (SANS 3001-CO3-3:2015). Pretoria: 2015

South African National Standard, 2006. Concrete Tests-Compressive Strength of Hardened Concrete. (SANS 5863:2006). Pretoria: SANS.

South African National Standard, 2011. Fly ash for concrete Part 1: Definition, specifications and conformity criteria. (SANS 50450-1:2011). Pretoria: SANS.

Soutsos, M., Kanavaris, F., and Hatzitheodorou, A, 2018, Critical analysis of strength estimates from maturity functions, Case Studies in Construction Materials

Soutsos, M., Hatzitheodorou, A., Kanavaris, F., & Kwasny, J. (2017). Effect of temperature on the strength development of mortar mixes with GGBS and fly ash. Magazine of Concrete Research, 69(15), 787-801.

Thomas, M. 1996, Chloride Thresholds In Marine Concrete, Cement and Concrete Research Journal, Vol. 26, No. 4, pp. 513-519,1996

Thomas, M., 2007, Optimising the Use of Fly Ash in Concrete, Portland Cement Association Publication, Retrieved, January 20, 2017 from www.cement.org

Thomas, M., Shehata, M., and Shashiprakash, S., 1999, The Use of Fly Ash in Concrete: Classification by Composition, Cement, Concrete and Aggregates, Vol. 21, No. 2

United Nations, 2015a, Sustainable Development Goals, [Online] Available at: https://www.un.org/sustainabledevelopment/climate-change-2/ [Accessed 15 February 2018]

United Nations, 2015b, Paris Agreement, retrieved March, 05, 2018 from https://unfccc.int/sites/default/files/english_paris_agreement.pdf

United Nations Framework Convention On Climate Change, 2008, Kyoto Protocol Reference Manual On Accounting Of Emissions And Assigned Amount

Wajahat H. M., Soliman I. A., Al-Bedawi W. H., (1991) Temperature effect on strength of mortars and concrete containing blended cements, Cement and Concrete Composites Volume 13, Issue 3, 1991, Pages 197-202

Yang, K., Mun, J. and Cho, M., 2015, Effect of Curing Temperature Histories on the Compressive Strength Development of High-Strength Concrete, Advances in Materials Science and Engineering Volume 2015

Ye, H. and Radlinska, A., 2017, Effect of Alkalis on Cementitious Materials: Understanding the Relationship between Composition, Structure and Volume Change Mechanism, Journal of Advanced Concrete Technology, Vol. 15, 166-177, April 2017

Yikici, T. A. and Chen, H. R., 2015, Use of maturity method to estimate compressive strength of mass concrete, Construction and Building Materials 95 (2015) 802–812

Yuan, Q., Shi, C., De-Schutter, G, Audenaert, K. and Deng, D, 2009, Chloride binding of cement-based materials subjected to external chloride environment – A Review, Construction and Building Materials 23 (2009) 1–13.

Zemajtis J. Z., 2014, Role of Concrete Curing, [Online] https://www.cement.org/learn/concrete - technology/concrete-construction/curing-in-construction

Zulu, S. and Allopi, D., 2015, Optimising the Usage of Fly Ash in Concrete in the Construction of Roadworks, 34th South African Transport Conference (SATC 2015)

9. Annexures

Annexure 1: Compressive Strength Results

Table 9-1: Compressive Strength Test Results

					23°C Curing Temperature		40°C Curing Temperature	
Mix	**Cementitious Material**	**w/c Ratio**	**Calcium Hydroxide Content**	**Ages (Days)**	**Average Compressive Strength of 3 Cubes (MPa)**	**Standard Deviation**	**Average Compressive strength of 3 Cubes (MPa)**	**Standard Deviation**
1	OPC	0.35	5%	1	59	1.10	73	2.86
				3	81	2.12	85	2.37
				7	95	2.34	92	4.16
				28	115	0.31	110	1.60
				90	120	2.72	112	1.53
				180	122	3.18	114	1.57
2	OPC	0.35	0%	1	55	1.44	69	2.96
				3	90	0.78	81	1.17
				7	98	1.29	86	2.68
				28	120	2.62	105	4.08
				90	124	1.40	110	1.20
				180	126	1.47	114	3.79
3	OPC	0.45	5%	1	24	0.38	33	0.62
				3	59	1.77	58	2.49
				7	70	0.67	68	1.72
				28	87	1.15	76	1.05
				90	92	0.76	78	1.22
				180	95	2.95	82	1.68
4	OPC	0.45	0%	1	19	1.02	31	1.81
				3	57	1.15	55	1.79
				7	69	1.05	63	1.13
				28	77	0.72	71	3.18
				90	88	1.52	74	4.20
				180	90	0.12	778	1.93
5	OPC+25%FA	0.35	5%	1	35	0.91	46	1.23
				3	62	3.21	73	1.41
				7	82	0.20	87	0.80
				28	108	2.20	117	3.72
				90	121	1.33	119	0.92
				180	124	1.60	121	1.01

					23°C Curing Temperature		40°C Curing Temperature	
Mix	**Cementitious Material**	**w/c Ratio**	**Calcium Hydroxide Content**	**Ages (Days)**	**Average Compressive Strength of 3 Cubes (MPa)**	**Standard Deviation**	**Average Compressive strength of 3 Cubes (MPa)**	**Standard Deviation**
6	OPC+25%FA	0.35	0%	1	31	0.83	41	1.21
				3	58	0.98	62	1.59
				7	75	0.81	80	4.97
				28	101	3.30	107	4.98
				90	126	2.39	116	3.83
				180	128	0.87	118	1.72
7	OPC+25%FA	0.45	5%	1	18	0.53	31	1.25
				3	44	0.46	52	0.51
				7	58	1.11	73	1.31
				28	81	2.46	97	1.07
				90	105	2.72	106	1.68
				180	109	3.61	108	1.00
8	OPC+25%FA	0.45	0%	1	16	0.25	25	0.76
				3	45	0.64	51	1.18
				7	59	1.78	70	0.30
				28	85	2.72	98	1.29
				90	107	1.92	105	6.47
				180	109	1.21	107	1.25
9	OPC+35%FA	0.35	5%	1	32	0.95	41	0.61
				3	50	1.55	58	0.76
				7	69	1.18	80	2.25
				28	96	3.00	114	3.41
				90	105	3.59	116	2.00
				180	113	2.91	119	1.82
10	OPC+35%FA	0.35	0%	1	28	1.19	38	1.75
				3	51	2.00	58	2.47
				7	64	2.55	80	0.90
				28	90	2.91	102	1.36
				90	100	1.97	106	1.51
				180	104	1.83	109	3.14
11	OPC+35%FA	0.45	5%	1	14	0.46	21	1.36
				3	37	1.79	43	0.60
				7	48	0.59	61	1.79
				28	70	2.09	88	3.92
				90	94	2.72	102	5.61
				180	103	2.85	107	5.03

					23°C Curing Temperature		40°C Curing Temperature	
Mix	**Cementitious Material**	**w/c Ratio**	**Calcium Hydroxide Content**	**Ages (Days)**	**Average Compressive Strength of 3 Cubes (MPa)**	**Standard Deviation**	**Average Compressive strength of 3 Cubes (MPa)**	**Standard Deviation**
12	OPC+35%FA	0.45	0%	1	13	0.36	20	0.38
				3	27	1.45	38	1.01
				7	39	1.10	54	2.37
				28	62	1.20	79	1.86
				90	79	0.62	91	3.79
				180	89	2.50	94	2.16
13	OPC+50%FA	0.35	5%	1	22	0.51	31	0.95
				3	38	0.29	51	3.36
				7	49	0.45	73	0.81
				28	77	1.10	95	1.60
				90	105	2.12	108	1.44
				180	115	1.53	114	3.59
14	OPC+50%FA	0.35	0%	1	21	0.57	27	1.48
				3	34	1.12	43	1.50
				7	44	0.87	62	1.91
				28	67	0.90	87	1.20
				90	89	5.21	97	2.25
				180	105	2.75	103	1.40
15	OPC+50%FA	0.45	5%	1	9	0.10	13	0.99
				3	23	0.15	32	1.48
				7	30	0.25	47	0.78
				28	51	1.60	70	2.36
				90	71	1.40	84	0.82
				180	83	2.00	86	0.78
16	OPC+50%FA	0.45	0%	1	7	0.10	11	0.62
				3	17	0.20	24	1.31
				7	25	0.96	36	1.23
				28	42	0.47	61	1.27
				90	62	2.72	71	1.56
				180	75	2.53	73	1.87

Annexure 2: Compressive Strength Line Graphs for Relationship Between Compressive Strength and Age of Concrete

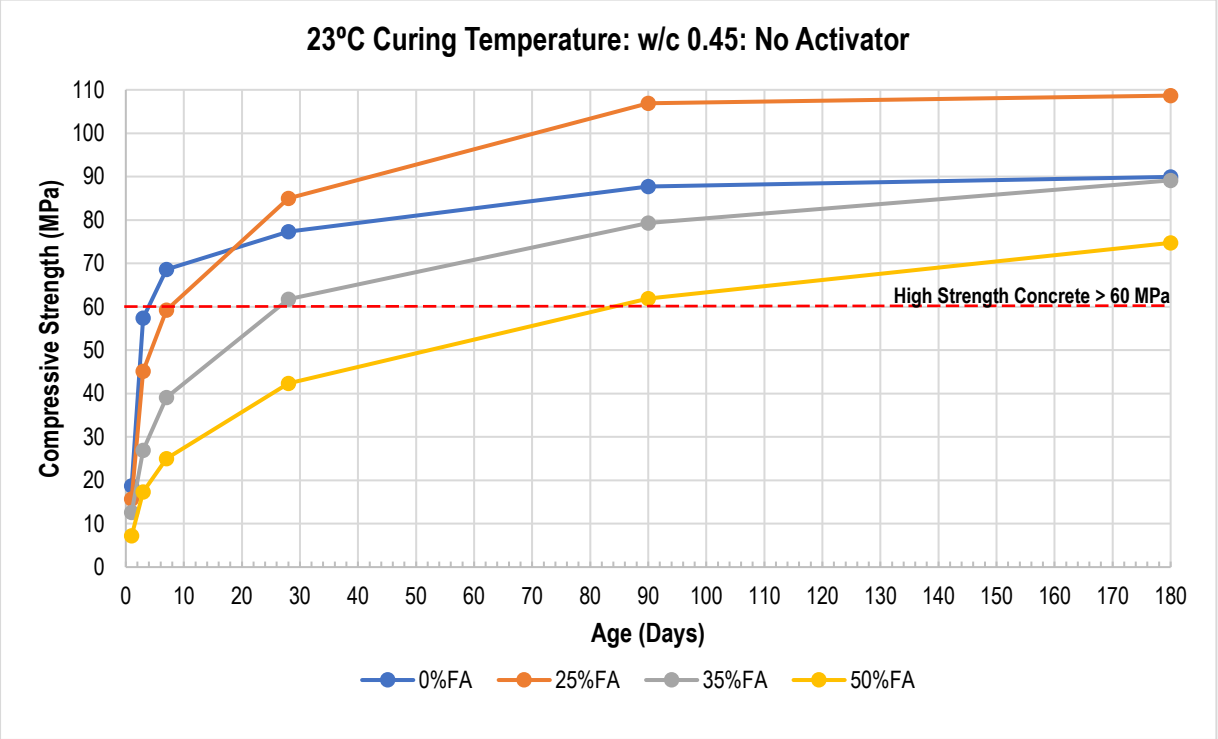

Figure 9.1: Compressive Strength for Concrete Cured at 23^{0}C without $Ca(OH)_2$ Activator (w/c = 0.45)

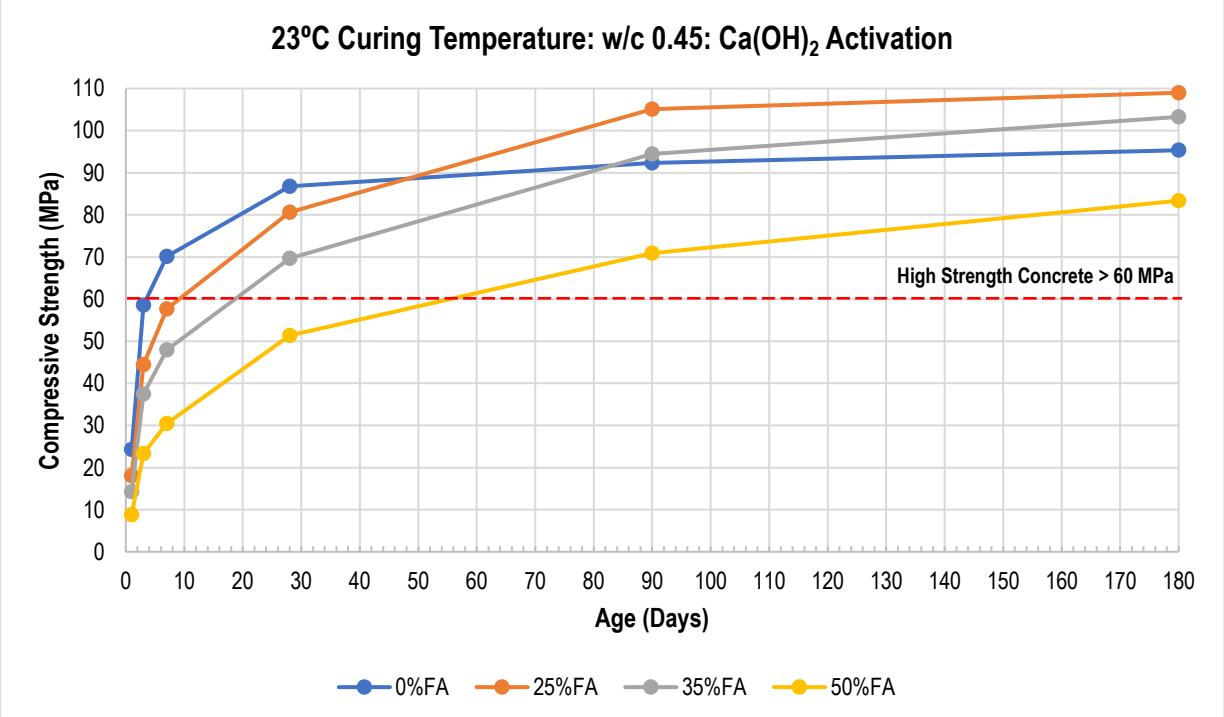

Figure 9.2: Compressive Strength for Concrete Cured at 23^{0}C with $Ca(OH)_2$ Activator (w/c = 0.45)

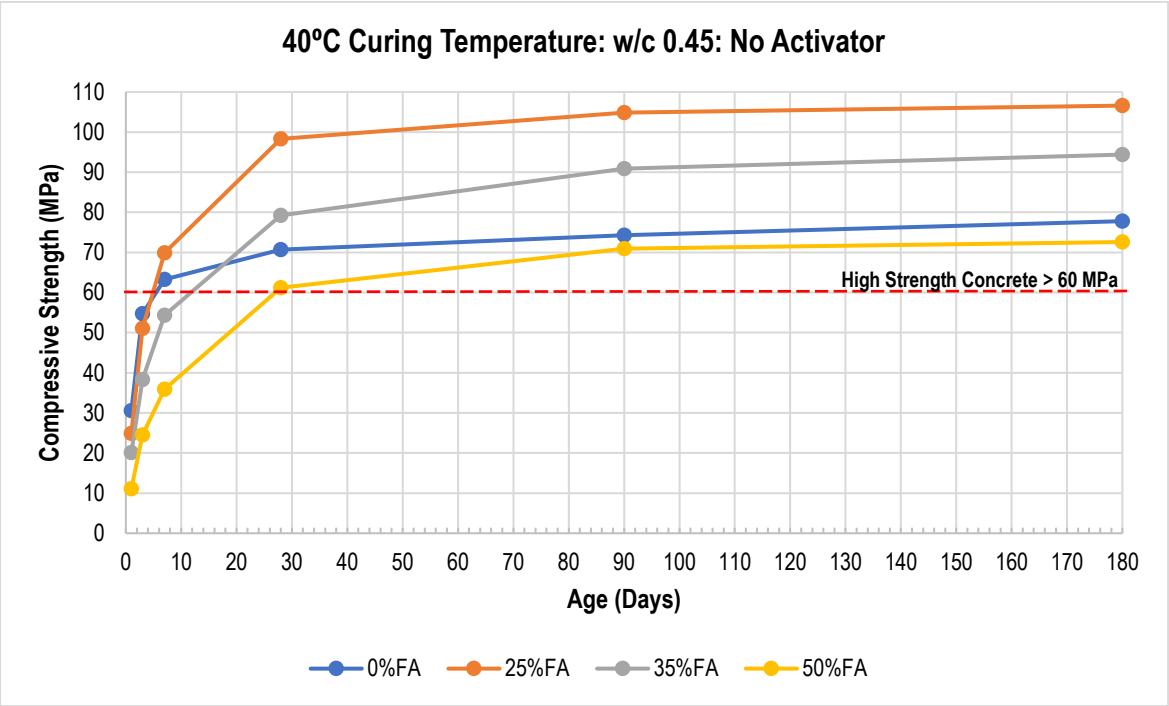

Figure 9.3: Compressive Strength for Concrete Cured at 40^{0}C without $Ca(OH)_2$ Activation (w/c = 0.45)

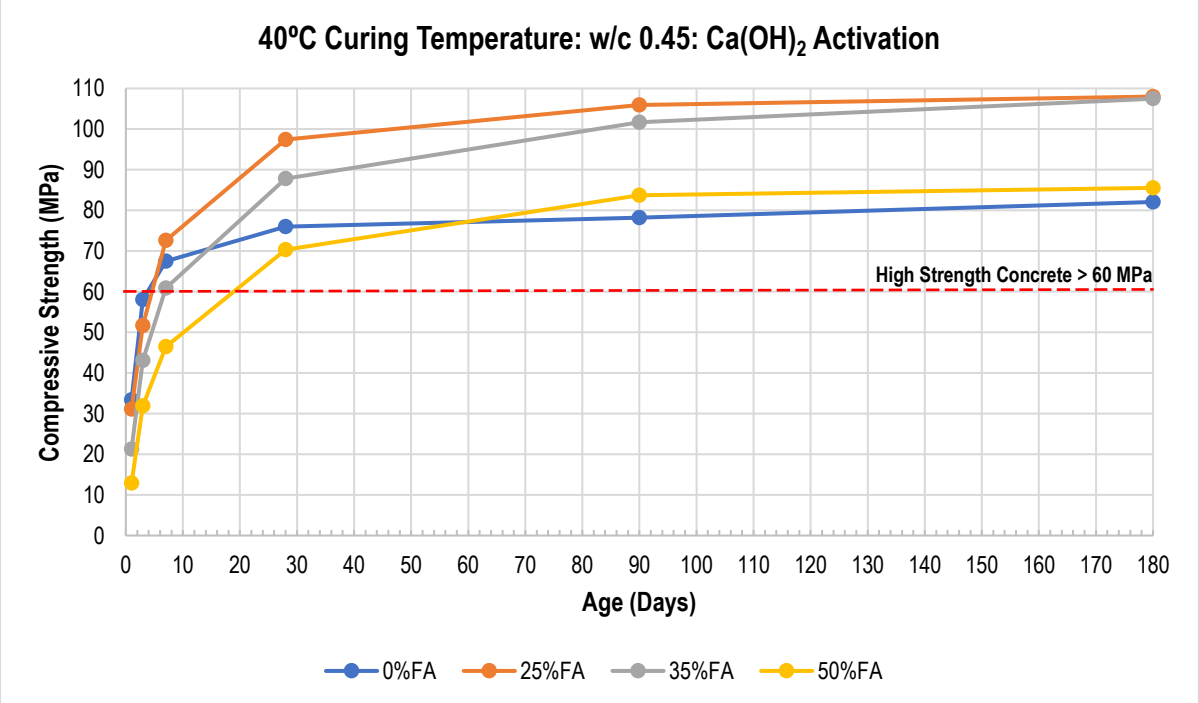

Figure 9.4: Compressive Strength for Concrete at 40^{0}C with $Ca(OH)_2$ Activator (w/c = 0.45)

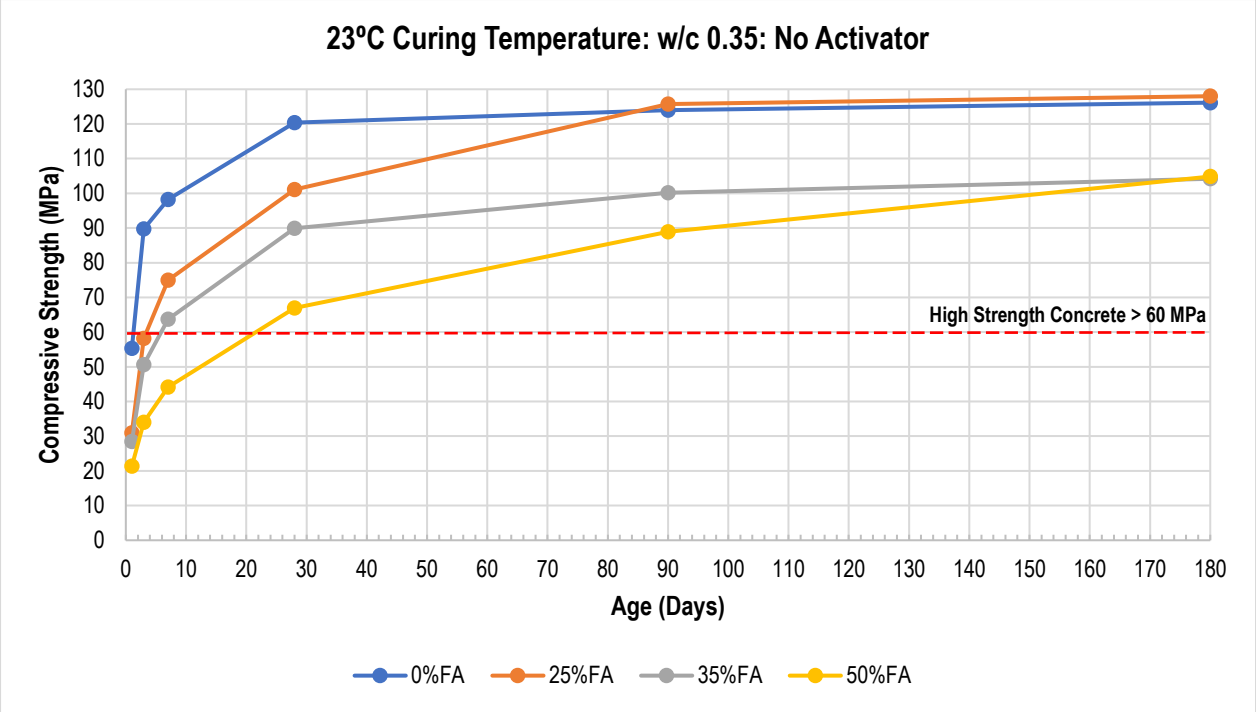

Figure 9.5: Compressive Strength for Concrete Cured at 23^{0}C without $Ca(OH)_2$ Activator (w/c = 0.35)

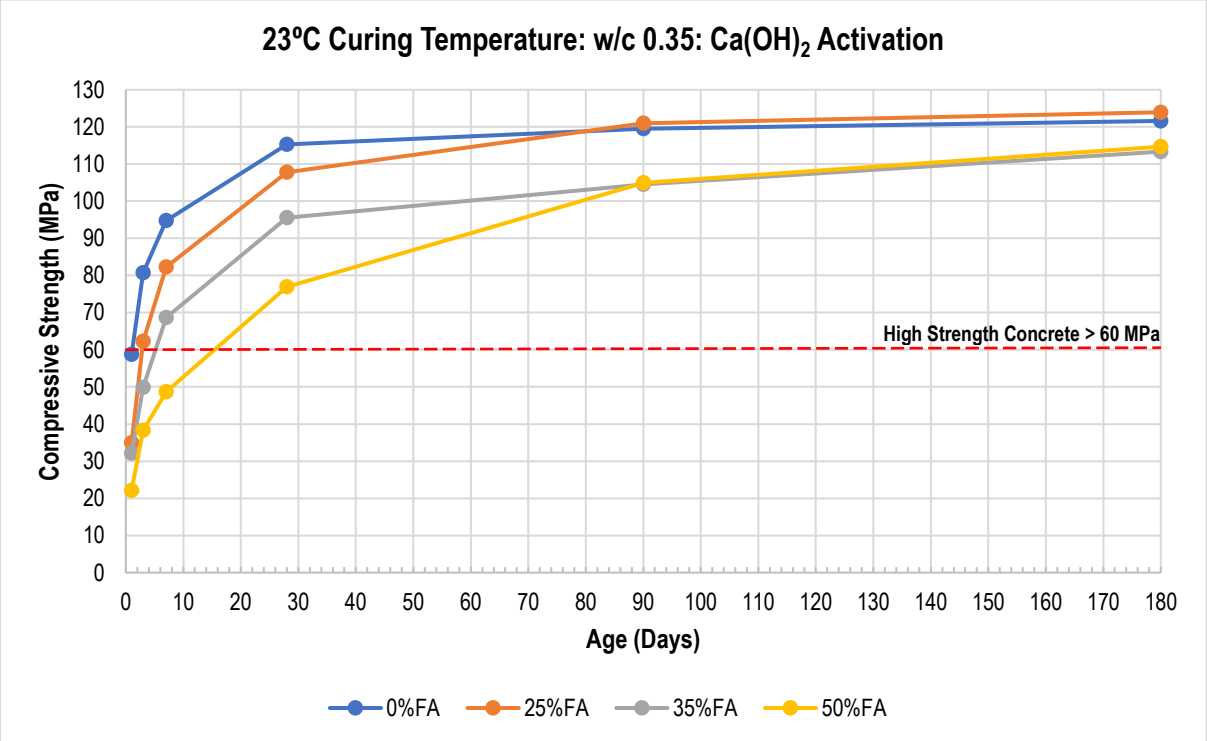

Figure 9.6: Compressive Strength for Concrete Cured at 23^{0}C with $Ca(OH)_2$ Activation (w/c = 0.35)

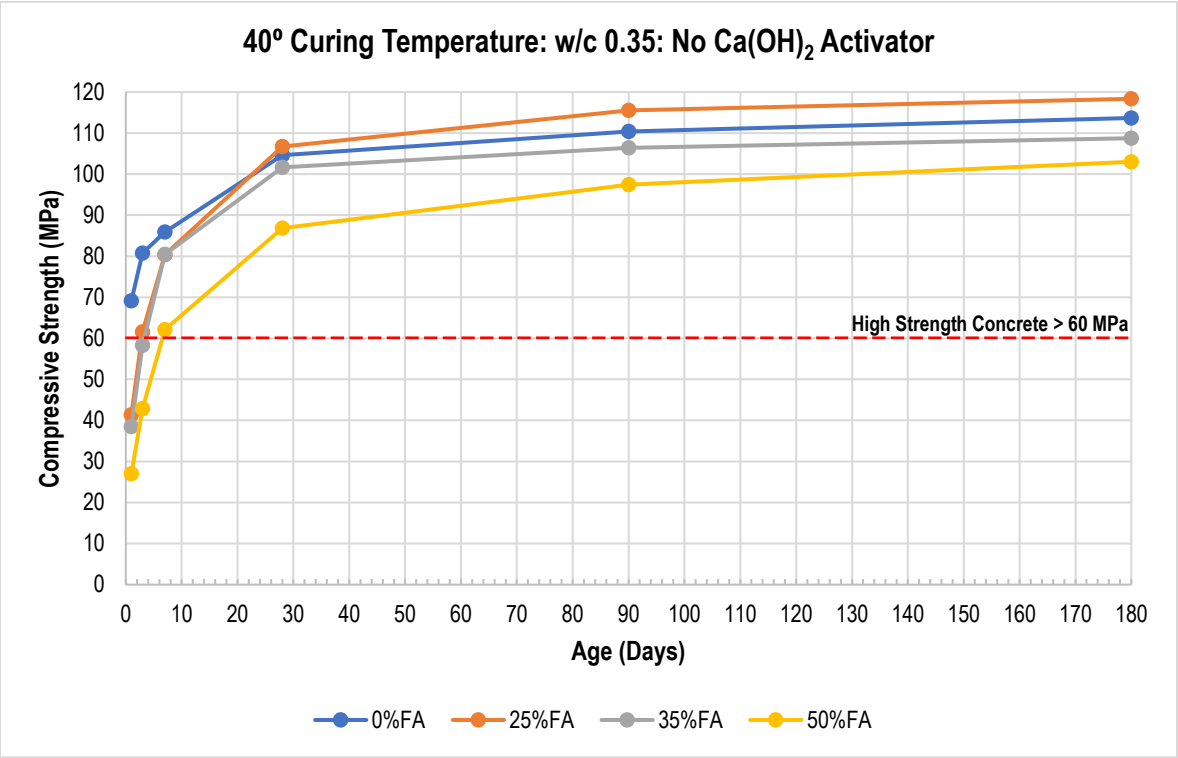

Figure 9.7: Compressive Strength for Concrete Cured at 40^{0}C without $Ca(OH)_2$ Activator (w/c = 0.35)

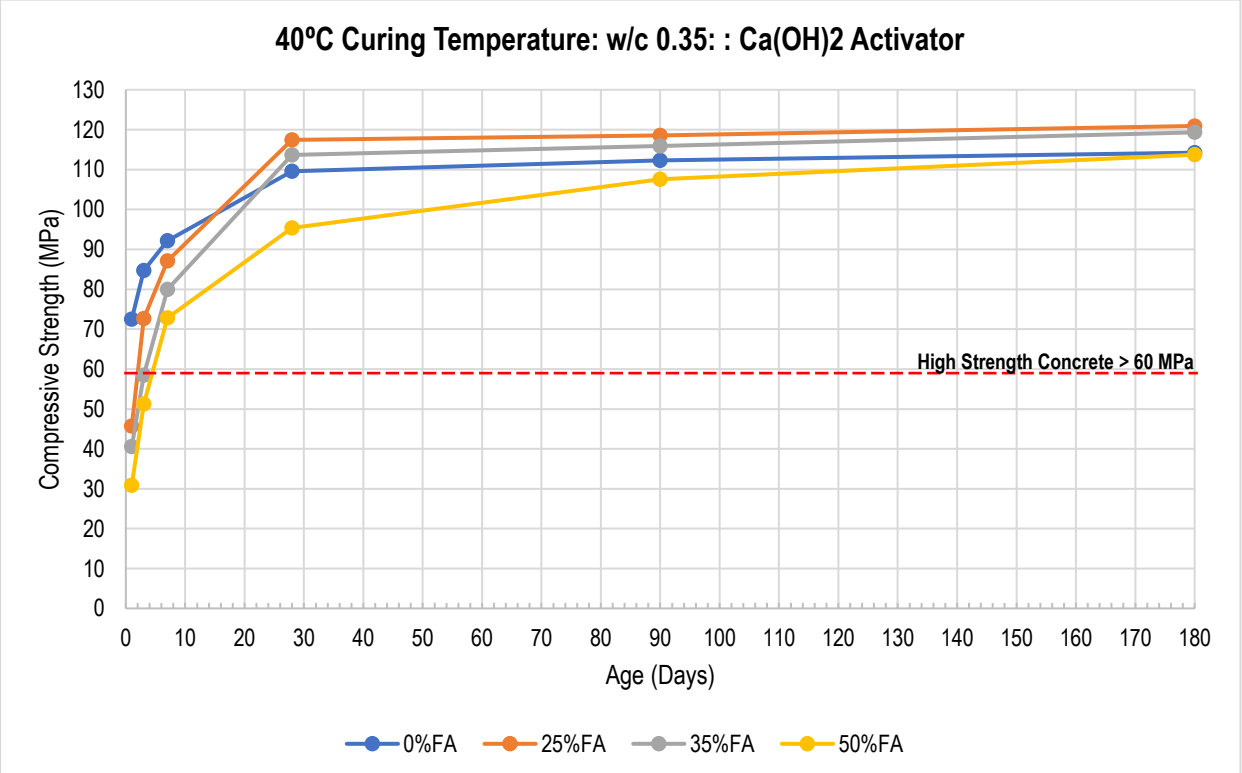

Figure 9.8: Compressive Strength for Concrete Cured at 40^{0}C with $Ca(OH)_2$ Activator (w/c = 0.35)

Annexure 3: Compressive Strength Line Graphs for Relationship Between Compressive Strength and Fly Ash Content

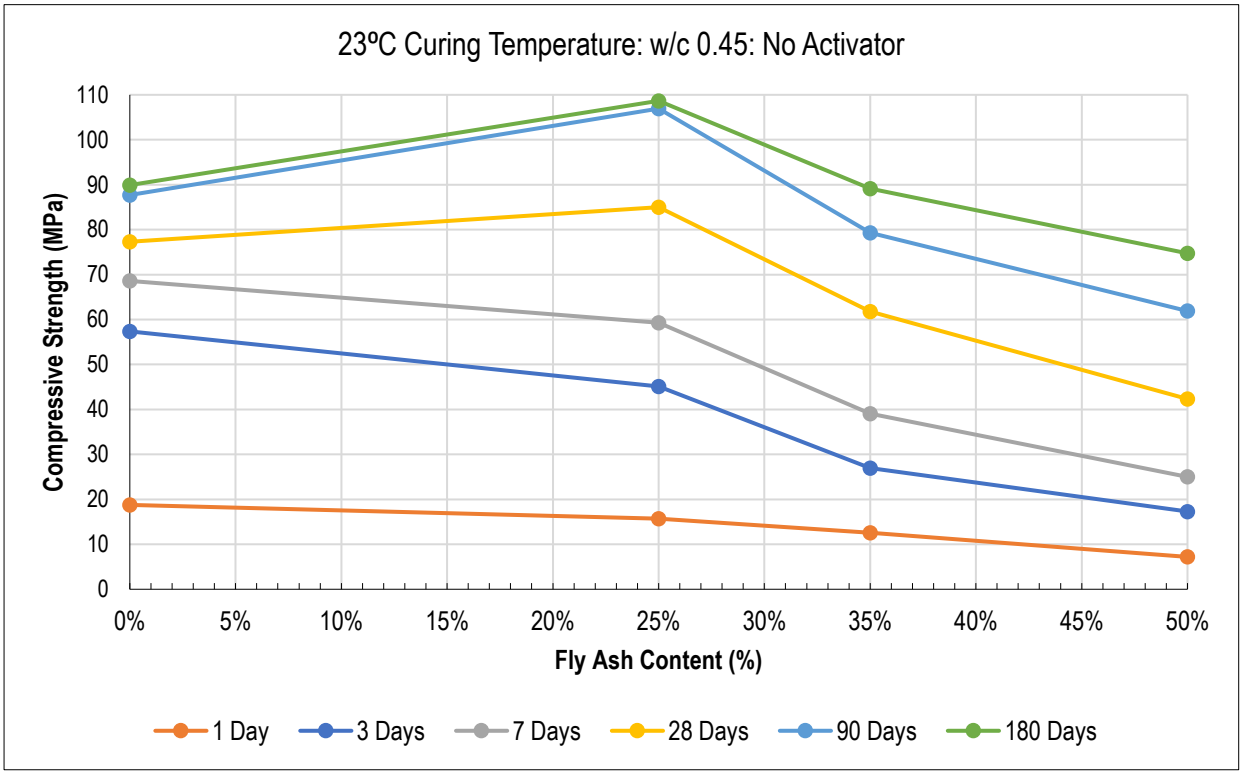

Figure 9.9: Relationship Between Compressive strength and FA Content (23°C: w/c 0.45: No Activator)

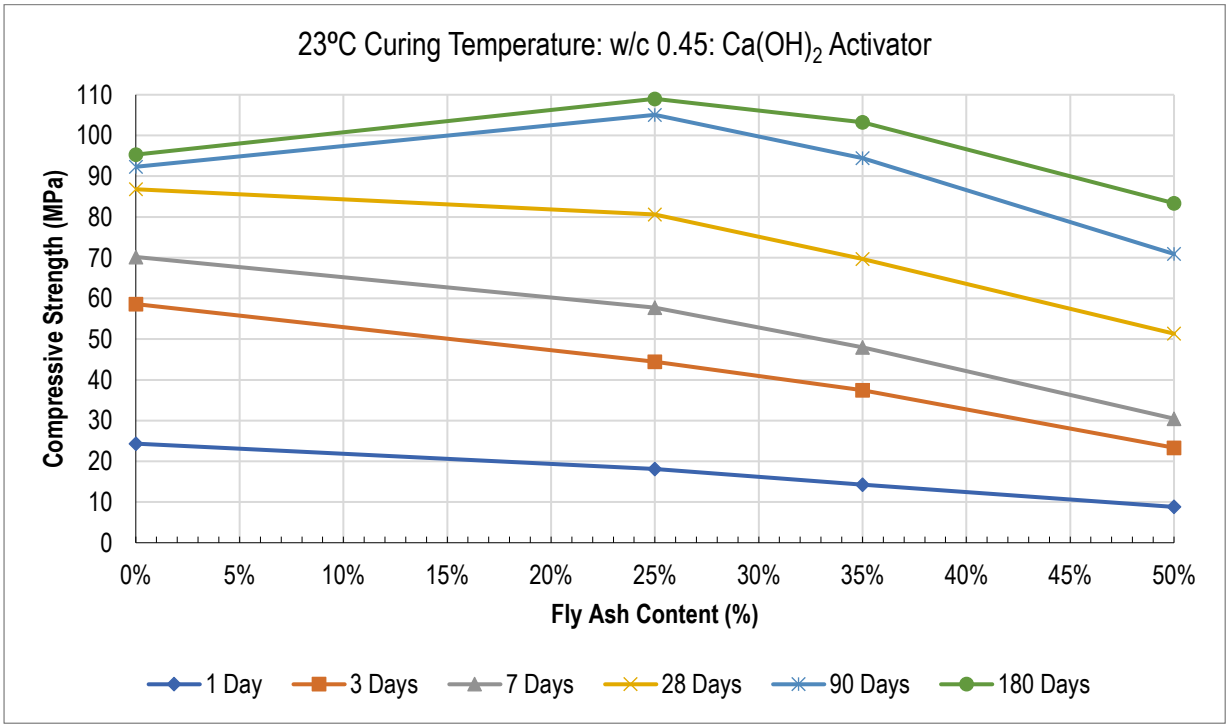

Figure 9.10: Relationship between Compressive strength and FA Content (23°C: w/c 0.45: $Ca(OH)_2$ Activator)

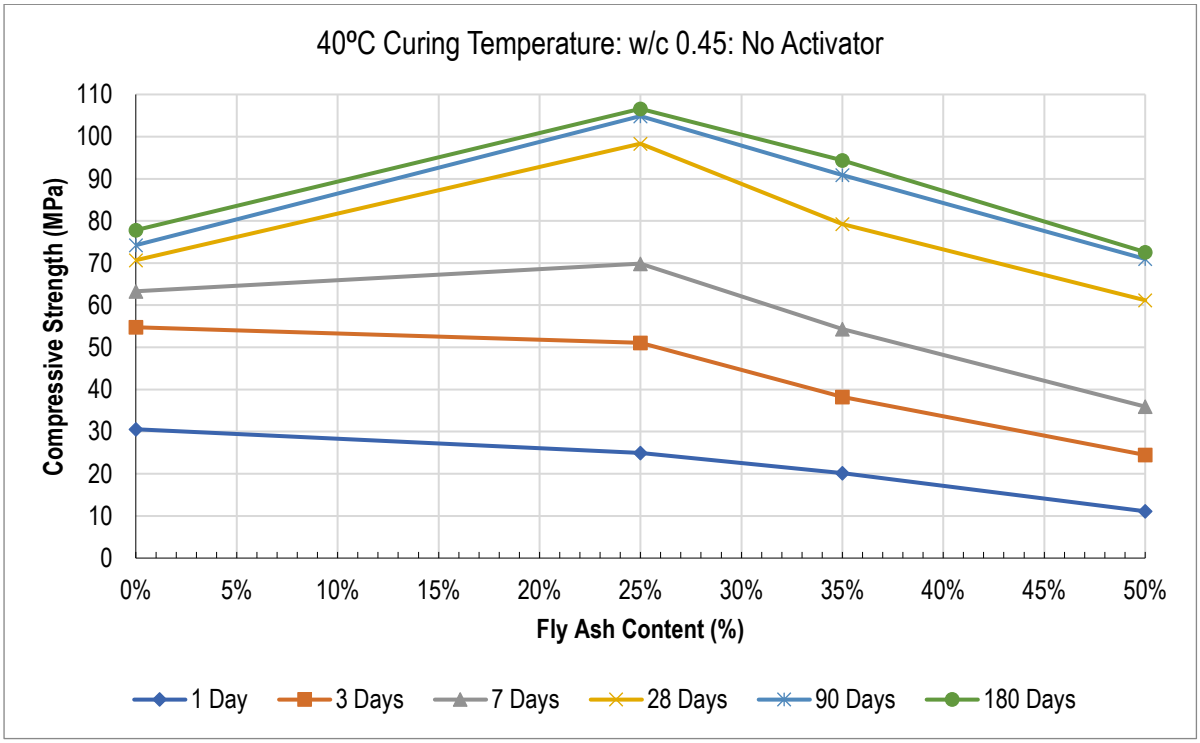

Figure 9.11: Relationship Between Compressive strength and FA Content ($40^{o}C$: w/c 0.45: No Activator)

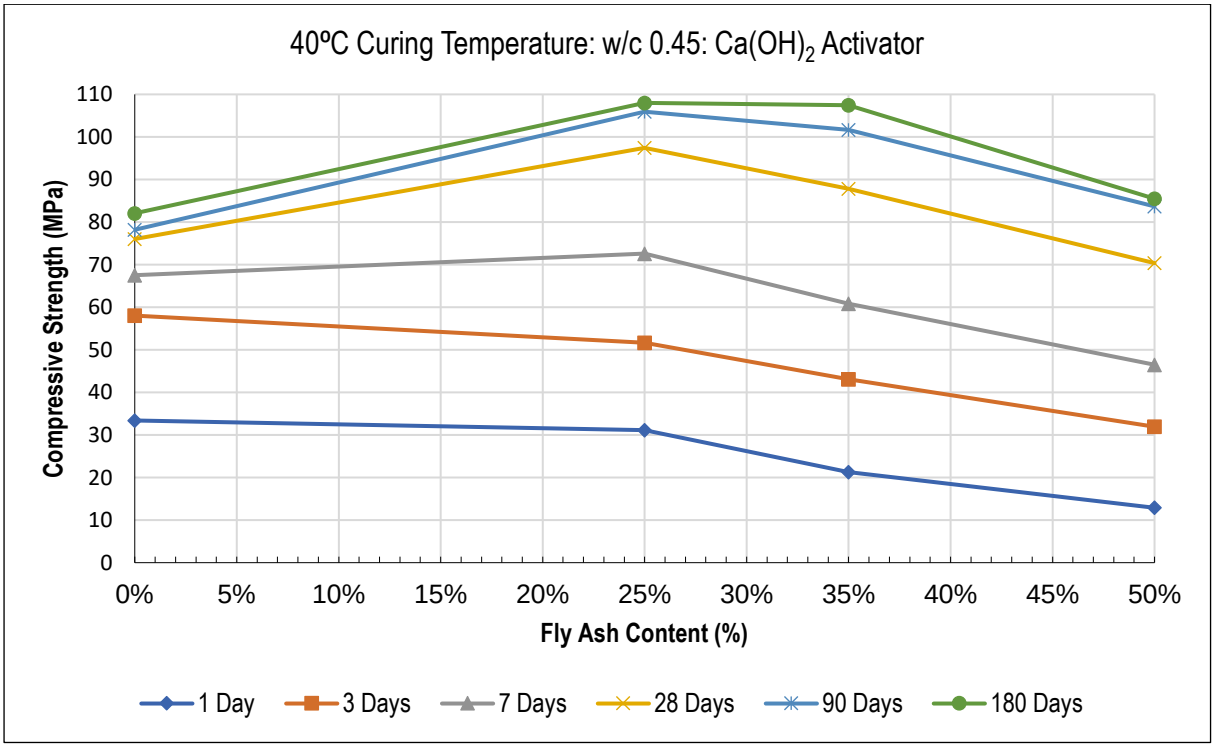

Figure 9.12: Relationship Between Compressive strength and FA Content ($40^{o}C$: w/c 0.45: $Ca(OH)_2$ Activator)

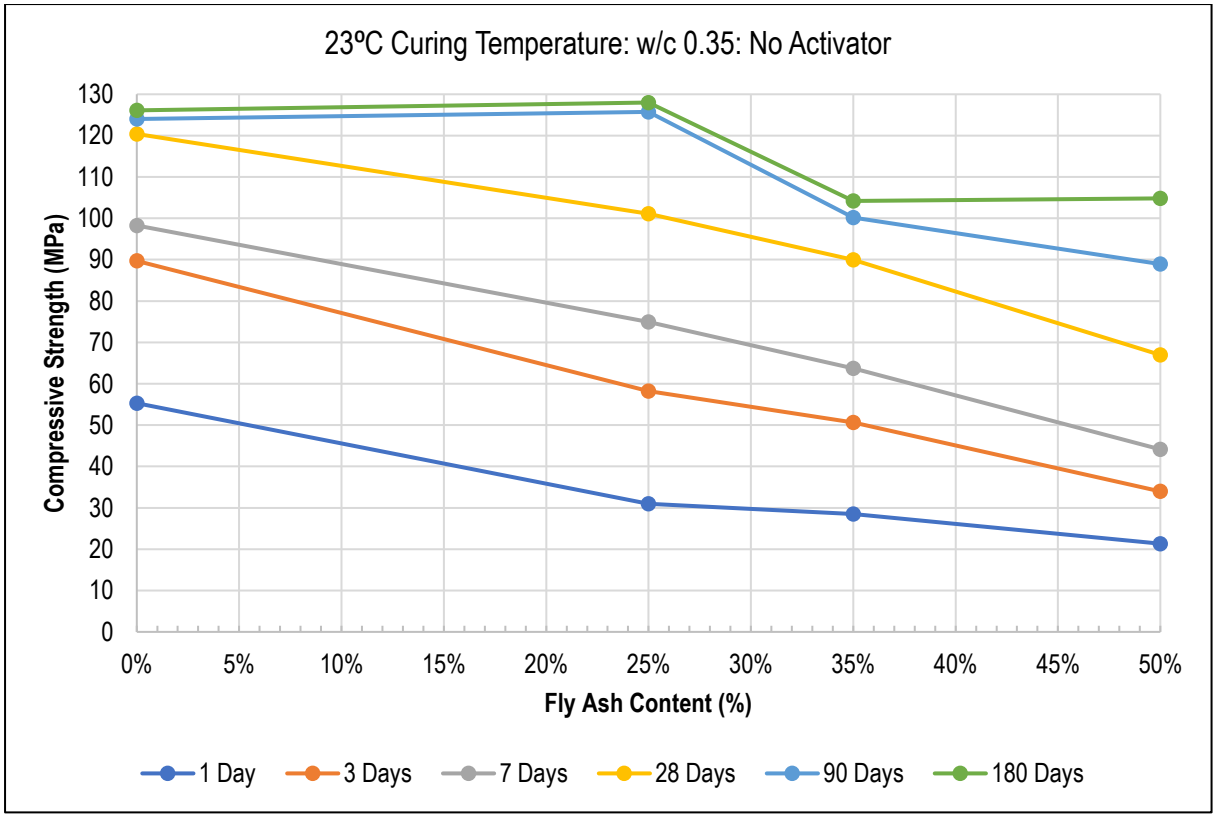

Figure 9.13: Relationship Between Compressive strength and FA Content (23°C: w/c 0.35: No Activator)

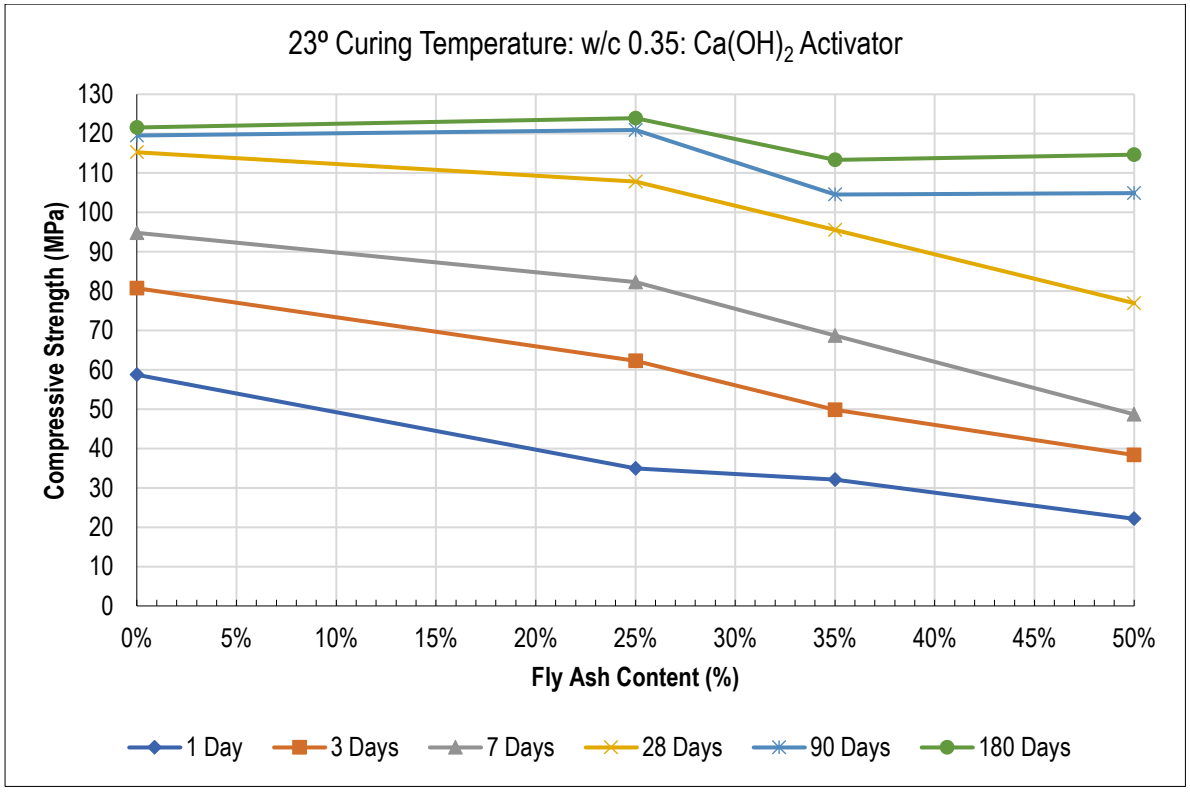

Figure 9.14: Relationship Between Compressive strength and FA Content (23°C: w/c 0.35: $Ca(OH)_2$ Activator)

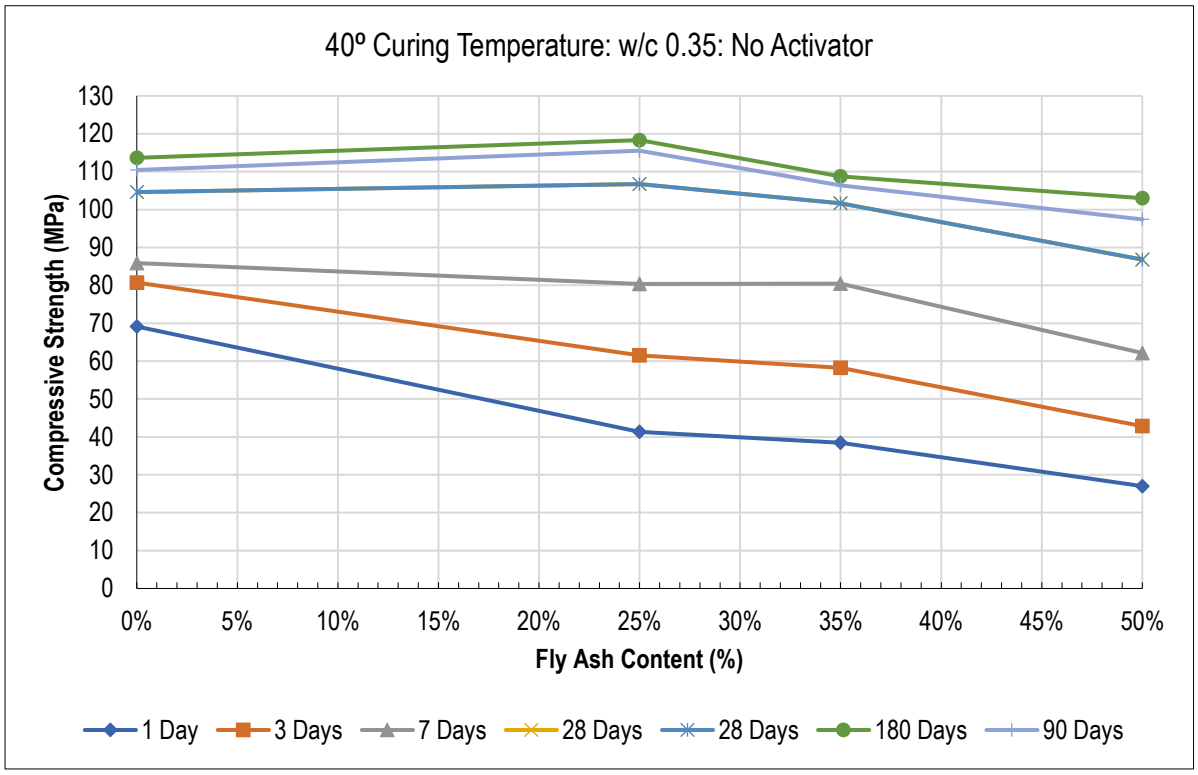

Figure 9.15: Relationship Between Compressive strength and FA Content (40°C: w/c 0.35: No Activator)

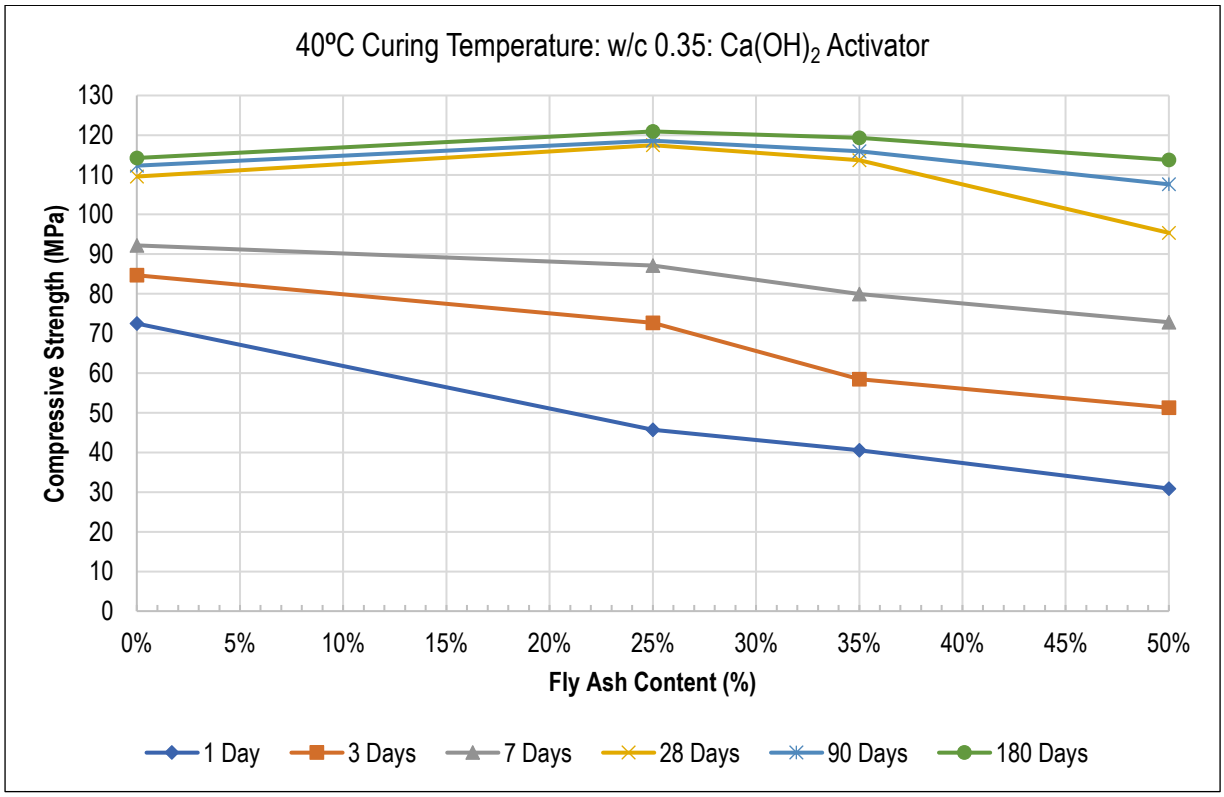

Figure 9.16: Relationship Between Compressive strength and FA Content (40°C: w/c 0.35: $Ca(OH)_2$ Activator)

Annexure 4: Chloride Conductivity Test and Porosity Results

The Chloride Conductivity Index results were processed using an Excel spreadsheet developed by University of Capetown and University of Witwatersrand (2017).

Table 9-2: Chloride Conductivity Index Test Results

					23°C Curing Temperature				40°C Curing Temperature			
Mix	Binder	w/c Ratio	$Ca(OH)_2$ Content	Sample No.	CCI Value (mS/cm)	Average CCI (mS/cm)		Coeff. Of Variation (%)	CCI Value (mS/cm)	Average CCI (mS/cm)		Coeff. Of Variation (%)
3	OPC	0.45	5%	1	0.75	0.76		11.88	0.74	0.74		10.95
				2	0.87				0.66			
				3	0.65				0.85			
				4	0.77				0.71			
4	OPC	0.45	0%	1	0.87	0.85		4.96	0.80	0.77		9.57
				2	0.79				0.67			
				3	0.89				0.75			
				4	0.86				0.84			
7	OPC+25%FA	0.45	5%	1	0.37	0.38		3.59	0.08	0.09		4.82
				2	0.36				0.09			
				3	0.38				0.09			
				4	0.39				0.09			
8	OPC+25%FA	0.45	0%	1	0.46	0.45		4.09	0.15	0.13		14.28
				2	0.45				0.11			
				3	0.42				0.13			
				4	0.46				0.12			
11	OPC+35%FA	0.45	5%	1	0.30	0.27		10.10	0.07	0.06		7.59
				2	0.28				0.07			
				3	0.28				0.06			
				4	0.23				0.06			
12	OPC+35%FA	0.45	0%	1	0.26	0.29		7.84	0.07	0.07		4.32
				2	0.32				007			
				3	0.29				0.08			
					0.30				0.08			

					23°C Curing Temperature				40°C Curing Temperature			
Mix	**Binder**	**w/c Ratio**	**$Ca(OH)_2$ Content**	**Sample No.**	**CCI Value (mS/cm)**	**Average CCI (mS/cm)**		**Coeff. Of Variation (%)**	**CCI Value (mS/cm)**	**Average CCI (mS/cm)**		**Coeff. Of Variation (%)**
15	OPC+50%FA	0.45	5%	1	0.38	0.37		5.55	0.05	0.08		30.76
				2	0.40				0.08			
				3	0.37				0.07			
				4	0.35				0.11			
16	OPC+50%FA	0.45	0%	1	0.37	0.39		2.48	0.07	0.07		3.58
				2	0.39				0.07			
				3	0.39				0.08			
				4	0.39				0.07			
1	OPC	0.35	5%	1	0.37	0.28		24.19	0.22	0.24		15.72
				2	0.28				0.21			
				3	0.21				0.22			
				4	0.26				0.29			
2	OPC	0.35	0%	1	0.28	0.28		6.17	0.27	0.28		15.28
				2	0.27				0.31			
				3	0.27				0.31			
				4	0.30				0.22			
5	OPC+25%FA	0.35	5%	1	0.15	0.15		8.79	0.03	0.04		12.09
				2	0.15				0.03			
				3	0.16				0.04			
				4	0.13				0.04			
6	OPC+25%FA	0.35	0%	1	0.16	0.18		9.01	0.05	0.05		11.15
				2	0.18				0.05			
				3	0.20				0.04			
				4	0.17				0.06			

					23°C Curing Temperature				40°C Curing Temperature			
Mix	**Binder**	**w/c Ratio**	**$Ca(OH)_2$ Content**	**Sample No.**	**CCI Value (mS/cm)**	**Average CCI (mS/cm)**		**Coeff. Of Variation (%)**	**CCI Value (mS/cm)**	**Average CCI (mS/cm)**		**Coeff. Of Variation (%)**
9	OPC+35%FA	0.35	5%	1	0.11	0.12		5.72	0.03	0.04		21.04
				2	0.12				0.04			
				3	0.12				0.04			
				4	0.12				0.03			
10	OPC+35%FA	0.35	0%	1	0.13	0.12		2.02	0.04	0.04		11.46
				2	0.13				0.03			
				3	0.12				0.04			
				4	0.12				0.04			
13	OPC+50%FA	0.35	5%	1	0.21	0.24		11.16	0.06	0.06		1.23
				2	0.23				0.06			
				3	0.27				0.06			
				4	0.24				0.06			
14	OPC+50%FA	0.35	0%	1	0.22	0.22		5.28	0.07	0.06		6.11
				2	0.21				0.06			
				3	0.22				0.06			
				4	0.24				0.06			

Table 9-3: Porosity Test Results Determined in Terms of CCl Test

					23°C Curing Temperature				40°C Curing Temperature			
Mix	Binder	w/c Ratio	$Ca(OH)_2$ Content	Sample No.	Porosity (%)	Average Porosity (%)	Standard Deviation	Coeff. Of Variation (%)	Porosity (%)	Average Porosity (%)	Standard Deviation	Coeff. Of Variation (%)
3	OPC	0.45	5%	1	3.27	3.28		2.45	3.13	3.27		4
				2	3.35				3.32			
				3	3.17				3.43			
				4	3.32				3.21			
4	OPC	0.45	0%	1	3.46	3.47		2.86	3.62	3.43		4.20
				2	3.61				3.32			
				3	3.40				3.32			
				4	3.40				3.48			
7	OPC+25%FA	0.45	5%	1	3.38	3.37		3.52	1.74	1.69		3.47
				2	3.29				1.63			
				3	3.31				1.73			
				4	3.52				1.64			
8	OPC+25%FA	0.45	0%	1	3.91	3.78		3.91	2.47	2.34		8.65
				2	3.70				2.05			
				3	3.61				2.49			
				4	3.91				2.35			
11	OPC+35%FA	0.45	5%	1	3.70	3.45		7.1	1.42	1.31		10.82
				2	3.60				1.45			
				3	3.34				1.18			
				4	3.16				1.19			
12	OPC+35%FA	0.45	0%	1	3.56	3.82		4.68	1.62	1.51		8.84
				2	3.98				1.52			
				3	3.85				1.32			
				4	3.89				1.56			

					23°C Curing Temperature				40°C Curing Temperature			
Mix	**Binder**	**w/c Ratio**	**$Ca(OH)_2$ Content**	**Sample No.**	**Porosity (%)**	**Average Porosity (%)**	**Standard Deviation**	**Coeff. Of Variation (%)**	**Porosity (%)**	**Average Porosity (%)**	**Standard Deviation**	**Coeff. Of Variation (%)**
15	OPC+50%FA	0.45	5%	1	3.38	3.37		1.08	1.31	1.49		11.04
				2	3.32				1.70			
				3	3.40				1.44			
				4	3.36				1.50			
16	OPC+50%FA	0.45	0%	1	3.39	3.55		4.39	1.57	1.58		2.29
				2	3.76				1.56			
				3	3.51				1.56			
				4	3.53				1.64			
1	OPC	0.35	5%	1	1.60	1.40		13.35	1.26	1.43		11.38
				2	1.47				1.41			
				3	1.15				1.39			
				4	1.40				1.65			
2	OPC	0.35	0%	1	2.13	2.13		4.39	2.47	2.48		10.66
				2	2.05				2.47			
				3	2.08				2.80			
				4	2.26				2.16			
5	OPC+25%FA	0.35	5%	1	1.99	1.96		5.36	0.71	0.79		7.28
				2	2.03				0.79			
				3	2.02				0.80			
				4	1.81				0.84			
6	OPC+25%FA	0.35	0%	1	1.98	2.16		5.87	1.05	1.12		11.50
				2	2.19				1.03			
				3	2.29				1.08			
				4	2.18				1.31			

					23°C Curing Temperature				40°C Curing Temperature			
Mix	**Binder**	**w/c Ratio**	**$Ca(OH)_2$ Content**	**Sample No.**	**Porosity (%)**	**Average Porosity (%)**	**Standard Deviation**	**Coeff. Of Variation (%)**	**Porosity (%)**	**Average Porosity (%)**	**Standard Deviation**	**Coeff. Of Variation (%)**
9	OPC+35%FA	0.35	5%	1	2.01	2.05		4.29	0.7	0.72		3.52
				2	1.95				0.75			
				3	2.14				0.7			
				4	2.12				0.74			
10	OPC+35%FA	0.35	0%	1	2.31	2.29		2.08	0.91	0.73		17.62
				2	2.34				0.71			
				3	2.24				0.59			
				4	2.25				0.72			
13	OPC+50%FA	0.35	5%	1	2.41	2.36		2.26	0.96	0.95		2.42
				2	2.29				0.96			
				3	2.36				0.91			
				4	2.39				0.95			
14	OPC+50%FA	0.35	0%	1	2.63	2.73		2.74	1.10	1.03		5.96
				2	2.79				0.98			
				3	2.78				1.06			
				4	2.70				0.97			

Annexure 5: Water Sorptivity Index and Porosity Test Results

The Water Sorptivity Index and porosity results were processed using an Excel spreadsheet developed by University of Capetown and University of Witwatersrand (2017).

Table 9-4: Water Sorptivity Index Test Results

					23°C Curing Temperature				40°C Curing Temperature			
Mix	**Binder**	**w/c Ratio**	**$Ca(OH)_2$ Content**	**Sample No.**	**WSI Value ($mm/hr^{0.5}$)**	**Average WSI ($mm/hr^{0.5}$)**		**Coeff. Of Variation (%)**	**WSI Value ($mm/hr^{0.5}$)**	**Average WSI ($mm/hr^{0.5}$)**		**Coeff. Of Variation (%)**
3	OPC	0.45	5%	1	5.59	5.69		2.0	4.62	4.55		4.9
				2	5.85				4.45			
				3	5.66				4.31			
				4	5.65				4.82			
4	OPC	0.45	0%	1	5.85	6.55		7.9	4.80	4.58		5.5
				2	6.62				4.21			
				3	6.63				4.63			
				4	7.10				4.67			
7	OPC+25%FA	0.45	5%	1	4.82	5.14		6.9	4.57	5.13		8.0
				2	4.85				5.50			
				3	5.41				5.38			
				4	5.48				5.09			
8	OPC+25%FA	0.45	0%	1	5.90	5.42		8.5	5.23	5.55		5.5
				2	5.23				5.77			
				3	4.87				5.34			
				4	5.67				5.85			
11	OPC+35%FA	0.45	5%	1	5.91	5.63		3.7	6.15	6.18		5.2
				2	5.41				5.78			
				3	5.60				6.57			
				4	5.60				6.21			
12	OPC+35%FA	0.45	0%	1	5.01	5.44		5.4	6.10	5.97		4.9
				2	5.57				5.82			
				3	5.68				5.65			
				4	5.49				6.31			

					23°C Curing Temperature				40°C Curing Temperature			
Mix	**Binder**	**w/c Ratio**	**$Ca(OH)_2$ Content**	**Sample No.**	**WSI Value ($mm/hr^{0.5}$)**	**Average WSI ($mm/hr^{0.5}$)**		**Coeff. Of Variation (%)**	**WSI Value ($mm/hr^{0.5}$)**	**Average WSI ($mm/hr^{0.5}$)**		**Coeff. Of Variation (%)**
15	OPC+50%FA	0.45	5%	1	5.15	5.28		6.1	5.63	5.53		3.8
				2	5.75				5.74			
				3	5.17				5.26			
				4	5.03				5.51			
16	OPC+50%FA	0.45	0%	1	6.10	5.96		3.1	4.74	4.95		3.5
				2	5.73				5.16			
				3	6.12				4.91			
				4	5.89				5.00			
1	OPC	0.35	5%	1	5.85	5.64		4.4	4.58	4.28.		13.5
				2	5.45				4.70			
				3	5.86				3.43			
				4	5.40				4.39			
2	OPC	0.35	0%	1	5.54	5.69		7.8	4.46	4.54		11.6
				2	5.34				5.10			
				3	6.19				3.85			
				4	-				4.76			
5	OPC+25%FA	0.35	5%	1	6.22	6.04		2.8	3.57	3.63		4.3
				2	6.13				3.52			
				3	5.84				3.81			
				4	5.97				-			
6	OPC+25%FA	0.35	0%	1	6.19	6.43		5.8	4.97	4.55		10.0
				2	6.83				3.94			
				3	6.66				4.81			
				4	6.04				4.46			

					23°C Curing Temperature				40°C Curing Temperature			
Mix	**Binder**	**w/c Ratio**	**$Ca(OH)_2$ Content**	**Sample No.**	**WSI Value ($mm/hr^{0.5}$)**	**Average WSI ($mm/hr^{0.5}$)**		**Coeff. Of Variation (%)**	**WSI Value ($mm/hr^{0.5}$)**	**Average WSI ($mm/hr^{0.5}$)**		**Coeff. Of Variation (%)**
9	OPC+35%FA	0.35	5%	1	7.23	6.66		8.6	3.25	3.17		33.1
				2	6.05				2.45			
				3	7.05				4.63			
				4	6.29				2.35			
10	OPC+35%FA	0.35	0%	1	5.53	5.16		5.8	4.01	4.30		18.8
				2	4.81				3.51			
				3	5.24				5.42			
				4	5.07				4.25			
13	OPC+50%FA	0.35	5%	1	4.95	4.85		5.2	4.80	4.36		9.3
				2	4.80				4.00			
				3	4.52				4.62			
				4	5.11				4.03			
14	OPC+50%FA	0.35	0%	1	4.73	5.06		6.5	3.33	3.55		5.1
				2	4.83				3.48			
				3	5.25				3.73			
				4	5.42				3.67			

Table 9-5: Porosity Test Results Determined In Terms of Water Sorptivity Test

					23°C Curing Temperature				40°C Curing Temperature			
Mix	Binder	w/c Ratio	$Ca(OH)_2$ Content	Sample No.	Porosity (%)	Average Porosity (%)		Coeff. Of Variation (%)	Porosity (%)	Average Porosity (%)		Coeff. Of Variation (%)
3	OPC	0.45	5%	1	7.19	7.37		3.2	6.86	6.78		2.0
				2	7.14				6.75			
				3	7.59				6.92			
				4	7.55				6.61			
4	OPC	0.45	0%	1	7.61	7.84		2.6	7.61	7.58		5.8
				2	7.73				7.12			
				3	7.98				7.41			
				4	8.05				8.16			
7	OPC+25%FA	0.45	5%	1	8.36	8.64		2.7	4.80	4.66		4.0
				2	8.76				4.52			
				3	8.89				4.47			
				4	8.54				4.83			
8	OPC+25%FA	0.45	0%	1	9.10	9.37		3.9	5.94	5.94		1.4
				2	9.03				6.05			
				3	9.74				5.86			
				4	9.62				5.91			
11	OPC+35%FA	0.45	5%	1	10.53	9.67		7.6	4.61	4.47		7.0
				2	8.81				4.82			
				3	9.94				4.37			
				4	9.39				4.09			
12	OPC+35%FA	0.45	0%	1	9.98	9.71		2.5	4.16	4.40		4.3
				2	9.53				4.49			
				3	9.85				4.60			
					9.49				4.34			

					23°C Curing Temperature				40°C Curing Temperature			
Mix	**Binder**	**w/c Ratio**	**$Ca(OH)_2$ Content**	**Sample No.**	**Porosity (%)**	**Average Porosity (%)**		**Coeff. Of Variation (%)**	**Porosity (%)**	**Average Porosity (%)**		**Coeff. Of Variation (%)**
15	OPC+50%FA	0.45	5%	1	8.80	8.90		1.3	4.26	4.08		9.4
				2	9.00				4.48			
				3	8.81				3.98			
				4	9.00				3.59			
16	OPC+50%FA	0.45	0%	1	10.34	9.78		6.4	4.55	4.43		6.7
				2	10.27				4.79			
				3	9.48				4.27			
				4	9.04				4.12			
1	OPC	0.35	5%	1	3.67	3.44		8.0	2.61	2.75		4.5
				2	3.11				2.79			
				3	3.66				2.72			
				4	3.33				2.90			
2	OPC	0.35	0%	1	5.94	5.67		5.5	4.87	4.46		10.3
				2	5.33				4.81			
				3	5.74				4.18			
				4	-				3.96			
5	OPC+25%FA	0.35	5%	1	3.71	3.86		3.1	1.84	2.25		16.2
				2	3.82				2.54			
				3	3.98				2.37			
				4	3.98				-			
6	OPC+25%FA	0.35	0%	1	4.04	4.02		4.1	2.10	2.15		7.0
				2	3.88				1.97			
				3	4.24				2.32			
				4	3.92				2.22			

					23°C Curing Temperature				40°C Curing Temperature			
Mix	**Binder**	**w/c Ratio**	**$Ca(OH)_2$ Content**	**Sample No.**	**Porosity (%)**	**Average Porosity (%)**		**Coeff. Of Variation (%)**	**Porosity (%)**	**Average Porosity (%)**		**Coeff. Of Variation (%)**
9	OPC+35%FA	0.35	5%	1	4.35	3.99		9.7	1.82	2.00		7.2
				2	4.22				2.16			
				3	3.89				2.06			
				4	3.49				1.96			
10	OPC+35%FA	0.35	0%	1	4.55	4.75		8.3	1.84	1.75		6.7
				2	4.68				1.86			
				3	4.46				1.64			
				4	5.33				1.66			
13	OPC+50%FA	0.35	5%	1	6.00	6.03		3.6	2.58	2.54		1.9
				2	6.35				2.47			
				3	5.85				2.55			
				4	5.94				2.55			
14	OPC+50%FA	0.35	0%	1	6.85	6.92		2.9	2.84	2.84		6.2
				2	7.10				2.63			
				3	6.67				3.06			
				4	7.07				2.84			

Annexure 6: Oxygen Permeability Test Results

The Oxygen Permeability Index results were processed using an Excel spreadsheet developed by University of Capetown and University of Witwatersrand (2017).

Table 9-6: Oxygen Permeability Index Test Results

					23°C Curing Temperature				40°C Curing Temperature			
Mix	**Binder**	**w/c Ratio**	**$Ca(OH)_2$ Content**	**Sample No.**	**OPI Value**	**Average OPI**	**Standard Deviation**	**Coeff. Of Variation (%)**	**OPI Value**	**Average OPI**	**Standard Deviation**	**Coeff. Of Variation (%)**
3	OPC	0.45	5%	1	11.44	11.58	0.18	1.5%	11.8	11.71	0.10	0.9%
				2	11.78				11.6			
				3	11.53				11.72			
				4	-				-			
4	OPC	0.45	0%	1	11.56	11.44	0.10	0.9%	11.6	11.49	0.14	1.2%
				2	11.33				11.58			
				3	11.48				11.5			
				4	11.39				11.29			
7	OPC+25%FA	0.45	5%	1	10.98	11.09	0.15	1.3%	11.7	11.48	0.20	1.7%
				2	11.07				11.24			
				3	11.3				11.56			
				4	10.99				11.44			
8	OPC+25%FA	0.45	0%	1	10.99	10.97	0.04	0.4%	11.21	11.24	0.20	1.8%
				2	10.91				11.03			
				3	11				11.52			
				4	10.96				11.19			
11	OPC+35%FA	0.45	5%	1	11.18	10.99	0.19	1.7%	11.19	11.30	0.26	2.2%
				2	11				11.12			
				3	10.8				11.59			
				-	-				-			
12	OPC+35%FA	0.45	0%	1	11	11.01	0.07	0.6%	11.93	11.56	0.36	3.2%
				2	11.09				11.56			
				3	10.95				11.2			

					23°C Curing Temperature				40°C Curing Temperature			
Mix	**Binder**	**w/c Ratio**	**$Ca(OH)_2$ Content**	**Sample No.**	**OPI Value**	**Average OPI**	**Standard Deviation**	**Coeff. Of Variation (%)**	**OPI Value**	**Average OPI**	**Standard Deviation**	**Coeff. Of Variation (%)**
15	OPC+50%FA	0.45	5%	1	11.32	11.26	0.07	0.6%	11.16	11.26	0.18	1.6%
				2	11.27				11.09			
				3	11.17				11.3			
				4	11.29				11.5			
16	OPC+50%FA	0.45	0%	1	10.8	10.83	0.08	0.7%	11.03	10.96	0.13	1.1%
				2	10.82				10.82			
				3	10.75				10.91			
				4	10.94				11.1			
1	OPC	0.35	5%	1	11.56	11.48	0.11	0.9%	11.2	11.25	0.25	2.3%
				2	11.34				11.53			
				3	11.45				11.03			
				4	11.57				-			
2	OPC	0.35	0%	1	11.04	11.16	0.11	1.0%	10.62	11.09	0.45	4.1%
				2	11.21				11.14			
				3	11.29				11.52			
				4	11.1							
13	OPC+50%FA	0.35	5%	1	11.06	11.1425	0.25	2.3%	11.58	11.23	0.34	3.0%
				2	10.82				11.2			
				3	11.36				10.91			
				4	11.33							
14	OPC+50%FA	0.35	0%	1	11.34	11.25	0.10	0.9%	11.48	11.50	0.12	1.3%
				2	11.32				11.63			
				3	11.19				11.34			
				4	11.14				11.54			

Annexure 7: Fly Ash and Cement Particle Size Distribution

MASTERSIZER 2000

Result Analysis Report

Sample Name:
sample FA01 - Average

Sample Source & type:
WITS UNIV

Sample bulk lot ref:

SOP Name:
Cement rdpt 2018

Measured by:
eol

Result Source:
Averaged

Measured:
11 July 2018 09:43:32

Analysed:
11 July 2018 09:43:34

Particle Name:
Cement 1.0

Particle RI:
1.680

Dispersant Name:

Accessory Name:
Scirocco 2000

Absorption:
1

Dispersant RI:
1.000

Analysis model:
General purpose (fine)

Size range:
0.020 to 2000.000 um

Weighted Residual:
1.556 %

Sensitivity:
Normal

Obscuration:
3.78 %

Result Emulation:
Off

Concentration:
0.0002 %Vol

Specific Surface Area:
2.78 m²/g

Span :
3.604

Surface Weighted Mean D[3,2]:
2.158 um

Uniformity:
1.08

Vol. Weighted Mean D[4,3]:
8.384 um

Result units:
Volume

---

d(0.1): 0.756 um **d(0.5):** 5.471 um **d(0.9):** 20.476 um

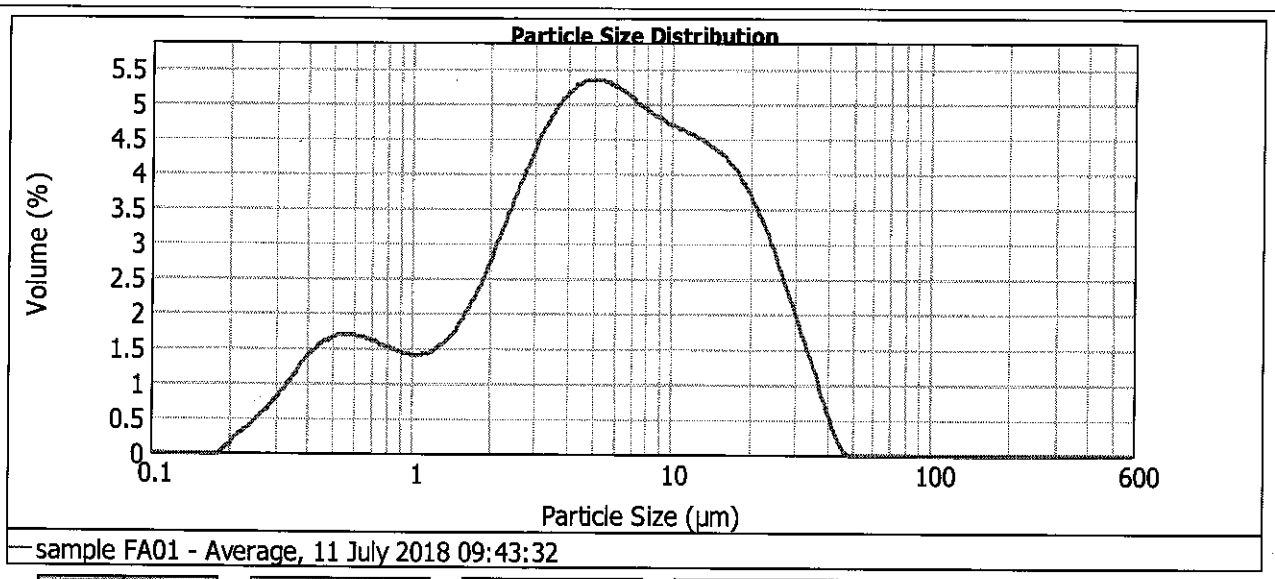

Size (µm)	Vol Over %	Size (µm)	Vol Over %	Size (µm)	Vol Over %	Size (µm)	Vol Over %	Size (µm)	Vol Over %	Size (µm)	Vol Over %
0.010	100.00	0.158	100.00	1.660	82.06	17.378	14.17	138.038	0.00	1445.440	0.00
0.013	100.00	0.182	100.00	1.905	80.01	19.953	10.63	158.489	0.00	1659.587	0.00
0.020	100.00	0.209	99.92	2.188	77.50	22.909	7.46	181.970	0.00	1905.461	0.00
0.023	100.00	0.240	99.63	2.512	74.47	26.303	4.80	208.930	0.00	2187.762	0.00
0.026	100.00	0.275	99.17	2.884	70.93	30.200	2.70	239.883	0.00	2511.886	0.00
0.030	100.00	0.316	98.49	3.311	66.91	32.000	2.00	275.423	0.00	2884.032	0.00
0.035	100.00	0.363	97.55	3.802	62.51	34.674	1.20	316.228	0.00	3311.311	0.00
0.040	100.00	0.417	96.34	4.365	57.85	39.811	0.30	363.078	0.00	3801.894	0.00
0.046	100.00	0.479	94.94	5.012	53.06	45.000	0.01	416.869	0.00	4365.158	0.00
0.052	100.00	0.550	93.44	5.754	48.25	45.709	0.00	478.630	0.00	5011.872	0.00
0.060	100.00	0.631	91.92	6.607	43.53	52.481	0.00	549.541	0.00	5754.399	0.00
0.069	100.00	0.724	90.44	7.586	38.95	60.256	0.00	630.957	0.00	6606.934	0.00
0.079	100.00	0.832	89.05	8.710	34.53	69.183	0.00	724.436	0.00	7585.776	0.00
0.091	100.00	0.955	87.74	10.000	30.24	79.433	0.00	831.764	0.00	8709.636	0.00
0.105	100.00	1.096	86.48	11.482	26.05	91.201	0.00	954.993	0.00	10000.000	0.00
0.120	100.00	1.259	85.18	13.183	21.96	104.713	0.00	1096.478	0.00		
0.138	100.00	1.445	83.75	15.136	17.98	120.226	0.00	1258.925	0.00		

Operator notes:

Malvern Instruments Ltd.
Malvern, UK
Tel := +[44] (0) 1684-892456 Fax +[44] (0) 1684-892789

Mastersizer 2000 Ver. 5.60
Serial Number : 34355-137

File name: July 2018
Record Number: 691
11/07/2018 09:44:57

MASTERSIZER 2000

Result Analysis Report

Sample Name:
SAMPLE C02 - Average

Sample Source & type:
WITS UNN

Sample bulk lot ref:

SOP Name:
Cement rdpt 2018

Measured by:
eol

Result Source:
Averaged

Measured:
11 July 2018 09:38:48

Analysed:
11 July 2018 09:38:50

Particle Name:
Cement 1.0

Particle RI:
1.680

Dispersant Name:

Accessory Name:
Scirocco 2000

Absorption:
1

Dispersant RI:
1.000

Analysis model:
General purpose (fine)

Size range:
0.020 to 2000.000 um

Weighted Residual:
1.127 %

Sensitivity:
Normal

Obscuration:
9.70 %

Result Emulation:
Off

Concentration:
0.0009 %Vol

Specific Surface Area:
1.98 m²/g

Span :
2.733

Surface Weighted Mean D[3,2]:
3.029 um

Uniformity:
0.856

Vol. Weighted Mean D[4,3]:
15.681 um

Result units:
Volume

---

d(0.1): 1.087 um **d(0.5):** 12.519 um **d(0.9):** 35.301 um

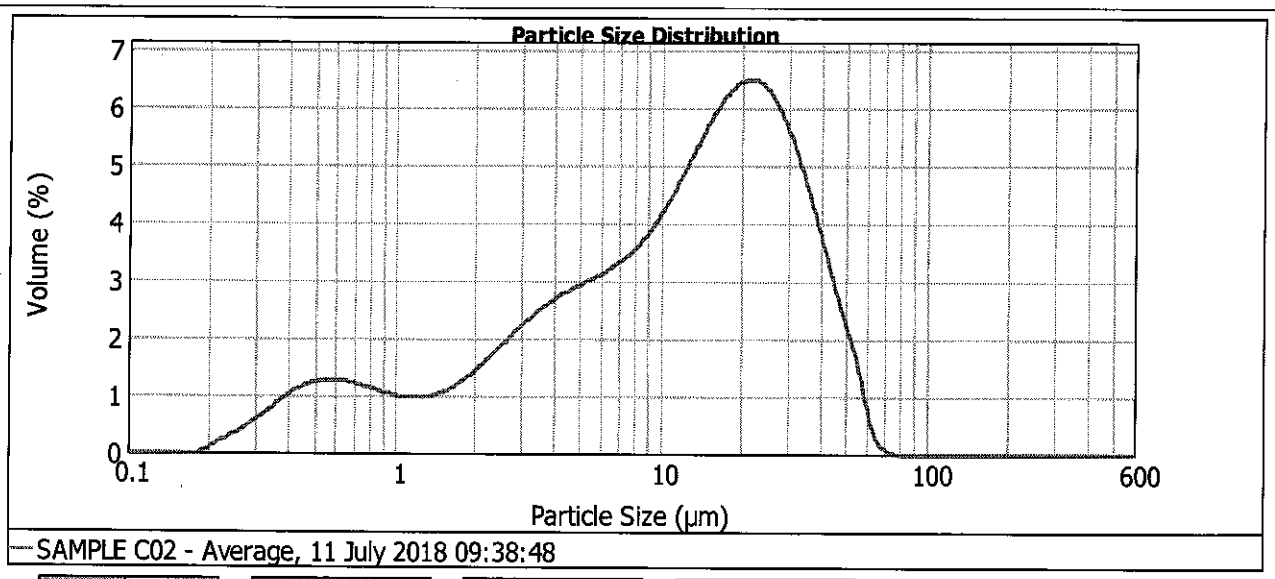

Size (µm)	Vol Over %	Size (µm)	Vol Over %	Size (µm)	Vol Over %	Size (µm)	Vol Over %	Size (µm)	Vol Over %	Size (µm)	Vol Over %
0.010	100.00	0.158	100.00	1.660	87.21	17.378	37.98	138.038	0.00	1445.440	0.00
0.013	100.00	0.182	100.00	1.905	86.09	19.953	32.26	158.489	0.00	1659.587	0.00
0.020	100.00	0.209	99.94	2.188	84.77	22.909	26.40	181.970	0.00	1905.461	0.00
0.023	100.00	0.240	99.74	2.512	83.20	26.303	20.66	208.930	0.00	2187.762	0.00
0.026	100.00	0.275	99.40	2.884	81.39	30.200	15.29	239.883	0.00	2511.886	0.00
0.030	100.00	0.316	98.90	3.311	79.33	32.000	13.22	275.423	0.00	2884.032	0.00
0.035	100.00	0.363	98.21	3.802	77.07	34.674	10.56	316.228	0.00	3311.311	0.00
0.040	100.00	0.417	97.31	4.365	74.62	39.811	6.84	363.078	0.00	3801.894	0.00
0.046	100.00	0.479	96.27	5.012	72.03	45.000	3.92	416.869	0.00	4365.158	0.00
0.052	100.00	0.550	95.14	5.754	69.32	45.709	3.62	478.630	0.00	5011.872	0.00
0.060	100.00	0.631	93.99	6.607	66.47	52.481	1.50	549.541	0.00	5754.399	0.00
0.069	100.00	0.724	92.88	7.586	63.46	60.256	0.24	630.957	0.00	6606.934	0.00
0.079	100.00	0.832	91.83	8.710	60.22	69.183	0.02	724.436	0.00	7585.776	0.00
0.091	100.00	0.955	90.85	10.000	56.67	79.433	0.00	831.764	0.00	8709.636	0.00
0.105	100.00	1.096	89.95	11.482	52.71	91.201	0.00	954.993	0.00	10000.000	0.00
0.120	100.00	1.259	89.08	13.183	48.29	104.713	0.00	1096.478	0.00		
0.138	100.00	1.445	88.19	15.136	43.36	120.226	0.00	1258.925	0.00		

Operator notes:

Malvern Instruments Ltd.
Malvern, UK
Tel := +[44] (0) 1684-892456 Fax +[44] (0) 1684-892789

Mastersizer 2000 Ver. 5.60
Serial Number : 34355-137

File name: July 2018
Record Number: 687
11/07/2018 09:40:04

Annexure 8: Ultra Fine Fly Ash Data Sheet

The Ultra-fine Fly Ash Data Sheet is Obtainable in the url below;

http://ashresources.co.za/wp-content/uploads/2018/02/05.29_SupaPozz-Brochure_PR.pdf

Annexure 9: Superplasticiser Data Sheet

The Superplasticiser Data Sheet is Obtainable in the url below;

http://files.autospec.com/za/sika/2018datasheets/sika-viscocrete-90he.pdf

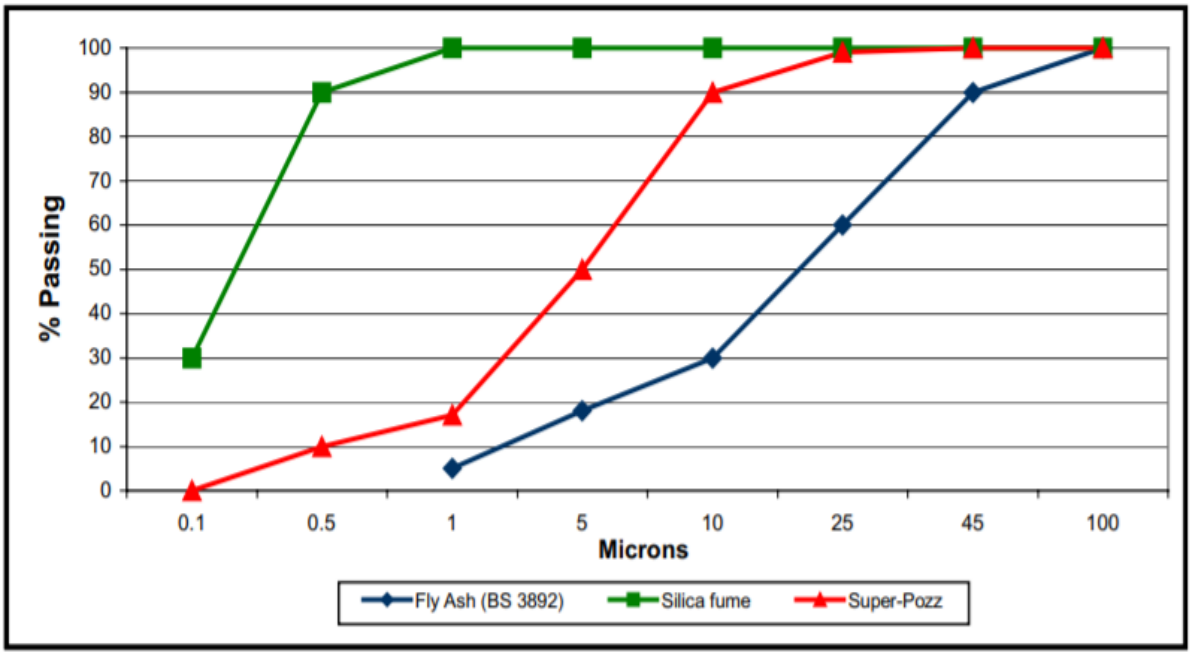

Figure 9.17: Particle Size Distribution for Ultra Fine Fly Ash, Silica Fume and Standard Fly Ash (Source: Seedat, 2003)